UNIVERSITAT DE BARCELONA

Categorització dels cossos de poliglucosà cerebrals basada en la presència de neoepítops reconeguts per IgMs naturals

Elisabet Augé Marí

Aquesta tesi doctoral està subjecta a la llicència ***Reconeixement 3.0. Espanya de Creative Commons***.

Esta tesis doctoral está sujeta a la licencia ***Reconocimiento 3.0. España de Creative Commons***.

This doctoral thesis is licensed under the ***Creative Commons Attribution 3.0. Spain License***.

Facultat de Farmàcia i Ciències de l'Alimentació
Departament de Bioquímica i Fisiologia

Categorització dels cossos de poliglucosà cerebrals basada en la presència de neo-epítops reconeguts per IgMs naturals

ELISABET AUGÉ MARÍ

2018

Facultat de Farmàcia i Ciències de l'Alimentació
Departament de Bioquímica i Fisiologia

Programa de doctorat:

Recerca, desenvolupament i control de medicaments

Categorització dels cossos de poliglucosà cerebrals basada en la presència de neo-epítops reconeguts per IgMs naturals

Memòria presentada per **Elisabet Augé Marí** per optar al títol de doctor per la Universitat de Barcelona

Dr. Jordi Vilaplana i Hortensi	Dra. Carme Pelegrí i Gabaldà	Elisabet Augé Marí
(director)	(directora)	(doctoranda)

ELISABET AUGÉ MARÍ
2018

The greatest glory in living lies not in never falling, but in rising every time we fall.

Nelson Mandela

Als meus pares, Roser i Jaume
Al meu germà, Xavi

A l'Ariadna

Després d'aquesta gran etapa, vull agrair a totes aquelles persones que m'han donat suport i ajudat durant els diferents moments (espero no deixar-me a ningú):

En primer lloc, m'agradaria agrair als meus directors, la Nanen i el Jordi, per haver-me donat la possibilitat de fer la tesi al seu grup i haver confiat en mi en tot moment. He tingut la oportunitat de desenvolupar-me, créixer i equivocar-me, sempre amb el vostre suport incondicional i plena confiança.

A les meves companyes de laboratori. Gemma, tot i haver coincidit en un període curt en el temps, agrair-te la teva disposició per ensenyar-me en els meus inicis, explicar-me el funcionament del lab i donar-me els millors consells. Itsaso, agradecerte todos los momentos vividos en el lab. Gracias por todos tus consejos, por resolver todas mis dudas y por todo tu apoyo.

A totes les professores i professors de la Secció de Fisiologia per haver compartit amb mi docència i recerca. Agrair-vos la proximitat, els vostres consells i el gran interès que heu mostrat en la meva etapa de doctoranda. Lluïsa, has estat dia si dia també procurant per mi, sobretot en aquesta última etapa. Gràcies pel teu suport a nivell professional, però sobretot personal.

A tots els estudiants, becaris i post-docs: Blanca, Ignasi, Mariona, Lídia, Paulina, Sheila, Marta, Malén, Mar, Rocío, Thalia, Ivana, Abi, Cristina, Alba, Teresa, David.... Gràcies per les estones a la coffee-room, pels dinars, per les festes de Nadal i per compartir preocupacions, riures i anècdotes. Al Joan per ser un gran company dins i fóra el departament.

Agrair al David, la Vanessa i el Quim el seu suport i la seva ajuda sempre que l'he necessitat.

Als becaris i estudiants de doctorat del Departament de Farmacologia: Miren, Oriol, Dolors, Christian... per haver compartit consells, algun que altra anticòs i anècdotes.

A Sebastián. Conocerte durante esta etapa ha sido un placer. Gracias por haber compartido conmigo tu proyecto, técnicas, preocupaciones, charlas, cafés... Deseo de corazón que tengas mucho éxito con tu tesis.

Al personal del Banc de Teixits Neurològics de l'Hospital Clínic de Barcelona. A la Dra. Ellen Gelpi, la Dra. Laura Molina, la Teresa Ximelis i tot l'equip tècnic del Biobanc per la seva disposició, amabilitat i confiança.

A la Míriam Osorio i tot el personal del Banc de Medicina Fetal, per la seva disposició i facilitat en l'entrega de mostres.

Al Dr. Joan J. Guinovart i al Dr. Jordi Duran. Agrair-vos l'oportunitat de col·laborar amb el vostre grup, així com també la vostra implicació en el projecte. Per estar sempre disposats a ensenyar, a ajudar i a compartir.

I am very grateful to Prof. Dr. med. Ingo Bechmann and Dr. med. Martin Krueger for hosting me in the Institut für Anatomie. Thank you very much for your kindness and your patience and for giving me the opportunity to learn new techniques. Thank you Julia, Judith, Alina, Jana, Henrike, Peter... for being so nice and for helping me inside and outside the lab!

Agrair també a tota la gent dels *Stammtisch*, en especial a l'Àlex, per fer-me sentir com a casa durant la meva estada a Leipzig.

A la Txell. Leipzig i Begur ens han unit i espero que així sigui per molt temps. T'he d'agrair molts dels moments viscuts allà, però també per mantenir l'amistat aquí, per seguir preocupant-te per la meva recerca i per mi. Ets una gran persona.

Al Brian, la Tere, la Judith i la Jordana. Compartir amb vosaltres les vivències del doctorat és impagable. Gràcies per tots els moments inoblidables viscuts al vostre costat. Sou unes persones fantàstiques. Molt èxit amb el vostre doctorat!

Al Sergi, l'Ivan, la Sílvia, la Marta i el Pau. Per acollir-me tan bé dins d'un grup que es fa anomenar els integradors del Sergi. Per compartir, escoltar i riure. Gràcies.

A l'Àlex, l'Adrià, la Jèssica, el Lluís i el David. Per ser-hi abans, per ser-hi ara. Més que mai.

A la Carla. És increïble que estigui escrivint aquestes línies d'agraïment a una persona que conec des de la infància. Hem viscut tants moments, Carla. Aquesta és una etapa més. Gràcies per ser aquí encara.

A l'Alba. Tot va començar aquí, a la Facultat de Farmàcia, amb tu. Sento que aquesta tesi també és teva. Ets l'amiga genial. Encara me'n recordo quan em vas dir: li he dit a la meva mare que he conegut a una persona que s'assembla molt a mi. Hem passat molts moments junts i se'm dibuixa un somriure d'orella a orella cada cop que en recordo algun. Has fet que Vilafranca sigui el poble que mai havia tingut. No és que em senti orgullosa de ser la teva amiga, sinó que em sento feliç.

A l’Anna que ha fet que la portada de la tesi sigui alegria, com ella. Tenia una idea al cap i l’has calcat. Mil gràcies per tot!

A la Marina, la Irene, el Gerardo i la Puri. Gracias por compartir conmigo esta etapa y recibir vuestro apoyo.

A la meva família. Tiets, cosins, avis... en especial, a la meva àvia, que estic segura que hagués estat molt orgullosa; i al Ramon, agrair-te la paciència infinita que vas tenir amb el papa quan et donava la tabarra amb la tesi i amb el meu viatge a Alemanya, ni que m’hagués anat a la fi del món...

Als meus pares i al Xavi, el meu germà petit que fa de germà gran. Gràcies per aguantar-me, però sobretot per estimar-me. Per estimar el que faig, per estimar el que penso, per estimar com sóc. Gràcies, aquesta tesi és per vosaltres.

A l’Ariadna. Ets la persona que més coneix aquesta tesi. Quantes vegades te n’hauré parlat? No hi ha paraules per descriure tot el que has fet, fas i sé que faràs per mi. Sense tu no hauria arribat aquí, Ari. Has escoltat, aconsellat, compartit i viscut amb mi. Però no només per això, sinó per totes les altres coses.

Aquesta tesi ha estat finançada per:

Generalitat de Catalunya
Projecte 2014 SGR 525
Projecte 2017 SGR 625
Ministerio de Economía y Competitividad
Proyecto BFU 2013-47382-P
Proyecto BFU 2016-78398-P

La doctoranda ha gaudit dels següents ajuts predoctorals durant la realització d'aquesta tesi:

Ajuts de Personal Investigador en Formació (APIF) per a alumnes de tercer cicle de la Universitat de Barcelona
Facultat de Farmàcia i Ciències de l'Alimentació, Universitat de Barcelona
Ajuts per a estudis o projectes fora de Catalunya 2016
Fundació Agustí Pedro i Pons, Universitat de Barcelona

ÍNDEX

ABSTRACT

ÍNDEX DE FIGURES

ÍNDEX DE TAULES

ABREVIATURES

AAN	autoanticòs natural
AGE	a*dvanced glycation end-products,* productes finals de glicosilació avançada
AN	anticòs natural
ApoE	apolipoproteïna E
AQP4	aquaporina 4
Aβ	*amyloid β*, β amiloide
CA	*corpora amylacea*, cossos amilacis
CAL	*corpora amylacea-like granules***,** grànuls semblants als cossos amilacis
CDR3	regió determinant de la complementarietat 3 o regió hipervariable 3
Fab	*antigen binding fragment*
Fc	*crystallizable fragment*
GFAP	*glial fibrillary acidic protein*, proteïna acídica fibril·lar glial
GS	glicogen sintasa
HDL	*high density lipoproteins*, lipoproteïnes d'alta densitat
HSP	*heat shock proteins,* proteïnes de xoc tèrmic
IgA	immunoglobulina A
IgG	immunoglobulina G
IgM	immunoglobulina M
KO	*knock-out*
LB	*Lafora body*, cos de Lafora
LDL	*low density lipoproteins*, lipoproteïnes de baixa densitat
LPC	*lysophosphatidylcholine*, lisofosfatidilcolina
MAO-B	monoamino-oxidasa B
MAP2	*microtubule-associated protein 2*, proteïna associada a microtúbuls 2
MMP2	*matrix metalloproteinase 2,* metal·loproteinasa de matriu 2
NeuN	*neuronal nuclei antigen,* antigen del nucli neuronal
nLB	*neuronal Lafora body*, cos de Lafora neuronal
OE	*overexpressed*
PAS	*periodic acid Schiff*, àcid periòdic de Schiff
PC	*phosphatidylcholine*, fosfatidilcolina
PGB	*polyglucosan body,* cos de poliglucosà
PTG	*protein targeting to glycogen*
SAMP8	*senescence-accelerated mouse prone 8*
SAMR1	*senescence-accelerated mouse resistant 1*

SNC	sistema nerviós central
SOPF	*Specific and Opportunistic Pathogen Free*
Tg	transgènic
VH	domini variable de la cadena pesada
WE	*waste elements*, productes de rebuig

ABSTRACT

The term polyglucosan bodies (PGBs) refers to complex aggregates composed of relatively large glucose polymers reaching diameters of tens of micrometres. PGBs have been reported in the central nervous system, but also in other organs and tissues, such as heart, skeletal muscle and liver. These aggregates have been described in humans and other species and they have been most widely studied in mammals. Different forms of PGBs have been related to particular situations or specific diseases. During the ageing process, human brain accumulates one type of PGBs called c*orpora amylacea* (CA). Although CA have been studied for several years, their origin and function remain unclear. PGBs are also associated with Lafora disease, a neurodegenerative disorder that is characterized by the presence of PGBs structures called Lafora bodies (LBs). On the other hand, brain ageing in mice leads to the progressive appearance and expansion of degenerative granular PGBs frequently referred to as *Periodic Acid Schiff* (PAS) granules. These granules, which are present mainly in the hippocampus, originate in astrocytes processes and tend to appear in clusters. Each cluster corresponds to the set of granules of a determined astrocyte. Recently, our research group have reported the presence of neo-epitopes recognized by IgMs on these structures. These IgMs, which are present as contaminants in many commercial antibodies, are responsible of numerous false positive staining on these bodies when immunohistochemical procedures are used.

This thesis aimed to study the origin, composition and function of PGBs that appear with age and in neurodegenerative conditions such as Alzheimer's disease and Lafora disease.

The results show that CA are similar structures to PAS granules from mice brain and that CA also contain neo-epitopes. In both cases, the neo-epitopes can be recognized by natural IgM antibodies, suggesting a new relation between PGBs and the natural immune system. Moreover, the false staining produced by the natural IgMs that bind to the neo-epitopes clarified some controversial results previously described about the presence of some components on CA and their function. We also determined that CA accumulate non-degradable products generated during ageing process and increased in neurodegenerative condictions, such as Alzheimer's disease. Taking all into account, we hypothesize that CA are waste containers in which deleterious or residual products are isolated to be later eliminated through the action of the innate immune system. On the other hand, we observed that malin deficient mice, a mouse model of Lafora disease, present high amounts of two distinct types of PGBs: PAS granules or CA-like granules,

originated in astrocytes and containing neo-epitopes, and neuronal LBs, which are exclusive of Lafora disease and do not contain neo-epitopes. Thus, the absence of malin triggers the formation of PGBs in neurons but also enhances their development in astrocytes. We postulate that, against to the current believe, astrocytes are involved in the etiopathogenesis of Lafora disease.

Overall results show that the distinct PGBs have been studied until now with a specific and limited perspective. A global or main picture is necessary to obtain the knowledgement of their significance.

I. INTRODUCCIÓ

1. COSSOS DE POLIGLUCOSÀ

El glicogen és una macromolècula que forma una partícula que pot atènyer fins a 20 nm de diàmetre. Està formada per llargues cadenes d'unitats de glucosa unides per enllaços α-1,4-glicosídics, que es ramifiquen a través d'enllaços α-1,6-glicosídics. El terme poliglucosà fa referència a polímers de glucosa semblants al glicogen, que es troben menys ramificats que aquest i que es poden agregar formant unes inclusions conegudes com a cossos de poliglucosà (*polyglucosan bodies*, PGBs) (Robitaille *et al*., 1980). Els PGBs inclouen petites quantitats de diferents proteïnes i es tenyeixen, igual que el glicogen, amb la tinció de l'àcid periòdic de Schiff (*periodic acid Schiff*, PAS). A diferència del glicogen, els PGBs són resistents, en un grau variable, a la digestió amb l'α-amilasa (Cavanagh, 1999). Amb microscòpia electrònica, es pot observar que els PGBs tenen una estructura fibril·lar.

La seva acumulació es pot trobar en diferents teixits durant l'envelliment, però també esdevé el tret característic d'algunes malalties associades a defectes en el metabolisme del glicogen (Hedberg-Oldfors i Oldfors, 2015). El present treball se centra en alguns d'aquests PGBs que es formen a nivell cerebral, concretament els cossos amilacis o *Corpora amylacea* (CA), els cossos de Lafora (*Lafora bodies*, LBs) i els grànuls PAS de ratolí, anomenats així perquè es marquen positivament per aquesta tinció. L'estudi d'altres PGBs, com per exemple els que apareixen en la malaltia de cossos de poliglucosà en adults (*adult polyglucosan body disease*), s'abordarà en futurs estudis.

1.1. Cossos amilacis

Els CA són unes inclusions glicoproteiques de tipus poliglucosà que s'acumulen en el cervell humà durant l'envelliment (Figura 1) i d'una manera notable en algunes malalties neurodegeneratives, com la malaltia d'Alzheimer, l'esclerosi múltiple, la malaltia de Parkinson o la malaltia de Pick, així com també en pacients amb epilèpsia del lòbul temporal acompanyada d'esclerosi hipocampal (Cavanagh, 1999; Cissé *et al*., 1993; Keller, 2006; Mizutani *et al*., 1987; Mrak *et al*., 1997; Nishio *et al*., 2001; Radhakrishnan *et al*., 2007; Song *et al*., 2014; Singhrao *et al*., 1993).

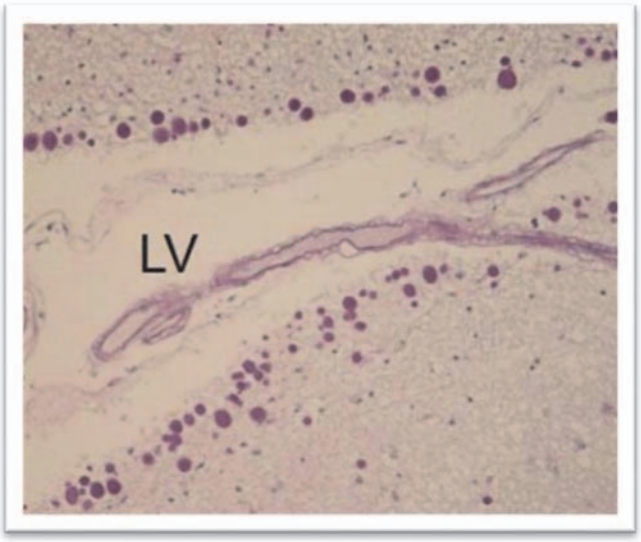

Figura 1. CA de la capa superficial de la matèria blanca propera al ventricle lateral del cervell d'un cas de 90 anys d'edat tenyits amb la reacció de PAS. LV: ventricle lateral (Nam *et al*., 2012).

Tot i que els CA van ser descrits per primer cop per Purkinje l'any 1837, el terme *corpora amylacea* va ser introduït posteriorment per Virchow (Virchow,1854) en base a la similitud d'aquests cossos cerebrals amb el midó (*amylacea* en llatí deriva del grec *amylon*, que significa midó).

1.1.1. Morfologia i distribució en el sistema nerviós central

Els CA són unes estructures habitualment esfèriques que varien en diàmetre entre 2-20 μm, tot i que en alguns casos poden arribar a 50 μm. Tot i que generalment són cossos esfèrics, també s'han descrit formes ovalades i elongades. Normalment la seva superfície és llisa, però no és infreqüent que de vegades sigui irregular, com si estigués recoberta de material (Cavanagh, 1999). Al còrtex cerebral, al nucli estriat i a la matèria gris de la medul·la espinal els CA són més petits que a les altres zones i només ocasionalment arriben a 10-12 μm (Averback, 1981; Leheskoki *et al*., 1991; Takahashi *et al*., 1975).

En individus d'edat avançada, els CA es troben en gairebé totes les regions del sistema nerviós central (SNC), però tendeixen a acumular-se en certes localitzacions. Al cervell, es troben congregats principalment en el recobriment glial, sota el revestiment de les cèl·lules ependimàries dels ventricles, particularment sota el cos callós, al sostre i terra del tercer i quart ventricles, i al sostre de l'aqüeducte cerebral. En les superfícies més externes del cervell, es troben generalment en el recobriment glial sota la piamàter, especialment en la base del cervell, en les superfícies medials dels lòbuls temporals i sobre les formacions de l'hipocamp. Quan estan presents a la matèria blanca cerebral,

tendeixen a acumular-se al voltant de vasos de mida mitjana i gran, i s'observen sovint als espais de Virchow-Robin (Cavanagh, 1999). Al cerebel, es troben a la profunditat del solc i és freqüent trobar-los a la línia de cèl·lules de Purkinje (Mittal i Olszewski, 1985). Al bulb raquidi també s'han descrit CA (Fujii *et al*., 1996). A la medul·la espinal també s'observen CA, els quals es localitzen principalment prop de les superfícies, ja sigui en el recobriment glial sota la piamàter o entre fibres nervioses mielinitzades (Cavanagh, 1999). A l'ull, especialment en subjectes d'edat avançada, s'han descrit CA prop de la lamina cribrosa i en les parts superficials del nervi òptic, sota la beina dural (Dolman *et al*., 1980). A la retina es troben en la capa de fibres del nervi òptic, la capa de cèl·lules ganglionars, la capa plexiforme interna i la capa nuclear interna, però no en les capes plexiforme o nuclear externes (Kubota *et al*., 1993; Kubota i Naumann, 1993). La presència de CA també s'ha descrit al nervi vestíbul-coclear, en la part superficial, sota la beina pia-aracnoide (Fujii *et al*., 1996).

1.1.2. Variacions amb l'edat

Ha estat àmpliament descrit que la formació dels CA cerebrals està relacionada amb l'edat. Cavanagh (1999), en mostres de medul·la espinal, va determinar que el nombre de CA és invariablement baix en grups d'individus d'edat més jove, malgrat que va puntualitzar que se'n poden trobar petits nombres en la medul·la espinal d'individus d'edat entre 10-15 anys, amb diàmetres que són quasi la meitat que els que es troben en individus d'edat adulta. A partir dels 30-40 anys, els CA generalment són més grans i més nombrosos. Chung i Horoupian (1996) van trobar una incidència baixa de CA en teixit hipocampal i parahipocampal en un grup de 20 subjectes control d'edats entre 16 i 51 anys amb diferents malalties. Busard *et al*. (1994) van estudiar sistemàticament la relació entre l'edat, el sexe i la presència de CA en 64 casos que no presentaven cap malaltia neurològica. Van determinar que el nombre de CA estava relacionat amb l'increment de l'edat i no van trobar cap relació amb el sexe de l'individu. Van observar que a edats inferiors a 40 anys, la presència de CA era esporàdica, mentre que a partir dels 40 anys es trobaven molt més augmentats, tot i que de manera variable. Estudis més recents mostren un increment significatiu de CA al lòbul frontal i a l'hipocamp amb l'edat i puntualitzen que aquests apareixen abans a la regió hipocampal (Maqbool i Tahir, 2008).

1.1.3. Ultraestructura

A nivell ultraestructural, els CA consisteixen en cabdells de filaments lineals curts, de 8-12 nm de diàmetre, que formen un patró espiral, i que semblen estar més concentrats

en el centre (Ramsey, 1965). Els cossos són regularment arrodonits però no estan envoltats per una membrana. La presència de partícules de glicogen al voltant del cossos és un tret característic (Leel-Ossy, 2001; Ramsey, 1965). En un estudi dut a terme per biòpsia de l'hipocamp i el lòbul temporal d'un pacient amb epilèpsia del lòbul temporal de 35 anys d'edat, es van trobar CA situats en el citoplasma d'astròcits fibrosos (Ramsey, 1965). Altres estudis també han posat de manifest l'associació d'aquestes estructures amb astròcits (Leel-Ossy, 2001; Palmucci *et al*., 1982; Sbarbati *et al*., 1996).

D'altra banda, Woodford i Tso (1980), en un estudi dut a terme en el nervi òptic de quatre subjectes, van arribar a la conclusió que els CA es trobaven inequívocament dins dels axons mielinitzats i no mielinizats. Van observar dins d'ells feixos de microtúbuls i formacions laminars que recordaven a mitocòndries en degeneració i no van veure cossos similars dins dels astròcits en aquesta regió. També s'han trobat CA intra-axonals amb les mateixes característiques ultraestructurals en d'altres regions com el tàlem (Mizutani *et al*., 1987), en petits axons mielinitzats de la matèria gris de la medul·la (Takahashi *et al*., 1975) o en el còrtex orbital (Anzil *et al*., 1974). Aquest últim autor, però, puntualitza que la presència de CA dins dels axons és menys freqüent que dins dels astròcits. Malgrat que diversos estudis demostren l'associació dels CA amb axons, és important fer èmfasi que cap d'ells ha demostrat que els CA es trobin dins dels somes neuronals en individus sans.

1.1.4. Composició

Els estudis histoquímics duts a terme per tal d'establir la naturalesa i composició dels CA, resumits a la Taula 1, indiquen que aquests estan formats principalment per polisacàrids, ja que es tenyeixen positivament amb la tinció de PAS, la tinció de Carmí de Best o el mètode de Gomori de metenamina de plata (Sakai, *et al*., 1969; Stam i Roukema, 1973). També es tenyeixen amb el mètode de PAS-dimedone, que no tenyeix mucopolisacàrids, glicoproteïnes o mucoproteïnes. La digestió prèvia amb α-amilasa redueix lleugerament la tinció de PAS (Sakai *et al*., 1969), fet que descarta una elevada quantitat de glicogen normal en aquestes estructures o bé indica una compactació elevada que dificulta la digestió enzimàtica. Amb la solució de iodina o d'àcid sulfúric, els CA es tenyeixen de color marró primerament i després violeta fosc, indicant que aquestes estructures presenten qualitats similars al midó. També es tenyeixen amb *Alcian blue* a pH baix (Sakai *et al*., 1969; Stam i Roukema, 1973) i el punt d'extinció amb blau de metilè és a pH inferior a 2 (Stam i Roukema, 1973), indicant, doncs, la naturalesa acídica d'alguns components dels CA.

Tinció	Marcatge	Referències
Acetat d'uranil-ferrocianida	+	Sakai *et al*., 1969; Stam i Roukema, 1973
Alcian blue	+	Sakai *et al*., 1969; Stam i Roukema, 1973
Blau de toluïdina	metacromàtic	Sakai *et al*., 1969; Stam i Roukema, 1973
Carmí de Best	+	Sakai *et al*., 1969; Stam i Roukema, 1973
Extinció blau de metilè	A pH<2	Stam i Roukema, 1973
Feulgen reaction per ADN	-	Stam i Roukema, 1973
Gallocianina per ADN i ARN	-	Stam i Roukema, 1973
Gomori de metenamina de plata	+	Stam i Roukema, 1973
Hematoxilina	blau pàl·lid	Cavanagh, 1999
Iodina i H_2SO_4	marró i violeta	Sakai *et al*., 1969; Stam i Roukema, 1973
Lípids	-	Sakai *et al*., 1969; Stam i Roukema, 1973
Luxol Fast blue	blau pàl·lid	Robitaille *et al*., 1980
PAS-dimedone	+	Sakai *et al*., 1969
Tinció de PAS	+	Sakai *et al*., 1969; Stam i Roukema, 1973
Nile blue sulphate	blau	Cavanagh, 1999
Tioflavina S	+	Stam i Roukema, 1973
Vermell Congo	-	Avendano *et al*., 1980; Stam i Roukema, 1973
Hale's dialysed iron	+	Avendano *et al*., 1980; Sakai *et al*., 1969; Stam i Roukema, 1973

Taula 1. Tincions histoquímiques dels CA cerebrals.

Tot i que a nivell histoquímic els CA no presenten ARN i ADN (Stam i Roukema, 1973), estudis recents mitjançant tècniques d'hibridació *in situ* mostren que els CA presenten afinitat per diferents oligonucleòtids (Balea *et al*., 2006).

L'anàlisi bioquímic dels CA indica que quan són purificats mitjançant un procés de centrifugació amb una extracció final en aigua donen lloc a una fracció aquosa que conté un 87,9% de polímers de glucosa, un 4,7 % de proteïnes i un 2,5 % de fosfats (Sakai *et al*., 1969). Aquests resultats van ser confirmats posteriorment per Stam i Roukema (1973), els quals van descriure la presència de petites quantitats de fosfats i sulfats en els CA. Van concloure que el glicogen era l'únic polímer al qual els fosfats i els sulfats s'hi podien unir, ja que els nivells d'àcid hexurònic i hexosamina, 0,2 i 0,3 % respectivament, eren baixos. Styaert *et al*. (1990), després de purificar els CA cerebrals evitant l'ús de proteases, van determinar que el contingut proteic dels CA aïllats corresponia al 4% del pes total. L'anàlisi SDS-PAGE de les fraccions de CA va mostrar

diferents bandes polipeptídiques amb pesos moleculars entre 24 i 133 KDa, essent els més abundants 24, 42, 94 i 133 KDa. Aquests resultats van ser confirmats per Cissé *et al*. (1991) que, a més a més, van analitzar la seqüència d'aminoàcids dels polipèptids de 24 i 42 KDa i van determinar que presentava homologia amb l'extrem N-terminal de la ubiqüitina humana. Ja que els pesos moleculars d'aquests polipèptids són més grans que els de la ubiqüitina (8,5 KDa), es va considerar que algunes proteïnes dels CA estaven conjugades a aquesta proteïna. En un estudi més recent, l'anàlisi proteòmic de CA obtinguts mitjançant la microdisseció làser en cervells de casos d'esclerosi múltiple va determinar la presència de 24 proteïnes diferents, la majoria de les quals eren proteïnes del citoesquelet cel·lular. A més a més, van trobar proteïnes implicades en la motilitat i plasticitat cel·lular, en la regulació de l'apoptosi i la senescència, i en rutes enzimàtiques (Selmaj *et al*., 2008).

En els darrers anys, una de les tècniques més utilitzades per a l'estudi de la composició dels CA és l'assaig immunohistoquímic. Diversos estudis immunohistoquímics han posat de manifest que els CA contenen diferents substàncies derivades de diversos tipus cel·lulars, però alguns dels resultats publicats presenten certa controvèrsia. Així doncs, mentre que alguns autors han determinat la presència de la proteïna tau (Day *et al*., 2015; Wilhelmus *et al*., 2011), d'altres no han estat capaços de reproduir aquests resultats (Notter i Knuesel, 2013). El mateix passa amb el pèptid β amiloide (Aβ), mentre que Notter i Knuesel (2013) van determinar la seva presència en els CA, altres autors no van arribar a la mateixa conclusió (Pirici i Margaritescu, 2014; Wilhelmus *et al*., 2011). Altres components descrits en els CA i vinculats amb un possible origen neuronal són l'α-sinucleïna (Buervenich *et al*., 2001; Notter i Knuesel, 2013; Wilhelmus *et al*., 2011), la reelina (Notter i Knuesel, 2013), la proteïna associada a microtúbuls 2 (MAP2) (Nam *et al*., 2012; Notter i Knuesel, 2013) i la β-tubulina classe III (Wilhelmus *et al*., 2011). També s'ha demostrat que presenten reactivitat per a l'antigen del nucli neuronal (NeuN) (Buervenich *et al*., 2001; Korzhevskii i Giliarov, 2007; Pirici i Margaritescu, 2014) i per a la nestina (Buervenich *et al*., 2001), tot i que aquesta última no ha pogut ser detectada en els estudis duts a terme per Pirici i Margaritescu (2014).

També han estat descrits alguns components vinculats a un possible origen glial. Reaccions positives en els CA amb anticossos dirigits contra la proteïna bàsica de mielina, la proteïna proteolipídica, el galactosilcerebroside i la glicoproteïna de mielina de l'oligodendròcit (Singhrao *et al*., 1994) indiquen que metabòlits oligodendroglials contribueixen també a la seva composició. També han estat determinades proteïnes vinculades a l'astroglia, com proteïnes específiques de la família S100 (Buervenich *et*

al., 2001; Hoyaux *et al*., 2000; Pirici i Margaritescu, 2014), l'aquaporina 4 (AQP4) (Pirici i Margaritescu, 2014) o la proteïna acídica fibril·lar glial (GFAP). Pel que fa a aquesta última, mentre que alguns autors descriuen un marcatge positiu dels CA (Buervenich *et al*., 2001; Pirici i Margaritescu, 2014), altres conclouen que la immunoreactivitat de GFAP es troba associada als CA, però es limita al marge d'aquests dipòsits (Nam *et al*., 2012; Notter i Knuesel, 2013; Pirici *et al*., 2014).

Els CA també són immunoreactius a proteïnes de xoc tèrmic (*Heat Shock Proteins*, HSP) (Cissé *et al*., 1993; Gáti i Leel-Ossy, 2001; Martin *et al*., 1991), tot i que Erdamar *et al*. (2000) no van poder reproduir el marcatge d'algunes d'elles i determinaven que la diferència podia ser deguda a algun factor desconegut, i a la ubiqüitina (Cissé *et al*., 1993; Day *et al*., 2015; Pirici i Margaritescu, 2014; Pirici *et al*., 2014; Wilhelmus *et al*., 2011).

Altres substàncies descrites en els CA mitjançant assaigs immunohistoquímics són proteïnes sanguínies, com l'ADAMTS13 i la thrombopondin-1 (Meng *et al*., 2009), components del sistema complement (Singhrao *et al*., 1995), epítops mitocondrials (Botez i Rami, 2001), productes finals de glicosilació avançada (*advanced glycation end-products*, AGE) (Iwaki *et al*., 1996) i proteoglicans (Liu *et al*., 1987).

A més a més, estudis recents, mitjançant anticossos policlonals dirigits contra diferents espècies de fongs, descriuen la presència de proteïnes fúngiques en els CA cerebrals de casos de malalties neurodegeneratives, suggerint una possible relació d'aquestes inclusions i les infeccions fúngiques (Pisa *et al*., 2016).

1.1.5. Origen cel·lular

Un dels aspectes que ha creat més debat en l'estudi dels CA és el seu origen cel·lular. Com s'ha descrit en els apartats anteriors, en base als estudis ultrastructurals, i sobretot, en base als estudis immunohistoquímics, tant l'origen neuronal com el glial han estat proposats.

L'origen neuronal s'ha hipotetitzat en base a l'observació a nivell ultrastructural de CA en axons neuronals de determinades regions del SNC (Anzil *et al*., 1974; Mizutani *et al*., 1987; Takahashi *et al*., 1975; Woodford i Tso, 1980). A més a més, els assaigs immunohistoquímics han permès descriure determinats components d'origen neuronal com a constituents dels CA, fet que assenyala l'origen neuronal, o si més no, la participació d'aquestes cèl·lules en la formació dels CA. També, Selmaj *et al.* (2008), mitjançant l'anàlisi proteòmic de CA aïllats de casos d'esclerosi múltiple, suggereixen

que els CA consisteixen en agregats de cèl·lules neuronals. Cap estudi, però, ha demostrat la presència de CA en els somes neuronals.

La majoria de CA s'acumulen en localitzacions íntimament relacionades amb l'astroglia. Diversos autors han determinat mitjançant un anàlisi ultrastructural la presència de CA en astròcits fibrosos (Leel-Ossy, 2001; Ramsey, 1965; Palmucci *et al*., 1982; Sbarbati *et al*., 1996). Anzil *et al*., l'any 1974, tot i observar la presència de CA en terminals postsinàptics, puntualitzen que l'observació de CA en neurones és molt menys freqüent que en astròcits. A més, diferents estudis (Nam *et al*., 2012; Notter i Knuesel, 2013; Schipper i Cissé, 1995; Singhrao *et al*., 1993) posen de manifest l'associació de CA i processos astrocítics GFAP positius, mentre que en descarten la seva associació amb oligodendròcits o micròglia (Nam *et al*., 2012; Notter i Knuesel, 2013). S'ha proposat, doncs, que aquesta associació podria ser o bé el resultat de la fagocitosi de romanents de neurites o neurones en estat de degeneració o de metabòlits vasculars per part dels astròcits (Singhrao *et al*., 1993; Meng *et al*., 2009), o bé un indicador de la fisiopatologia o la degeneració pròpia d'aquestes cèl·lules (Suzuki *et al*., 2012). A més a més, un estudi recent ha aportat evidències de que els CA deriven d'una font glial mediada per hemo-oxigenasa-1, la qual promou dany mitocondrial i formació de CA. Els autors van arribar a aquesta conclusió mitjançant l´ús de cultius d'astròcits on l'hemo-oxigenasa-1 es trobava sobreexpressada a nivells semblants als que es troba en el cervell de malalts d'Alzheimer. Els cossos semblants a CA van ser observats en astròcits sota aquestes condicions, les quals no es complien en les cèl·lules control (Song *et al*., 2014).

1.1.6. Significat fisiopatològic

Els CA, que van ser descrits per J.E. Purkinje l'any 1837, van ser considerats durant molt de temps irrellevants per als neuropatòlegs. Tot i que van ser àmpliament estudiats durant l'inici del segle XX, alguns autors van considerar que no tenien cap significat fisiopatològic (Buzzard i Greenfield, 1921). No va ser fins a les últimes dècades de segle, amb l'aplicació de noves i més refinades tècniques histoquímiques, ultrastructurals i immunohistoquímiques, que va sorgir l'interès en el seu significat i la seva relació amb certes condicions neuropatològiques. Així doncs, moltes de les interpretacions sobre els CA deriven dels estudis sobre la seva composició, igual que succeeix a l'hora de postular el seu origen cel·lular. Tot i que s'han fet diverses interpretacions, la seva funció fisiopatològica encara és desconeguda.

Singhrao *et al.* (1995) proposen, en base a la seva composició, que els CA són matrius inertes de mucopolisacàrid que recullen proteïnes ubiquitinades resultants de la mort

neuronal o del dany a mielina durant l'envelliment i en diferents malalties neurològiques. Així doncs, els CA esdevindrien mecanismes comuns i eficients que tindrien la funció de prevenir el reconeixement de proteïnes immunogèniques per part de la micròglia o els limfòcits i així protegir el SNC de dany inflamatori.

Altres autors, en la mateixa línia, han proposat que la funció dels CA estaria orientada a la captura i segrest de productes potencialment nocius derivats del metabolisme cel·lular, principalment derivats del procés d'envelliment, però probablement també de qualsevol estat de malaltia que generi quantitats excessives de productes metabòlics potencialment nocius (Cavanagh, 1999; Cissé *et al*., 1993). Cavanagh (1999) proposa, doncs, que es tractaria d'un altre mecanisme paral·lel al sistema de lisosoma/lipofuscina. Els productes relacionats amb l'envelliment resultants del procés de glicació de proteïnes de llarga durada poden ser detectats en els dos sistemes, però mentre que el sistema de lisosoma/lipofuscina és un sistema de degradació enzimàtic, en els CA els productes s'incorporen en un polímer de glucosa. A més a més, Sbarbati *et al*. (1996), després d'observar CA sobresortint del SNC cap al teixit connectiu pial, suggereixen que després de la seva producció en astròcits, els CA es transfereixen al teixit connectiu pial a través de la membrana glial limitant. Així doncs, conclouen que els CA no només representen una acumulació de material anòmal, sinó que podrien formar part d'un sistema glio-pial d'eliminació de substàncies del sistema nerviós.

Els diferents treballs duts a terme per Schipper (2004) permeten concloure que els CA deriven dels gränuls peroxidasa/Gomori-positius que estan presents en astròcits, i que la seva formació podria ser mediada per l'activitat hemo-oxigenasa 1 i el dany a mitocòndries. Així doncs, conclouen que els CA representarien la presència d'estrès oxidatiu, d'anomalies mitocondrials i de desequilibris del ferro durant l'envelliment dels astròcits. Estudis recents indiquen que la formació de CA es veu incrementada a l'hipocamp d'individus que es troben en un estat pre-malaltia d'Alzheimer i suggereixen que el dany mitocondrial mediat per hemo-oxigenasa 1, la mitofàgia i la formació de CA serien els esdeveniments primerencs en la patogènesi d'aquesta malaltia (Song *et al*., 2014).

Altres autors, després d'analitzar els CA presents en cervell de pacients d'esclerosi múltiple, sostenen que els CA representen cèl·lules d'origen neuronal agregades i degenerades, i suggereixen que podrien constituir un fenomen secundari a la patologia de la malaltia (Selmaj *et al*., 2008).

En una línia similar, Meng *et al*. (2009), després de descriure la presència de dues proteïnes sanguínies en els CA, suggereixen que aquestes estructures representen conglomeracions de proteïnes que interaccionen, les quals provenen de neurones en degeneració i d'elements sanguinis alliberats després del trencament de la barrera hematoencefàlica.

Notter i Knuesel (2013), en canvi, apunten que la presència de reelina en els CA, que ells mateixos identifiquen, podria estar relacionada amb deficiències en el transport neuronal donant lloc a l'acumulació d'orgànuls i metabòlits proteics en les varicositats neurítiques. Els autors conclouen que els canvis que es produeixen en els nivells de reelina associats a l'envelliment i a certes malalties neurodegeneratives podrien jugar un paper important en la formació dels CA a través de l'alteració de la dinàmica del citoesquelet cel·lular.

Finalment, cal destacar que estudis recents (Pisa *et al*., 2016) apunten a una possible associació entre els CA cerebrals i certes infeccions fúngiques després de descriure la presència de proteïnes d'origen fúngic en aquestes estructures, predominantment en els CA de casos de malalties neurodegeneratives, mitjançant estudis immunohistoquímics.

1.1.7. Cossos amilacis en altres teixits

En altres òrgans com el cor, el fetge, la pròstata, la tiroide i els pulmons, s'han descrit inclusions anomenades també "cossos amilacis". Tot i així, aquests cossos no presenten sempre les mateixes característiques ni les mateixes reaccions histoquímiques que els CA cerebrals. Normalment, presenten peculiaritats pròpies de cada òrgan, i en els casos de la pròstata i el pulmó, no estan relacionats amb la naturalesa de poliglucosà (Cavanagh, 1999).

1.2. Cossos de Lafora

Els LBs són un tipus de PGBs que apareixen en els pacients de la malaltia de Lafora i que s'acumulen en diferents teixits, però majoritàriament al cervell (Ramachandran *et al*., 2009). Aquests cossos són un signe patognòmic de la malaltia i s'ha postulat que podrien ser la seva causa.

1.2.1. Malaltia de Lafora

La malaltia va ser descrita l'any 1911 per Gonzalo Rodríguez-Lafora, un deixeble de Santiago Ramón i Cajal, quan estava exercint com a neuropatòleg a Washington. No només va descriure les inclusions en cervell, que posteriorment rebrien el seu nom, sinó

que també va estudiar les característiques clíniques de la malaltia, el seu curs i el seu patró d'herència (Lafora, 1911; Lafora i Glueck, 1911; Nanduri *et al*., 2008).

La malaltia de Lafora és un tipus d'epilèpsia mioclònica progressiva que es caracteritza per una neurodegeneració progressiva d'inici insidiós en edats d'entre 8 i 18 anys. És una malaltia neurodegenerativa autosòmica recessiva causada majoritàriament per mutacions en un dels següents gens: *EPM2A*, el qual codifica per a la laforina, una proteïna fosfatasa dual-específica amb un domini d'unió a carbohidrats (Minassian *et al*., 1998; Serratosa *et al*., 1999); i *EPM2B* (també anomenat NHLRC1), el qual codifica per a la malina, una E3 ubiquitin-ligasa (Chan *et al*., 2003; Gómez-Abad *et al*., 2005; Singh *et al.,* 2005, 2006). Els individus amb mutacions en un dels dos gens són neurològicament i histològicament indistingibles (Singh i Ganesh, 2009).

La malaltia es manifesta normalment durant l'adolescència amb convulsions tònico-clòniques generalitzades, mioclònies o crisis d'absència, entre d'altres. A mesura que la malaltia progressa, els individus afectats pateixen una demència progressiva acompanyada d'apràxia, afàsia i pèrdua visual, que acaba donant lloc a la mort, normalment en la primera dècada des de l'aparició dels símptomes inicials (Acharya *et al.,* 1995; Berkovic *et al*., 1993; Gómez-Abad *et al*., 2005; Kobayashi *et al*., 1990; Minassian, 2001).

La malaltia de Lafora presenta un procés de neurodegeneració progressiva. A l'autòpsia s'observa una abundant pèrdua neuronal sense desmielinització ni inflamació. Totes les regions del SNC es veuen involucrades en aquest procés, tot i que en diferents graus. Aquestes regions inclouen l'escorça cerebral i cerebel·losa, els ganglis basals, els nuclis del cerebel, el tàlem i l'hipocamp. A més a més, també s'observa neurodegeneració a la retina (Busard *et al*., 1987b; Minassian, 2001; Schwarz i Yanoff, 1965; Van Heycop Ten Ham i De Jager, 1963).

1.2.2. Característiques dels cossos de Lafora

Els LBs es troben principalment localitzats al cervell, on tendeixen a acumular-se en diferents regions. Es troben exclusivament a les neurones, i s'ha descrit que els LBs més grans, d'uns 10-30 μm de diàmetre, es localitzen principalment als somes neuronals. També s'han descrit LBs més petits, d'1-5 μm de diàmetre, que es troben a les dendrites i a les neurites corticals (Busard *et al*., 1987b; Jenis *et al*., 1970; Ramon y Cajal *et al*., 1974; Vanderhaeghen, 1971).

Pel que fa a la distribució en el cervell, els LBs es troben principalment a l'escorça cerebral, essent més abundants a les capes III i V (Busard *et al*., 1987b; Van Heycop Ten Ham i De Jager, 1963). Altres regions on s'ha descrit la presència de LBs són el tàlem, la substància negra i els nuclis dentats (Van Heycop Ten Ham i De Jager, 1963), així com també la retina (Berart-Badier *et al*., 1980; Schwarz i Yanoff, 1965).

Els LBs normalment són arrodonits o ovalats, tot i que els que es troben en dendrites poden tenir una estructura més elongada (Busard *et al*., 1987b). Les dues característiques histològiques que distingeixen els LBs dels altres PGBs són la presència d'una regió central densa envoltada d'una regió menys compacta, i la seva localització intraneuronal (Figura 2) (Cavanagh, 1999).

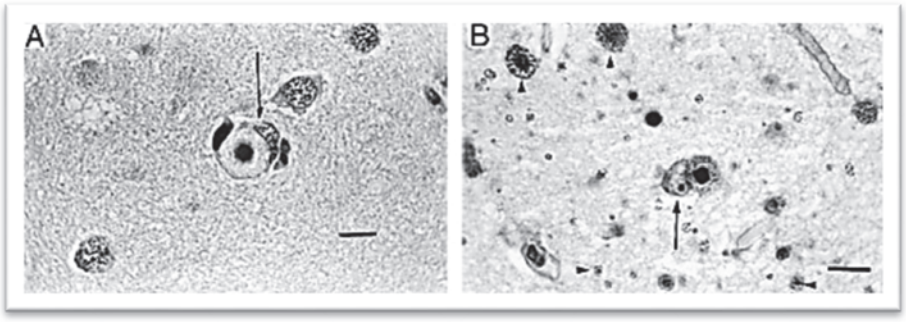

Figura 2. LBs localitzats al soma neuronal de l'escorça cerebral. (A) Tinció hematoxilina-eosina. (B) Tinció de PAS-hematoxilina. Fletxes: nucli neuronal desplaçat. Caps de fletxa: altres LBs (Cavanagh, 1999).

Els LBs són positius per a la tinció de PAS, la tinció de Carmí de Best i la tinció de PAS-dimedone. S'ha determinat també que es tenyeixen amb iodina donant lloc a una coloració marró, i es tenyeixen amb *Alcian blue* a pH baix (Sakai *et al*., 1970). A més a més, pel que fa al seu anàlisi bioquímic, Sakai *et al*. (1970) i Yokoi *et al*. (1975) van determinar que aquests cossos contenen un 80-93 % de glucosa, un 9% de contingut proteic i un 1,26% de fosfats. Així doncs, en conjunt, les propietats histoquímiques i químiques dels LBs són molt semblants a les determinades per als CA, exceptuant un petit increment en el contingut proteic i un contingut una mica més baix de fosfats.

L'anàlisi ultrastructural dels LBs mostra que aquests estan formats per filaments de 8-12 nm de diàmetre semblants als que es descriuen a l'anàlisis ultrastructural dels CA, tot i que en els LBs la quantitat de material electrodens en la part central és més gran (Vanderhaeghen, 1971).

Tot i que s'han dut a terme pocs estudis immunohistoquímics en casos de malalts de Lafora per tal de caracteritzar el contingut proteic dels cossos, estudis duts a terme en

alguns casos de la malaltia revelen que els LBs contenen neurofilaments de 160 i 200 KDa (Lewis *et al*., 1990), ubiqüitina i proteïna tau (Greene i Papasozomenos, 1987).

1.2.3. Cossos de Lafora en altres teixits

Els LBs també han estat descrits en altres òrgans com fetge, múscul esquelètic, cor o pell. A diferència dels LBs neuronals, els cossos d'altres teixits no tenen una morfologia esfèrica (Minassian, 2001).

A la pell, aquests cossos es troben localitzats principalment a les cèl·lules ductals de les glàndules sudorípares ecrines i a les cèl·lules mioepitelials de les glàndules sudorípares apocrines. La biòpsia cutània es pot utilitzar per al diagnòstic i és el mètode menys invasiu amb sensibilitat alta quan les proves genètiques no són possibles (Carpenter i Karpati, 1981; Busard *et al*., 1987a; Andrade *et al*., 2003).

Malgrat l'àmplia distribució dels LBs en l'organisme, els pacients habitualment no presenten manifestacions extra-neurològiques, com a mínim no abans de sucumbir a la malaltia neurològica (Minassian, 2001; Tagliabracci *et al*., 2007).

1.2.4. Models murins de la malaltia

S'han desenvolupat diferents models murins de la malaltia de Lafora. El primer model murí es va crear a través de la supressió de la regió codificant del domini fosfatasa dual-específic del gen *EPM2A*. Els ratolins que no expressen *EPM2A* mostren evidències patològiques de la malaltia a partir dels 2 mesos d'edat. Fenotípicament, tenen un creixement i desenvolupament normals fins als 4 mesos, quan es comencen a produir canvis de comportament. Les convulsions mioclòniques, l'atàxia i els canvis electroencefalogràfics s'observen als 9 mesos d'edat. Aquests animals mostren un mecanisme peculiar de neurodegeneració en el que es produeix desintegració d'alguns orgànuls cel·lulars, com les mitocòndries o el reticle endoplasmàtic. A més a més, s'observa que la degeneració neuronal i l'aparició de les inclusions de tipus Lafora es produeixen abans de qualsevol anormalitat de comportament (Ganesh *et al*., 2002).

Un altre model desenvolupat per a l'estudi de la malaltia de Lafora és el ratolí deficient de malina. Tot i que DePaoli-Roach *et al*. (2010) i Turnbull *et al*. (2010) descriuen el model a 3 i 6 mesos d'edat, respectivament, Vallès-Ortega *et al.* (2011) estenen l'estudi dels ratolins deficients de malina a 11 mesos i descriuen que a aquesta edat presenten neurodegeneració, increment de l'excitabilitat sinàptica i propensió a patir convulsions mioclòniques, juntament amb l'increment dels nivells de glicogen sintasa (GS) muscular

al cervell. També analitzen la progressió dels LBs a l'hipocamp, i descriuen l'expressió de GS muscular i malina en un subconjunt particular d'interneurones, les parvalabúmina positives, l'aparició posterior de LBs en aquestes cèl·lules i la seva degeneració i pèrdua progressiva en absència de malina.

També es va desenvolupar un model transgènic (Tg) creat a través de la sobreexpressió de laforina inactivada (Cys26-6Ser). El ratolí Tg va proporcionar informació valuosa sobre la localització de la proteïna laforina. En cervell, aquesta proteïna es localitza al soma neuronal i a les dendrites. També es va demostrar que la laforina es localitza al reticle endoplasmàtic, però no als ribosomes, com es pensava inicialment. És important destacar que aquest model va permetre la caracterització de la unió de la laforina a diferents polisacàrids i determinar la unió preferent de la laforina als PGBs respecte al glicogen (Chan *et al*., 2004).

1.2.5. Laforina i malina

Recentment s'ha descrit que les dues proteïnes implicades en la malaltia formen un complex i regulen l'acumulació de glicogen a través del control proteasoma dependent de proteïnes relacionades amb el glicogen, com la *protein targeting to glycogen* (PTG), la GS muscular, l'enzim desramificant del glicogen o la neuronatina (Cheng *et al*., 2007; Sharma *et al*., 2011; Vilchez *et al*., 2007; Worby *et al*., 2008). A més a més, també s'ha descrit que l'activitat fosfatasa de la laforina permet mantenir la qualitat del glicogen mitjançant la prevenció de la seva hiperfosforilació (Tagliabracci *et al*., 2011; Turnbull *et al*., 2010).

Tot i així, també s'ha descrit que tant la laforina com la malina estan involucrades en sistemes de degradació cel·lular, com les vies endosomals, lisosomals i d'autofàgia (Aguado *et al*., 2010; Criado *et al*., 2012; Knecht *et al*., 2010; Puri *et al*., 2012), així com també en l'eliminació de proteïnes mal plegades a través del sistema ubiqüitina-proteasoma (Garyali *et al*., 2009; Rao *et al*., 2010). S'ha proposat, també, que les activitats d'ambdues proteïnes són protectores enfront l'estrès de reticle endoplasmàtic (Liu *et al*., 2009; Vernia *et al*., 2009) o l'estrès tèrmic (Sengupta *et al*., 2011).

Tot i que es desconeix encara avui dia el mecanisme pel qual actuen aquestes dues proteïnes en la malaltia de Lafora, s'ha pogut demostrar que estarien implicades en el metabolisme de glicogen i que la formació dels cossos tindria un paper patogènic. Així doncs, estudis recents (Duran *et al*., 2014) posen de manifest que ratolins dobles Tg deficients de malina i de GS cerebral no acumulen LBs al cervell i no mostren augment de marcadors de neurodegeneració, així com tampoc mostren canvis en les propietats

electrofisiològiques ni en la succeptibilitat a l'epilèpsia induïda per àcid kaínic observats en el model deficient de malina. Tampoc mostren deficiències en l'autofàgia, fet que sí que mostrava el model murí de la malaltia. A més a més, els animals deficients de laforina i GS tampoc presenten LBs, i les alteracions neurològiques inherents a la malaltia són rescatades en aquest model (Pederson *et al*., 2013; Turnbull *et al*., 2011, 2014). D'altra banda, en ratolins dobles Tg amb deficiència de PTG (proteïna implicada en l'activació de la GS) i deficiència de malina o de laforina, s'atura la formació dels LBs, la susceptibilitat a les convulsions i la neurodegeneració (Turnbull *et al*., 2011, 2014). En canvi, un increment de l'activitat de la GS mitjançant la sobreexpressió de PTG implica l'acumulació de glicogen i deficiències en l'autofàgia (Durant *et al*., 2014). També s'ha vist que la sobreexpressió de GS constitutivament activa en neurones de ratolí comporta l'acumulació de glicogen insoluble i neurodegeneració (Duran *et al*., 2012). Tot això indica que l'acumulació de glicogen en els LBs és un procés crucial en el desenvolupament de la malaltia. A més a més, és possible que les deficiències en l'autofàgia siguin secundàries a l'acumulació dels cossos. Com que hi ha estudis que demostren que l'autofàgia alterada pot causar neurodegeneració (Komatsu *et al*., 2006; Hara *et al*., 2006; McMahon *et al*., 2012), sembla que seria possible que un deteriorament de l'autofàgia fos el vincle entre els LBs i la neurodegeneració.

1.3. Grànuls *Periodic Acid Schiff*

L'envelliment cerebral en ratolins condueix a una sèrie de canvis morfològics i funcionals que es poden considerar el resultat de processos anormals o patològics. Un d'aquests canvis és l'aparició d'unes estructures granulars degeneratives al seu hipocamp que s'expandeixen progressivament amb l'edat. Aquestes estructures es caracteritzen per presentar una reacció positiva per a la tinció de PAS. És per aquesta raó que sovint s'han anomenat grànuls PAS.

Aquestes estructures van ser descrites inicialment per Lamar *et al*. (1976) a l'hipocamp de ratolins de la soca C57BL/6 envellits. La presència dels grànuls PAS s'ha observat extensivament a l'hipocamp de diverses soques de ratolins, però una quantitat notable de grànuls s'ha observat en la soca *senescence-accelerated mouse prone 8* (SAMP8), la qual es caracteritza per presentar un procés d'envelliment accelerat (Figura 3) (Akiyama *et al*., 1986; Del Valle *et al*., 2010; Kuo *et al*., 1996).

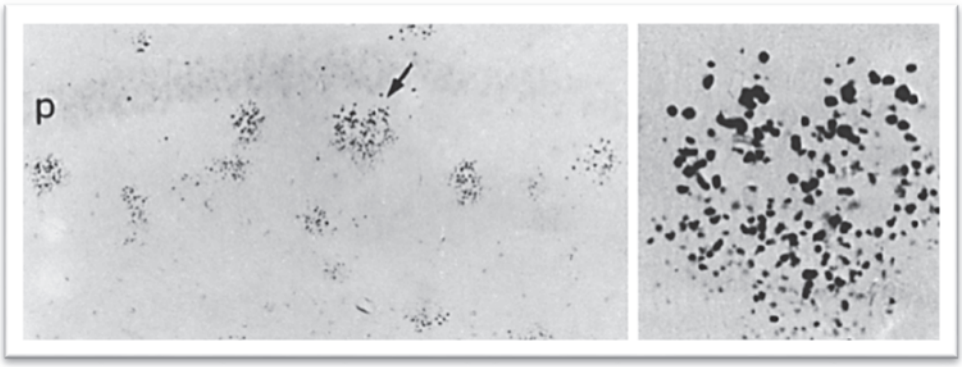

Figura 3. Gràmuls PAS a l'hipocamp d'un ratolí SAMP8 de 16 mesos d'edat tenyits amb la reacció de PAS-dimedone (Akiyama *et al*., 1986).

1.3.1. Morfologia i distribució en el sistema nerviós central

Els gràmuls PAS són unes estructures arrodonides o ovoides que es troben en el parènquima cerebral de diferents soques de ratolí. Es localitzen principalment a l'hipocamp, on apareixen primerament a l'*stratum radiatum* de la regió CA1, i des d'aquí s'estenen gradualment a altres regions i capes de l'hipocamp. Els gràmuls fan aproximadament 3 μm de diàmetre i tendeixen a agrupar-se en forma de clústers que ocupen una àrea més o menys esfèrica de 80 μm de diàmetre, cadascun dels quals conté entre 40-50 gràmuls (Akiyama *et al*., 1986; Jucker *et al*., 1994b; Kuo *et al*., 1996; Ye *et al*., 2004).

Els clústers de gràmuls s'han estudiat principalment a l'hipocamp de ratolí, tot i que també s'han trobat en altres regions. Estudis sobre la distribució topogràfica d'aquestes estructures indiquen que també es troben presents als còrtex piriforme i entorrinal, al bulb olfactori, al cerebel i al cos trapezoide (Akiyama *et al*., 1986; Jucker *et al*., 1994b ; Knuesel *et al*., 2009; Kern *et al*., 2011; Mitsuno *et al*., 1999; Robertson *et al*., 1998). Els clústers de gràmuls es troben presents en grans quantitats a les capes *stratum radiatum* i *lacunosum moleculare* de l'hipocamp, i es distribueixen al llarg de les regions CA1, CA2, CA3 i gir dentat (Nakamura *et al*., 1995). En el cerebel, els clústers es troben principalment localitzats a les capes de cèl·lules granulars i de Purkinje (Jucker *et al*., 1994b; Mitsuno *et al*., 1999). S'han descrit petites diferències morfològiques entre els clústers del cerebel i els de l'hipocamp: els del cerebel presenten un menor nombre de gràmuls per clúster i un patró més difós respecte els clústers de l'hipocamp. Tot i així, la seva morfologia i el seu patró de reactivitat indiquen que els gràmuls de cerebel i d'hipocamp són el resultat del mateix procés (Jucker *et al*., 1994b; Knuesel *et al*., 2009). Ocasionalment, en edats avançades, s'han observat gràmuls al diencèfal, al cos estriat i a l'amígdala (Jucker *et al*., 1994b; Knuesel *et al*., 2009).

En general, els resultats dels diversos estudis realitzats en quant a la distribució i progressió dels grànuls PAS en cervell mostren un mateix patró que es desenvolupa de la mateixa manera a totes les soques de ratolins. De fet, l'edat d'inici d'aparició dels grànuls i la rapidesa de proliferació dels clústers són els fets que diferencien les diverses soques de ratolins entre elles, més que la possible diferència de morfologia o localització dels grànuls.

1.3.2. Presència i cronologia en ratolins

Els grànuls PAS s'han descrit en ratolins envellits de diferents soques, i han estat extensament estudiats en els cervells de ratolins de la soca C57BL/6 (Jucker *et al.*, 1992; 1994b; Lamar *et al*., 1976; Soontornniyomkij *et al*., 2012), AKR (Mitsuno *et al*., 1999), SAMP8 i *senescence-accelerated mouse resistant-1* (SAMR1) (Akiyama *et al*., 1986; Del Valle *et al*., 2010; Kuo *et al*., 1996; Porquet *et al*., 2013). S'ha de destacar, però, que hi ha algunes soques de ratolins que presenten pocs grànuls PAS a edats avançades, com són BALB/c, DBA/2, C3H i CBA (Jucker *et al.*, 1992, 1994a, 1994b; Krass *et al*., 2003). També s'ha descrit la presència de grànuls PAS en ratolins Tg que tenen el rerefons genètic d'una soca que desenvolupa els clústers de grànuls. Alguns d'aquests ratolins Tg presenten variacions en quant a la velocitat d'aparició i a la quantitat de grànuls respecte els ratolins control, com es comenta a continuació.

A nivell cronològic, l'increment progressiu dels grànuls a l'hipocamp, al còrtex entorrinal i al còrtex piriforme s'ha associat de forma estadísticament significativa al procés d'envelliment (Madhusudan *et al*., 2009). Tot i així, a partir de certes edats es trenca la tendència acumulativa d'aquestes estructures i en edats avançades els estudis mostren un estancament del nombre de clústers, a més d'una major dispersió dels clústers de grànuls (Jucker *et al*., 1992, 1994b). En edats avançades també s'ha observat que apareix un nombre superior de grànuls de mida més gran, probablement a causa de la unió entre diversos grànuls més petits (Jucker *et al*., 1994b; Robertson *et al*., 1998). L'edat en la qual els clústers de grànuls apareixen i creixen, però, difereix en funció de la soca. Cal destacar l'inici precoç dels grànuls PAS en el ratolins SAMP8, al voltant dels 3 mesos d'edat, i el seu augment significatiu amb l'edat (Figura 4), el qual és més gran i més ràpid respecte altres soques (Del Valle *et al*., 2010; Jucker *et al*., 1994a, 1994b; Kuo *et al*., 1996). Del Valle *et al*. (2010) van comparar en un estudi el nombre de clústers de grànuls hipocampals entre les soques ICR-CD1, SAMR1 i SAMP8 des de 3 fins a 15 mesos d'edat i van observar que els ratolins SAMP8 presentaven un major increment amb l'edat del nombre de grànuls. També s'han observat diferències en l'increment del nombre de clústers de grànuls amb l'edat en alguns ratolins Tg respecte els seus

corresponents controls. Aquest és el cas dels ratolins *reeler* (Kocherhans *et al*., 2010), els ratolins triple Tg de la malaltia d'Alzheimer (Knuesel *et al*., 2009; Oddo *et al*., 2003), els ratolins TDP-43 Tg (Tsuiji *et al*., 2017), els ratolins Tg2576 (Lodeiro *et al*., 2017), els ratolins trisòmics Ts65Dn (Kern *et al*., 2011; Rachubinski *et al.*, 2012) o els ratolins deficients d'apolipoproteïna E (ApoE) (Robertson *et al*., 1998, 2000). Aquests últims comencen a desenvolupar grànuls PAS a partir de les 4-6 setmanes d'edat, convertint-se en els animals que tenen un inici més primerenc de desenvolupament d'aquestes estructures.

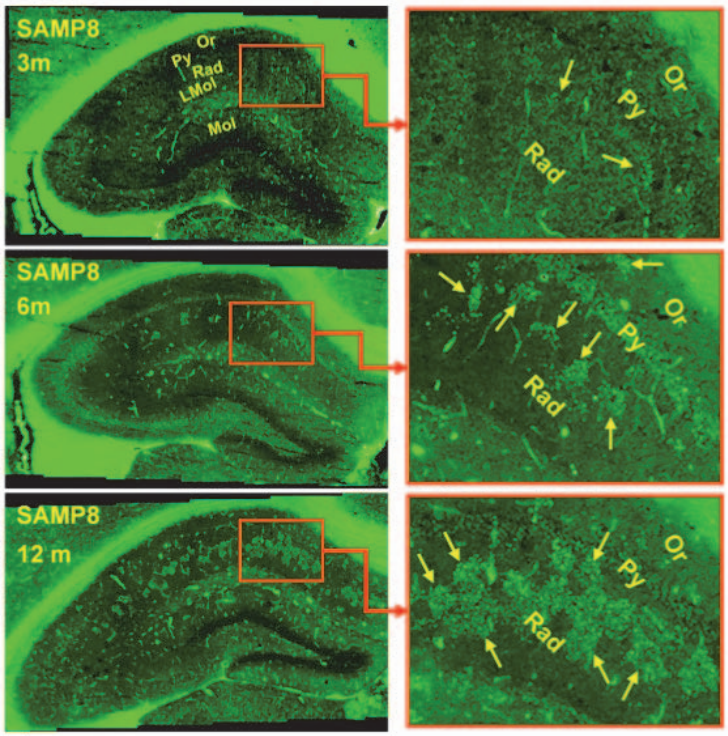

Figura 4. Clústers de grànuls PAS en seccions coronals d'hipocamp de ratolins SAMP8 de 3, 6 i 12 mesos d'edat tenyits amb un anticòs dirigit contra Aβ. Or: capa *oriens*, Py: capa *pyramidal*, Rad: *stratum radiatum*, LMol: capa *lacunosum moleculare*, Mol: capa molecular del gir dentat (Del Valle *et al*., 2010).

1.3.3. Ultraestructura

A l'anàlisi ultraestructural dels grànuls PAS s'observa una regió central fibril·lar electrodensa, que sovint està envoltada per una regió translúcida o halo. Aquest halo està delimitat per una membrana plasmàtica discontínua, fet que suggereix una localització intracel·lular del grànul (Figura 5). La regió central, que presenta una forma arrodonida o ovoide, conté estructures membranoses agregades desordenades de 5-8 nm de diàmetre que no tenen similitud amb cap orgànul cel·lular (Kuo *et al*., 1996; Manich *et al*., 2014a; Robertson *et al*., 2000). De fet, alguns orgànuls citoplasmàtics, com ara el reticle endoplasmàtic, els poliribosomes, els filaments intermedis i els mitocondris s'han trobat ocasionalment a la regió translúcida, sovint en un estat de

degeneració (Doehner *et al*., 2010; Kuo *et al*., 1996; Manich *et al*., 2014a; Mitsuno *et al*., 1999; Robertson *et al*., 1998). Aquests orgànuls s'acompanyen per unes bosses o bombolles, algunes de les quals s'originen de les invaginacions de la membrana plasmàtica, que es localitzen a la regió translúcida però estan també en contacte amb la regió central del grànul (Manich *et al*., 2014a). La membrana plasmàtica que envolta el grànul presenta unions característiques astròcit-astròcit (Kuo *et al*., 1996; Manich *et al*., 2014a). En general, el parènquima cerebral proper que envolta els grànuls madurs no presenta alteracions morfològiques. Tot i així, ocasionalment s'han observat alguns símptomes de deteriorament, com per exemple dendrites en degeneració (Manich *et al*., 2014a).

L'estudi ultrastructural dels grànuls PAS també ha permès caracteritzar aquestes estructures en estat immadur. Els grànuls immadurs presenten una regió central menys compacta, envoltada per una regió translúcida que conté estructures que formen bosses o bombolles de formes i mides irregulars. Algunes de les bosses semblen originar-se en la membrana plasmàtica que envolta el grànul, mentre que d'altres es troben en contacte amb la matriu que conforma la part central del grànul. En alguns casos, les bosses que es troben properes a la regió central semblen fragmentar-se, i els fragments membranosos semblen incorporar-se a la matriu central. En la regió translúcida també s'observen mitocòndries en degeneració, i en alguns casos, fragments de la membrana mitocondrial semblen projectar-se a la part central del grànul que s'està formant. La membrana plasmàtica dels grànuls immadurs està sovint fragmentada o és inestable, com també ho estan les membranes de les cèl·lules adjacents (Manich *et al*., 2014a).

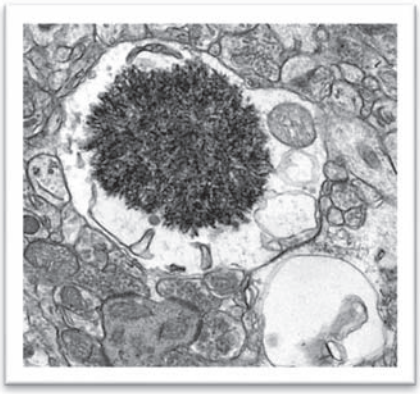

Figura 5. Ultrastructura d'un grànul PAS madur de l'hipocamp d'un ratolí SAMP8 de 14 mesos d'edat (Manich *et al*., 2014a).

1.3.4. Composició

Per estudiar la naturalesa i composició dels grànuls PAS, s'ha dut a terme un ampli ventall de tincions. Algunes d'elles es mostren a la Taula 2.

Tinció	Marcatge	Referències
Alcian blue	-	Akiyama *et al*., 1986
Bielchowsky silver	-	Lamar *et al*., 1976
Blau de toluïdina	-	Akiyama *et al*., 1986; Robertson *et al*., 1998
Blumer-PAS-dimedone	+	Akiyama *et al*., 1986
Gomori de metenamina de plata	+	Jucker *et al*., 1992; Jucker *et al*., 1994a; Jucker *et al*., 1994b
Hematoxilina-Eosina	-	Akiyama *et al*., 1986; Lamar *et al*., 1976
Iodina	+	Mitsuno *et al*., 1999
Luxol Fast blue	-	Jucker *et al*., 1992
Tinció de PAS	+	Akiyama *et al*., 1986; Jucker *et al*., 1992; Lamar *et al*., 1976; Mitsuno *et al*., 1999
Tinció de plata	+	Doehner *et al*., 2012
Tioflavina S	+ (alguns)	Doehner *et al*., 2010; Jucker *et al*., 1992; Jucker *et al*., 1994a; Jucker *et al*., 1994b; Kocherhans *et al*., 2010
Tioflavina S	-	Mandybur *et al*., 1989; Manich *et al*., 2014b; Takemura *et al*., 1993
Vermell Congo	-	Akiyama *et al*., 1986; Jucker *et al*., 1992; Jucker *et al*., 1994a; Mandybur *et al*., 1989; Mitsuno *et al*., 1999; Takemura *et al*., 1993
Vermell Congo (modificació Askanas)	+	Robertson *et al*., 1998; Robertson *et al*., 2000
Violeta de cresil	-	Jucker et al., 1992; Kern *et al*., 2011; Knuesel *et al*., 2009; Mandybur *et al*., 1989

Taula 2. Tincions histoquímiques dels grànuls cerebrals de ratolí.

Com el seu nom indica, els grànuls PAS es caracteritzen per tenyir-se positivament amb la reacció de PAS (Lamar *et al*., 1976). A més a més, altres tincions relacionades amb els glicoconjugats també tenyeixen aquestes estructures, com per exemple, la tinció de iodina (Mitsuno *et al*., 1999) o la tinció de Gomori de metenamina de plata (Jucker *et al*., 1992; 1994a; 1994b). La digestió prèvia de les seccions cerebrals amb α-amilasa o diastasa només redueixen dèbilment la tinció de PAS (Akiyama *et al*.,1986; Mitsuno *et al*., 1999).

D'altra banda, existeix certa controvèrsia pel que fa a les tincions de tioflavina S i vermell Congo. Tot i que alguns autors descriuen positivitat per a alguns grànuls amb la tinció de tioflavina S (Doehner *et al*., 2010; Jucker *et al*., 1992; 1994a; 1994b; Kocherhans *et al*., 2010), d'altres no descriuen cap marcatge positiu per als grànuls amb aquesta tinció (Mandybur *et al*., 1989; Manich *et al.*, 2014b; Takemura *et al*., 1993). En el cas de la tinció amb vermell Congo, tot i que en uns estudis s'ha descrit una reacció positiva d'alguns grànuls (Robertson *et al*., 1998; 2000), la majoria d'estudis mostren negativitat dels grànuls per a aquesta tinció (Akiyama *et al*., 1986; Jucker *et al*., 1992; 1994a; 1994b; Mandybur *et al*., 1989; Mitsuno *et al*., 1999; Takemura *et al*., 1993).

A part de les tincions, s'ha analitzat també l'activitat enzimàtica de la monoamino oxidasa (MAO)-B en els grànuls PAS de l'hipocamp de ratolins SAMP8 envellits (Nakamura *et al.,* 1995), i s'ha vist que presenten una reactivitat positiva.

Els marcatges immunohistoquímics realitzats en talls histològics i seccions ultrafines han estat àmpliament utilitzats per descriure la presència de determinats components dels grànuls PAS. Així doncs, en concordança amb la reactivitat PAS positiva, s'han detectat glicoproteïnes i proteoglicans (Akiyama *et al*., 1986; Kuo *et al*., 1996; Takemura *et al*., 1993), així com també proteïnes de matriu extracel·lular, com l'heparan sulfat proteoglicà, la laminina (Jucker *et al*., 1992; Jucker *et al*., 1994b; Kuo *et al*., 1996), el *syndecan*-2 (Manich *et al*., 2011) o la reelina (Knuesel *et al*., 2009).

Mitjançant estudis immunohistoquímics, també s'han detectat als grànuls PAS algunes proteïnes involucrades en malalties neurodegeneratives, com el pèptid Aβ (Del Valle *et al*., 2010; Doehner *et al*., 2012; Knuesel *et al*., 2009; Oddo *et al*., 2003; Robertson *et al*., 1998; Wirak *et al*., 1991), la ubiqüitina (Robertson *et al*., 1998; Soontornniyomkij *et al*., 2012; Tsuiji *et al*., 2017), l'α-sinucleïna (Krass *et al*., 2003) i la proteïna tau (Kern *et al*., 2011; Manich *et al*., 2011; Rachubinski *et al*., 2012), així com també s'hi ha descrit la presència de MAP2, NeuN (Manich *et al*., 2011), p62, calretinina, parvalbúmina (Tsuiji *et al*., 2017) i S100A8 (Lodeiro *et al*., 2017).

Tot i que aquests resultats suggereixen que els grànuls PAS podrien presentar certa concordança amb diferents lesions cerebrals observades en malalties neurodegeneratives i permeten postular un origen neuronal d'aquestes estructures, un estudi posterior (Manich *et al*., 2014b) va descartar la presència d'alguns d'aquests components en comprovar que el marcatge d'aquestes proteïnes no era específic.

1.3.5. Presència de neo-epítops

Manich *et al*. (2014b) van descriure la presència d'uns epítops en els grànuls PAS que no es trobaven en altres zones cerebrals i es formaven durant el procés de formació dels grànuls (Manich *et al*., 2014a), fet que els va permetre concloure que eren neo-epítops. Aquests neo-epítops eren reconeguts per immunoglobulines (Ig) de l'isotip IgM.

Estudis ultrastructurals van permetre determinar que els neo-epítops es troben localitzats en la regió central dels grànuls, específicament en els fragments membranosos. Tot i així, alguns d'ells s'observen en la membrana plasmàtica dels processos astrocítics i en les membranes de les estructures més properes al neuropil. Els neo-epítops s'observen de manera similar en les mateixes àrees en els grànuls immadurs i en la matriu dispersa de la regió central (Manich *et al*., 2014a).

Aquests neo-epítops són els responsables de falsos marcatges positius d'aquestes estructures quan es duen a terme estudis immunohistoquímics perquè les IgMs que els reconeixen es troben com a contaminants en molts anticossos comercials. Gràcies a aquest estudi, es va descartar la presència de la proteïna tau i el pèptid Aβ en els grànuls PAS (Manich *et al*. 2014b).

1.3.6. Origen cel·lular

Existeix controvèrsia respecte l'origen cel·lular dels grànuls PAS. Alguns treballs han apuntat a un possible origen astrocític mentre que d'altres a un possible origen neuronal.

L'origen neuronal dels grànuls PAS ha estat postulat en base a l'observació de vesícules i contactes sinàptics amb la membrana plasmàtica dels grànuls (Mitsuno *et al*., 1999), la localització de grànuls en terminals presinàptics o postsinàptics anòmals (Irino *et al*., 1994), o la presència de grànuls interconnectats en processos neuronals identificats com a dendrites (Doehner *et al*., 2012; Wirak *et al*., 1991). L'origen neuronal també ha estat postulat per la descripció de components neuronals en aquestes estructures. Posteriorment, però, com s'ha comentat en l'apartat anterior, s'ha demostrat que alguns d'aquests components no es troben realment en els grànuls PAS (Manich *et al*., 2014b).

S'ha observat que existeix una relació molt estreta entre els grànuls PAS i els astròcits. En estudis de microscòpia electrònica s'han localitzat grànuls PAS en els cossos cel·lulars i especialment en els processos astrocítics d'astròcits protoplàsmics expandits (Robertson *et al.,* 1998). A més a més, s'ha vist que entre el 60-80 % dels grànuls PAS estan associats a processos astrocítics GFAP-positius (Akiyama *et al*., 1986; Jucker *et*

al., 1994b; Madhusudan *et al*., 2009; Nakamura *et al*., 1995), i s'han descrit clústers de grànuls sencers associats directament amb astròcits GFAP-positius, fins i tot amb una situació astrocítica del nucli central respecte el clúster de grànuls (Jucker *et al*., 1994b; Manich *et al*., 2014a; Nakamura *et al*., 1995). Estudis ultraestructurals han permès identificar grànuls madurs en processos astrocítics degeneratius que contenen acumulacions de glicogen, fibril·les GFAP-positives i unions astròcit-astròcit específiques amb membranes adjacents (Kuo *et al*., 1996; Manich *et al*., 2014a). S'ha trobat que els grànuls immadurs sempre s'originen en astròcits i la formació dels grànuls en els diferents processos d'un astròcit específic causa el patró de clúster dels grànuls PAS. Així doncs, cada agrupació de grànuls que forma el clúster està formada per un mateix astròcit (Manich *et al*., 2014a). També s'ha vist que els grànuls PAS s'associen en alguns casos amb capil·lars sanguinis i estan situats en els astròcits que els envolten (Doehner *et al*., 2010; Manich *et al*., 2014a; Robertson *et al*., 1998 Ye *et al*., 2004).

Així doncs, en conjunt, els resultats publicats fins a l'actualitat reforcen l'origen astrocític dels grànuls PAS, més que l'origen neuronal.

1.3.7. Significat fisiopatològic

Malgrat que s'ha realitzat un ampli ventall d'estudis sobre els grànuls PAS i el seu desenvolupament en diverses soques de ratolins, les diferents interpretacions sobre el significat fisiopatològic d'aquestes estructures són quasi tan nombroses com els treballs que les estudien.

En múltiples ocasions, els grànuls s'han interpretat com a agregats amiloides (Del Valle *et al*., 2010; Doehner *et al*., 2010; Robertson *et al*., 2000; Wirak *et al*., 1991), a causa dels marcatges produïts amb anticossos dirigits contra diferents fragments del pèptid Aβ, així com també per les tincions de vermell Congo o tioflavina S. Tot i així, aquesta interpretació s'ha descartat finalment després d'observar que els marcatges immunohistoquímics eren falsos marcatges positius (Manich *et al*., 2014b), així com també després que alguns autors no van poder reproduir els resultats obtinguts en les tincions (Akiyama *et al*., 1986; Jucker *et al*., 1992; 1994a; 1994b; Mandybur *et al*., 1989; Manich *et al*., 2014b; Takemura *et al*., 1993). De la mateixa manera, la reactivitat dels grànuls PAS en marcatges immunohistoquímics realitzats amb anticossos dirigits contra la proteïna tau ha afavorit la interpretació dels grànuls PAS com a lesions pròpies de taupaties (Kern *et al*., 2011; Krass *et al*., 2003; Manich *et al*., 2011), però, com en el cas anterior, aquesta interpretació ha estat descartada (Manich *et al*., 2014b).

Diferents treballs han associat els grànuls PAS de ratolí amb els CA humans (Jucker *et al*., 1992; 1994a; 1994b; Jucker i Ingram, 1994; Mitsuno *et al*., 1999; Robertson *et al*., 1998; Sinadinos *et al*., 2014). La seva tinció PAS positiva i el seu increment durant l'envelliment són dues de les principals característiques compartides per ambdues estructures. Tot i així, existeixen algunes característiques, com la distribució cerebral o algunes reaccions histoquímiques, que difereixen.

D'altra banda, Soontornniyomkij *et al*., (2012) van concloure que les estructures hipocampals observades en ratolins ICR-CD1 envellits corresponien a autofagosomes formats com a conseqüència d'una ineficiència en l'aclariment de les acumulacions proteiques i l'alteració de la proteòstasi associada a l'augment de l'edat. Cal remarcar que aquesta interpretació es va fer en base a estudis immunohistoquímics amb diferents marcadors d'autofàgia sense tenir en compte els falsos marcatges positius que se'n poden derivar a causa de la presència dels neo-epítops en els grànuls.

Un altre grup d'estudis ha hipotetitzat que els grànuls PAS són dipòsits de reelina extruïts per neurones envellides i fagocitats per cèl·lules glials degut a la disfunció dels sistemes d'eliminació del proteasoma i l'autofagosoma, procés que esdevindria paral·lel a la pèrdua de reelina neuronal (Doehner *et al*., 2010, 2012; Knuesel *et al*., 2009; Kocherhans *et al*., 2010; Madhusudan *et al*., 2009). La presència de reelina en els grànuls, però, va ser detectada mitjançant anticossos anti-reelina, els quals podrien estar contaminats amb IgMs i donar lloc a falsos marcatges positius.

Estudis recents (Lodeiro *et al*., 2017) conclouen que els grànuls PAS són agregats extracel·lulars que es formen prèviament a la formació dels dipòsits d'Aβ i constitueixen un procés inflamatori previ al desenvolupament de la malaltia. De nou, aquestes conclusions s'extreuen en base al marcatge dels grànuls amb anticossos dirigits contra la proteïna S100A8, sense considerar els possibles falsos marcatges positius.

Així doncs, l'establiment de la presència de neo-epítops en les estructures granulars (Manich *et al*., 2014b) posa en dubte algunes hipòtesis, explica algunes controvèrsies generades i obre un nou camí cap a l'estudi del seu significat fisiopatològic.

2. ANTICOSSOS NATURALS

Els anticossos presents a l'organisme sense necessitat d'una infecció prèvia o d'una immunització deliberada s'anomenen anticossos naturals (ANs). Una proporció significativa d'aquests anticossos, els anomenats autoanticossos naturals (AANs), actua reconeixent components del propi organisme. Els AANs poden intervenir en el manteniment de l'homeòstasi de l'organisme a través de diferents funcions, com l'eliminació de cèl·lules alterades o la modulació del sistema immunitari. Aquestes funcions reguladores permeten que els AANs actuïn beneficiosament en diferents situacions patològiques, com ara l'aterosclerosi o el càncer (Lutz *et al*., 2009).

2.1. Origen

Els limfòcits o cèl·lules B1, que es subdivideixen en cèl·lules B1a, les quals són CD5+, i cèl·lules B1b, les quals són CD5-, han tingut molta rellevància durant els últims anys a causa principalment de les seves característiques especials. Aquestes cèl·lules resideixen en la cavitat pleural i peritoneal i es caracteritzen per tenir una vida llarga i autorenovar-se. Les cèl·lules B1a i B1b tenen diferents funcions: les cèl·lules B1a són la font principal d'ANs, mentre que els anticossos produïts per les cèl·lules B1b són induïts per l'exposició a antígens foranis (Duan i Morel, 2006; Montecino-Rodriguez i Dorshkind, 2006). Es pot assumir, doncs, que els AANs són originats per limfòcits B1a.

2.2. Característiques

Els AANs constitueixen una proporció important dels anticossos sèrics (Dighiero *et al*., 1983; Wardemann *et al*., 2003). Es caracteritzen per trobar-se presents a la sang de cordó umbilical de nounats (Merbl *et al*., 2007) i de ratolins nounats (Dighiero *et al*., 1985), així com també en ratolins mantinguts en condicions lliures de gèrmens i alimentats amb dietes lliures d'antígens (Hooijkaas *et al*., 1984). Els AANs es troben conservats evolutivament: han estat descrits en tots els vertebrats amb mandíbula, des de peixos cartilaginosos fins a amfibis, ocells i mamífers (Gonzalez *et al*., 1988; Flajnik i Rumfelt, 2000). La majoria d'AANs són de l'isotip IgM, però també s'han descrit AANs dels isotips IgG i IgA (Avrameas *et al*., 2007).

Poc després que Avrameas a França i Notkins a Regne Unit establissin l'existència dels AANs, es va produir un progrés constant en la seva caracterització pel que fa a aspectes d'especificitat, afinitat i configuració genètica (Avrameas, 1991; Notkins, 2004). La majoria dels AANs caracteritzats fins ara són polireactius, ja que són capaços de reconèixer diferents antígens, ja siguin antígens propis, o fins i tot antígens foranis. Cada

AAN té la capacitat d'unir-se a múltiples antígens que no estan relacionats estructuralment com per exemple proteïnes, polisacàrids, nucleòtids i fosfolípids (Notkins, 2004). Les capacitats d'unió a l'antigen dels AANs són més sensibles als canvis de temperatura o al tractament amb agents dissociatius que la dels anticossos monoreactius. Aquest fet suggereix que el paratop dels AANs és més plàstic que el dels anticossos monoreactius (Avrameas *et al*., 2007; Casali i Schettino, 1996). S'ha demostrat que un estat conformacional determinat del paratop de l'AAN es pot unir a epítops diferents en llocs espacialment diferents en la regió de combinació amb l'antigen (Mariuzza, 2006; Sethi *et al*., 2006). Polireactivitat no significa manca d'especificitat: cada AAN presenta el seu propi conjunt d'especificitats epitòpiques, i per tant, és únic.

Cal tenir en compte que els AANs són diferents dels autoanticossos associats a malalties autoimmunitàries. Els autoanticossos associats a malalties autoimmunitàries són monoreactius, presenten elevada afinitat i són mutats somàticament. La principal diferència estructural entre autoanticossos monoreactius associats a malalties autoimmunitàries i AANs polireactius resideix en la tercera regió hipervariable (CDR3) del domini variable de la cadena pesada (VH). L'anàlisi estructural dels anticossos ha demostrat que la regió CDR3 del VH forma el centre físic del lloc d'unió de molts anticossos, i és la regió que té el grau més alt de variació en la composició d'aminoàcids i longitud. Per tant, és probable que la regió CDR3 del VH jugui el paper més important en la determinació de la poli/auto reactivitat dels AANs (Mannoor *et al*., 2013).

Tenint en compte que l'avidesa és la força d'unió global entre l'anticòs i l'antigen, publicacions inicials descriuen els AANs com a molècules de baixa afinitat i elevada avidesa per als antígens propis (Casali i Notkins, 1989; Ternynck i Avrameas, 1986). La noció que un anticòs ha de ser d'elevada afinitat per tal de ser biològicament rellevant s'origina principalment a partir de l'anàlisi dels requisits per a una resposta immunològica eficient contra els patògens. Aquest concepte no s'aplica necessàriament als AANs, ja que, malgrat la baixa afinitat, presenten una elevada avidesa. A més, la reacció d'unió monovalent d'un anticòs pot ser de baixa afinitat mentre que la unió multivalent pot ser d'una elevada avidesa (Avrameas i Ternynck, 1995) i la rellevància biològica de la interacció antigen-anticòs depèn de la concentració local d'antigen i anticòs, tant com de les pròpies característiques d'unió de la molècula d'anticòs (Lacroix-Desmazes *et al*., 1998).

La connectivitat caracteritza el grau en que les regions variables dels anticossos interactuen amb les regions variables de les Ig sèriques i amb les regions variables dels receptors antigènics dels limfòcits. Els AANs han demostrat expressar graus més

elevats de connectivitat que els anticossos generats per la immunitat desencadenada per un antigen forani (Lacroix-Desmazes *et al*., 1998).

L'anàlisi dels gens de la regió variable dels AANs, dels anticossos induïts per antígens i dels anticossos associats a malalties autoimmunitàries ha permès conèixer algunes característiques estructurals dels respectius llocs d'unió a l'antigen. La majoria dels AANs es codifiquen directament pels gens de la línea germinal i no se sotmeten pràcticament a cap mutació somàtica (Chen *et al*., 1991; Lacroix-Desmazes *et al*., 1998).

2.3. Funcions

Els ANs tenen funcions immunològiques importants i diverses (Figura 6). Així, proporcionen protecció immunitària innata quan actuen, per exemple, com a primera línia de defensa contra diferents patògens. Poden actuar, també, en el manteniment de l'homeòstasi tissular quan participen, per exemple, en l'eliminació de cèl·lules apoptòtiques mitjançant el reconeixement d'estructures pròpies (és quan són referits com AANs) (Wootla *et al*., 2015). En molts casos, aquestes estructures pròpies representen neo-estructures alterades o induïdes per l'estrès que es generen durant diversos processos biològics. Aquesta propietat permet que els AANs reconeguin i identifiquin selectivament substàncies alterades, les quals contenen diverses *eat-me tags* que són reconegudes pels AANs. Així doncs, els AANs intervenen en funcions d'homeòstasi facilitant l'eliminació de cèl·lules alterades i restes cel·lulars. Aquesta funció és important perquè una acumulació excessiva de restes cel·lulars pot activar respostes immunitàries adaptatives i desencadenar autoimmunitat (Lutz *et al*., 2009).

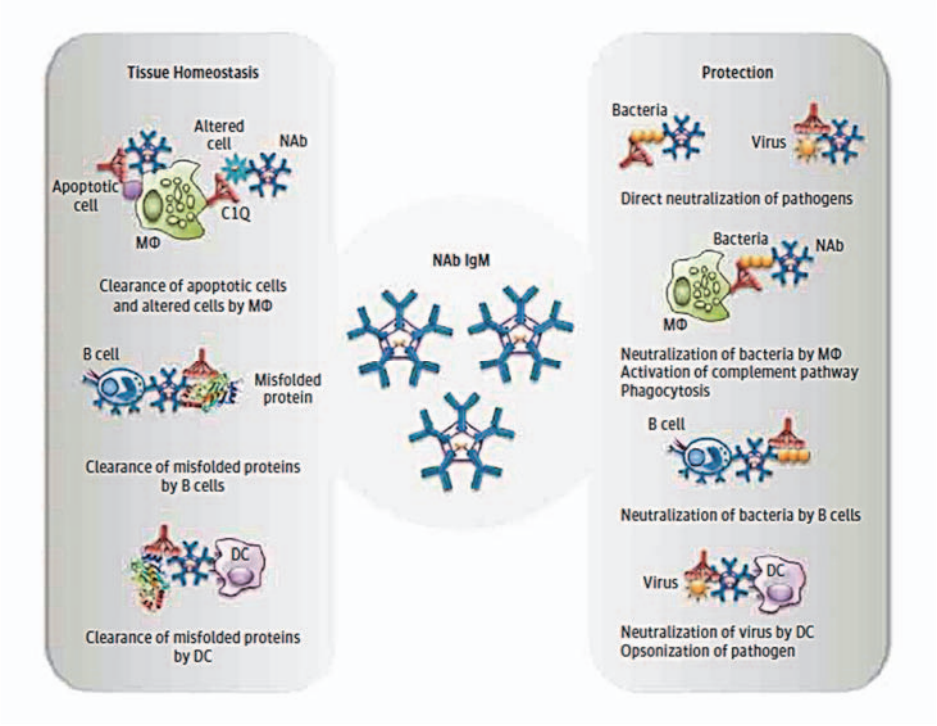

Figura 6. Funcions dels ANs (Wootla *et al*., 2015).

2.3.1. Eliminació d'estructures danyades per oxidació

L'aparició d'epítops específics d'oxidació representa un exemple prominent d'estructures pròpies alterades induïdes per estrès, ja que són generats de manera ubiqua com a conseqüència de la peroxidació de lípids durant diverses situacions fisiològiques i patològiques, i es troben també presents a les membranes de cèl·lules apoptòtiques. Aquests epítops específics d'oxidació confereixen una diana dels AANs, fet que indica un paper important dels AANs en la seva eliminació i en la neutralització de les seves propietats proinflamatòries (Binder, 2010).

La peroxidació de fosfolípids, procés complex en el qual l'oxigen molecular reacciona amb els lípids, provoca la generació d'un gran nombre de productes lipídics peroxidats altament reactius que poden modificar proteïnes i lípids, i que a la vegada formen estructures alterades. Molts d'aquests lípids oxidats tenen propietats proinflamatòries i s'ha demostrat que alguns d'ells poden ser reconeguts per una part del sistema immunitari innat. Per tal d'assenyalar la seva naturalesa antigènica, aquestes estructures han estat denominades epítops específics d'oxidació. La presència dels fosfolípids a les membranes cel·lulars i a les partícules de lipoproteïnes permet la generació d'epítops específics d'oxidació per múltiples mecanismes oxidatius

involucrats en processos fisiològics i en diverses malalties inflamatòries en les que la peroxidació de lípids s'accelera en gran mesura (Binder, 2010; Leibundgut *et al*., 2013).

Una de les patologies on s'exemplifica aquest fenomen és l'aterosclerosi. L'aterosclerosi és una malaltia inflamatòria crònica de les parets vasculars, i és la causa subjacent dels atacs de cor i de la majoria dels accidents cerebrovasculars. És una malaltia prototípica de l'increment de l'estrés oxidatiu amb una patogènesis complexa que està influenciada per diverses variables. Un dels principals factors que contribueixen al desenvolupament de les lesions ateroscleròtiques és un augment dels nivells de les lipoproteïnes de baixa densitat (LDL). L'oxidació de les LDL en la túnica íntima dels vasos és un dels esdeveniments iniciadors de l'aterosclerosi (Miller *et al*., 2011; Palinski *et al*., 1989; Weismann i Binder, 2012).

Quan la fosfatidilcolina (PC), present en partícules o cèl·lules, s'oxida, es formen productes altament reactius, com el malondialdehid, el 4-hidroxinonenal o el 1-palmitoil-2-(-oxovaleroil)-*sn*-glicero-3-fosfatidilcolina. Aquests aldehids formen adductes covalents amb els grups amino de les proteïnes i els lípids i s'ha demostrat que poden ser reconeguts per AANs específics (Figura 7) (Binder *et al*., 2005; Faria-Neto *et al*., 2006; Horkko *et al*., 1999; Lutz *et al*., 2009).

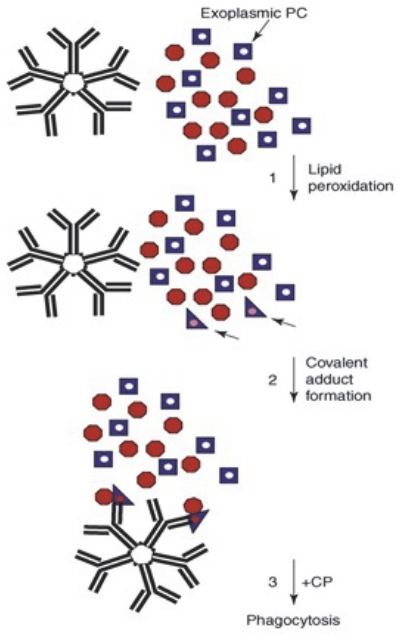

Figura 7. Interacció dels AANs de l'isotip IgM amb epítops específics d'oxidació de cèl·lules i partícules. Un parell de molècules de PC amb el cap de la fosforilcolina ocult (rectangles blaus amb punt blanc) se sotmeten a la peroxidació lipídica i exposen aldehids reactius (els rectangles blaus esdevenen triangles amb el cap de la fosforilcolina parcialment alterat). Algunes proteïnes (cercle vermell) reaccionen covalentment amb els grups aldehids dels fosfolípids oxidats i així generen neo-antígens en que el cap de la fosforilcolina queda exposat (punt vermell en el triangle). La unió multivalent de l'autoanticòs IgM al residu de fosforilcolina activa la via clàssica del sistema complement de manera suficient per opsonitzar les partícules per dur a terme una eliminació eficient produïda pels fagòcits (Lutz *et al*., 2009).

2.3.2. Eliminació de cèl·lules apoptòtiques o restes cel·lulars

L'eliminació de restes cel·lulars pot ser induïda per una varietat de molècules, però els AANs proporcionen un medi addicional d'eliminació. Aquesta funció dels AANs permet prevenir els efectes adversos derivats de l'acumulació de restes cel·lulars que podrien desencadenar la resposta immune adaptativa i acabar culminant en alguna malaltia autoimmunitària.

L'apoptosi és un mecanisme per a l'eliminació cel·lular. Com a tal, condueix a la inactivació de l'aparell de replicació de la cèl·lula i a la seva mort programada. També involucra canvis en la superfície de la cèl·lula que condueixen al seu reconeixement i eliminació final (Gardai i Bratton, 2006). Una cèl·lula apoptòtica pot ser identificada per la seva morfologia i pels canvis associats a la seva membrana, com la condensació de la cromatina, la condensació citoplasmàtica, la fragmentació nuclear, el moviment de fosfolípids a la membrana, i la formació de protuberàncies o vesícules a la superfície de la cèl·lula. Els fagòcits poden internalitzar la cèl·lula sencera o les vesícules. Els fosfolípids com la fosfatidilserina envolten la membrana cel·lular com a resultat de la finalització de la funció de l'aminofosfolipid translocasa, l'enzim responsable de restringir la fosfatidilserina a la capa interna de la membrana cel·lular (Litvack i Palaniyar, 2010). Està ben documentat que aquesta exposició de la fosfatidilserina cap a l'exterior de la cèl·lula apoptòtica millora la seva capacitat de ser fagocitada (Gardai i Bratton, 2006). A més a més de l'exposició de la fosfatidilserina en les cèl·lules apoptòtiques, s'exposen també altres molècules com lisofosfolípids, àcid fosfatídic, cardiolipina, aminosucres, manosa i molècules d'adhesió. Durant les últimes etapes de l'apoptosi, quan la membrana cel·lular és més permeable, la PC és hidrolitzada per la fosfolipasa A2 calci-independent i la resultant lisofosfatildilcolina (LPC) queda exposada a la membrana i esdevé una diana dels AANs (Figura 8) (Kim *et al*., 2002).

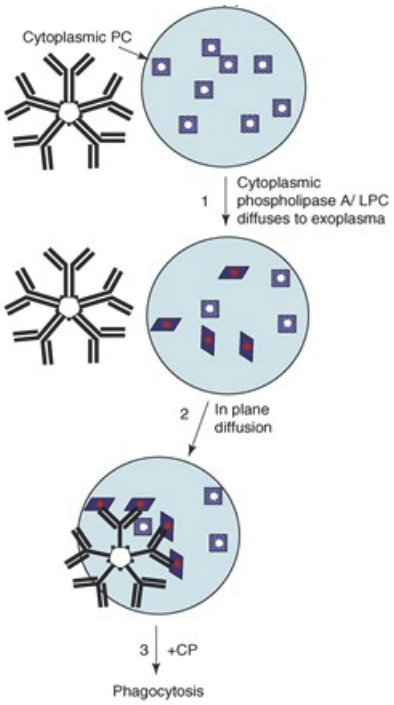

Figura 8. Reconeixement de cèl·lules apoptòtiques per part dels AANs de l'isotip IgM. Algunes molècules de PC són hidrolitzades per la fosfolipasa A2 a LPC que difon ràpidament al costat exoplàsmic i exposa el seu cap de fosforilcolina (els quadres blaus esdevenen rombes i exposen la fosforilcolina exoplàsmica representada amb un punt vermell). Les IgMs s'uneixen a la LPC i promouen l'activació de la via clàssica del sistema complement per opsonitzar les cèl·lules i dur a terme una eliminació eficient mitjançada per fagòcits (Lutz *et al*., 2009).

2.3.3. Altres funcions

Les cèl·lules tumorals sovint es caracteritzen pels canvis que es produeixen en l'expressió de certes proteïnes i pels canvis del patró de glicosilació d'aquestes. Els canvis que es produeixen en aquest tipus de cèl·lules proporcionen una major supervivència del tumor, que permeten, per exemple, la suspensió del control del creixement, un major potencial metastàsic o escapar de la vigilància del sistema immunitari. Sota certes circumstàncies, però, els carbohidrats antigènics de glicolípids i glicoproteïnes de les cèl·lules tumorals poden esdevenir un altre patró de reconeixement per als AANs. Així doncs, s'ha evidenciat que els AANs, presents en individus sans, tenen la capacitat d'unir-se a carbohidrats antigènics de diferents cèl·lules tumorals i produir la mort d'aquestes. Per tant, aquests anticossos podrien jugar un paper important en el sistema de vigilància tumoral i esdevenir futures estratègies immunoterapèutiques (Schwartz-Albiez, 2012; Schwartz-Albiez *et al*,, 2008; Vollmers i Brandlein, 2007).

II. OBJECTIUS

Aquesta tesi està estructurada en una sèrie de treballs encadenats en els quals alguns dels objectius concrets s'han plantejat de manera seqüencial tenint en compte els resultats i les conclusions que s'anaven obtenint. Els objectius concrets s'agrupen en dos grans objectius generals.

L'objectiu general primer és completar els estudis previs sobre els grànuls PAS presents en l'hipocamp de ratolí, determinant si les IgMs que reconeixen els neo-epítops presents en aquestes estructures són AANs. Aquest fet posaria de manifest una relació important entre aquestes estructures degeneratives i el sistema immunitari innat.

L'objectiu general segon és estudiar si la presència de neo-epítops en els grànuls PAS del cervell de ratolí és un fet exclusiu d'aquest tipus de PGBs o és un fet generalitzable a altres PGBs cerebrals, com els CA del cervell humà o els LBs. Per abordar aquest segon objectiu general, s'estudiarà la presència de neo-epítops en els CA presents en cervell humà en situacions d'envelliment i en la malaltia d'Alzheimer, així com també en els LBs que apareixen en el cervell d'un model murí de la malaltia de Lafora.

Conjuntament, l'abordatge d'aquests objectius generals donarà una nova visió sobre els PGBs i permetrà avançar en el coneixement sobre l'origen, la composició i la funció dels diferents tipus de PGBs que apareixen en el cervell.

Els objectius concrets que se'n deriven són els següents:

1. Determinar si les IgMs que reconeixen els neo-epítops presents en els grànuls PAS de l'hipocamp cerebral de ratolí són AANs.

2. Estudiar la presència de neo-epítops en els CA del cervell humà i en cas afirmatiu, estudiar la localització dels neo-epítops en aquests cossos.

3. Avaluar la presència d'ANs que puguin reconèixer els neo-epítops presents en els CA cerebrals humans.

4. Estudiar la ultraestructura dels CA presents en hipocamp humà tant en l'inici de la seva formació com en els estadis més avançats.

5. Comparar la ultraestructura dels CA humans amb la dels grànuls PAS de ratolí.

6. Estudiar la composició dels CA de l'hipocamp humà.

7. Determinar els tipus de PGBs que apareixen en un model murí de la malaltia de Lafora, concretament ratolins deficients de malina.

8. Estudiar si els PGBs dels ratolins deficients de malina estan associats a determinats tipus cel·lulars.

9. Estudiar la presència de neo-epítops en els cossos que apareixen en el model murí de la malaltia de Lafora.

10. Elucidar el paper de la glicogen sintasa en el desenvolupament dels PGBs i en la presència dels neo-epítops utilitzant ratolins deficients d'aquest enzim i ratolins que sobreexpressen la PTG.

III. RESULTATS

ARTICLE 1

NEO-EPITOPES EMERGING IN THE DEGENERATIVE HIPPOCAMPAL GRANULES OF AGED MICE CAN BE RECOGNIZED BY NATURAL IgM AUTO-ANTIBODIES

Gemma Manich, Elisabet Augé, Itsaso Cabezón, Mercè Pallàs, Jordi Vilaplana i Carme Pelegrí

Immunity & Ageing 2015; 12:23
DOI: 10.1186/s12979-015-0050-z

RESUM

Objectius: En aquest treball es pretén determinar si les IgMs que reconeixen els neo-epítops presents en els grànuls PAS de l'hipocamp de ratolí, i que es troben com a contaminants en diversos anticossos comercials, són AANs. Tenint en compte que els AANs s'originen de manera natural, ja en les primeres etapes de la vida, sense necessitat de cap contacte previ amb antígens externs, i que són interespecífics, l'objectiu és demostrar la presència d'aquests anticossos en el sèrum de ratolins, independentment de la seva edat, de l'exposició prèvia a patògens o de la presència de grànuls en el seu hipocamp, així com també determinar la seva presència en el sèrum d'altres espècies animals.

Material i mètodes: Es van utilitzar ratolins mascle SAMP8, ICR-CD1 i BALB/C de diferents edats (1-9 mesos d'edat) i ratolins mascle ICR-CD1 i BALB/C mantinguts en condicions *specific and opportunistic pathogen-free* (SOPF) de 3 mesos d'edat. Per a cada grup es van utilitzar entre 4 i 6 animals. Els animals es van anestesiar i se'n va obtenir sang per punció cardíaca, de la qual se'n va obtenir posteriorment el sèrum que es va congelar a -80ºC. Després de la punció cardíaca, els animals es van perfondre amb sèrum fisiològic i es va procedir a l'extracció del seu encèfal, que es va congelar en isopentà i es va guardar a -80ºC. Es van realitzar seccions criostàtiques de la zona central de l'hipocamp que es van fixar amb acetona i es van congelar a -20ºC. També es van realitzar seccions criostàtiques de cervells de ratolins ICR-CD1 de 12-15 mesos d'edat que es van obtenir seguint el procediment comentat anteriorment, però sense realitzar la punció cardíaca. Es van realitzar diferents assaigs immunohistoquímics utilitzant els diferents sèrums obtinguts, així com també sèrums de rata, conill i cabra, com a anticossos primaris. Les mostres es van analitzar per microscòpia de fluorescència.

Resultats: Els assaigs immunohistoquímics duts a terme amb els sèrums de ratolí de diferents soques i edats i d'animals SOPF i amb els sèrums d'altres espècies animals sobre seccions cerebrals de ratolins ICR-CD1 de 12-15 mesos d'edat van mostrar en tots els casos un marcatge positiu dels grànuls PAS quan s'utilitzen anticossos secundaris dirigits específicament contra les IgMs de les espècies corresponents. També es van realitzar immunomarcatges amb els sèrums dels diferents ratolins sobre les seves pròpies seccions cerebrals, i aquests també van mostrar un marcatge positiu per als grànuls PAS, sempre i quan l'animal tingués aquestes estructures en el seu hipocamp. Aquests resultats indiquen que tots els sèrums avaluats contenen IgMs que reconeixen els neo-epítops presents en els grànuls PAS cerebrals de ratolí.

Conclusions: El present treball mostra que els neo-epítops presents en els grànuls PAS de cervell de ratolí són reconeguts per IgMs que són AANs. Són anticossos que es troben presents en el sèrum de ratolí de diferents soques i edats, independentment de la presència de grànuls en el seu hipocamp, i també en el sèrum de ratolins mantinguts en condicions SOPF i en el sèrum d'altres espècies animals. Aquest fet posa de manifest una possible interacció entre el sistema immunitari innat i els grànuls PAS de ratolí.

Aquest treball és l'últim d'una primera sèrie d'estudis sobre els grànuls PAS de ratolí. Agrupant tota aquesta informació s'ha realitzat el següent article de revisió:

PERIODIC ACID-SCHIFF GRANULES IN THE BRAIN OF AGED MICE: FROM AMYLOID AGGREGATES TO DEGENERATIVE STRUCTURES CONTAINING NEO-EPITOPES

Gemma Manich, Itsaso Cabezón, Elisabet Augé, Carme Pelegrí i Jordi Vilaplana

Ageing Research Reviews 2016; 27: 42-55
DOI: 10.1016/j.arr.2016.03.001

Aquest article de revisió es troba a l'Annex de la present tesi.

Manich et al. Immunity & Ageing (2015) 12:23
DOI 10.1186/s12979-015-0050-z

Immunity & Ageing

SHORT REPORT Open Access

Neo-epitopes emerging in the degenerative hippocampal granules of aged mice can be recognized by natural IgM auto-antibodies

Gemma Manich[1], Elisabet Augé[1], Itsaso Cabezón[1,2], Mercè Pallàs[2,3], Jordi Vilaplana[1,3*] and Carme Pelegrí[1,3]

Abstract

Background: Degenerative granular structures appear progressively with age in the hippocampus of most mouse strains. We recently reported that these granules contain a neo-epitope that is recognised by IgM antibodies present as contaminants in many commercial antibodies obtained from mouse ascites and mouse or rabbit serum. We hypothesise that these anti-neo-epitope IgMs are in fact natural auto-antibodies that are generated spontaneously during the foetal stage without previous contact with external antigens and whose repertoire and reactivity pattern have been determined through evolution, being remarkably stable within species and even between species.

Findings: In the present work we found that mice from the ICR-CD1, BALB/C and SAMP8 strains have anti-neo-epitope IgM antibodies in their plasma at all ages tested and even when maintained under specific opportunistic pathogen-free conditions. Moreover, we determined that these anti-neo-epitope IgMs are also present in rabbit, goat and rat serum. We also found that, in each mouse that presented hippocampal granules, the anti-neo-epitope IgMs contained in its plasma recognised the neo-epitopes in its own granules.

Conclusions: This study led to the conclusion that anti-neo-epitope IgMs are widespread natural auto-antibodies contained in the plasma of mice and other species. The presence of these natural auto-antibodies not only explains why they are frequently found as contaminants in commercial antibodies, but also paves the way for a new approach to a treatment and diagnosis of pathological brain processes based on natural IgMs and neo-epitopes.

Keywords: Ageing, Hippocampus, Auto-antibody, IgM, Neo-epitope, Periodic acid-Schiff

Findings

Introduction

Pathological granular structures, originally described as periodic acid-Schiff granules due to their reactivity to this staining, appear progressively with age in the hippocampus of most mouse strains, especially in the senescence-accelerated mouse prone 8 (SAMP8) strain [1–4]. They are round-to-ovoid structures that measure up to 3 μm in diameter and tend to form clusters, each with approximately 40–50 granules [1, 4, 5]. The ultrastructural analysis of the granules showed a central electron-dense core formed by an accumulation of membranous fragments and a peripheral zone, or halo, externally delimited by a slightly discontinuous plasma membrane. The peripheral zone contains degenerating organelles, especially mitochondria, and unstable membranous structures that lead to the formation of blebs or bubbles, which cover an extensive area of this zone [2, 5–7]. In recent studies, we observed that these granules are formed by degenerative mechanisms that occur mainly in astrocytic processes, with each affected astrocyte generating one cluster of granules [8]. This degenerative process can also affect the structures of the surrounding neuropil, including neuronal structures

* Correspondence: vilaplana@ub.edu
[1]Departament de Fisiologia, Facultat de Farmàcia, Universitat de Barcelona, Av. Joan XXIII s/n., 08028 Barcelona, Spain
[3]CIBERNED Centros de Biomedicina en Red de Enfermedades Neurodegenerativas, Spain
Full list of author information is available at the end of the article

BioMed Central

© 2015 Manich et al. **Open Access** This article is distributed under the terms of the Creative Commons Attribution 4.0 International License (http://creativecommons.org/licenses/by/4.0/), which permits unrestricted use, distribution, and reproduction in any medium, provided you give appropriate credit to the original author(s) and the source, provide a link to the Creative Commons license, and indicate if changes were made. The Creative Commons Public Domain Dedication waiver (http://creativecommons.org/publicdomain/zero/1.0/) applies to the data made available in this article, unless otherwise stated.

such as synaptic buttons and dendritic spines [8]. In another recent study, we reported the presence of specific epitopes in the granules that are not present in healthy brain structures and are formed at the same time as the granules, which led us to conclude that they were neo-epitopes [9]. These neo-epitopes are mainly located in the membranous fragments of the centre of the granules, although during the granule formation they can also be found in the membranes of the adjacent neuropil. Moreover, we showed that this neo-epitope is recognised by contaminant IgM antibodies present in many commercial antibodies obtained from mouse ascites and mouse or rabbit serum.

All these findings suggest that the contaminant IgMs found in antibodies obtained from mouse serum and ascites and directed against the neo-epitope could in fact be natural auto-antibodies. Natural antibodies are generated spontaneously from the foetal stage without previous contact with external antigens [10, 11]. Their repertoire and reactivity pattern have been determined through evolution and are remarkably stable within species and even between species [12, 13]. They constitute a first line of immune defence and also have other important functions in the physiology of the organism. Some of these natural antibodies are able to recognise the neo-epitopes that are formed, for example, in cell remnants or in apoptotic or altered cells, and thus intervene in their controlled elimination [12]. Consequently, we hypothesise that mouse plasma contains natural IgM auto-antibodies that recognise the neo-epitopes present in the degenerative hippocampal granular structures formed with ageing.

If our hypothesis is correct and the anti-neo-epitope IgMs are natural antibodies, all mice of the different strains should have anti-neo-epitope IgMs in their blood plasma at all ages, regardless of any previous exposure to external pathogens, or whether the animals develop pathological granular structures in their hippocampus or not. Moreover, they are probably also found in the plasma of mammals other than mice. Besides, in order to consider them as auto-antibodies, it is necessary to demonstrate that the anti-neo-epitope IgMs in the plasma of animals with granules recognise the neo-epitopes in their own granules.

Methods

Mice

Male SAMP8, ICR-CD1 and Balb/cOlaHsd (BALB/C) mice aged from 1 to 15-month were used. These strains were selected because their progressive formation of hippocampal granule clusters is accelerated, moderate or nearly absent, respectively. ICR-CD1 and SAMP8 mice were obtained from the Servei d'Estabulari de la Facultat de Farmàcia (Universitat de Barcelona), while BALB/C mice were obtained from Harlan Laboratories Models (Sant Feliu de Codines, Spain). Animals were kept under standard temperature conditions (22 ± 2 °C) and 12:12 h light–dark cycles (300 lux / 0 lux), and had access to food and water *ad libitum* throughout the study. We also used 3-month-old male ICR-CD1 (Janvier Labs, Le Genest-Saint-Isle, France) and BALB/C mice (Harlan Laboratories Models), which were kept under specific opportunistic pathogen-free (SOPF) conditions from birth and until the day of sacrifice. All experimental procedures were reviewed and approved by the University of Barcelona Animal Experimentation Ethics Committee (DAAM 7504).

Serum obtention and brain removal and processing

One to nine-months-old SAMP8, ICR-CD1 and BALB/C mice (4–6 animals per group) were anaesthetised i.p. with sodium pentobarbital (80 mg/kg), the thoracic cage was opened and blood was obtained by cardiac puncture. Blood was left to clot, centrifuged at 14,850 rpm for 5 min in a Biofuge Pico centrifuge (Heraeus, Madrid, Spain), and serum was collected and stored at −80 °C until use. After cardiac puncture, animals received an intracardiac gravity-dependent perfusion of 50 mL saline solution (0.9 % NaCl). Brains were dissected and cryostatic brain sections were obtained as described previously [8]. Some brain sections from 12 and 15-month-old ICR-CD1 mice were obtained following the same procedure, but without the cardiac puncture to obtain blood, in order to obtain hipocampal sections with degenerative granules.

Immunohistochemical staining for fluorescence microscopy and image acquisition

In order to determine if the plasma of the animals (including those born and maintained in SOPF conditions) contained anti-neo-epitope IgMs, immunohistochemical staining procedures were performed on brain sections from 12 or 15-months-old ICR-CD1 animals by using the mouse serum in the first incubation and an anti-mouse IgM conjugated to a fluorocrom as a secondary antibody. The staining was performed as follows. Sections were rehydrated with PBS and then blocked and permeabilised with 1 % bovine serum albumin (Sigma-Aldrich) and 0.1 % Triton X-100 (Sigma-Aldrich) in PBS for 20 min. They were washed with PBS and the primary incubation was performed overnight at 4 °C with a solution containing both a mouse serum diluted 1/100 and the rabbit anti-MMP2 IgG antibody (Merck Millipore, Darmstadt, Germany) diluted 1/200 in blocking buffer (BB; 1 % bovine serum albumin in PBS). The anti-MMP2 antibody was added as a specific marker of the granules, as we previously described [9]. Thereafter, slides were washed again and incubated for 1 h with a solution containing 1/50 tetramethyl rhodamine-conjugated (TRITC) goat anti-mouse IgM (Jackson ImmunoResearch Laboratories, Newmarket,

UK) and 1/250 AlexaFluor (AF)-488-conjugated donkey anti-rabbit IgG antibody (Life Technologies, Carlsbad, CA) in BB. Nuclear staining was performed with Hoechst (2 μg/mL, H-33258, Fluka, Madrid, Spain). The slides were coverslipped with Fluoromount (Electron Microscopy Sciences, Hatfield, PA, USA). As the positive control for the anti-neo-epitope IgM staining of the granules the anti-neo-epitope IgMs contained as a contaminant in the OX52 antibody (obtained from mouse ascites) were used instead of the animal serum. Negative controls were performed with a first incubation without mouse serum. To verify that the anti-neo-epitope IgMs contained in mouse serum were auto-antibodies, we performed the same immunohistochemical procedure detailed above but on brain sections of the same animal that provided the serum instead of the brain sections from aged ICR-CD1 animals.

To determine the presence of the anti-neo-epitope IgMs in the serum of other species than mouse we performed the same immunohistochemical staining procedures by using rat serum (obtained from our laboratory), rabbit serum and goat serum (both from Jackson ImmunoResearch Laboratories) at a 1/50 dilution instead of mouse serum. AF-594-conjugated goat anti-rat IgM (Life Technologies), fluorescein isothiocyanate (FITC)-conjugated goat anti-rabbit IgM, FITC-conjugated rabbit anti-goat IgM (Abcam, Cambridge, UK) and AF-555-conjugated donkey anti-rabbit IgG (Life Technologies) were used at a dilution 1/250 in the secondary incubations.

In all cases, fluorescence images were taken with a fluorescence laser microscope BX41 (Olympus, Germany) and images where stored in tiff format. Image compositions were performed with the ImageJ programme (National Institute of Health, USA).

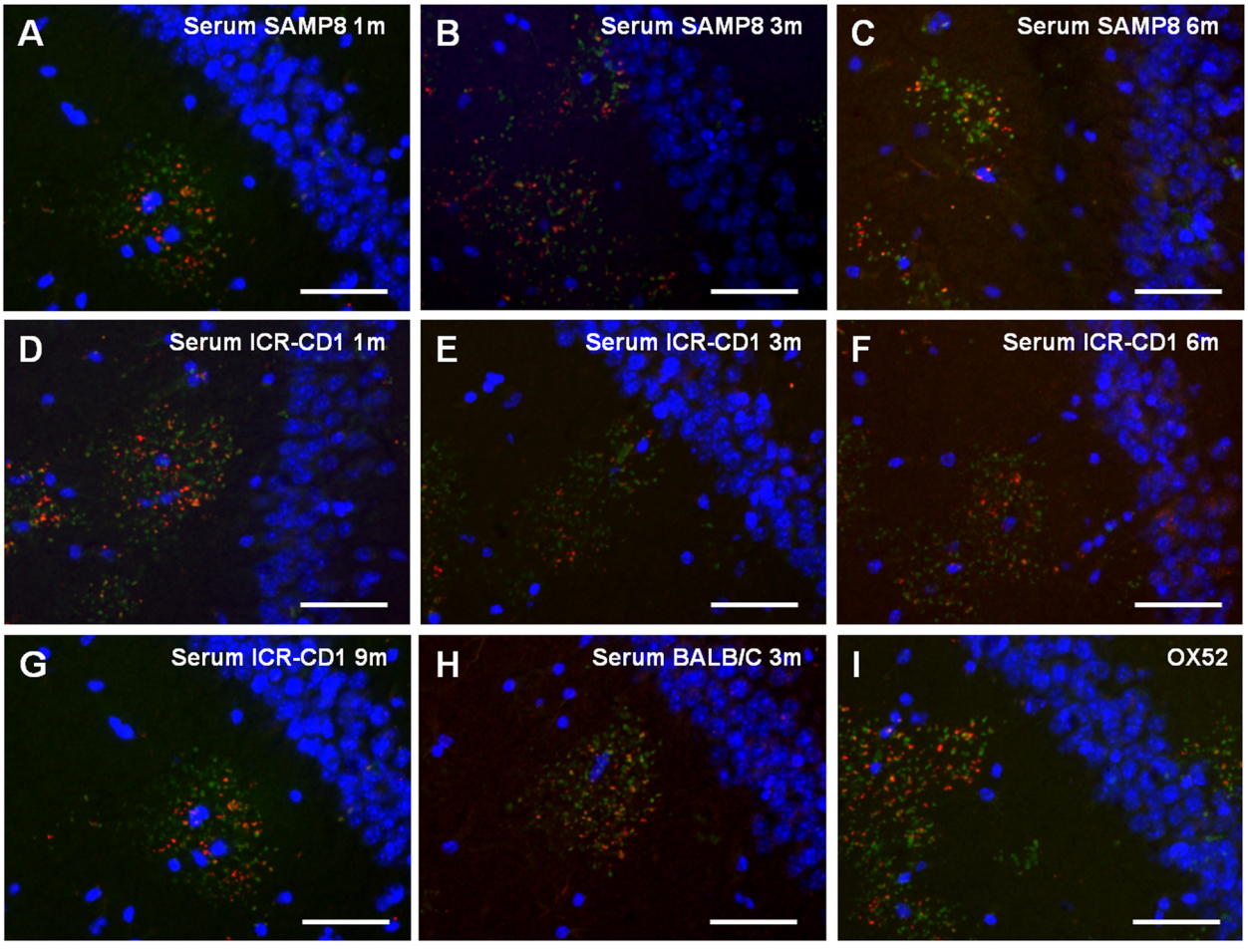

Fig. 1 Sera from SAMP8, ICR-CD1 and BALB/C mice contain anti-neo-epitope IgMs. Representative images of the hippocampal region of brain sections from 15-month-old ICR-CD1 mice simultaneously stained with Hoechst (blue), anti-MMP-2 antibody (green) and mouse sera (red) from each experimental group as detailed next. **a**-**c**: Sera from SAMP8 mice aged 1, 3 and 6 months, respectively. **d**-**g**: Sera from ICR-CD1 mice aged 1, 3, 6 and 9 months, respectively. **h**: Serum from a BALB/C mouse aged 3 months. **i**: Control staining of the granules with anti-neo-epitope IgMs contained in the OX52 antibody. In all cases the anti-MMP-2 staining showed the clusters of granules. Some granules of the clusters are stained with the serum, indicating that all sera contained anti-neo-epitope IgMs. Scale bar: 50 μm

Results

In order to determine whether the anti-neo-epitope IgMs are natural antibodies we first examined their presence in the serum of mice from different strains at different ages, i.e., 1, 3, 6 and 9 month-old ICR-CD1 mice, 1, 3 and 6 month-old SAMP8 mice and 3 month-old BALB/C mice ($n = 4–6$ per group). The IgM presence was evaluated by immunostaining brain sections from 15-month-old ICR-CD1 mice with the mouse sera and the anti-MMP2 antibody. In all cases the sera stained hippocampal granules, which are also labelled with the anti-MMP2 antibody, indicating that all tested mouse sera contained the anti-neo-epitope IgMs (Fig. 1a–h). In the positive control performed with the anti-neo-epitope IgMs contained in the OX52 antibody, granules were also stained (Fig. 1i).

On the other hand, as natural antibodies are present regardless of any previous exposure to external pathogens, we also tested for the presence of the anti-neo-epitope IgMs in the serum of 3-month-old ICR-CD1 and BALB/C mice maintained under SOPF conditions ($n = 6$ per group). All mouse sera positively stained the hippocampal granules contained in the brain sections from 15-month-old ICR-CD1 mice, which are also labelled with the anti-MMP2 antibody (Fig. 2), indicating that mice kept under SOPF conditions contained the anti-neo-epitope IgMs in their plasma.

Furthermore, as natural antibodies are remarkably stable not only within species but even between species, we also tested the presence of these IgMs in the serum of species other than mice. Thus, we immunostained brain sections of a 12-month old ICR-CD1 mouse with rat, rabbit and goat serum. In all cases the granules were positively stained, which indicated that the serum of the different species assayed contained the anti-neo-epitope IgMs (Fig. 3).

On the other hand, in order to establish whether the anti-neo-epitope IgM is an auto-antibody, brain sections from each mouse were immunostained with its own sera combined with the staining with the anti-MMP2 antibody. In the cases in which MMP2 indicated the presence of granules, the granules were also stained with the own serum, indicating that the anti-neo-epitope IgM contained in serum is an auto-antibody that recognises the own hippocampal granules (Fig. 4). It must be pointed out that some young animals, especially BALB/C mice, do not present granules in their hippocampus and thus the staining of the granules with their own

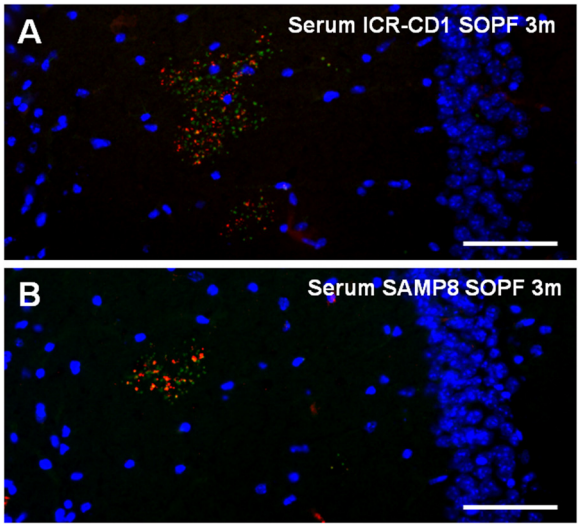

Fig. 2 Previous contact with external pathogens is not necessary for the presence of anti-neo-epitope IgMs in mouse serum. Representative images of the hippocampal region of brain sections from 12-month old ICR-CD1 mice simultaneously stained with Hoechst (blue), anti-MMP-2 antibody (green) and sera (red) from a 3-month-old ICR-CD1 SOPF animal (**a**) or from a 3-month-old BALB/C SOPF animal (**b**). In both cases the anti-MMP-2 staining showed the clusters of granules. Some granules of the clusters are stained with the serum, indicating that the sera of SOPF animals contained anti-neo-epitope IgMs. Scale bar: 50 μm

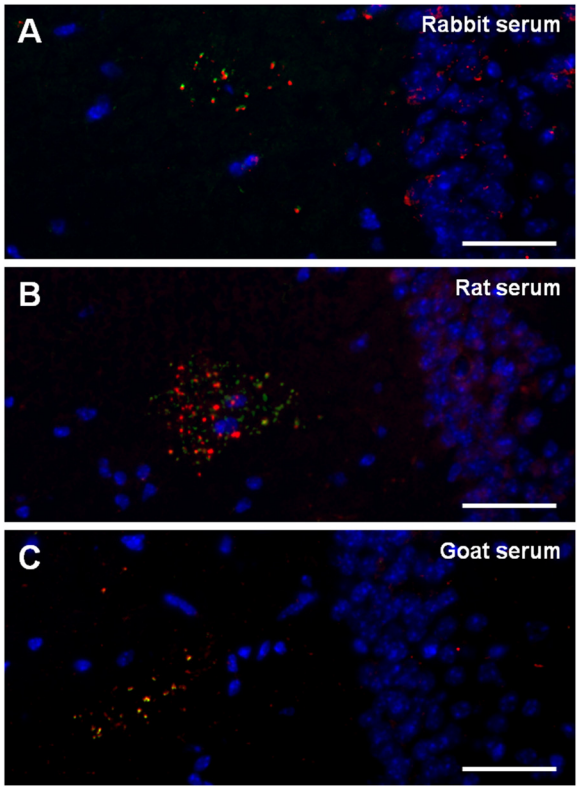

Fig. 3 Anti-neo-epitope IgMs are present in the serum from other species than mice. Representative images of the hippocampal region of brain sections from 12-month-old ICR-CD1 mice simultaneously stained with Hoechst (blue), anti-MMP-2 antibody and rabbit (**a**), rat (**b**) and goat (**c**) serum. Clusters of granules can be observed with the anti-MMP-2 staining (red in **a** and **c** and green in **b**) and some granules of the clusters are stained with the different sera (green in **a** and **c** and red in **b**), which indicates that the serum of these species contained anti-neo-epitope IgMs. Scale bar: 50 μm

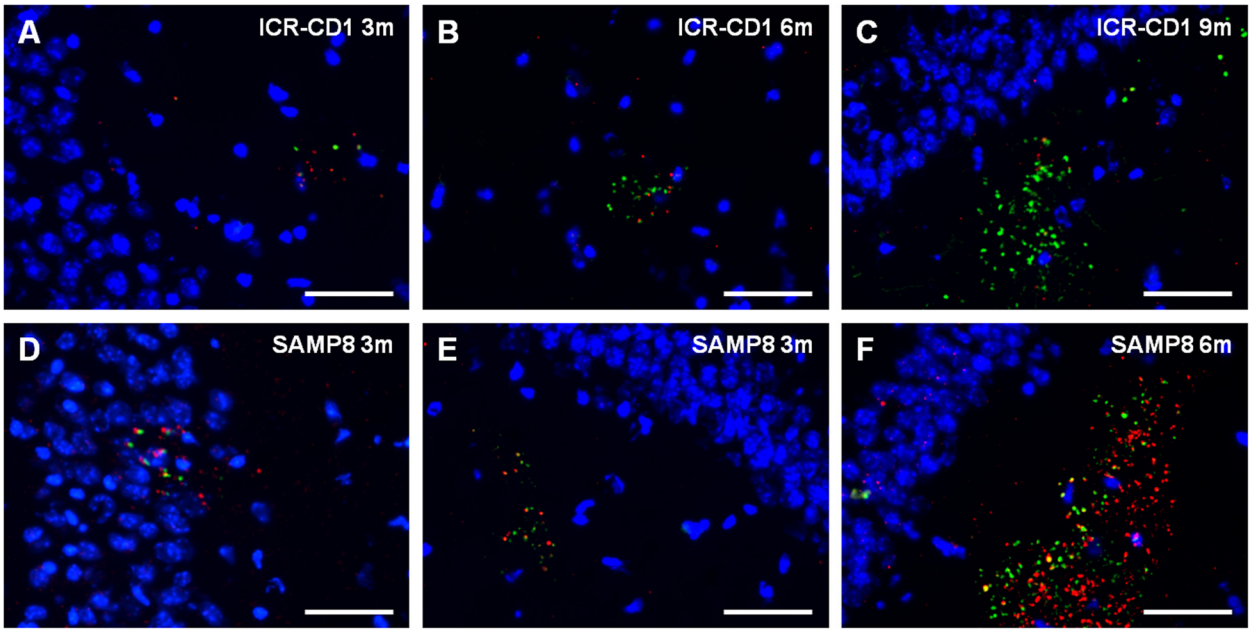

Fig. 4 Anti-neo-epitope IgMs are auto-antibodies. Representative images of the hippocampal region of brain sections from different mice stained with their own serum (*red*) and both the anti-MMP2 antibody (*green*) and Hoechst (*blue*). **a**-**c**: Representative ICR-CD1 mice aged 3, 6 and 9 months, respectively. **d**-**f**: Representative SAMP8 mice aged 3 and 6 months. As can be observed, the granules are stained by the serum of the own mouse. Thus, each serum recognize the own neo-epitope present in its clusters of granules. Scale bar: 50 μm

IgMs cannot be tested. Moreover, as all sera from all ages contain anti-neo-epitope IgMs, these results also indicate that the presence of the granules in the brain is not necessary for the existence of the anti-neo-epitope IgMs in the plasma.

Moreover, it should be pointed out that, under physiological conditions, the IgMs present in mouse plasma do not reach the granules of the hippocampus. The immunostaining with a primary incubation containing only the antibody directed against MMP2 and a secondary incubation with antibodies directed against the anti-MMP2 and against the mouse IgMs show the clusters of granules stained with the anti-MMP2 antibody but not with the anti-IgM antibody (Fig. 5). Thus, the anti-neoepitope IgMs existing in the plasma of the animals do not have access to the brain neo-epitopes.

Discussion and conclusions

The results of this study led us to conclude that the IgMs directed against the neo-epitope are common natural auto-antibodies that are always contained in mouse plasma independently of the existence of granules in the brain, and are also present in plasma of species other than mouse.

The presence of both these neo-epitopes in the granules and the natural anti-neo-epitope IgMs could be due to the fact that the neo-epitopes are formed by widespread mechanisms related to pathological ageing processes such as those associated with the increase of oxidative stress caused by the production of reactive oxygen or nitrogen species. Note that the number of granules seems to be modulated by antioxidant treatments or increases in oxidative stress [5, 14–16]. Oxidative stress may cause advanced glycation end products or oxidised phospholipids, which are a target of natural auto-antibodies and may trigger immune responses aimed at eliminating them and removing the structures that contain them [17–19].

Oxidation-specific epitopes have been documented in some pathological situations as in atherosclerotic lesions but also in pulmonary, renal and liver diseases as well as central nervous system lesions of multiple sclerosis and Alzheimer disease. Moreover, cells undergoing apoptosis have also been shown to contain multiple oxidation-specific epitopes in their plasma membranes. Therefore, oxidation-specific epitopes constitute perfect tags for the identification of biological waste and the discrimination of dying cells from viable cells by specific immune responses [20]. From this point of view, we can consider that the neo-epitopes found in the granules of the hippocampus of aged mice and the presence of natural anti-neo-epitope IgMs in their plasma could be related to a general mechanism that is effective in some tissues. However, the brain avoids these responses, probably due to the existence of the blood–brain barrier. It is worth noting that natural IgMs and neo-epitopes that have received little attention are now back on stage, as demonstrated by a

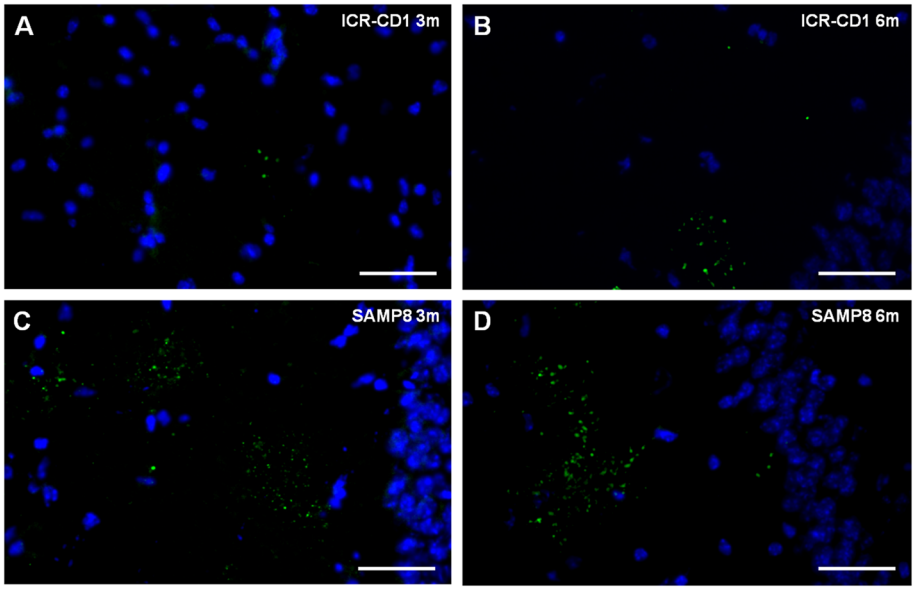

Fig. 5 IgMs from mouse plasma do not reach the granules of the hippocampus under physiological conditions. Representative images of the hippocampal region of brain sections from different mice stained with both the anti-MMP2 antibody (*green*) and Hoechst (*blue*). In the second incubation, an anti-mouse IgM antibody *(red)* is added. **a** and **b**: brain sections from representative ICR-CD1 mice aged 3 and 6 months, respectively. **c** and **d**: brain sections from representative SAMP8 mice aged 3 and 6 months, respectively. The granules are stained with the MMP2 antibody but the secondary anti-mouse IgM antibody did not stain the granules in any of the assayed mice, thus indicating that the anti-neo-epitope IgMs contained in their plasma do not reach the granules. Scale bar: 50 μm

new field of activity relating to the diagnosis and treatment of some cancers based on the presence of specific tumour neo-epitopes, which can be recognised by natural IgMs [21–23]. The results of this study led us to believe that treatment and diagnostics based on natural IgMs and neo-epitopes can probably be extended to brain diseases and pathological processes that occur in the brain, and could therefore pave the way for a new field of study in this area.

Abbreviations

BB: blocking buffer; FITC: fluorescein isothiocyanate-conjugated; IgM: immunoglobulin M; PBS: phosphate-buffered saline; SAMP8: senescence-accelerated mouse prone 8; SOPF: specific opportunistic pathogen free; TRITC: tetramethyl rhodamine-conjugated.

Competing interests

The authors declare that they have no competing interests.

Authors' contributions

GM, CP and JV participated in the design of the study. GM, EA, IC, CP and JV performed the experimental procedures, the microscope analysis and data analysis and interpretation. GM, EA, MP, CP and JV drafted the manuscript and participated in the critical review. All authors have read and approved the final manuscript. CP and JV contributed equally to this study.

Acknowledgments

This study was funded by grant BFU2010-22149 from the Spanish Ministerio de Ciencia e Innovación and grant BFU2013-47382-P from the Spanish Ministerio de Economía y Competitividad, and by the Centros de Investigación Biomédica en Red (CIBER) at the Instituto de Salud Carlos III. We thank the Generalitat de Catalunya for funding the research group (2009/SGR00853, 2014/SGR525) and for awarding a predoctoral fellowship to GM (FI-DGR 2011). IC and EA received an Ajuts de Personal Investigador en Formació predoctoral fellowship from the Universitat de Barcelona (APIF-UB). The authors thank Christopher Evans for revising the English language.

Author details

[1]Departament de Fisiologia, Facultat de Farmàcia, Universitat de Barcelona, Av. Joan XXIII s/n., 08028 Barcelona, Spain. [2]Unitat de Farmacologia i Farmacognòsia, Facultat de Farmàcia, Institut de Biomedicina (IBUB), Universitat de Barcelona, Av. Joan XXIII s/n., 08028 Barcelona, Spain. [3]CIBERNED Centros de Biomedicina en Red de Enfermedades Neurodegenerativas, Spain.

Received: 31 July 2015 Accepted: 15 November 2015
Published online: 24 November 2015

References

1. Akiyama H, Kameyama M, Akiguchi I, Sugiyama H, Kawamata T, Fukuyama H, et al. Periodic acid-Schiff (PAS)-positive, granular structures increase in the brain of senescence accelerated mouse (SAM). Acta Neuropathol. 1986;72:124–9.
2. Kuo H, Ingram DK, Walker LC, Tian M, Hengemihle JM, Jucker M. Similarities in the age-related hippocampal deposition of periodic acid-schiff-positive granules in the senescence-accelerated mouse P8 and C57BL/6 mouse strains. Neuroscience. 1996;74:733–40.
3. Del Valle J, Duran-Vilaregut J, Manich G, Casadesús G, Smith MA, Camins A, et al. Early amyloid accumulation in the hippocampus of SAMP8 mice. J Alzheimers Dis. 2010;19:1303–15.
4. Jucker M, Walker LC, Schwarb P, Hengemihle J, Kuo H, Snow AD, et al. Age-related deposition of glia-associated fibrillar material in brains of C57BL/6 mice. Neuroscience. 1994;60:875–89.
5. Robertson TA, Dutton NS, Martins RN, Roses AD, Kakulas BA, Papadimitriou JM. Age-related congophilic inclusions in the brains of apolipoprotein E-deficient mice. Neuroscience. 1998;82:171–80.
6. Mitsuno S, Takahashi M, Gondo T, Hoshii Y, Hanai N, Ishihara T, et al. Immunohistochemical, conventional and immunoelectron microscopical characteristics of periodic acid-Schiff-positive granules in the mouse brain. Acta Neuropathol. 1999;98:31–8.

7. Doehner J, Genoud C, Imhof C, Krstic D, Knuesel I. Extrusion of misfolded and aggregated proteins - a protective strategy of aging neurons? Eur J Neurosci. 2012;35:1938–50.
8. Manich G, Cabezón I, Camins A, Pallàs M, Liberski PP, Vilaplana J, Pelegrí C. Clustered granules present in the hippocampus of aged mice result from a degenerative process affecting astrocytes and their surrounding neuropil. Age 2014; 36:9690.
9. Manich G, Del Valle J, Cabezon I, Camins A, Pallas M, Pelegri C, et al. Presence of a neo-epitope and absence of amyloid beta and tau protein in degenerative hippocampal granules of aged mice. Age. 2014;36:151–65.
10. Ehrenstein MR, Notley CA. The importance of natural IgM: scavenger, protector and regulator. Nat Rev Immunol. 2010;10:778–86.
11. Mannoor K, Xu Y, Chen C. Natural autoantibodies and associated B cells in immunity and autoimmunity. Autoimmunity. 2013;46:138–47.
12. Baumgarth N, Tung JW, Herzenberg LA. Inherent specificities in natural antibodies: a key to immune defense against pathogen invasion. Springer Semin Immunopathol. 2005;26:347–62.
13. Avrameas S. Natural autoantibodies: from "horror autotoxicus" to "gnothi seauton". Immunol Today. 1991;12:154–9.
14. Porquet D, Casadesús G, Bayod S, Vicente A, Canudas AM, Vilaplana J, et al. Dietary resveratrol prevents Alzheimer's markers and increases life span in SAMP8. Age (Dordr). 2013;35:1851–6.
15. Veurink G, Liu DAN, Taddei K, Perry G, Smith MA, Robertson TA, et al. Reduction of inclusion body pathology in ApoE-deficient mice fed a combination of antioxidants. Free Radic Biol Med. 2003;34:1070–7.
16. Nakamura S, Akiguchi I, Seriu N, Ohnishi K, Takemura M, Ueno M, et al. Monoamine oxidase-B-positive granular structures in the hippocampus of aged senescence-accelerated mouse (SAMP8). Acta Neuropathol. 1995;90:626–32.
17. Goldin A, Beckman JA, Schmidt AM, Creager MA. Advanced glycation end products: sparking the development of diabetic vascular injury. Circulation. 2006;597–605.
18. Singh R, Barden A, Mori T, Beilin L. Advanced glycation end-products: a review. Diabetologia. 2001;44:129–46.
19. Binder CJ, Hörkkö S, Dewan A, Chang M-K, Kieu EP, Goodyear CS, et al. Pneumococcal vaccination decreases atherosclerotic lesion formation: molecular mimicry between Streptococcus pneumoniae and oxidized LDL. Nat Med. 2003;9:736–43.
20. Binder CJ. Natural IgM antibodies against oxidation-specific epitopes. J Clin Immunol. 2010;30 Suppl 1:S56–60.
21. Vollmers HP, Brändlein S. Natural antibodies and cancer. N Biotechnol. 2009;294–8.
22. Vázquez AM, Rodrèguez-Zhurbenko N, López AM. Anti-ganglioside anti-idiotypic vaccination: more than molecular mimicry. Front Oncol. 2012;2:170.
23. Lutz HU, Miescher S. Natural antibodies in health and disease: an overview of the first international workshop on natural antibodies in health and disease. Autoimmun Rev. 2008;7:405–9.

Submit your next manuscript to BioMed Central and we will help you at every step:

- We accept pre-submission inquiries
- Our selector tool helps you to find the most relevant journal
- We provide round the clock customer support
- Convenient online submission
- Thorough peer review
- Inclusion in PubMed and all major indexing services
- Maximum visibility for your research

Submit your manuscript at
www.biomedcentral.com/submit

ARTICLE 2

NEW PERSPECTIVES ON CORPORA AMYLACEA IN THE HUMAN BRAIN

Elisabet Augé, Itsaso Cabezón, Carme Pelegrí i Jordi Vilaplana

Scientific Reports 2017; 7:41807

DOI: 10.1038/srep41807

RESUM

Objectius: Estudiar la presència de neo-epítops que puguin ser reconeguts per IgMs naturals ens els CA de cervell humà. A més a més, determinar si la presència de neo-epítops en els CA pot ser responsable de falsos marcatges positius en aquestes estructures quan es duen a terme assaigs immunohistoquímics.

Material i mètodes: Es van utilitzar seccions criostàtiques d'hipocamp humà de 7 casos de malaltia d'Alzheimer (73-92 anys) i 3 casos no associats a malaltia d'Alzheimer (79-95 anys, referits com a casos control) i es va realitzar la tinció de PAS per tal de verificar la presència de CA en tots ells. Per determinar l'existència d'ANs dirigits contra possibles neo-epítops dels CA es van utilitzar tècniques d'immunofluorescència utilitzant com a anticossos primaris els sèrums obtinguts de mostres sanguínies humanes provinents de donants sans (n=8), sèrums procedents de sang de cordó umbilical, els quals contenen IgMs naturals generades durant la vida fetal i sense contacte previ amb antígens externs (n=3) i sèrums de diferents espècies animals: ratolí (alguns mantinguts en condicions SOPF), rata, cabra i conill. També es van utilitzar IgMs comercials humanes i la regió *crystallizable fragment* (Fc) de les IgMs humanes. Per determinar l'existència de possibles falsos marcatges positius en els CA humans es va utilitzar l'anticòs JJ319, un anticòs dirigit contra el CD28 de rata i sense reactivitat en el cervell humà, del qual es va obtenir la fracció IgG mitjançant una columna de proteïna A i la fracció IgM mitjançant una columna MBP agarosa. També es van realitzar marcatges amb anticossos primaris dirigits contra la proteïna tau i el pèptid Aβ, realitzant els seus corresponents controls de pre-adsorció, per determinar si la presència d'aquests dos components en els CA, descrita per diverses autors, és real o és el resultat de falsos marcatges causats per les IgMs.

Resultats: Els marcatges amb els sèrums humans va posar de manifest l'existència d'IgMs plasmàtiques humanes que reconeixen uns neo-epítops que es troben situats en els CA humans. Aquestes IgMs també es troben presents en els sèrums de cordó umbilical, així com també en els sèrums d'altres espècies animals. No s'observa marcatge, en canvi, quan s'utilitza la regió Fc de les IgMs i el secundari anti-IgM corresponent o quan no s'incuba cap sèrum en la primera incubació. Això posa de manifest que els CA contenen neo-epítops reconeguts per IgMs naturals. D'altra banda, els marcatges amb l'anticòs JJ319 mostren un marcatge positiu dels CA quan s'utilitzen anticossos secundaris dirigits contra les cadenes pesades i lleugeres de les IgG, així com també anticossos secundaris dirigits contra les IgMs, però no quan s'utilitza l'anticòs secundari isotip específic corresponent. També s'observa marcatge positiu utilitzant la

fracció IgM obtinguda de l'anticòs JJ319 i el secundari anti-IgM. Quan s'utilitza el mateix secundari i la fracció IgG, no s'observa marcatge. Tampoc s'observa marcatge en utilitzar la fracció IgG i el secundari dirigit contra les cadenes pesades i lleugeres de les IgG. Els resultats obtinguts amb l'anticòs JJ319 posen de manifest que el marcatge inicial observat a l'utilitzar l'anticòs JJ319 no purificat i un anticòs secundari no isotip específic de ratolí és causat pel creuament d'aquest anticòs secundari amb les IgMs naturals que es troben com a contaminants a l'anticòs JJ319 que s'uneixen als neo-epítops dels CA. Les IgMs, doncs, produeixen falsos marcatges. Per últim, els assaigs immunohistoquímics amb els anticossos dirigits contra la proteïna tau i el pèptid Aβ mostren, quan s'utilitza l'anticòs secundari isotip específic, el marcatge de cabdells neurofibril·lars i plaques amiloides, però no el dels CA. El marcatge de cabdells i plaques desapareix quan l'anticòs és pre-adsorbit amb la proteïna corresponent. Quan s'utilitzen anticossos secundaris dirigits contra les IgMs, en alguns casos s'observa marcatge positiu dels CA, fet que indica la presència d'IgMs contaminants. Aquests marcatges no desapareixen quan es fa el control de pre-adsorció corresponent, i són, doncs, falsos marcatges positius produïts per les IgMs.

Conclusions: Els CA de l'hipocamp de cervell humà contenen neo-epítops que són reconeguts per IgMs naturals. Aquest fet posa de manifest una possible interacció entre el sistema immunitari innat i els CA, i reforça la hipòtesi que considera els CA com a elements implicats en l'eliminació de substàncies de rebuig. Aquests anticossos es troben presents en el sèrum de diferents espècies animals (inclosos animals mantinguts en condicions SOPF), així com també en el sèrum de cordó umbilical humà. En condicions fisiològiques, però, aquests anticossos no poden accedir al parènquima cerebral. S'ha vist que la presència dels neo-epítops és la responsable de falsos marcatges positius d'aquestes estructures en els estudis immunohistoquímics perquè les IgMs naturals es poden trobar com a contaminants en alguns anticossos comercials i unir-se als neo-epítops. Tenint en compte aquest fet, s'ha pogut descartar la presència de proteïna tau i del pèptid Aβ en els CA, tot i que havia estat descrita en estudis publicats amb anterioritat. Es planteja finalment la necessitat de revisar tots els estudis previs sobre els CA realitzats mitjançant tècniques immunohistoquímiques.

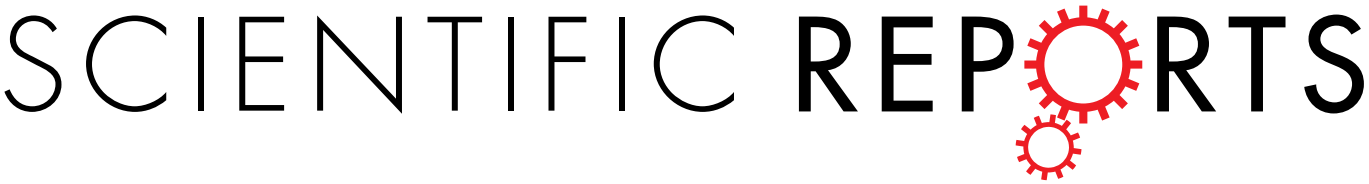

OPEN

New perspectives on *corpora amylacea* in the human brain

Elisabet Augé[1,2], Itsaso Cabezón[1,2], Carme Pelegrí[1,2,3,*] & Jordi Vilaplana[1,2,3,*]

Received: 25 July 2016
Accepted: 28 December 2016
Published: 03 Febraury 2017

Corpora amylacea **are structures of unknown origin and function that appear with age in human brains and are profuse in selected brain areas in several neurodegenerative conditions. They are constituted of glucose polymers and may contain waste elements derived from different cell types. As we previously found on particular polyglucosan bodies in mouse brain, we report here that *corpora amylacea* present some neo-epitopes that can be recognized by natural antibodies, a certain kind of antibodies that are involved in tissue homeostasis. We hypothesize that *corpora amylacea*, and probably some other polyglucosan bodies, are waste containers in which deleterious or residual products are isolated to be later eliminated through the action of the innate immune system. In any case, the presence of neo-epitopes on these structures and the existence of natural antibodies directed against them could become a new focal point for the study of both age-related and degenerative brain processes.**

Corpora amylacea (CA) are glycoproteinaceous structures that were first reported in the brains of elderly patients by J.E. Purkinje at a scientific conference held in Prague in 1837. Although extensively discussed around the beginning of the nineteenth century, they were not considered to be of any pathological significance for many years. It was not until recent decades, with the development of new techniques, that interest in their nature and their relation with certain diseases awakened[1]. CA usually increase in number with age in normal human brains, but they are also profuse in selected areas of the brain in several neurodegenerative conditions, including Alzheimer's, Parkinson's, Huntington's and Pick's diseases, multiple and hippocampal sclerosis, and in patients with temporal lobe epilepsy and focal cortical dysplasia[2,3]. While essentially constituted of glucose polymers, an extraordinary number of components mainly derived from neurons, oligodendrocytes and astrocytes have been proposed to accompany them[1,2]. However, the presence of several of these components remains controversial and some results seem to be inconsistent. It is in part due to the uncertainty regarding their composition that the origin and role of CA still remain unclear; and CA are probably the cerebral structures that have been considered in the most different ways over the years. CA have been considered as: merely post-mortem artifacts[4]; the result of a defect in glycogen metabolism[5]; protein precipitates of lymphatic or hematogenous origin[4]; accumulations of breakdown products from neurons and oligodendroglial cells[6]; aggregated remnants of degenerated neuronal cells[7]; conglomerations of interacting proteins from degenerating neurons and extravasated blood elements released after the breakdown of the blood–brain barrier[8]; structures formed from degenerating astrocytes[9]; and recently, as pathological structures related to fungal infections[10]. The presence of waste elements is a recurrent feature, and CA may be involved in the trapping and sequestration of potentially hazardous products[1], or they may act as a system that cleans the central nervous system (CNS)[11]. In any case, such diverse interpretations have not allowed for a comprehensive overview of CA.

CA are positive to periodic acid-Schiff (PAS) staining due to their high polysaccharide content. They have been associated with some pathological polyglucosan bodies (PGBs) that appear with age in mouse brain and are frequently referred to as "PAS granules" because they are also stained in the PAS reaction[12]. Studies we recently performed on mouse PAS granules determined that these structures result from a degenerative process affecting astrocytic processes and their surrounding neuropil[13]. We found that during their formation, some epitopes emerge and these epitopes should be considered as neo-epitopes because they are not present in healthy structures[14]. We also observed that these neo-epitopes are recognized by natural IgM antibodies which, as they are natural, are present in the blood plasma of mice from birth and without prior contact with external antigens[15]. These results indicate that the organism permanently has antibodies prepared to react against the neo-epitopes that arise in

[1]Secció de Fisiologia, Departament de Bioquímica i Fisiologia, Facultat de Farmàcia i Ciències de l'Alimentació, Universitat de Barcelona, Av. Joan XXIII 27-31, 08028 Barcelona, Spain. [2]Institut de Neurociències, Universitat de Barcelona, Barcelona, Spain. [3]CIBERNED Centros de Biomedicina en Red de Enfermedades Neurodegenerativas, Spain. *These authors contributed equally to this work. Correspondence and requests for materials should be addressed to J.V. (email: vilaplana@ub.edu)

PAS granules. We also found that the IgM antibodies that recognize these neo-epitopes are also present in the plasma of other mammal species[15], which is in accordance with the fact that natural antibodies have been fixed by natural selection during evolution and are therefore interspecific. Meanwhile, we also observed that these natural IgM antibodies are present as contaminants in a high percentage (around 70%) of commercial antibodies originated from mouse, rabbit, goat or rat, and obtained from ascites or serum, being monoclonal or polyclonal, and even supplied as purified[14,15]. Since these contaminant IgMs are recognized by the majority of anti-IgG antibodies used as secondary antibodies in immunohistochemical studies, these IgMs are the cause of numerous cases of false positive immunostaining of PAS granules, and they therefore account for some inconsistencies in some of the theories concerning PAS granules[12].

Taking all the above into account and based on certain similarities between CA in human brains and PAS granules in mouse brains, we hypothesized that CA in human brains would also contain neo-epitopes and that human plasma, as well as plasma from other mammal species, would contain natural IgMs directed against them. If this hypothesis is confirmed, a new perspective on and interpretation of CA will be opened up. Moreover, we also hypothesized that the presence of contaminant IgMs in commercial antibodies causes much false positive immunostaining of CA and hence, several conclusions drawn from some of the studies published to date are unfounded, making it necessary to revise the current view of these structures.

Results

CA contain neo-epitopes that can be recognized by plasma IgMs. The presence of CA in brain hippocampal slices from Alzheimer's disease (AD) and control donors was confirmed by carrying out standard PAS staining (Fig. 1a). Thereafter, we tested whether human plasma contains plasma IgMs directed against some components of the CA in these brains. We used brain slices from 3 AD and 3 control donors. From each brain donor, 8 brain slices were immunostained respectively with human blood plasma from 8 different donors in the first incubation and an anti-human IgM (μ chain specific) antibody conjugated to a fluorochrome in the second incubation. In all cases the CA become stained (Fig. 1b–e). Positive staining of CA was also observed when using commercial purified human IgM immunoglobulins in the first incubation (Fig. 1f). The absence of staining when using blocking buffer (BB) in the first incubation indicated that the IgMs are necessary for such staining (Fig. 1g). The presence of a receptor for the Fc region of the IgM in CA was ruled out on the basis of the absence of staining when using just the Fc fragment of the human IgM in the first incubation (Fig. 1h). Moreover, this was reinforced as previous incubation with a universal Fc receptor blocker did not block the staining with purified human IgM immunoglobulins (Fig. 1i). All these results suggest the presence of some neo-epitopes on CA that can be recognized by some human plasmatic IgMs.

The IgMs that recognize the neo-epitopes contained on CA are natural IgMs. As natural IgMs are usually interspecific because their repertoire and reactivity pattern were determined by evolution, we checked for the existence of IgMs directed against the neo-epitopes of CA in sera from different mammal species. We used brain slices from 4 different AD brain donors. For each donor, 4 different brain sections were immunostained using sera from goat, rat, rabbit and mouse in the first incubation and the appropriate fluorochrome-labeled anti-IgM antibodies in the second. In all cases, CA become stained (Fig. 2a–d). Negative controls performed with BB in the first incubation and the different fluorochrome-labeled anti-IgM antibodies in the second did not stain CA (Fig. 2e), indicating that IgMs are essential for such staining. Therefore, the presence of IgMs directed against the neo-epitopes of CA in all the mammal species tested suggests that these IgMs are natural antibodies.

Meanwhile, taking into account that natural antibodies are present from birth, without any need for previous contact with external antigens, we also immunostained different brain sections from the 4 AD brain donors with sera obtained from mice maintained from birth in specific opportunistic pathogen free (SOPF) conditions. In all cases, CA became stained, indicating that also in SOPF conditions mice can contain IgMs that recognize some CA components (Fig. 2f), and reinforcing that these IgMs are in fact natural antibodies.

We also tested whether the IgMs directed against the neo-epitopes of CA were also contained in sera obtained from human umbilical cords. It must be pointed that, unlike IgGs, IgMs cannot cross the placenta and those contained in serum from the umbilical cord are produced by the fetus and are considered natural antibodies[16]. We immunostained different brain slices from an AD donor with purified IgMs obtained from 3 different umbilical cord sera in the first incubation and human anti-IgM antibodies in the second; and CA become stained in all cases (Fig. 2g-h). Moreover, as indicated before, the staining was not present when using BB in the first incubation and human anti-IgM antibodies in the second. These results strongly support the finding that the IgMs that recognize some components of CA are natural antibodies.

The IgMs that recognize the neo-epitopes contained in CA do not reach these neo-epitopes *in vivo*. As indicated earlier, when using BB in the first incubation and fluorochrome-labeled anti-human IgM specific antibody in the second, there was no positive staining of CA in any of the slices tested from the different brain donors (Fig. 1g). As natural antibodies are permanently present in the plasma of organisms, and consequently it can be assumed that they were also present in the plasma of the brain donors, we can deduce that in neither AD or control patients had the plasma IgMs reached the CA. This observation is equivalent to that made when studying the PAS granules of mice, in which we were able to demonstrate that all mice with granules in their hippocampus contained IgMs directed against the neo-epitopes in their plasma; but that *in vivo*, and due to the blood–brain barrier, these IgMs do not reach the PAS granules in any of these animals[15].

The anti-neo-epitopes IgMs can cause false positive staining of CA. In our previous studies on PAS granules in mice, we observed that a high number of commercial antibodies contain contaminant natural IgMs that produce false immunostaining of them[14]. We therefore checked whether contaminant IgMs also produce

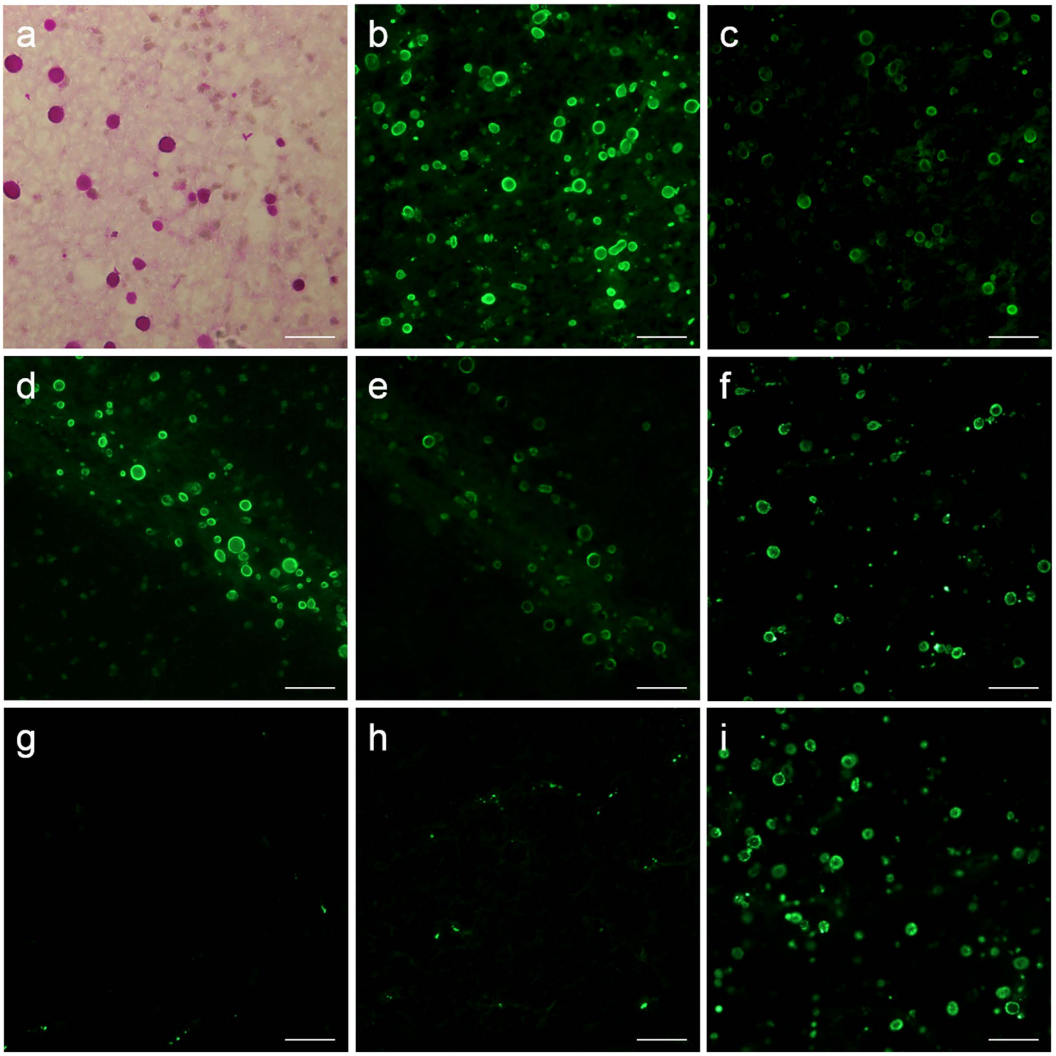

Figure 1. CA contain neo-epitopes that can be recognized by plasma IgMs. A representative image of PAS staining illustrating the presence of CA in a hippocampal brain section from an AD donor is shown in (**a**). Representative images from brain sections from an AD donor (**b** and **c**) and a control donor (**d** and **e**) immunostained with two different human blood plasma in the first incubation and anti-human IgM (μ chain specific) conjugated to a fluorochrome in the second incubation (**b** and **d** correspond to one plasma donor, and **c** and **e** to the other donor). As can be observed, CA were positively stained in all cases. If commercial purified human IgM antibodies were used in the first incubation, CA were also stained (**f**). Negative staining was observed when BB (**g**) and the Fc fragment of human IgM (**h**) were used in the first incubation, instead of human IgMs. Previous incubation with an Fc receptor blocker did not block the positive staining obtained when commercial purified human IgM was used in the first incubation (**i**). The last four representative images (**f–i**) were obtained from the same AD donor. Scale bar: 50 μm.

false positive immunostaining of CA, and the results obtained confirmed that they do. One example of such false positive staining can be observed when using the JJ319 mouse IgG_1 primary antibody directed against rat CD28 surface antigen of lymphocytes, with no reactivity in brain, but containing contaminant IgMs. The immunostaining of CA contained in hippocampal sections from 4 different AD donors with the JJ319 primary antibody and a secondary fluorochrome-labeled antibody against heavy and light chains of mouse IgG appeared to be positive in all cases (Fig. 3a). This positive staining, however, is just a misinterpretation. CA were not stained when using the specific anti-γ-chain of mouse IgG_1 as the secondary antibody, indicating the absence of IgG_1 bound to the CA (Fig. 3b). The staining was positive when using a secondary antibody directed against the μ-chain of mouse IgM, indicating the presence of contaminant IgMs bound to the CA (Fig. 3c). The staining with secondary antibodies directed against the μ-chain of mouse IgM remained when using the IgM fraction of the JJ319 in the first incubation (Fig. 3d), whereas it disappeared when using its IgG fraction in the first incubation (Fig. 3e). Finally, the staining of CA with the IgG fraction in the first incubation also failed when using the secondary fluorochrome-labeled antibody against heavy and light chains of mouse IgG (Fig. 3f). We can therefore conclude that the initial staining observed when using the unpurified JJ319 antibody in the first incubation and the

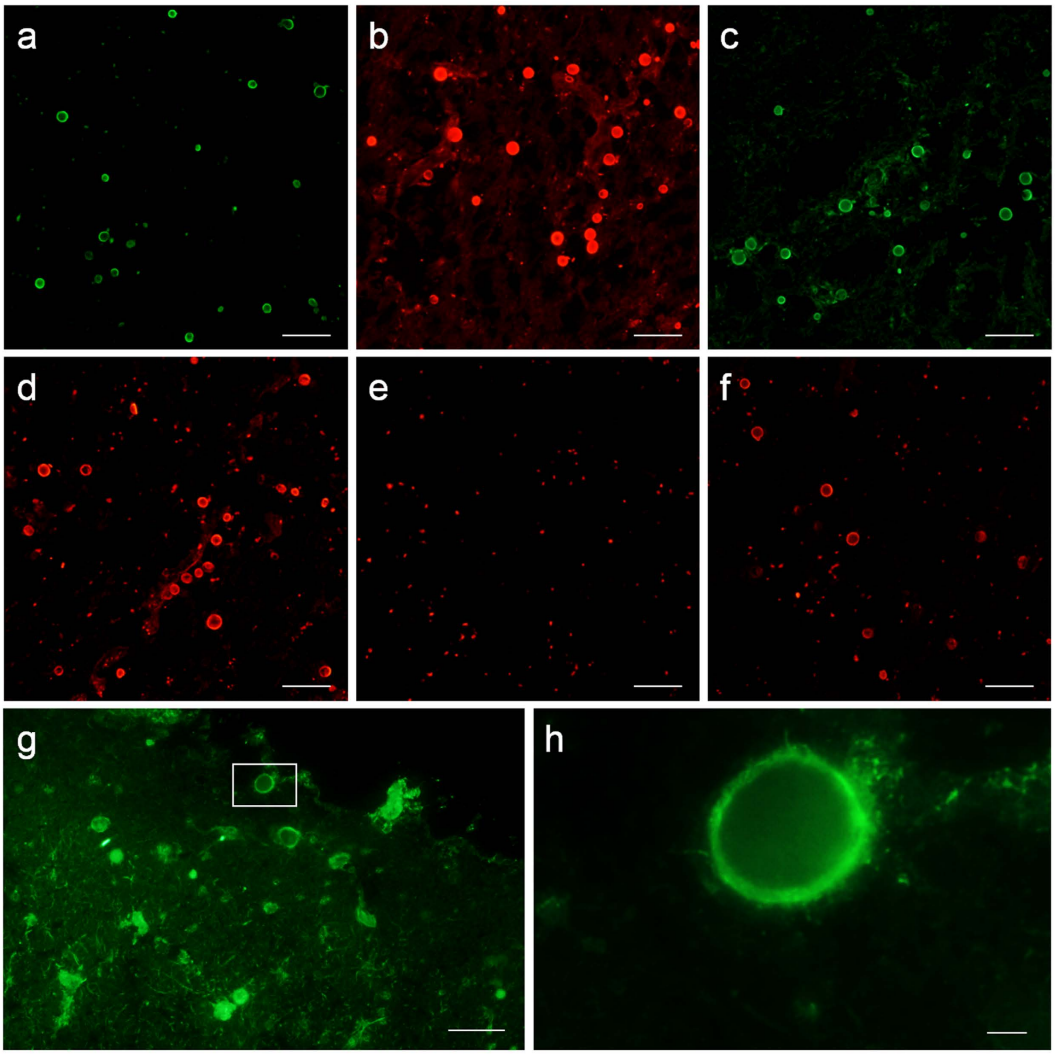

Figure 2. The IgMs that recognize CA neo-epitopes are natural antibodies. Representative images from an AD donor showing the positive staining of CA when using goat (**a**), rat (**b**), rabbit (**c**) and mouse (**d**) sera in the first incubation and an appropriate fluorochrome-labeled anti-IgM antibody in the second. Negative staining was obtained when BB was used in the first incubation instead of the different mammal sera and a representative image obtained when an anti-mouse IgM was used in the second incubation is shown (**e**). A representative image from the same AD donor showing the positive staining of CA with sera from SOPF mice is shown (**f**). Purified IgMs from umbilical cord sera positively stained the CA of an AD patient and a representative image is shown in (**g**). (**h**) Inset in (**g**). Scale bar (**a**–**g**) 50 μm; scale bar (**h**) 5 μm.

secondary antibody directed against heavy and light chains of mouse IgG was simply due to the cross-reaction of this secondary antibody with the contaminant IgMs bound to the CA. As the secondary antibodies used in immunohistochemical studies are usually directed against heavy and light chains, misinterpretation due to the presence of contaminant natural IgMs could be frequent and could explain some of the contradictory results regarding the composition of CA.

CA do not contain tau protein or amyloid–β peptides. Some contradictory results concerning the composition of CA are related to their content of tau protein or the presence of amyloid-β protein precursor (AβPP) or their derived amyloid-β (Aβ) peptides[3,17–22]. Therefore, we revised the immunostaining of CA using different commercial antibodies directed against these components. Taking into account the possible presence of contaminant IgMs, we ruled out the use of secondary antibodies directed against the heavy and light chains of IgGs, because they can cross-react with the IgMs. Instead, we used secondary antibodies directed against the γ_1-chain specific for IgG_1 and secondary antibodies directed against the μ-chain specific for IgMs.

In order to check the presence of tau, we used an anti-tau protein IgG_1 antibody (clone Tau5) and brain slices from 4 AD donors. When the second incubation contained both the antibody against the μ-chain (green fluorescence) and the antibody directed against the γ_1-chain (red fluorescence), we observed positive staining of CA corresponding to the μ-chain but not to the γ_1-chain, indicating that the vial contained contaminant IgMs

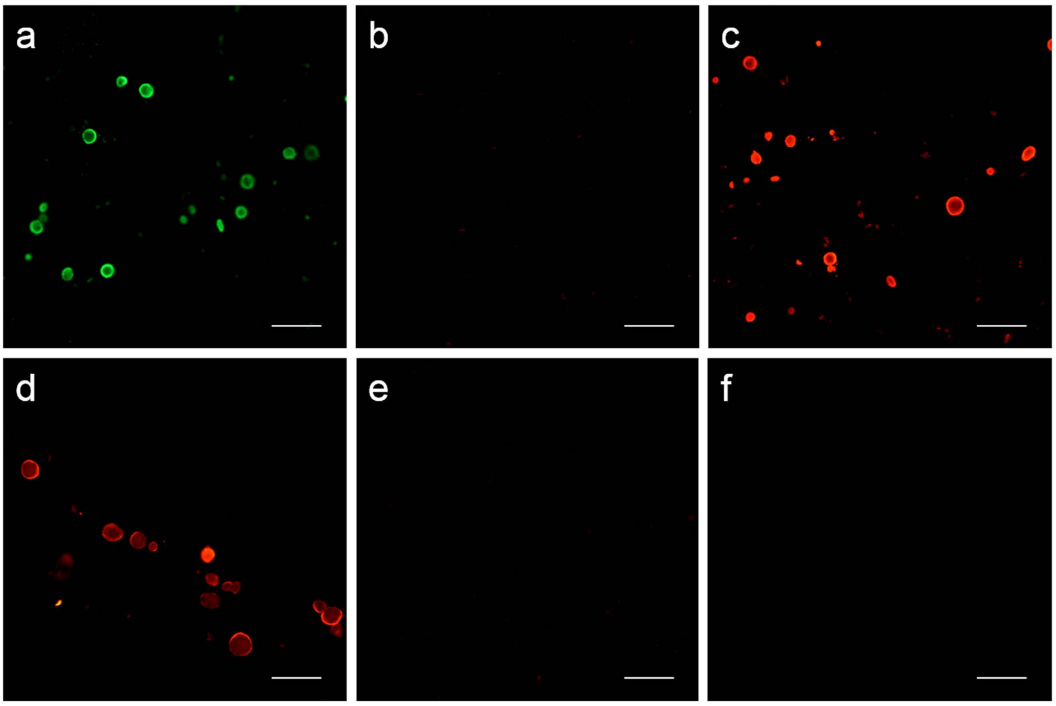

Figure 3. IgMs can produce false positive staining of CA. Representative images of brain sections from an AD patient stained with JJ319 mouse IgG_1 primary antibody and: a secondary fluorochrome-labeled antibody against heavy and light chains of mouse IgG (**a**) a secondary fluorochrome-labeled antibody against the γ_1 chain of mouse IgG (**b**) and a secondary fluorochrome-labeled antibody against the μ chain of mouse IgM (**c**). As can be observed, CA are not stained when the secondary antibody against the γ_1 chain of mouse IgG is used. When purified IgMs or purified IgGs from JJ319 antibody were used in the first incubation (**d** and **e** respectively) and a fluorochrome-labeled antibody against the μ chain was used in both cases in the second incubation, positive staining of CA was obtained when using purified IgMs while it was negative when using purified IgGs. Negative staining of CA was also obtained when purified IgGs were incubated followed by a secondary antibody against heavy and light chains of mouse IgG (**f**). It can therefore be concluded that only IgM bind to the CA and that the staining when using a secondary antibody against heavy and light chains of mouse IgG is just a cross-reaction with IgMs. Scale bar: 50 μm.

that bind to the CA, but that anti-tau IgG_1 does not bind to them. We also observed that neurofibrillary tangles were positively stained with the IgGs but not with the IgMs, denoting the presence of tau protein and the absence of neo-epitopes recognized by IgMs in these pathological structures (Fig. 4a). Consistent with this, when the anti-tau antibody was pre-adsorbed with tau protein, the staining of the neurofibrillary tangles with IgG disappeared; but that of the IgM on CA did not (Fig. 4b). The same procedure was repeated with another primary antibody directed against the tau protein (clone 5E2), and the results were reproduced exactly (Fig. 4c and d). It can therefore be concluded that CA do not contain tau protein, at least not at levels that are detected by our immunostaining procedures.

The presence of AβPP or some of their derived Aβ peptides on CA was also checked with two different primary antibodies in brain slices from 4 different AD donors. We used one primary antibody directed against the 1–16 region of the $Aβ_{42}$ (clone 6E10), which also recognizes the AβPP, and another primary antibody directed against $Aβ_{42}$ (clone 12F4) which only recognizes the $Aβ_{42}$ peptide. In all cases, the secondary incubations contained both the anti-γ_1-chain (red fluorescence) and the anti-μ-chain (green fluorescence) antibodies. The 6E10 antibody, which did not contain IgM contamination, indicated the presence of Aβ in amyloid plaques but not in CA (Fig. 4e). Moreover, the positive staining of amyloid plaques disappeared when the primary antibody was pre-adsorbed with Aβ protein (Fig. 4f). The antibody 12F4 corroborated the presence of Aβ on amyloid plaques and its absence in CA. In this case, however, the vial contained contaminant IgMs that bound to CA but not to amyloid plaques (Fig. 4g). Now, when pre-adsorbing the primary antibody with Aβ protein, the positive staining of the amyloid plaques disappeared; while the staining of CA with IgM was maintained (Fig. 4f). All together, these results indicate that CA do not contain AβPP or Aβ peptides, at least not at levels that are detected by our immunostaining procedures.

Discussion

The most important outcome of the present work is the presence of natural IgM antibodies in human plasma that are capable of recognizing some neo-epitopes on human brain CA. This conclusion is derived from the different sequential findings. In the first place, the fact that human plasma from different donors are capable of immunostaining CA when using fluorochrome-labeled anti-IgMs as the secondary antibodies suggests that there

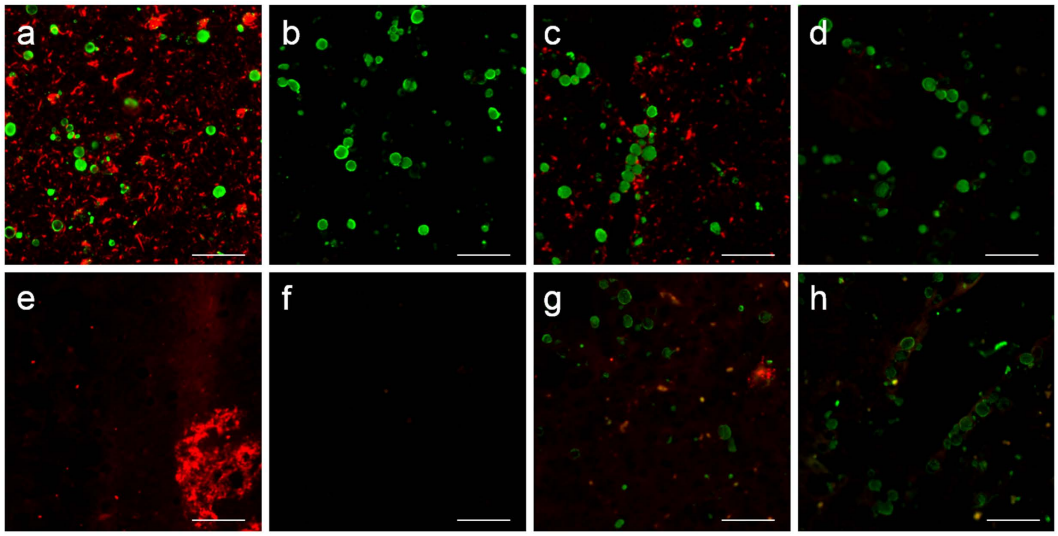

Figure 4. CA do not contain tau protein or amyloid–β peptides. Representative images obtained from brain samples from an AD donor stained with: anti-tau clone tau 5 (**a**) pre-adsorbed anti-tau clone tau 5 (**b**) anti-tau clone tau 5E2 (**c**) and pre-adsorbed anti-tau clone tau 5E2 (**d**), followed by both fluorochrome-labeled secondary antibodies directed against the μ chain of mouse IgM (green) and against the γ_1 chain of mouse IgG (red). When using non-pre-adsorbed antibodies, CA were positively stained with the contaminant IgMs contained in the anti-tau antibodies (green) and neurofibrillary tangles and neurons were stained with the anti-tau IgG_1 (red) (**a** and **c**). When the antibodies were pre-adsorbed with tau protein, the staining of the neuro fibrillary tangles and neurons disappeared while that of CA by contaminant IgMs remained (**b** and **d**). Representative images obtained from brain samples from an AD donor stained with: the 6E10 antibody (**e**) pre-adsorbed 6E10 (**f**) the 12F4 antibody (**g**) and pre-adsorbed 12F4 (**h**), followed by both fluorochrome-labeled secondary antibodies directed against the μ chain of mouse IgM (green) and against the γ_1 chain of mouse IgG (red). When using non-pre-adsorbed anti-Aβ IgG_1 antibodies, amyloid plaques appeared positively stained with IgGs (red) (**e** and **g**). CA did not stain after 6E10 staining because this antibody did not contain contaminant IgM (**e**) while they appeared stained with 12F4 (green), denoting contamination of IgMs in this antibody (**g**). When the antibodies were pre-adsorbed with Aβ fragments, the staining of the amyloid plaques disappeared while that of CA by contaminant IgMs remained (**h**). Scale bar: 50 μm.

are IgMs in human plasma that recognize some of their components. Secondly, as plasma contains more than IgMs, we subsequently checked for the staining with purified IgMs to rule out some possible staining artifacts, and positive staining was also observed. Moreover, we observed that the Fc fragments of the IgMs are insufficient to stain the CA and we verified that a universal Fc receptor blocker does not block the staining with IgMs. Thus, the staining with the IgMs seems to be related to the variable regions of the IgMs, which are those that contain the antigen-binding sites. In order to determine if the IgMs are natural antibodies, we used different approaches. The most noteworthy was the use of purified IgMs obtained from sera of human umbilical cords. As IgMs do not cross the placenta, these IgMs are generated by the fetus before exposure to external antigens, and are part of the repertoire of natural antibodies. We observed that IgMs from umbilical cords can stain CA. Moreover, IgMs that recognize some CA components are also found in sera from mammals other than human, which is consistent with the fact that natural antibodies are often interspecific. We also observed that they are present in sera from mice maintained from birth in SOPF conditions, without any contact with opportunistic pathogens. Altogether, these sequential findings reveal a connection between the natural immune system and CA, and seem to indicate some useful aspects concerning CA.

Natural antibodies, which can act as a first line of defense against external elements, also play an important role in the maintenance of tissue homeostasis. They act, among others, on neo-epitopes that appear in situations of cellular stress and tissue damage; but also even during conventional tissue cell turnover[23–25]. Taking into account that CA may be involved in the trapping and sequestering of potentially hazardous products[1], the presence of neo-epitopes in CA could just be a consequence of the presence of some altered components in them, such as oxidized lipids like phosphorylcholine or the oxidation-associated determinant malondialdehyde, which can become an adduct on proteins[23,26]. However, not only are CA a random accumulation of several components, but they are also concretions or compact structures with a high glucidic content and often with a periventricular or perivascular location. This could be related to their extrusion from brain tissue. CA seem to be elements in an organized process and in fact, they have been considered as a part of a physiological cleaning system of the CNS[11]. The existence of natural antibodies directed against the neo-epitopes located on CA seems to be congruent with their possible pre-programed elimination. The clearance of dying cells is one of the most essential roles of the natural immune system and, in mouse, natural IgM antibodies that recognize apoptotic cells have been shown to enhance the phagocytic clearance of these cells without triggering harmful inflammatory responses in the tissue[23,27]. The enhancement of phagocytosis processes mediated by natural IgMs and the presence of neo-epitopes on CA

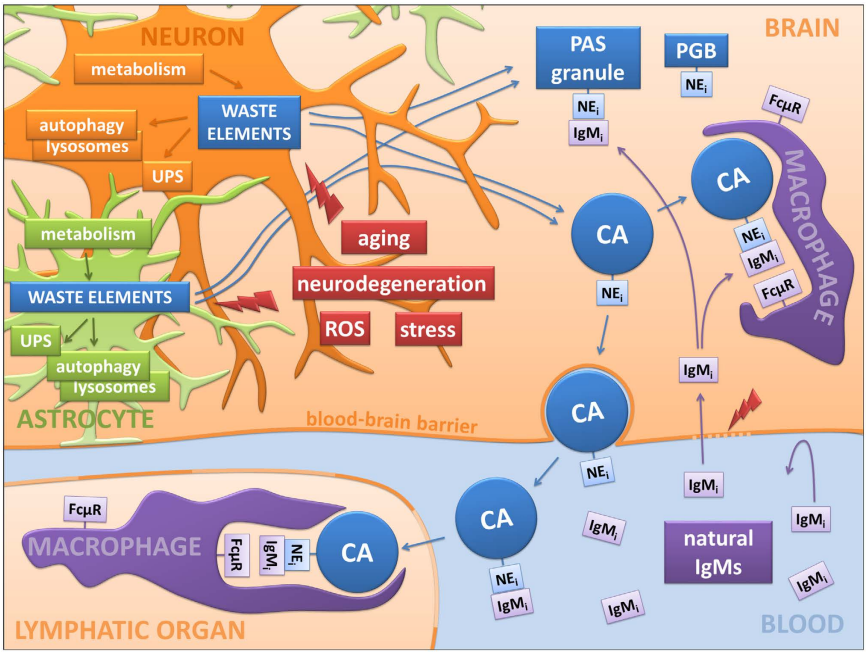

Figure 5. Schematic integrative proposal. Waste elements generated from neurons, astrocytes, oligodendrocytes and other brain cells are removed intracellularly via the ubiquitin proteasome system (UPS) or via autophagic processes linked to lysosomal digestion. However, some of these waste elements can be found in polyglucosan bodies (PGBs) like CA in human brains or PAS granules in mouse brains, mainly when the production of waste elements is strengthened by factors such as aging, neurodegenerative disorders, reactive oxygen species or cellular stress. These PGBs contain some neo-epitopes (NEi) that are targeted by natural antibodies of the IgM type (IgMi). Since in physiological conditions the blood –brain barrier prevents access of IgMs to the brain parenchyma, the linkage between IgMs and CA is produced outside the brain after CA extrusion or inside the brain if the barrier is disrupted, thus allowing the passage of the IgMs. Macrophages, which contain specific receptors for the activated IgMs (FcμR), can subsequently phagocytize them. The new relationship shown here between PGBs and the natural immune system suggests that these PGBs could be waste containers ready to be eliminated by the action of this predetermined immune system.

suggest that these structures may be phagocyted, which is in agreement with the potential cleaning mechanism attributed to CA. Reinforcing this possibility, it should be pointed out that the presence of CA in the brain does not correlate with local inflammatory processes and moreover, in *neuromyelitis optica*, CA located in the injured regions are collected and engulfed by infiltrating macrophages[9].

As we have shown in this study, these IgMs directed against the neo-epitopes of CA are widely present in human plasma and in serum from umbilical cord, as well as in the serum of different species of mammals, including animals kept in SOPF conditions. Together, this indicates that these antibodies are directed against ubiquitous antigens. By using antigen microarray informatics, it has been determined that IgM natural antibodies are directed to a specific and limited set of self-molecules that are highly constant between newborns[16,28]. However, the number of molecules studied was limited, and it is still unknown in which specific structures these interactions occur *in vivo* or what the exact function of this self-reactivity against each one of these molecules would be. To the best of our knowledge, little is known about natural antibodies directed against neo-epitopes located on CNS structures. One study reported two human monoclonal natural antibodies targeting myelin and cell-surface antigens on oligodendrocytes; those antibodies seemed to promote the remyelination of neuronal fibers[29,30]. Other studies proposed the presence of natural antibodies targeting Aβ peptides in the serum and cerebrospinal fluid of healthy individuals[31,32]. However, these last findings were not confirmed by our present studies, in which we did not observe natural antibodies against amyloid plaques in samples from AD donors. Based on the components assumed to be present in CA, we can conjecture as to the possible nature of the neo-epitopes contained in them. However, given the false positive staining that the contaminant IgMs present in commercial antibodies has produced in immunohistochemical studies of CA, there is a need to revise their composition. As we point out in this work, it will be necessary to revise the papers that consider the presence of tau and Aβ in CA; and there is also a need to clarify the presence of other doubtful components, such as nestin[33], alpha-synuclein[20,21,33], GFAP[3,21,33,34] or some Heat-shock proteins like HSP70[33,35–37]. There is, nonetheless, general consensus as to the accumulation of waste products in CA[1–3] and the presence of ubiquitin in these structures[3,19,20,35,38]. It should be pointed out that ubiquitin is associated with mechanisms for the cleaning of waste products, which reinforces the idea that CA are organized structures that can eliminate waste products. Consistently with this, PAS granules from mice, which have a high glucidic content and seem to contain waste products from different cellular origins, also contain ubiquitin[39,40].

In the CNS, the presence of the blood–brain barrier generally restricts the access of plasma IgMs to the brain parenchyma and, as we describe herein, in AD and control donors, the IgMs do not have access to the neo-epitopes present in CA. However, as indicated above, in the case of *neuromyelitis optica*, in which the blood–brain barrier is altered in the injured regions, the CA are collected and engulfed by infiltrating macrophages[9]. Meanwhile, some studies indicate that CA can be extruded from the marginal glia at the vestibular root entry, and it has been proposed that they could be a component of the glio-pial system of clearance that can remove different molecules from the CNS[11]. Taken as a whole, the binding between IgMs and CA could take place inside the CNS when the blood–brain barrier is altered or outside the CNS after CA extrusion.

Taking all the above into account, the picture obtained supports the idea that CA are waste containers involved in protective or cleaning mechanisms, in which potentially deleterious or residual cellular products arising through different processes and in different cell types are sequestered to be later eliminated via phagocytic processes or other mechanisms in which the innate immune system plays an important role (Fig. 5).

In the present work we highlight a new link between CA and the innate immune system, and this link will certainly help to ascertain the nature and functions of CA. Moreover, as the neo-epitopes that are target of natural IgMs have also been observed in PAS granules in mice[12,15], these properties could perhaps be expanded to other PGBs, making it necessary to study the presence of neo-epitopes in other related brain degenerative bodies such as Lafora bodies from Lafora disease or Bielschowsky bodies from Bielschowsky body disease. In the same way in which the presence of neo-epitopes in certain malignant tumor cells and the presence of IgMs directed against these neo-epitopes is a recent field of study in the therapy and diagnosis of cancerous processes[25,41,42], so the existence of neo-epitopes on CA and other degenerative brain structures and the presence of natural IgM antibodies directed against them could become a new focus of the study of age-related or pathological degenerative brain processes. It may open up new lines of research into PGBs and their physiopathological roles.

Methods

Human brain samples and blood. Post-mortem brain samples were purchased from the Banc de Teixits Neurològics (Biobanc-Hospital Clínic-IDIBAPS, Barcelona). Brain samples were taken from seven cases of neuropathologically confirmed Alzheimer's disease patients (A3B3C3 stage, 73–92 years old) and three non-AD patients (79–95 years old, referred as control donors). On arrival at the laboratory, frozen hippocampal sections (6 μm) were stored at −80 °C. The number of brain samples used in each staining is indicated in the result section. For the most part, a minimum of three AD and three control brain donors were used for each specific staining.

Human blood samples (n = 8) collected with K3-EDTA were obtained from healthy donors from the Banc de Sang i Teixits de Barcelona. The samples were centrifuged at 12,000 rpm for 5 min in a Biofuge Pico centrifuge (Heraeus, Madrid, Spain) at 4 °C and plasma was collected and stored at −20 °C until use.

Foetal blood samples (n = 3) were obtained from the Maternal/Fetal Medicine Biobanc, I + D Fetal Medicine Research Center (IDIBAPS).

Rabbit and goat sera were obtained from Jackson ImmunoResearch Laboratories (Newmarket, UK) and rat, mouse and mouse SOPF sera were obtained from our laboratory as described previously[15].

All methods involving animals and human samples were performed in accordance with appropriate guidelines and regulations. All experiments involving human tissue were approved by the Bioethical Committee of the University of Barcelona and all the animal experimental procedures were reviewed and approved by the University of Barcelona Animal Experimentation Ethics Committee (DAAM 7504).

Periodic acid-Schiff staining. Brain sections were stained with PAS according to the standard procedure. Briefly, sections were fixed for 10 min in Carnoy's solution (60% ethanol, 30% chloroform and 10% glacial acetic acid). Then the slides were pretreated for 10 minutes with 0.25% periodic acid (19324–50, Electron Microscopy Sciences) in distilled water followed by a washing step for 3 min. Then the slides were immersed in Schiff's reagent (26052–06, Electron Microscopy Sciences) for 10 min. After the Schiff's reagent, the slides were washed for 5 min in distilled water. Nuclei were counterstained for 6 min with a hematoxylin solution according to Mayer (3870, J.T. Baker, Center Valley, USA). Then the slides were washed, dehydrated to xylene and coverslipped with quick-mounting medium (Eukitt, Fluka Analytical, Germany).

Antibodies and reagents. The following antibodies were used as primary antibodies: human IgM purified immunoglobulins (1:2; OBT1524; AbD Serotec, Kidlington, UK), mouse monoclonal IgG_1 against Aβ peptide 1–42 (12F4; 1:100; SIG-39142; Covance, Princeton, USA), mouse monoclonal IgG_1 anti-Aβ 1–16 (6E10; 1:50; SIG-39320; Covance), mouse monoclonal IgG_1 anti-tau, a.a.210–241 (clone Tau-5; 1:100; MAB361; Merck Millipore, Darmstadt, Germany), mouse monoclonal IgG_1 anti-tau (clone 5E2; 1:50; 05–348; Merck Millipore) and mouse polyclonal IgG_1 anti-rat CD28 (JJ319; 1:50; kindly provided by Prof. T. Hünig). The IgM fraction of JJ319 was obtained from JJ319 using an MBP agarose column (PierceTM IgM Purification Kit; Thermo Scientific, Rockford, IL, USA), and the IgG fraction of JJ319 was obtained using a protein A column. Human adult sera were used as the primary antibodies at 1:100 dilution. Rabbit, rat and goat sera were used at 1:50 dilution, while mouse and SOPF mouse sera were pooled (n = 3, respectively, ICR-CD1, 3 months) and used at 1:100 dilution. The IgM fractions from human umbilical cord sera were purified from umbilical cord sera also with MBP agarose column, and were concentrated using the Pierce Protein Concentrators PES, 30 K MWCO (Thermo Scientific).

The following antibodies were used as secondary antibodies: AF488 goat anti-human IgM heavy chain (1:200; A-21215; Life Technologies, Eugene, OR, USA), AF594 goat anti-rat IgM heavy chain (1:250; A-21213; Life Technologies), rabbit anti-goat IgM conjugated to fluorescein isothiocyanate (FITC) (1:250; ab112861; Abcam, Cambridge, UK), goat anti-rabbit IgM μ chain-FITC (1:250; ab98458; Abcam), goat anti-mouse IgM μ chain specific conjugated to tetramethyl rhodamine-isothiocyanate (TRITC) (1:250; 115–025–020; Jackson ImmunoResearch Laboratories), AF488 goat anti-mouse IgM μ chain specific (1:250; 115–545–075; Jackson

ImmunoResearch Laboratories), AF594 goat anti-mouse IgG_1 (1:250; A-21125; Life Technologies) and AF488 donkey anti-mouse IgG (H + L) (1:250; A-21202; Life Technologies).

Immunohistochemistry. For the immunohistochemistry, human brain sections were air dried for 10 min and then fixed with acetone for 10 min at 4 °C. After 2 h of drying, sections were rehydrated with phosphate-buffered saline (PBS) and then blocked and permeabilized with 1% bovine serum albumin in PBS (Sigma-Aldrich) (Blocking buffer, BB) with 0.1% Triton X-100 (Sigma-Aldrich) for 20 min. They were washed with PBS and the primary incubation was overnight at 4 °C. Afterwards, the slides were washed and incubated for 1 h at room temperature with the secondary antibody. Nuclear staining was performed with Hoechst (2 μg/mL, H-33258, Fluka, Madrid, Spain) and the slides were washed and coverslipped with Fluoromount (Electron Microscopy Sciences, Hatfield, PA, USA). Negative controls of staining were performed using BB in the first incubation instead of the primary antibodies. Pre-adsorption controls for tau and Aβ immunostaining were performed by incubating the antibodies overnight at 4 °C with mild agitation with a 10–20 molar-fold concentration of tau protein (AG952; Merck Millipore), Aβ protein fragment 1–42 (A9810; Sigma, Saint Louis, Missouri) or Aβ 1–40 (AS-24235; Anaspec, Fremont, CA). To rule out the presence of Fc receptors in CA, a universal Fc receptor blocker (NB309–15; Innovex Bioscience, Richmond, CA) was incubated before the incubation of the human IgMs, and the staining with Natural Human IgM Fc fragment protein (1:2; ab90287; Abcam) was also tested in the first incubation instead of complete IgMs.

Image acquisition. Images were captured with a fluorescence laser and optical microscope (BX41, Olympus, Germany) and stored in tiff format. All the images were acquired using the same microscope, laser and software settings. The time of exposition was adapted to each staining, but the respective control images were acquired with the same time of exposition. Image analysis and treatment were performed using the ImageJ program (National Institute of Health, USA). Images that were modified for contrast and brightness to enhance their visualization were processed in the same way as the images corresponding to their respective controls.

References

1. Cavanagh, J. B. Corpora-amylacea and the family of polyglucosan diseases. *Brain Res. Rev.* **29,** 265–295 (1999).
2. Rohn, T. T. Corpora amylacea in neurodegenerative diseases: cause or effect? *Int. J. Neurol. Neurother.* **2,** 31 (2015).
3. Pirici, D. & Margaritescu, C. Corpora amylacea in aging brain and age-related brain disorders. *J. Aging Gerontol.* **2,** 33–57 (2014).
4. Ferraro, A. & Damon, L. A. The histogenesis of amyloid bodies in the central nervous system. *Arch. Pathol.* **12,** 229–244 (1931).
5. Sakai, M., Austin, J., Witmer, F. & Trueb, L. Studies of corpora amylacea: Isolation and preliminary characterization by chemical and histochemical techniques. *Arch. Neurol.* **21,** 526–544 (1969).
6. Singhrao, S. K., Neal, J. W., Piddlesden, S. J. & Newman, G. R. New immunocytochemical evidence for a neuronal/oligodendroglial origin for corpora amylacea. *Neuropathol. Appl. Neurobiol.* **20,** 66–73 (1994).
7. Selmaj, K. *et al.* Corpora amylacea from multiple sclerosis brain tissue consists of aggregated neuronal cells. *Acta Biochim. Pol.* **55,** 43–49 (2008).
8. Meng, H., Zhang, X., Blaivas, M. & Wang, M. M. Localization of blood proteins thrombospondin1 and ADAMTS13 to cerebral corpora amylacea. *Neuropathology* **29,** 664–671 (2009).
9. Suzuki, A. *et al.* Phagocytized corpora amylacea as a histological hallmark of astrocytic injury in neuromyelitis optica. *Neuropathology* **32,** 597–594 (2012).
10. Pisa, D., Alonso, R., Rábano, A. & Carrasco, L. Corpora amylacea of brain tissue from neurodegenerative diseases are stained with specific antifungal antibodies. *Front. Neurosci.* **10,** 86 (2016).
11. Sbarbati, A., Carner, M., Colletti, V. & Osculati, F. Extrusion of corpora amylacea from the marginal glia at the vestibular root entry zone. *J. Neuropathol. Exp. Neurol.* **55,** 196–201 (1996).
12. Manich, G., Cabezón, I., Augé, E., Pelegrí, C. & Vilaplana, J. Periodic acid-Schiff granules in the brain of aged mice: From amyloid aggregates to degenerative structures containing neo-epitopes. *Ageing Res. Rev.* **27,** 42–55 (2016).
13. Manich, G. *et al.* Clustered granules present in the hippocampus of aged mice result from a degenerative process affecting astrocytes and their surrounding neuropil. *Age* **36,** 9690 (2014).
14. Manich, G. *et al.* Presence of a neo-epitope and absence of amyloid beta and tau protein in degenerative hippocampal granules of aged mice. *Age* **36,** 151–165 (2014).
15. Manich, G. *et al.* Neo-epitopes emerging in the neurodegenerative hippocampal granules of aged mice can be recognized by natural IgM auto-antibodies. *Immun. Ageing* **12,** 23–30 (2015).
16. Merbl, Y., Zucker-Toledano, M., Quintana, F. J. & Cohen, I. Newborn humans manifest autoantibodies to defined self molecules detected by antigen microarray informatics. *J. Clin. Invest.* **117,** 712–718 (2007).
17. Loeffler, K. U., Edward, D. P. & Tso, M. O. M. Tau-2 immunoreactivity of corpora amylacea in the human retina and optic nerve. *Invest. Ophthalmol. Vis. Sci.* **34,** 2600–2603 (1993).
18. Nolan, C. C. & Brown, A. W. Reversible neuronal damage hippocampal pyramidal cells with triethyllead: the role of astrocytes. *Neuropathol. Appl. Neurobiol.* **15,** 441–457 (1989).
19. Day, R. J., Mason, M. J., Thomas, C., Poon, W. W. & Rohn, T. T. Caspase-cleaved tau co-localizes with early tangle markers in the human vascular dementia brain. *PLoS ONE.* **10,** e0132637; 10.1371/journal.pone.0132637 (2015).
20. Wilhelmus, M. M. M. *et al.* Novel role of transglutaminase 1 in corpora amylacea formation? *Neurobiol. Aging* **32,** 845–856 (2011).
21. Notter, T. & Knuesel, I. Reelin immunoreactivity in neuritic varicosities in the human hippocampal formation of non-demented subjects and Alzheimer's disease patients. *Acta Neuropathol. Commun.* **1,** 27 (2013).
22. Tate-Ostroff, B., Majocha, R. E. & Marotta, C. A. Identification of cellular and extracellular sites of amyloid precursor protein extracytoplasmic domain in normal and Alzheimer disease brains. *Proc. Natl. Acad. Sci. USA* **86,** 745–749 (1989).
23. Grönwall, C., Vas, J. & Silverman, G. J. Protective roles of natural IgM antibodies. *Front. Immunol.* **3,** 66 (2012).
24. Lutz, H. U., Binder, C. J. & Kaveri, S.Naturally occurring auto-antibodies in homeostasis and disease. *Trends Immunol.* **30,** 43–51 (2009).
25. Vollmers, H. P. & Brändlein, S. Natural IgM antibodies: the orphaned molecules in immune surveillance. *Adv. Drug Deliv. Rev.* **58,** 755–765 (2006).
26. Chou, M. Y. *et al.* Oxidation-specific epitopes are dominant targets of innate natural antibodies in mice and humans. *J. Clin. Invest.* **119,** 1335–1349 (2009).
27. Wang, H., Coligan, J. E. & Morse, H. C. Emerging functions of natural IgM and its Fc receptor FCMR in immune homeostasis. *Front. Immunol.* **7,** 99 (2016).

28. Mouthon, L. *et al.* Invariance and restriction toward a limited set of sel-antigens characterize neonatal IgM antibody repertoires and prevail in autoreactive repertoires of healthy adults. *Proc. Natl. Acad. Sci. U. S. A.* **92,** 3839–3843 (1995).
29. Lang, W., Rodriguez, M., Lennon, V. A. & Lampert, P. W. Demyelination and remyelination in murine viral encephalomyelitis. *Ann. N. Y. Acad. Sci.* **436,** 98–102 (1984).
30. Rodriguez, M., Lennon, V. A., Benveniste, E. N. & Merrill, J. E. Remyelination by oligodendrocytes stimulated by antiserum to spinal cord. *J. Neuropathol. Exp. Neurol.* **46,** 84–95 (1987).
31. Du, Y. *et al.* Reduced levels of amyloid β-peptide antibody in Alzheimer disease. *Neurology* **57,** 801–805 (2001).
32. Szabo, P., Relkin, N. & Weksler, M. E. Natural human antibodies to amyloid beta peptide. *Autoimmun. Rev.* **7,** 415–420 (2008).
33. Buervenich, S., Olson, L. & Galter, D. Nestin-like immunoreactivity of corpora amylacea in aged human brain. *Brain Res. Mol. Brain Res.* **94,** 204–208 (2001).
34. Nam, I. H. *et al.* Association of corpora amylacea formation with astrocytes and cerebrospinal fluid in the aged human brain. *Korean J. Phys. Anthropol.* **25,** 177–184 (2012).
35. Cissé, S., Perry, G., Lacoste-Royal, G., Cabana, T. & Gauvreau, D. Immunochemical identification of ubiquitin and heat-shock proteins in corpora amylacea from normal aged and Alzheimer's disease brains. *Acta Neuropathol.* **85,** 233–240 (1993).
36. Martin, J. E. *et al.* Heat shock protein expression in corpora amylacea in the central nervous system: clues to their origin. *Neuropathol. Appl. Neurobiol.* **17,** 113–119 (1991).
37. Gáti, I. & Leel-Ossy, L. Heat shock protein 60 in corpora amylacea. *Pathol. Oncol. Res.* **7,** 140–144 (2001).
38. Pirici, I. *et al.* Corpora amylacea in the brain form highly branched three-dimensional lattices. *Rom. J. Morphol. Embryol.* **55,** 1071–1077 (2014).
39. Robertson, T. A., Dutton, N. S., Martins, R. N., Taddei, K. & Papadimitriou, J. M. Comparison of astrocytic and myocytic metabolic dysregulation in apolipoprotein E deficient and human apolipoprotein E transgenic mice. *Neuroscience* **98,** 353–359 (2000).
40. Soontornniyomkij, V. *et al.* Increased hippocampal accumulation of autophagosomes predicts short-term recognition memory impairment in aged mice. *Age* **34,** 305–316 (2012).
41. Lutz, H. U. & Miescher, S. Natural antibodies in health and disease: an overview of the first international workshop on natural antibodies in health and disease. *Autoimmun. Rev.* **7,** 405–409 (2008).
42. Vázquez, A. M., Rodríguez-Zhurbenko, N. & López, A. M. Anti-ganglioside anti-idiotypic vaccination: more than molecular mimicry. *Front. Oncol.* **2,** 170 (2012).

Acknowledgements

This study was funded by grant BFU2013-47382-P and BFU2016-78398-P from the Spanish *Ministerio de Economía y Competitividad*, and by the *Centros de Investigación Biomédica en Red* (CIBER) at the *Instituto de Salud Carlos III*. We thank the *Generalitat de Catalunya* for funding our research group (2014/SGR525). I. Cabezón and E. Augé received the pre-doctoral *Ajuts de Personal Investigador en Formació* fellowship from the *Universitat de Barcelona* (APIF-UB).

Author Contributions

E.A., C.P. and J.V. participated in the design of the study. E.A., I.C., C.P. and J.V performed the experimental procedures, the microscope and data analysis, and the interpretation of results. E.A., C.P. and J.V. drafted the manuscript and participated in the critical review. All the authors have read and approved the final manuscript. C.P. and J.V. contributed equally to this study.

Additional Information

Competing financial interests: The authors declare no competing financial interests.

How to cite this article: Augé, E. *et al.* New perspectives on *corpora amylacea* in the human brain. *Sci. Rep.* **7**, 41807; doi: 10.1038/srep41807 (2017).

Publisher's note: Springer Nature remains neutral with regard to jurisdictional claims in published maps and institutional affiliations.

This work is licensed under a Creative Commons Attribution 4.0 International License. The images or other third party material in this article are included in the article's Creative Commons license, unless indicated otherwise in the credit line; if the material is not included under the Creative Commons license, users will need to obtain permission from the license holder to reproduce the material. To view a copy of this license, visit http://creativecommons.org/licenses/by/4.0/

© The Author(s) 2017

ARTICLE 3

CORPORA AMYLACEA IN HUMAN HIPPOCAMPAL BRAIN TISSUE ARE INTRACELLULAR BODIES THAT EXHIBIT A HOMOGENEOUS DISTRIBUTION OF NEO-EPITOPES

Elisabet Augé, Ingo Bechmann, Núria Llor, Jordi Vilaplana, Martin Krueger i Carme Pelegrí

2018, publicació en curs

RESUM

Objectius: Determinar la localització dels neo-epítops en els CA i estudiar la ultraestructura d'aquests cossos per aportar noves dades en quant a la seva formació i possible funció.

Material i mètodes: Es van utilitzar mostres post-mortem de cervell humà de 3 casos sense evidència de cap malaltia neurodegenerativa (63-76 anys) conservades amb formaldehid al 4%. Les mostres de teixit es van extreure de la regió d'hipocamp i es van tallar amb un vibràtom en seccions de 60 µm de gruix. Un grup d'aquestes seccions es van post-fixar durant una hora amb paraformaldehid al 4% i glutaraldehid al 0,1% en PBS i es van incubar amb IgMs anti-neo-epítop com a anticòs primari i un anticòs secundari biotinilat. El marcatge es va visualitzar amb DAB. L'altre grup de seccions es va post-fixar durant sis hores amb paraformaldehid al 4% i glutaraldehid a l'1 % en PBS. Posteriorment, totes les seccions es van processar per fer l'anàlisi ultrastructural fins obtenir seccions ultra-fines que es van visualitzar per microscòpia electrònica. Paral·lelament, es van dur a terme estudis d'immunofluorescència i microscòpia confocal, duent a terme marcatges dels neo-epítops en seccions de vibràtom de 60 µm de gruix i en seccions semifines de 0,5-1 µm de gruix.

Resultats: Els CA es troben delimitats per una membrana plasmàtica, fet que indica que són estructures intracel·lulars. La majoria presenten una estructura interna formada per fibres linears compactes, que en alguns casos semblen estar més concentrades a la part central. En alguns casos, s'observa també granulació fina en aquesta part interna. Al voltant de l'estructura interna s'observen amb freqüència mitocòndries, grànuls de glicogen i estructures membranoses en forma de vesícules o bombolles, que poden estar en contacte amb la part interna que conforma el cos. Aquests CA sovint es troben envoltats de filaments intermedis que podrien correspondre a filaments GFAP, com s'havia descrit prèviament (Leel-Ossy, 2001). Un petit nombre de CA, en canvi, presenta una zona interna menys compacta i menys estructurada que la majoria de CA. Aquests CA es caracteritzen per presentar, a la part interna, les estructures membranoses i les mitocòndries, així com també una absència de filaments intermedis al voltant del cos. Aquestes observacions suggereixen que aquests cossos corresponen a estadis primerencs de la formació dels CA. Els CA madurs tenen diàmetres més grans respecte els CA immadurs. Els marcatges dels neo-epítops en seccions de vibràtom i ens seccions semi-fines permeten posar de manifest que la immunoreactivitat de les IgMs es distribueix de manera homogènia en tot el cos, indicant una distribució homogènia dels neo-epítops en els CA.

Conclusions: El present treball mostra que els CA són inclusions citoplasmàtiques que es troben localitzades presumiblement en astròcits. La seva formació és intracel·lular on s'observa com mitocòndries i estructures membranoses s'integren a les fibres linears que conformen el cos. A més a més, s'han localitzat els neo-epítops en tota l'estructura dels CA. En concordança amb estudis previs, es corrobora que els CA presents en el cervell humà i en els grànuls PAS de ratolí comparteixen característiques morfològiques i tenen orígens similars.

Manuscript Click here to download Manuscript Auge CA.docx

Click here to view linked References

Title

Corpora amylacea in human hippocampal brain tissue are intracellular bodies that exhibit a homogeneous distribution of neo-epitopes

Authors

Elisabet Augé, PharM[1,2], Ingo Bechmann, MD, PhD[3], Núria Llor, PhD[4], Jordi Vilaplana, PhD[1,2,5], Martin Krueger, MD, PhD[3]*, Carme Pelegrí, PhD[1,2,5]*

ORCID Carme Pelegrí: 0000-0002-7734-1546
ORCID Jordi Vilaplana: 0000-0003-2113-238X

Affiliations:

[1] Secció de Fisiologia, Departament de Bioquímica i Fisiologia, Universitat de Barcelona, Barcelona, Spain

[2] Institut de Neurociències, Universitat de Barcelona, Barcelona, Spain

[3] Institute for Anatomy, University of Leipzig, Leipzig, Germany

[4] Secció de Química Terapèutica, Departament de Farmacologia, Toxicologia i Química Terapèutica, Universitat de Barcelona, Barcelona, Spain

[5] Centros de Biomedicina en Red de Enfermedades Neurodegenerativas (CIBERNED), Spain.

*** Corresponding authors** (these authors contributed equally to these work):

- Dr. Carme Pelegrí, Secció de Fisiologia, Departament de Bioquímica i Fisiologia, Facultat de Farmàcia i Ciències de l'Alimentació, Av. Joan XXIII 27-31, 08028 Barcelona, Spain. Phone: (+34) 93 4024505. E-mail: carmepelegri@ub.edu

- Dr. Martin Krueger, Institute for Anatomy, University of Leipzig, Eilenburger Str. 14-15, 04317 Leipzig, Germany. Phone: 49-341-9722 073. e-mail: martin.krueger@medizin.uni-leipzig.de

Acknowledgements:

This study was funded by grants BFU2013-47382-P and BFU2016-78398-P from MINECO, by Agencia Estatal de Investigación (AEI) and by European Regional Development Funds. It was also funded by *CIBER de Enfermedades Neurodegenerativas* from the *Instituto de Salud Carlos III*. We thank the *Generalitat de Catalunya* for funding our research group (2014/SGR525). E. Augé received a pre-doctoral "Ajuts de Personal Investigador en Formació" fellowship from the *Universitat de Barcelona* (APIF-UB). Collaboration with the Institute of Anatomy at the University of Leipzig was supported by a grant from the Fundació Agustí Pedro i Pons (UB). We are sincerely grateful to Christopher Evans and Michael Maudsley for correcting the English version of the manuscript. The authors thank Judith Craatz for her technical assistance in tissue preparation for electron microscopy.

Abstract

Corpora amylacea are spherical bodies of unknown origin and function, which accumulate in the human brain during the aging process and neurodegenerative disorders. In recent work, we reported that they contain some neo-epitopes that are recognized by natural IgMs, revealing a possible link between them and the natural immune system. Here, we performed an ultrastructural study complemented with confocal microscopy in order to shed light on the formation of corpora amylacea and to precisely localize the neo-epitopes. We show that immature corpora amylacea are intracellular astrocytic structures formed by profuse cellular debris and membranous blebs entrapped in a scattered mass of randomly oriented short linear fibers. In mature corpora amylacea, the structure becomes compacted and fibrillary material constitutes the principal component. We also determined that the neo-epitopes were uniformly localized throughout the whole structure. All these observations support the hypothesis that corpora amylacea are involved in the entrapment of damaged materials and non-degradable products. Moreover, they reinforce that the corpora amylacea of human brain are equivalent to another type of polyglucosan bodies named PAS granules. Further studies of both these structures will help to ascertain the function of corpora amylacea and their relationship with aging and neurodegenerative diseases.

Keywords

Polyglucosan body; Corpora amylacea; ultrastructure; neo-epitope; natural antibody

Introduction

Corpora amylacea (CA) are spherical or ovoid structures that measure 2 to 20 μm in diameter and accumulate primarily in the periventricular and subpial regions of the human brain during the aging process (Cavanagh 1999). They are positive to periodic acid-Schiff staining due to their high polysaccharide content, and when purified by a centrifugation procedure with final extraction in hot water, they yield a clear water-soluble fraction containing 87.9% hexose, 4.7% protein and 2.5% phosphate (Sakai et al. 1969). Although CA were described by J.E. Purkinje as far back as 1837, their origin and function remain unknown.

Ultrastructural analyses revealed that CA exhibit a complex structure in which the most conspicuous component is a compact mass of randomly oriented short linear fibers (8-12 nm). The bodies are regularly rounded, not membrane bound and often surrounded by glial fibrils (Ramsey 1965). Several authors indicate that CA are located within astrocytic processes (Leel-Ossy 2001; Palmucci et al. 1982; Ramsey 1965; Sbarbati et al. 1996), while others described them as intra-axonal inclusions (Agari et al. 1975; Mizutani et al. 1987; Woodford and Tso 1980). However, they have not been reported within neuronal perikarya. In any case, it seems that CA are seen less often within neuronal processes than within astrocytic processes (Anzil et al. 1974), and there is no doubt that, in the subpial region, they are found mainly within astrocyte processes. Sbarbati et al. (1996) observed them in astroglial processes in biopsy material from the vestibular root entry zone in cases of Ménière's disease and suggested that CA escape across the glia-limiting lamina into the pial connective tissue or subpial space. It appears, thus, that this may be a feasible escape route into the cerebrospinal fluid. The presence of waste elements is a recurrent feature of CA. CA may be involved in the trapping and sequestration of potentially hazardous products (Cavanagh 1999) and they may act as a system that cleans the central nervous system (Augé et al. 2017, Sbarbati et al. 1996).

CA have been associated with PAS granules, degenerative granular structures that appear progressively with age in the mouse brain (Augé et al. 2017; Manich et al. 2016). The analysis of the PAS granule ultrastructure has been subject to extensive studies. PAS granules contain a central core of electron-dense crystalline-like fibrillary

deposits that appear to be composed of degenerated membrane-like structures, surrounded by a halo or translucent region that is separated by a slightly discontinuous plasma membrane, thus confirming the intracellular location of these structures (Kuo et al. 1996; Manich et al. 2014a; Robertson et al. 2000). The presence of GFAP fibrils in the halo of the granule, glycogen accumulations and specific astrocyte-astrocyte junctions with adjacent membranes made it possible to determine that the granules were located in astrocytic processes. Although mature PAS granules are highly structured, immature PAS granules do not present the compact central core, and are characterized by sparse fibrils or scattered membranous-like structures in which some components as degenerating mitochondria can be integrated. Thus, PAS granules seem to be formed via the aggregations of damaged components of various kinds (Manich et al. 2014a). Although mouse PAS granules and human CA may be equivalent structures, and so the genesis of CA may be similar to that of PAS granules, their formation has not yet been described. This is one of the focuses of the present study.

Recently we reported that both CA and PAS granules contain neo-epitopes that can be recognized by natural IgMs (Augé et al. 2017; Manich et al. 2014b, 2015). Neo-epitopes are epitopes that originate de novo in certain circumstances and can trigger an immune response. Natural IgM antibodies are antibodies that have been fixed by natural selection during evolution and are thus interspecific; they are present in the blood plasma from birth without prior contact with external antigens. Accordingly, we found that the IgMs directed against the neo-epitopes sited on CA and PAS granules are present in sera from different species such as human, mouse, rat, goat or rabbit, and also in sera from both human umbilical cord and mouse maintained under specific opportunistic pathogen-free conditions, i.e., before external antigen exposure. Thus, the presence of neo-epitopes that can be recognized by natural IgMs on both CA and PAS granules indicates that organisms are permanently equipped with antibodies prepared to react against them. These studies highlighted a new link between these age-related deposits and the innate immune system. In the case of PAS granules, ultrastructural studies revealed that the neo-epitopes are located in the core of the granules, specifically in the membranous-like fragments (Manich et al. 2014a). However, we do not yet know the site of the neo-epitopes present on CA.

Therefore, the present study aimed to investigate the ultrastructure of CA in order to shed light on its formation and compare it with mouse PAS granules, and to determine the location of neo-epitopes in CA using immunofluorescence and electron microscopy in human autoptic brain tissue.

Material and methods

Tissue

Three human post-mortem brain samples were obtained from body donors (63-76 years old, without evidence of any neurodegenerative diseases) from the Institute of Anatomy at Leipzig University after institutional approval for the use of post-mortem tissues from the Institute of Anatomy at Leipzig University and in accordance with the Saxonian Death and Funeral Act of 1994, third section, paragraph 18, item 8. All authors declare that all experiments were conducted according to the principles of the Declaration of Helsinki.

Human brain samples were stored in 4% buffered formaldehyde and tissue was taken from the hippocampal region. Tissue samples were cut at 60 µm on a vibrating microtome (Leica) in phosphate buffered saline (PBS) at pH 7.4.

Electron microscopy

Some 60 µm vibratome sections were post-fixed for 1 h using a fixative containing freshly prepared 4% paraformaldehyde and 0.1% glutaraldehyde in PBS and incubated with anti-tau IgG antibody produced in mouse ascites (clone Tau5, ref. MAB361, lot #2890998, Merck Millipore, dilution 1/100). We took the same antibody used in previous work (Augé et al. 2017), in which we determined that the vial contained contaminant mouse IgMs directed against the neo-epitopes present in CA and can be used to label these structures. This staining was visualized with an anti-mouse IgM biotin-conjugated secondary antibody and 3,3'-Diaminobenzidine (DAB). These sections will be referred to as immunostained sections. Other sections, referred to as native sections, were post-fixed for 6 h using a PBS solution with 4% paraformaldehyde and 1% glutaraldehyde. Immunostained and native sections were then processed for

electron microscopy, stained with 0.5% OsO_4 followed by dehydration in graded alcohol and additional staining with 1% uranyl acetate in 70% alcohol for 60 min. After subjecting the section to the corresponding progressive dehydration, they were embedded in Durcupan (Sigma-Aldrich) between coated microscope slides and cover glasses and the resin was polymerized for 48 h at 56ºC. It was therefore possible to identify and precisely trim areas containing CA at the level of light microscopy. Semi-thin (500 nm to 1 μm) and ultra-thin (55 nm) sections were obtained using an ultra-microtome (Leica Ultracut R, Leica). Ultra-thin serial sections were collected using Formvar-coated single-slot grids and then incubated in lead citrate for 5 min. The ultrastructural analysis was performed with a Zeiss SIGMA electron microscope.

Immunofluorescence

In order to study the location of neo-epitopes in CA, immunofluorescence studies were performed. Vibratome sections were blocked and permeabilized with 3% bovine serum albumin (Sigma-Aldrich) in PBS with 0.3% Triton X-100 (Sigma-Aldrich) for 30 min. After washing the sections with PBS, they were incubated with the anti-tau IgG antibody previously referenced, which contains mouse anti-neo-epitope IgMs, and chicken polyclonal 200kDa neurofilament heavy (NEFH) primary antibody (1/200, OriGene) overnight at 4ºC. Afterwards, the sections were washed and incubated for 2 h at room temperature using fluorochrome-labeled secondary antibodies (Alexa Fluor (AF) 488 goat anti-mouse IgM, 1/250, Jackson ImmunoResearch Laboratories; AF647 goat anti-chicken IgG, 1/250, Invitrogen). 4’6-Diamidin-2-phenylindol (DAPI) was used to visualize nuclei. Omitting the primary antibodies in control experiments resulted in the absence of staining, as expected.

In addition, semi-thin native sections were used to perform immunofluorescence staining. These sections were obtained as described previously for the electron microscopy study, whereas OsO4 and uranyl acetate staining were omitted and Epon resin was used instead of Durcupan. After removing the resin with a mixture of sodium methoxide solution (Sigma) and a methanol/toluene solution, sections were blocked and permeabilized with 3% bovine serum albumin (Sigma-Aldrich) in PBS with 0.3% Triton X-100 (Sigma-Aldrich) for 30 min. After washing the sections with PBS, they were incubated with anti-tau IgG antibody produced in mouse ascites (1/100, Merck

Millipore), which contains mouse anti-neo-epitope IgMs, and rabbit polyclonal α-GFAP primary antibody (1/200, Dako) for 1.5 h at room temperature. Afterwards, the sections were washed and incubated for 1.5 h at room temperature using fluorochrome-labeled secondary antibodies (AF488 goat anti-mouse IgM, 1/250, Jackson ImmunoResearch Laboratories; AF568 goat anti-rabbit IgG, 1/250, Invitrogen).

To assess the IgM staining of CA in vibratome and semi-thin sections, confocal laser scanning microscopy (Olympus Fluoview 1000 confocal microscope) and Fluoview software were used.

Measurement of CA diameter and statistical analysis

The diameters of different CA were measured on obtained images by using the Image J program (National Institute of Health, USA). For each CA, we first defined the region of interest (ROI) manually tracing the contour of the CA by using the "freehand selection" tool of the image J program. Thereafter, for each ROI, the Feret's diameter (the longest distance between any two points along the selection boundary, also known as maximum calliper) was obtained. To compare the Feret's diameter of mature and immature CA, statistical analyses were performed by means of t-test for independent samples by using Statistica for Windows (Stat Soft Inc.). Differences were considered statistically significant when $p < 0.05$.

Results

Ultrastructural study of corpora amylacea in the human hippocampal brain

Native electron microscopy analysis was used to characterize CA. Since the number of CA in the human brain increases during aging and also during the progression of neurodegenerative diseases, we assumed that the human brain samples used would present not only a high number of already constituted CA but also a number of CA in formation.

The majority of CA observed were similar to the ones previously described in the literature and summarized in Fig. 1. They were delimited by a plasma membrane, confirming their intracellular location, and they exhibited an internal structure of densely packed, randomly oriented short linear fibers, which in some cases seemed to concentrate more in the central region. Some fine granulation was often observed in these internal structures. Moreover, mitochondria and glycogen granules were recurrently observed around the body, and irregularly shaped membranous blebs were seen near or in contact with the packed fibers. These CA were usually surrounded by intermediate filaments. This latter observation was also made by Leel-Ossy (2001), who described these filaments as astrocytic GFAP filaments.

A small number of CA, however, presented a less compact internal structure and were poorly structured and smaller than the majority (Fig. 2). The core of these CA was characterized by sparse fibrils, and the irregularly shaped membranous blebs were found not only around but also inside the fiber region, forming some multilamellar bodies. Some mitochondria were also observed around the fiber region, and some inside the internal structure. There was no evidence of intermediate filaments surrounding the bodies. Being less numerous, smaller, less compact, and more poorly structured than the CA previously described, we concluded that these structures corresponded to CA in early stages of their formation, i.e. immature CA. All these observations are analogous to the ones described previously for PAS granules in the mouse brain, which are equivalent to CA in the human brain (Manich et al. 2014a). Thus, in both cases, the bodies appear to be formed from the aggregation of certain components.

When quantifying the diameter of both types of CA, we obtained a mean Feret's diameter of mature CA (n=31) of 12.13 μm (±0.69 μm), with a maximum diameter of 18.41 μm and a minimum of 4.49 μm, and a mean Feret's diameter of immature CA (n=10) of 5.37 μm (±0.77 μm), with a maximum diameter of 11.36 μm and a minimum of 1.87 μm. The Student's t-test for non-paired data showed statistically significant differences between the Feret's diameters of the two types of CA, being t_{39}=5.18 and $p<0.001$. We thus conclude that mature CA are larger than the immature ones.

Localization of neo-epitopes in corpora amylacea

Electron-microscopic analysis of ultra-thin sections obtained from immunostained vibratome sections revealed that IgM staining was confined to the periphery of the body, while the surrounding plasma membrane was often partially lost due to the immunoperoxidase reactivity. The core of the structures regularly appeared to be devoid of IgM immunoreactivity (Fig. 3).

These findings were confirmed by immunofluorescence labeling of anti-neo-epitope IgMs in combination with anti-NEFH in 60µm vibratome sections. Here, the IgM-related immunoreactivity was confined to the surface of CA, while the core regularly appeared to be devoid of any immunolabeling (Fig. 4a-b). Importantly, NEFH immunoreactivity did not co-localize with IgM immunolabeling of neo epitopes.

However, the rather peripheral staining pattern may not reflect the actual distribution of neo-epitopes throughout the entire body of individual CA. In fact, the densely packed structure is likely to prevent complete penetration of the antibody applied, rendering the immunolabeling in the center of the structures impossible. In order to exclude the hypothesized penetration problems, we further performed immunofluorescence labeling of IgM-related neo-epitopes in combination with anti-GFAP in serially cut semi-thin sections of 500nm - 1µm thickness. Here, cross-sectioning respective CA uniformly reveals the antigens at the sectioned surface throughout the whole body of CA. With this approach, cross-sectioned CA revealed a homogeneous immunoreactivity of IgM-related neo-epitopes, which included the core regions (Fig. 4c-d). Moreover, and in line with the NEFH-related immunoreactivity, immunolabeling for GFAP did not co-localize with IgM immunoreactivity, although individual CA appeared to be ensheathed in astrocytic GFAP-filaments.

Discussion

This study was designed to investigate the ultrastructure of CA from the human hippocampal brain in order to shed light on its formation and to provide new data about the location of neo-epitopes within these structures.

Our results confirm that CA are intracellular formations. Leel-Ossy (2001) suggested that the cytoplasmic localization of CA could be proven by the presence of a nearby shrunken nucleus of an astrocyte. Here, we demonstrate that CA are surrounded by a plasma membrane and contain cytoplasmic organelles such as mitochondria, which confirms their intracellular location. Further, most CA appeared to be surrounded by intermediate filaments, which were shown to represent GFAP filaments at the level of fluorescence microscopy. These results are in line with earlier reports suggesting that the surrounding intermediate filaments correspond to astrocytic GFAP (Leel-Ossy 2001; Notter and Knuesel 2013; Palmucci et al. 1982; Ramsey 1965), although other authors have pointed out that the presence of CA in axons cannot be ruled out (Agari et al. 1975; Anzil et al. 1974; Mizutani et al. 1987; Woodford and Tso 1980). We show here that most CA consist of a compacted mass of randomly oriented short linear structures, which are usually surrounded by some membranous elements and mitochondria. This is consistent with previous descriptions of the ultrastructure of CA (Leel-Ossy 2001; Ramsey 1965; Woodford and Tso 1980).

Moreover, in this study we observed some CA in early stages. To our knowledge, this is the first study to show the ultrastructure of the immature CA. We observed that immature CA present certain distinctive characteristics with respect to mature CA: early CA contain an inner region that is less structured and less compact than in mature CA. They also contain abundant cellular debris, membranous blebs and mitochondria, which are located not only surrounding the inner structure but also included in it. Although little is known about the formation of CA and their role, these results are consistent with the suggestions made by other authors that CA are bodies involved in the entrapment of damaged materials and non-degradable products. Products of oxidative damage from mitochondria and other proteins, and other potentially damaging materials or non-degradable products generated in the process of aging, are likely to become entrapped in these structures formed in astrocytes and with a content based on polymerized sugar molecules (Augé et al. 2017; Cavanagh 1999; Leel-Ossy 2001; Schipper 2004).

A wide range of studies have linked CA to mouse PAS granules (Jucker et al. 1992, 1994a, b; Jucker and Ingram 1994; Manich et al. 2016; Mitsuno et al. 1999; Robertson et al. 1998; Sinadinos et al. 2014). In previous studies (Augé et al. 2017; Manich et al.

2015), we demonstrated that CA from the human brain and PAS granules from mice present neo-epitopes that can be recognized by natural antibodies. The present study identifies other similarities between CA from the human brain and PAS granules from mice, as indicated by some shared ultrastructural characteristics. Being ensheathed by a plasma membrane, both structures present a fibrillar core, usually surrounded by GFAP filaments, and membranous structures that form blebs as well as mitochondria adjacent to the core (Fig. 5). In addition, the ultrastructural study of immature PAS granules (Manich et al. 2014a) demonstrated that such granules presented a central core with sparse fibrils rather than an electron-dense core, in line with the results of the present study with respect to less compact CA. Although their size, distribution and some staining properties are different and should be taken into consideration, our results reinforce the idea that CA and PAS granules are similar structures and that the study of mouse granules might help clarify certain aspects of the nature and development of human CA.

Regarding the neo-epitopes present in CA, immunofluorescence labeling demonstrated that IgM-labeled neo-epitopes are homogeneously distributed throughout the whole body of CA. Although pre-embedding staining in vibratome sections and the subsequent electron microscopy analysis showed that IgM-related immunoreactivity was confined to the periphery of the structure, analysis of semi-thin sections (500 nm to 1 μm) demonstrated that neo-epitopes did not appear exclusively in the periphery of the CA, but also inside the core of the structures. These results are consistent with the study of neo-epitope localization in mouse granules, in which the post-embedding labeling immunoelectron microscopy showed that the neo-epitopes were located mainly in the membrane-like fragments of the whole granule (Manich et al. 2014a). Although the post-embedding labeling immunoelectron microscopy technique seems to perform better for determining the location of the neo-epitopes, with human brain samples the tissue preservation and manipulation made this procedure difficult, particularly because of the postmortem delay. In fact, few studies of post-embedding labeling immunoelectron microscopy in human brain tissue are available. In any case, the results indicate that neo-epitopes are located throughout the CA. They also show that, in immunohistochemical studies of CA, some epitopes of the central part (compact zone) are not always accessible and can only be labeled when CA has been sliced. Therefore, the immunohistochemical studies of CA in which the authors indicate that the

component analysed is located only in the periphery of the body must be revised in order to rule out this methodological problem.

In conclusion, the present study suggests that CA are intracytoplasmic inclusions presumably located in astrocytes. Their formation takes place inside the cell, where non-degradable products become aggregated. Moreover, the neo-epitopes they contain are located throughout the whole structure. In concordance with previous studies, we also corroborate that CA from human brain and PAS granules from mice share morphological features and probably a similar origin. However, further studies are required to clarify the cause of CA formation and to reveal the nature and function of neo-epitopes.

References

Agari KM, Nakamura H (1975) Intra-axonal corpora amylacea in ventral and lateral horns of the spinal cord. Acta Neuropathol 11:151–8

Anzil AP, Herrlinger H, Blinzinger K et al (1974) Intraneuritic corpora amylacea. Virchows Arch A Pathol Anat Histol 364: 297–301

Augé E, Cabezón I, Pelegrí C et al (2017) New perspectives on corpora amylacea in the human brain. Sci Rep 7: 41807

Cavanagh JB (1999) Corpora-amylacea and the family of polyglucosan diseases. Brain Res Rev 29: 265-95

Jucker M, Ingram DK (1994) Age-related fibrillary material in mouse brain: assessing its potential as a biomarker of aging and as a model of human neurodegenerative disease. Ann NY Acad Sci 719: 238-47

Jucker M, Walker LC, Kuo H et al (1994a) Age-related fibrillar deposits in brains of C57BL/6 mice. A review of localization, staining characteristics, and strain specificity. Mol Neurobiol 1994; 9: 125–33

Jucker M, Walker LC, Martin LJ et al (1992) Age-associated inclusions in normal and transgenic mouse brain. Science 255:1445

Jucker M, Walker LC, Schwarb P et al (1994b) Age-related deposition of glia-associated fibrillar material in brains of C57BL/6 mice. Neuroscience 60: 875–89

Kuo H, Ingram DK, Walker LC et al (1996) Similarities in the age-related hippocampal deposition of periodic acid-schiff-positive granules in the senescence-accelerated mouse P8 and C57BL/6 mouse strains. Neuroscience 74: 733–40

Leel-Ossy L (2001) New data on the ultrastructure of the corpus amylaceum (polyglucoan body). Pathol Oncol Res 7: 145-50

Manich G, Augé E, Cabezón I et al (2015) Neo-epitopes emerging in the neurodegenerative hippocampal granules of aged mice can be recognized by natural IgM auto-antibodies. Immun Ageing 12: 23

Manich G, Cabezón I, Augé E et al (2016) Periodic acid-Schiff granules in the brain of aged mice: From amyloid aggregates to degenerative structures containing neo-epitopes. Ageing Res Rev 2016; 27: 42–55

Manich G, Cabezón I, Camins A et al (2014a) Clustered granules present in the hippocampus of aged mice result from a degenerative process affecting astrocytes and their surrounding neuropil. Age 2014; 36: 9690

Manich G, Del Valle J, Cabezón I et al (2014b) Presence of a neo-epitope and absence of amyloid beta and tau protein in degenerative hippocampal granules of aged mice. Age 36: 151– 65

Mitsuno S, Takahashi M, Gondo T et al (1999) Immunohistochemical, conventional and immunoelectron microscopical characteristics of periodic acid-Schiff-positive granules in the mouse brain. Acta Neuropathol 98: 31–8

Mizutani T, Satoh J, Morimatsu Y (1987) Axonal polyglucosan body in the ventral posterolateral nucleus of the human thalamus in relation to aging. Acta Neuropathol 74: 9–12

Notter T, Knuesel I (2013) Reelin immunoreactivity in neuritic varicosities in the human hippocampal formation of non-demented subjects and Alzheimer's disease patients. Acta Neuropathol Commun 1: 27

Palmucci L, Anzil AP, Luh S (1982) Intra-astrocytic glycogen granules and corpora amylacea stain positively for polyglucosans: a cytochemical contribution on the fine structure polymorphism of particulate polysaccharides. Acta Neuropathol 57: 99–102

Ramsey HJ (1965) Ultrastructure of corpora amylacea. J Neuropathol Exp Neurol 24: 25-39

Robertson TA, Dutton NS, Martins RN et al (1998) Age-related congophilic inclusions in the brains of apolipoprotein E-deficient mice. Neuroscience 82: 171–80

Robertson TA, Dutton NS, Martins RN et al (2000) Comparison of astrocytic and myocytic metabolic dysregulation in apolipoprotein E deficient and human apolipoprotein E transgenic mice. Neuroscience 98: 353–9

Sakai M, Austin J, Witmer F et al (1969) Studies of corpora amylacea: I. Isolation and preliminary characterization by chemical and histochemical techniques. Arch Neurol 21:526–44

Sbarbati A, Carner M, Colletti V et al (1996) Extrusion of corpora amylacea from the marginal glia at the vestibular root entry zone. J Neuropathol Exp Neurol 55: 196–201

Schipper HM (2004) Brain iron deposition and the free radical-mitochondrial theory of ageing. Ageing Res Rev 3:264-301

Sinadinos C, Valles-Ortega J, Boulan L et al (2014) Neuronal glycogen synthesis contributes to physiological aging. Aging Cell 13: 935–45

Woodford B, Tso MO (1980) An ultrastructural study of the corpora amylacea of the optic nerve head and retina. Am J Ophthalmol 90: 492–502

Figure legends

Fig. 1 Electron microscopy images of hippocampal corpora amylacea (CA) from the human brain. a, c and **e:** Images of different CA**.** As shown in **b** (inset of **a**), CA consist of short linear structures that appear to be concentrated in the central part. In **d** (inset of **c**), the presence of a plasma membrane (full arrows) surrounding the CA confirms their intracellular location. Some mitochondria (full arrowheads) and glycogen granules can be observed near the body. As shown in **f** (inset of **e**), CA show membranous structures that form irregularly shaped blebs (asterisks), as well as intermediate filaments (empty arrowheads) surrounding the central part. Scale bar in **a**, **c** and **e** 3 μm. Scale bar in **b**, **d** and **f** 1 μm

Fig. 2 Electron microscopy images of less compact corpora amylacea (CA) from the human hippocampal brain. a, c and **f:** Images of different less compact CA. These CA present a different pattern of compaction that could correspond to an early stage in the formation of these structures. These pattern of compaction can be shown magnified in **b** (inset of **a**). In **d** and **e** (insets of **c**), a higher number of mitochondria can be observed in the space between the CA and the plasma membrane. Moreover, some cellular debris (empty arrowheads), multilamellar bodies (full arrowheads) and membranous structures forming blebs (asterisks) can be observed in **g** and **h** (insets of **f**). Scale bar in **a**, **c** and **f** 2 μm. Scale bar in **b**, **d**, **e**, **g** and **h** 500 nm

Fig. 3 Electron microscopy images of IgM labeled hippocampal corpora amylacea (CA) from the human brain. a and **c:** IgM staining, shown as dark regions due to DAB grains, was confined mainly to the periphery of the body, while the core of the structure was free from IgM immunoreactivity. **b** and **d** are insets of **a** and **c**, respectively. Scale bar in **a** and **c** 5 μm. Scale bar in **b** and **d** 1 μm

Fig. 4 Confocal microscopy images of hippocampal corpora amylacea (CA) from the human brain. a and **b:** 60 μm vibratome sections simultaneously immunostained with mouse IgMs against neo-epitopes (green) and with anti-neurofilament heavy (NEFH) (red). 4'6-Diamidin-2-phenylindol (DAPI) (blue) was used for nuclear staining. Of note, IgM-related immunolabeling is limited to the outer surface. **c** and **d:** Semi-thin 500 nm sections simultaneously immunostained with mouse IgMs against neo-epitopes

(green) and with anti-glial fibrillary acidic protein (GFAP) (red). In semi-thin sections, but not in vibratome sections, CA become sliced and IgMs can reach the centre of the structure. These results indicate that neo-epitopes are present in the whole CA. CA appear to be ensheathed in astrocytic GFAP-filaments (arrowheads), but not NEFH. Scale bar: 10 μm

Fig. 5 Comparison of hippocampal human corpora amylacea **(**CA) (**a**) and hippocampal mouse PAS granules (**b)** (Manich et al. 2014a) at an ultrastructural level. Short fibrillar elements constitute the inner structure of both bodies, which present a plasma membrane surrounding them, membranous structures that form blebs and some mitochondria close to the central part. Differences in the staining intensity are due to methodological procedures, while differences in the quality of the ultrastructure within the surrounding neuropil are related to the unavoidable post mortem delay in human samples. Scale bar 1 μm

Figure 1

Click here to download colour figure Fig1.tif

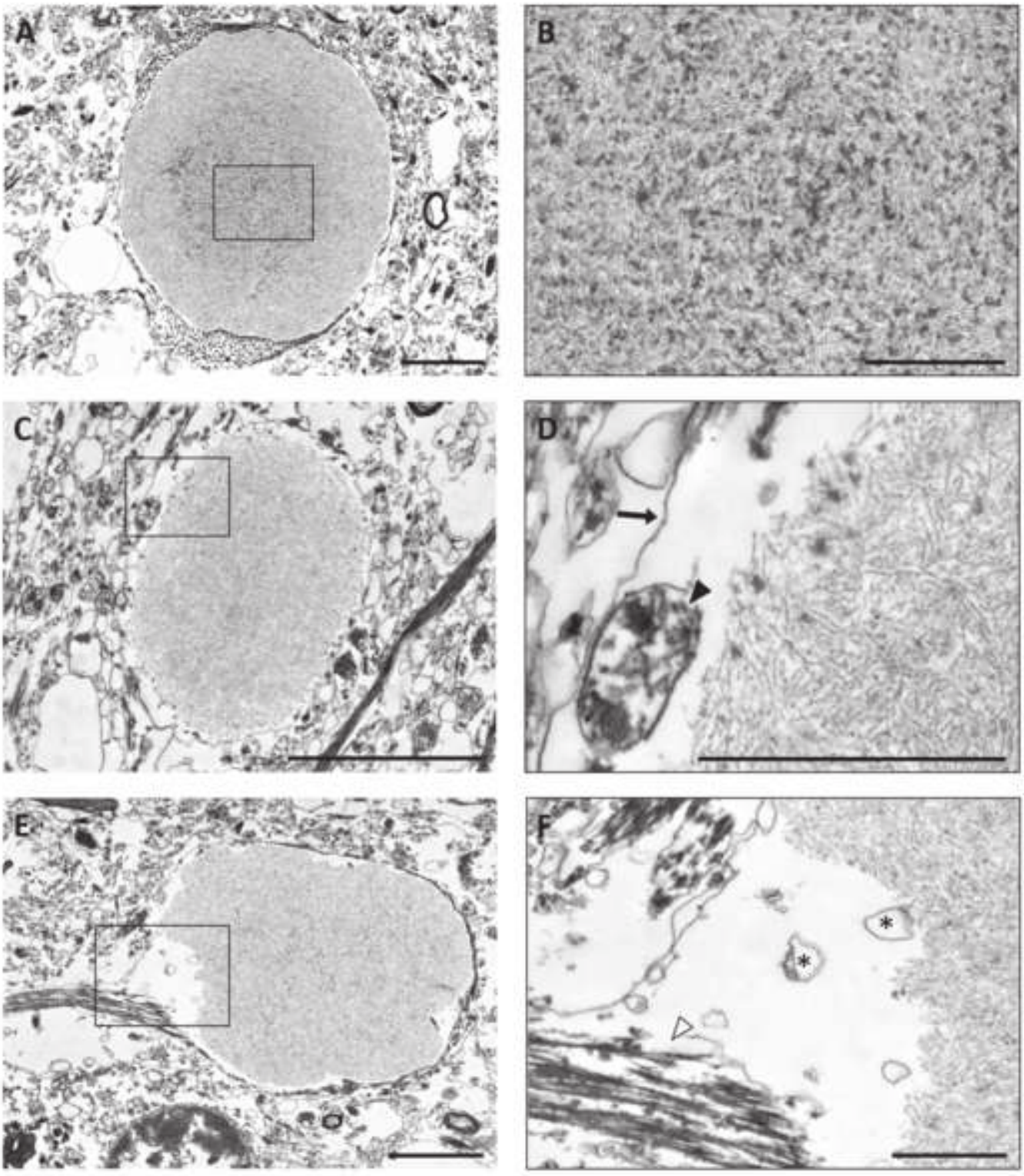

Figure 2

Click here to download colour figure Fig2.tif

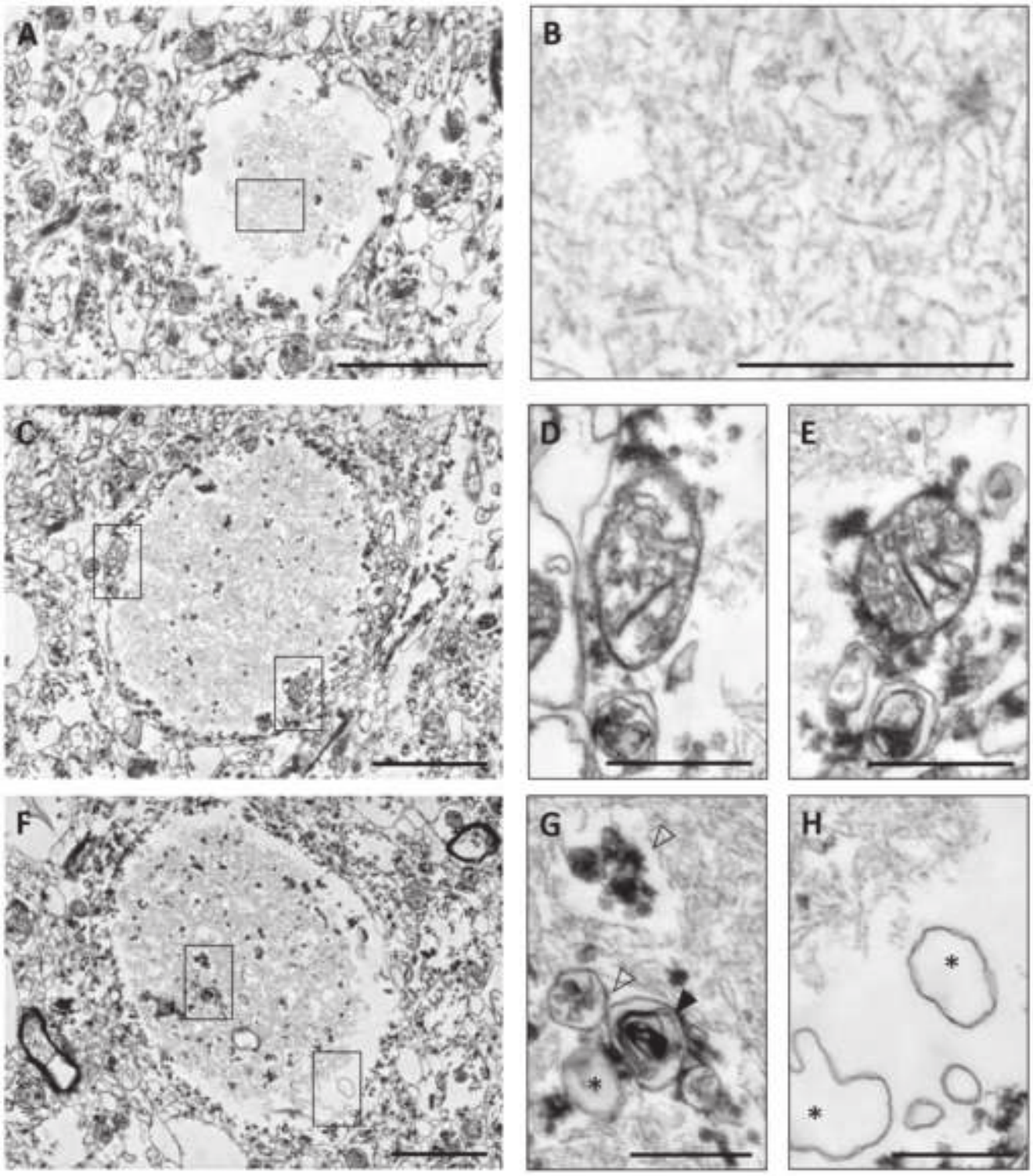

Figure 3

Click here to download colour figure Fig3.tif

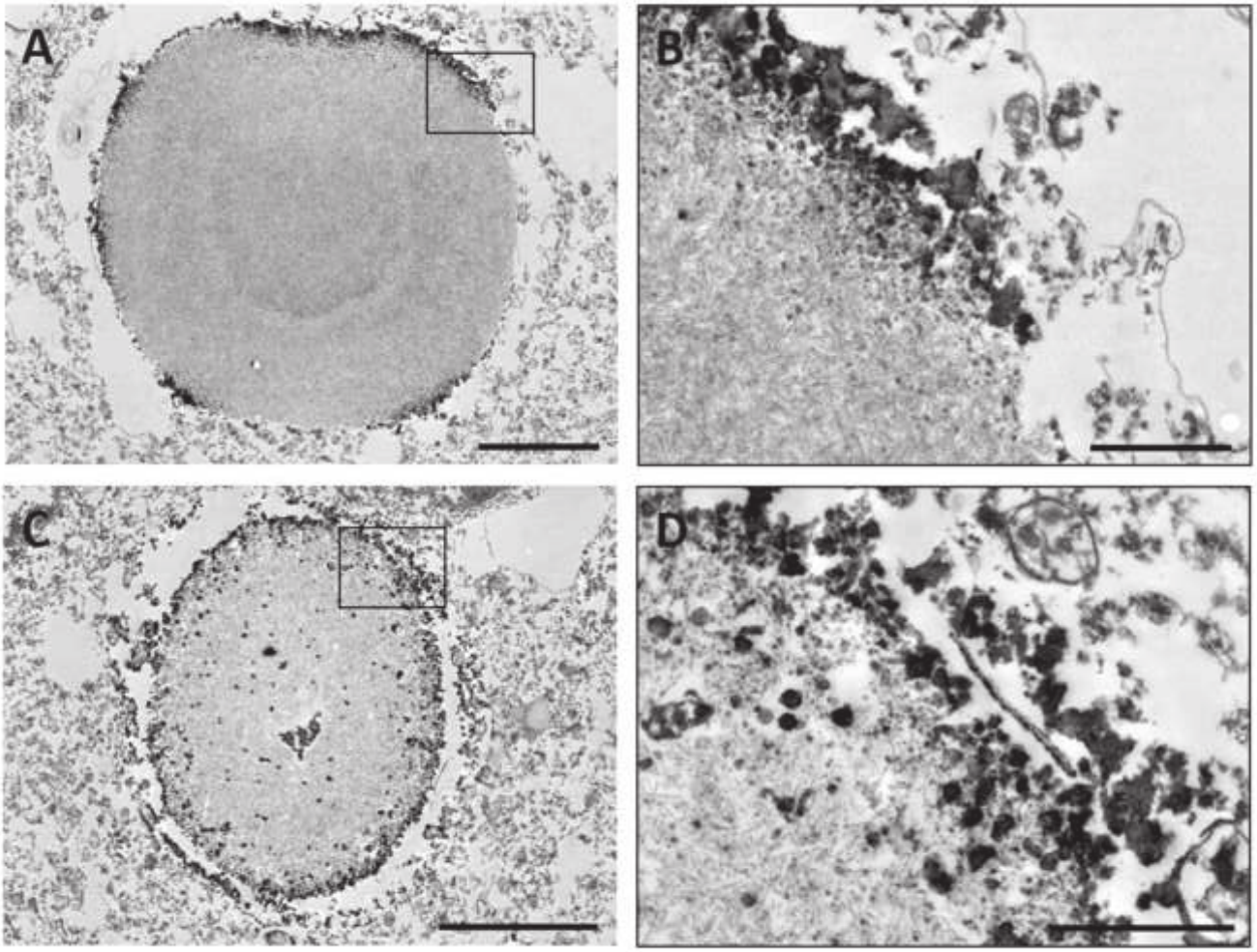

Figure 4

Click here to download colour figure Fig4.tif

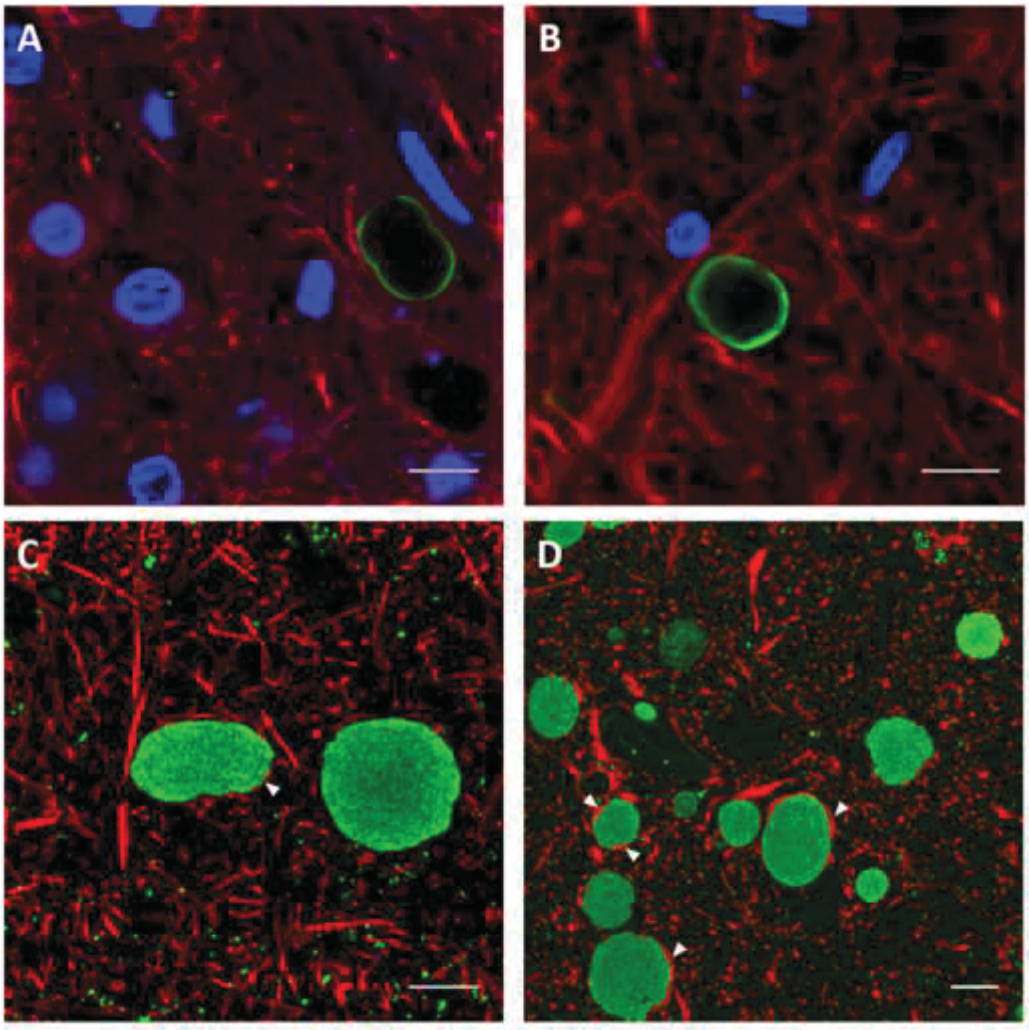

Figure 5

Click here to download colour figure Fig5.tif

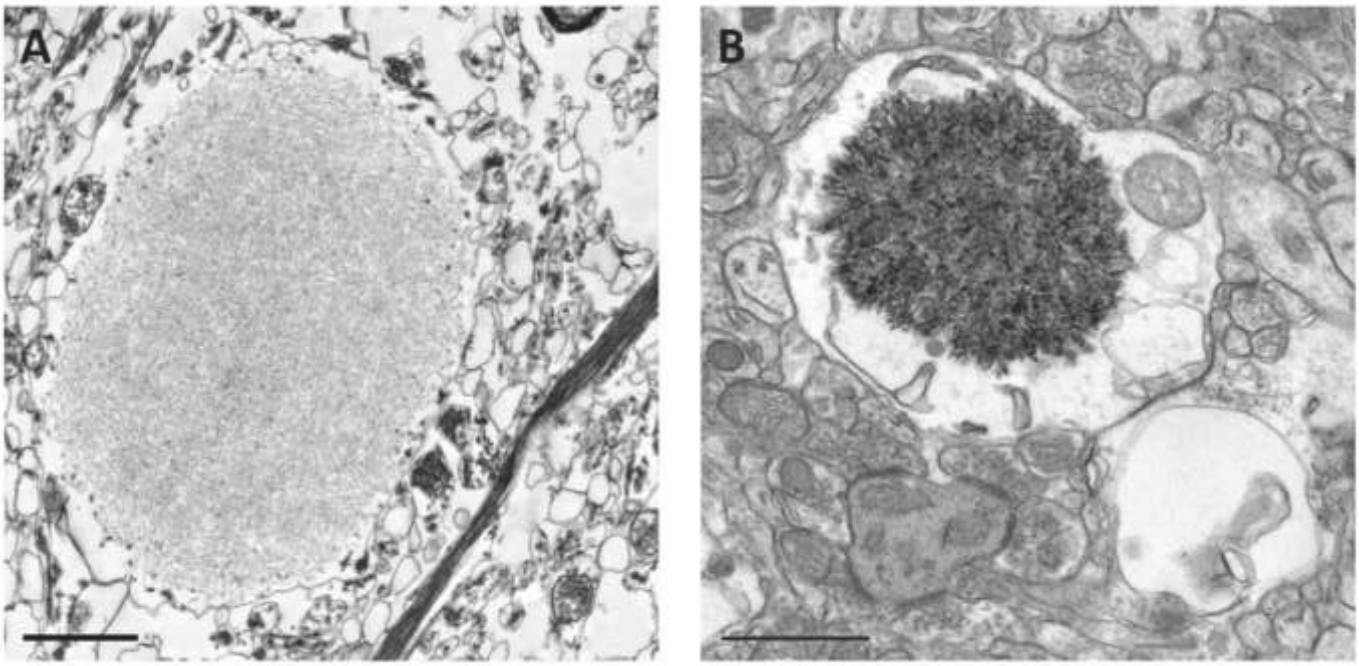

ARTICLE 4

DEFINING THE COMPOSITION OF CORPORA AMYLACEA IN HUMAN BRAIN: HITS AND MISSES

Elisabet Augé, Jordi Duran, Joan J. Guinovart, Carme Pelegrí i Jordi Vilaplana

Scientific Reports 2018, en fase de revisió

RESUM

Objectius: D'una banda, revisar la presència de determinats components descrits prèviament en els CA humans i determinar també la presència de determinats components potencials que no havien estat descrits amb anterioritat. D'altra banda, i com a objectiu relacionat amb l'anterior, conèixer la funció d'aquestes estructures cerebrals.

Material i mètodes: Es van utilitzar seccions criostàtiques d'hipocamp humà de quatre casos de malaltia d'Alzheimer (81-88 anys) i d'un cas no associat a malaltia d'Alzheimer (70 anys). Es va realitzar la tinció de PAS per verificar la presència de CA en tots ells. Es van aplicar tècniques d'immunofluorescència utilitzant diferents anticossos primaris dirigits contra diferents proteïnes que havien estat descrites amb anterioritat (GFAP, S100B, AQP4, NeuN, β-tubulina classe III i ubiqüitina) així com també d'altres que no havien estat descrites prèviament (p62, GS i metal·loproteinasa de matriu 2 (MMP2)). També en alguns casos es van dur a terme dobles marcatges. Les mostres es van analitzar per microscòpia de fluorescència i confocal. Tots els marcatges es van realitzar evitant possibles falsos marcatges causats per IgMs contaminants.

Resultats: Mitjançant l'ús d'anticossos secundaris isotip específics i tenint en compte la presència d'IgMs naturals com a contaminants en alguns dels anticossos comercials, es va descartar la presència dels marcadors astrocítics GFAP, S100B i AQP4, i dels marcadors neuronals NeuN i β-tubulina classe III, els quals havien estat descrits amb anterioritat per alguns autors. Es va confirmar, en canvi, la presència d'ubiqüitina en els CA humans. En avaluar la presència d'altres possibles components, es va determinar que els CA contenen p62, GS i MMP2. La ubiqüitina i la p62 són proteïnes que poden interaccionar, i per tant, es van fer estudis de co-localització d'aquestes dues proteïnes, i es van complementar també amb estudis de co-localització amb la GS. Els resultats obtinguts mostren que la GS i la p62 es troben majoritàriament localitzades a la perifèria dels CA, mentre que la ubiqüitina mostra marcatge perifèric i central. Aquests resultats suggereixen que els CA no constitueixen únicament l'agregació de polímers de glucosa insolubles que contenen proteïnes, sinó estructures amb dues regions diferenciades. La part perifèrica esdevindria la part activa o en creixement, on la GS aniria formant nous polímers de glucosa i la p62 podria interaccionar amb les substàncies ubiqüitinades, mentre que la part central seria la regió estable on els polímers de glucosa retindrien les substàncies ubiqüitinades. No s'han trobat diferències entre els CA dels cervells dels malalts d'Alzheimer i els CA dels cervells no associats a aquesta malaltia.

Conclusions: El present treball mostra que els CA no contenen alguns dels marcadors que havien estat descrits amb anterioritat i exposa que les IgMs naturals podrien ser les responsables d'altres marcatges que s'haurien de revisar. Per altra banda, es posa de manifest que els CA contenen ubiqüitina, GS, p62 i MMP2. La presència d'alguns d'aquests marcadors reforça la hipòtesi que diu que els CA són unes estructures que podrien estar involucrades en mecanismes de neteja cerebral.

Defining the composition of *corpora amylacea* in human brain: hits and misses

Authors: Elisabet Augé[1,2], Jordi Duran[3,4], Joan Guinovart[3,4,5], Carme Pelegrí [1,2,6,◊], Jordi Vilaplana [1,2,6,◊,*]

[◊]These authors contributed equally to this study

Affiliations: [1]Secció de Fisiologia, Departament de Bioquímica i Fisiologia, Facultat de Farmàcia i Ciències de l'Alimentació, Universitat de Barcelona, Barcelona, Spain. [2]Institut de Neurociències, Universitat de Barcelona, Barcelona, Spain. [3]Institute for Research in Biomedicine (IRB Barcelona), The Barcelona Institute of Science and Technology, Barcelona, Spain. [4]Centro de Investigación Biomédica en Red de Diabetes y Enfermedades Metabólicas Asociadas (CIBERDEM), Spain. [5]Departament de Bioquímica i Biomedicina Molecular, Universitat de Barcelona, Barcelona, Spain. [6]Centro de Investigación Biomédica en Red de Enfermedades Neurodegenerativas (CIBERNED), Spain.

[*]**Corresponding author:** Dr. Jordi Vilaplana, Secció de Fisiologia, Departament de Bioquímica i Fisiologia, Facultat de Farmàcia i Ciències de l'Alimentació, Av. Joan XXIII 27-31. 08028 Barcelona, Spain. Tel. (+34) 93 4024505. E-mail: vilaplana@ub.edu

Keywords: Polyglucosan body, *corpora amylacea*, neo-epitope, natural antibody, p62, ubiquitin, aging.

ABSTRACT

Corpora amylacea (CA) are polyglucosan bodies that accumulate in the human brain during ageing and are also present in large numbers in neurodegenerative conditions. Theories regarding the function of CA are regularly updated as new components are described. In previous work, we revealed the presence of some neo-epitopes in CA and the existence of some natural antibodies directed against these neo-epitopes. We also noted that these neo-epitopes and natural IgMs were the cause of false staining in CA immunohistochemical studies, and disproved the proposed presence of β-amyloid peptides and tau protein in them. Here we extend the list of components erroneously attributed to CA. We show that, contrary to previous descriptions, CA do not contain GFAP, S100, AQP4, NeuN or class III β-tubulin, and we question the presence of other components. Nonetheless, we observe that CA contains ubiquitin and p62, both of them associated with processes of elimination of waste substances, and also glycogen synthase, an indispensable enzyme for polyglucosan formation. In summary, this study shows that it is imperative to continue reviewing previous studies about CA but, more importantly, it shows that the vision of CA as structures involved in protective or cleaning mechanisms remains the most consistent theory.

INTRODUCTION

Corpora amylacea (CA) are polyglucosan bodies (PGBs) that accumulate primarily in periventricular and subpial regions of the human brain during the ageing process, but are also present in large numbers in selected areas of the brain in several neurodegenerative conditions including Alzheimer's, Parkinson's, Huntington's and Pick's diseases, as well as in patients with temporal lobe epilepsy[1-9]. Although CA were described by Purkinje as far back as 1837, their origin and function remain unknown.

While essentially constituted of glucose polymers[10], many components have been attributed to CA, mainly derived from neurons, oligodendrocytes, astrocytes and blood[1,11]. Due to this diversity, many theories have been put forward to explain the origin and functions of CA. Over the years, they have been considered to be protein precipitates of lymphatic or hematogenous origin[12]; the result of a defect in glycogen metabolism[10]; accumulations of breakdown products from neurons and oligodendroglial cells[9]; aggregated remnants of degenerated neuronal cells[13]; conglomerations of interacting proteins from degenerating neurons and extravasated blood elements released after the breakdown of the blood–brain barrier[14]; structures formed from degenerating astrocytes[15]; structures related to a latent human cytomegalovirus infection[16]; and most recently pathological structures related to fungal infections[17].

CA of human brain share some features with a type of PGB which appear in mouse brain also during the ageing process and frequently named PAS granules because of their positive staining with the periodic acid Schiff (PAS). We recently reported that both CA and PAS granules contain some neo-epitopes that can be recognized by plasmatic natural IgM antibodies[18,19]. Natural antibodies are permanently present in the organisms, even without prior contact with external antigens, and we found that the antibodies directed against the neo-epitopes are present in plasma from mice maintained under specific opportunistic pathogen-free conditions and also in human umbilical cord sera[18, 20]. The results indicated that these organisms are permanently equipped with antibodies prepared to react against the neo-epitopes that arise in CA. We also found that the IgM antibodies that recognize these neo-epitopes are present in the plasma of other mammal species, corroborating the fact that natural antibodies have been fixed by natural selection during evolution and are therefore interspecific[18, 20]. Meanwhile, we observed that these natural IgM antibodies are present as contaminants in a high percentage (around 70%) of commercial antibodies obtained from mouse, rabbit, goat and rat, obtained from ascites or serum, being monoclonal or polyclonal, and even supplied as purified[19, 20]. Since these contaminant IgMs are recognized by the majority of the anti-IgG antibodies used as secondary antibodies in immunohistochemical studies, they very frequently cause false positive immunostaining in CA. These IgMs therefore account for some of the inconsistencies concerning CA composition and underlie the controversies and the wide variety of theories about their origin and functions.

In this connection, some studies have indicated that CA contain tau protein[21-23], but

others have not reproduced these findings[24]. Contradictory results have also been described with regard to the amyloid-β peptide or its precursor: Notter and Knuesel[24] reported that it is indeed present in CA, while other authors reached the opposite conclusion[23,25]. In a recent study of the presence of both tau protein and amyloid-β peptides using different IgG antibodies directed against these components[18], our group observed that: a) in all cases in which the vials of primary antibodies were contaminated by IgMs, CA became stained when using a secondary antibody specifically directed against IgM; b) if the vials of primary antibodies were contaminated by IgMs, CA became stained when using non-isotype-specific anti-IgG secondary antibodies; c) pre-adsorption controls prevented the staining of fibrillary tangles and amyloid plaques, but not the staining of CA; and d) with or without IgM contamination, no positive staining of CA was observed when using isotype-specific anti-IgG secondary antibodies. Taken together, these results indicate that the positive staining on CA, when present, was produced by contaminant IgMs but not by the specific IgG antibodies directed against tau protein or amyloid-β peptides; thus, these findings rule out the presence of these components on CA.

Consequently, the presence of other components on CA determined by immunohistochemical procedures and summarized in table I requires clarification. Regarding neuronal markers, positive staining of CA has been observed using NeuN, an antibody directed against neuronal perikarya[25-27], as well as class III β-tubulin[23]. Components of astrocytic origin have also been described, including specific proteins of the S-100 family[25, 26, 28], aquaporin 4 (AQP4)[25] and the glial fibrillary acidic protein (GFAP). In this case, while some authors have reported that the immunoreactivity for GFAP is located throughout the CA[25,26], other reports specified that CA were outlined by the GFAP signal but that there was no staining within the bodies [24, 28-30]. Moreover, CA were reported to contain heat-shock proteins (HSP)[2, 31, 32] and there is a general consensus on the presence of ubiquitin [2, 21, 23, 25, 30]. In the present study, these components will be re-analysed in order to determine which ones are indeed present in CA, taking into account the possible false-positive staining produced by contaminant IgMs.

It has also been postulated that CA may be involved in trapping and sequestering potentially hazardous products[1]. Moreover, in view of their extrusion from the marginal glia, it has been proposed that they could be a component of the glio-pial clearance system that removes different molecules from the central nervous system[33]. These theories are based, among other points, on the presence of waste elements in CA as well as the presence of ubiquitin, which is involved in the signaling of substrates for degradation. Moreover, the existence of neo-epitopes on CA and the presence of natural IgM antibodies directed against them reinforce the idea that CA might be structures that are prepared for elimination via the natural immune system, perhaps via phagocytosis processes once extruded from the brain[18]. Accordingly, in the present study we also analyse the presence of certain components that may be related to these functions: specifically, p62, LC3 and matrix-metalloproteinase-2 (MMP2) proteins. The p62 protein is an ubiquitin-binding scaffold protein that collects ubiquitinated proteins

via their C-terminal Ubiquitin-Associated (UBA) domain, and recent studies suggest that the binding of ligands to the p62 ZZ domain induces p62 self-oligomerization and aggregation[34]. As p62 also binds directly to LC3 and GABARAP family proteins, it can therefore escort the ubiquitinated proteins to the autophagosomes, which can then be directed to autophagy processes[35] or to secretory autophagy, in which the content of the autophagosome becomes extruded from the cell[36]. The MMP2 protein is a metalloproteinase protein involved in the extracellular remodelling[37], a process necessary for the extrusion of CA from marginal astrocytes to the cerebrospinal fluid. We also analysed the presence of glucose synthase (GS) on CA. GS is the only enzyme able to synthesize glucose polymers in mammals and, as indicated above, glucose polymers are the most abundant component of CA. Remarkably, genetic ablation of glycogen synthase in mouse brain avoids the formation of PGBs in this organ[38]. Although the presence of GS on CA has not been studied to date, its presence has been observed in other PGBs such as Lafora bodies in malin^{KO} mice, a mouse model of Lafora disease[39].

Accordingly, in order to shed light on CA composition and function, the present study has two main objectives: 1) to verify the presence on CA of some previously described components, and 2) to determine the presence of certain potential components that have not been studied to date.

RESULTS

Revision of the presence of some components previously described in CA

Immunohistochemical studies were performed in order to verify the presence of some of the proposed components in CA. It must be taken into account that in previous studies with samples from AD and non-AD patients, we did not observe morphological or staining differences on CA depending on the presence or the absence of AD pathology[18] and so did happen in the present work, in which sections from a minimum of one non-AD and three AD brain donors were used for each specific staining (supplementary Figure S1). Thereafter, we considered the following results as general observations for all CA, and all representative images presented in the article are obtained from brain sections of AD patients. Some of the proposed components in CA are the astrocytic GFAP and S100B proteins. For these markers we tested the staining on different hippocampal sections from each patient, using the isotype-specific anti-IgG secondary antibody and also a specific anti-IgM secondary antibody. A positive staining with the specific anti-IgG secondary antibody would indicate the presence of the specific marker, while positive staining with the secondary anti-IgM antibody would indicate the presence of contaminant IgMs directed against the neo-epitopes of CA in the vial of the primary antibody. Figure 1 shows representative images from the different staining. When using the appropriate isotype-specific anti-IgG secondary antibodies, the astrocytic processes became stained with the GFAP or S100B primary

antibodies, and in some cases the whole astrocyte could be visualized (Figures 1 a1 and b1). These observations become the positive control of the staining, because they exhibited the expected staining of astrocytes with the GFAP and S100 markers. However, none of these markers were present in CA (Figure 1 a2 and b2). In the case of GFAP staining, some CA appeared as unstained black spheres surrounded by astrocytic processes (Figure 1 a2). When the staining was performed with the respective anti-IgMs, in both cases CA became stained (Figure 1 a3 and b3). These results indicated the presence of contaminant IgMs in the vials of primary antibodies, which recognize the neo-epitopes of CA; they also indicated that if a non-isotype-specific anti-IgG secondary antibody had been used, such as an anti-IgG against heavy and light chains (anti-IgG(H&L)), CA would have become stained due to the cross-reaction of this secondary antibody with the contaminant IgMs. We also tested the presence of AQP4 in CA. In this case, although the commercial isotype-specific anti-IgG secondary antibody was not available, the presence of this marker in CA was ruled out because there was no positive labeling of CA either with the anti-IgG(H&L) or with the anti-IgM antibody (Figure 1 c1-c3). If contaminant IgMs had been present, a positive staining with anti-IgG(H+L) antibody would have been observed in CA. This hypothetical case would have led to a controversial result because of the possible cross-reaction of this secondary antibody with the IgMs. It should be pointed out that when using anti-IgG(H+L) there was no staining in CA, but there was positive labeling of astrocytes (Figure 1 c1), confirming the correct functionality of the primary antibody. As in the case of the GFAP staining, AQP4 signals appeared surrounding CA, leading to empty spheres. The double staining with GFAP and AQP4 showed that these two markers are mainly located surrounding the CA (Figure 1 d1 and d2), and the color histogram profiles showed a similar distribution of both markers around the CA. Taken together, these results indicate that CA do not contain either GFAP, S100B or AQP4, and the presence of these astrocytic markers reported elsewhere were probably due to false staining caused by the contaminant IgMs.

We also verified the presence of the neuronal markers NeuN and class III β-tubulin on CA. When using isotype-specific anti-IgG secondary antibodies, the presence of these components is observed in the expected structures, i.e., the neuronal perikarya in the case of NeuN (Figure 2 a1) and certain neurons and neurites in the case of class III β-tubulin (Figure 2 b1). However, neither NeuN nor class III β-tubulin labeled CA (Figure 2 a1 and b2). When simple immunofluorescences were performed using the anti-IgMs as secondary antibodies, in both cases CA appeared labeled, confirming the presence of contaminant natural IgMs on the vials of the primary antibodies (Figure 2 a2 and b3). Again, these IgMs would have produced false-positive staining on CA, if a non-isotype-specific anti-IgG antibody had been used. All things considered, NeuN and TUJ1 do not label CA, and the previous descriptions are also probably based on false-positive staining produced by contaminant IgMs.

We also rechecked the presence of some components associated with the possible role of CA, including the ubiquitin protein and the HSP70. In the case of ubiquitin, CA became labeled when using the isotype-specific anti-IgG secondary antibody, as well

as some dystrophic neurites (Figure 2 c1), but not when using the anti-IgM secondary antibody (Figure 2 c2). Thus, the presence of ubiquitin on CA was confirmed. In the case of HSP70, CA was not labeled when using the isotype-specific anti-IgG secondary antibody (data not shown). However, in this case we did not observe any positive region or structure that could be used as a positive control, and so we could not rule out the possibility of a methodological problem with the primary antibody or epitope preservation. Consequently, the presence of HSP70 on CA remains doubtful. In any case, we observed that the CA became stained when using the anti-IgM secondary antibody, indicating that the vial of the primary antibody is also contaminated by IgM. Consequently, if a non-isotype-specific anti-IgG had been used, the CA labeling might have been positive, but due to a false-positive staining of CA.

Study of the presence of certain components predicted in CA

As indicated in the introduction section, and because CA could be involved in the sequestration of potentially hazardous products and their brain extrusion, we studied here the presence of p62, LC3 and MMP2 in CA. The presence of GS, the only enzyme able to synthesize glucose polymers, was also evaluated.

First, we checked the presence of contaminant natural IgMs in each of these four commercial antibodies by performing the immunohistochemistry with the appropriate anti-IgM secondary antibodies. With this approach, the only case in which the CA became stained was when LC3B was used (data not shown). Thereafter, the only primary antibody that contained IgMs was the LC3B. As LC3B is a polyclonal antibody obtained in rabbit, and the available anti-rabbit IgG antibodies are not isotype-specific, these anti-IgG antibodies could crossreact with the IgMs. Therefore, in this case we were not able to determine whether or not LC3B was present in the CA. In the other cases, i.e., p62, GS and MMP2, whose antibodies are free of contaminant IgMs, we observed a positive staining of CA by using the respective anti-IgG secondary antibodies (Figure 3 a-c). We therefore concluded that the three components (p62, GS and MMP2) were present in CA. On the other hand, taking into account that p62 and ubiquitin may interact due to the UBA domain present in p62, we also studied the co-localization pattern of these two proteins in CA and the co-localization of GS and p62 and that of GS and Ubi. After performing double staining with Ubi and p62, we observed different staining patterns in CA. Most of them presented p62 and Ubi in the peripheral area, generating a ring or a circle, and can contain Ubi, but no p62, concentrated in the central part (Figure 3 d1 and d2). In some cases CA presented p62 staining uniformly throughout the body, which is produced by the section in a tangential plane on the surface of the CA. The double staining with Ubi and GS presented similar patterns to those previously described. GS was located mainly on the periphery of the CA, where it might be accompanied by Ubi, and in the center of the CA there was in some occasions a region with high Ubi labeling (Figure 3 e1 and e2). Like the previous staining, the double staining with GS and p62 showed that these two components are mainly located at the periphery of the CA, with GS staining predominating in some cases and p62 staining in others (Figures 3 f1 and f2). Neither of these two last

components appeared concentrated in the central part of the CA. The histogram profiles shown in Figure 3 indicate that the Ubi pattern in CA differs from those of GS and p62. GS and p62 are located mainly in the periphery of the structure, while Ubi is located in the peripheral region but may also appear concentrated in the center. In order to corroborate these points, we obtained the 3D reconstruction of some representative CA stained with the different markers. As can be observed in supplementary figures S2-S5, and as indicated before, GS, p62 and Ubi stain the periphery of CA, while Ubi can also be concentrated in the central region of the structure. The double staining with GS and GFAP showed that GFAP staining is surrounding that of GS, which indicated that the astrocytic processes are surrounding CA (Figure 3 g1). This is clearly shown when CA is magnified (Figure 3 g2). When the histogram profiles are traced, it can be observed that the peaks of intensity of GFAP staining appear externally to those of GS staining. In some cases, CA become sliced in a tangential plane, and then the GS staining appear throughout the surface of the CA, and the astrocytic processes stained with GFAP are covering this surface (Fig 3 g3).

The results of the immunostaining performed in this study, including both the rechecking of the components described in CA and the study of the presence of some previously unreported components, are summarized in Table II.

DISCUSSION

The interpretation of the function of *corpora amylacea* has varied over time, and in fact numerous theories about these bodies have been formulated, due mainly to the continuous description of new components. In previous work, we were able to rule out the presence of some of these components, specifically the β-amyloid peptides and the tau protein[18]. In the present study we have expanded the list of components erroneously attributed to CA. *Contra* the previous descriptions summarized in Table I, we have seen that CA do not contain any of the following astrocytic or neuronal markers: GFAP, S100, AQP4, NeuN and class III β-tubulin. Except for the antibody against AQP4, all the antibodies tested contained contaminant IgMs that would have given false positives if non-isotype-specific secondary antibodies had been used. Thus, it is not surprising that conflicting results regarding the presence of these markers in CA have been reported. According to the descriptions in Table I, there remains some compounds whose presence should be verified in CA, notably the ones that present discrepancies, such as nestin, α-sinuclein or the transglutaminases, but also the components that do not present discrepancies at present but have been described only once, such as thrombospondin1, reelin, some markers related to cytomegalovirus infections or some fungal components. Elucidating which components really belong to CA will help to focus the theories about CA functionality.

Remarkably, interpretations of CA often omit the fact that these bodies are mainly formed by aggregates of glucose polymers, and the presence of minority components,

which are often erroneously identified, may have been overestimated. In this study, we identified ubiquitin, p62 and GS as some of these minority components. The presence of GS, the only enzyme capable of generating these polymers in animal cells, had already been described in other types of PGB such as Lafora bodies in the malinKO mouse model of Lafora disease[39]. Its presence is not surprising if we take into account that both the CA and the other PGBs are structures that can reach tens of microns in diameter, requiring large amounts of polyglucosans to be formed. Our results show that the staining of GS is mainly located in the peripheral area of CA. In some cases, the peripheral immunostaing of a specific globular structure is an artifact produced by problems of antibody penetration. However, this cannot be the present situation: CA attain up to 30 µm of diameter and, as brain sections in our study are 6 µm-thick, most of them must have been sliced and their central part exposed. In fact, sliced CA can be observed in the 3D animations shown in supplementary figures. Thus, the peripheral staining of GS indicates that a) GS is mainly located in the peripheral area of CA or b) GS located inside have suffered some physical or chemical modification that prevents its detection via immunohistochemistry. For its part, p62 stain was also mainly present in the peripheral area. As this protein has been related with the collection of ubiquitinated proteins, we expected some colocalization between p62 and Ubi. Indeed, we found a certain amount of Ubi staining in the periphery of the CA, but in some cases Ubi also appeared concentrated in the central part of CA, where p62, as GS, is absent or perhaps is physically or chemically altered.

Accordingly, all these findings indicate that CA are not just the aggregation of different insoluble glucose polymers amassing some proteins like GS, p62 and Ubi, but polyglucosan structures with two differentiated regions: the outer part, in which predominates the GS and p62 but also contain Ubi, and the central part, in which high amount of Ubi, but not GS or p62, can be immunohistochemically detected. It can be speculated that the outer part of CA is a dynamic or growing region, where GS are forming the glucose polymers and where p62 might capture the ubiquitinated substances, and that the central part is a stable region where the polyglucosans become accumulated and retain the ubiquitinated substances. This conjecture is consistent with the recent hypothesis indicating that corpora amylacea are waste containers in which deleterious or residual products are isolated for later elimination through the action of the innate immune system[18]. An alternative explanation is that the glucose polymers themselves are the waste substance. In fact, the polyglucosans of all PGBs present alterations in the frequency of branching, in the phosphate levels and water solubility with respect to physiologically functional glycogen[1]. In this regard, in Lafora disease a high number of PGBs accumulate in the brain and the elimination of GS prevents the progression of the disease[40], suggesting that glycogen is indeed the waste product in this case. However, if glucose polymers are the waste substance in CA, it must be determined the nature of the ubiquitinated substance which become accumulated, and it is necessary to explain why p62 and GS are found mainly in the peripheral region.

In a recent study using electronic microscopy techniques (article in press), we

observed that CA are found in astrocytic processes, and therefore all these events would occur inside them. In ultrastructural studies we also observed an interruption of astrocytic fibers in the area where CA are formed. In the present study we found that, although there were no astrocytic markers in the CA, they often surrounded and/or were in contact with these bodies. In addition, ultrastructural studies show that some CA present a central highly dense region, which might be the dense region observed here with a high content of ubiquitin. The ultrastructural studies also showed that the neo-epitopes recognized by natural IgMs are distributed throughout the CA, including the central part. It is then consistent that we found the ubiquitin, a marker of waste substances, in the same areas where we found these neo-epitopes, which can be markers of substances to be eliminated by the response of the natural immune system.

In summary this study shows that it is imperative to continue reviewing previous studies about CA. But, more importantly, it shows that the vision of CA as structures involved in protective or cleaning mechanisms remains the most consistent theory.

METHODS

Human brain samples

Post-mortem brain samples were purchased from the Banc de Teixits Neurològics (Biobanc-Hospital Clínic-IDIBAPS, Barcelona). Brain samples were taken from four cases of neuropathologically confirmed Alzheimer's disease patients (A3B3C3 stage, 81-88 years old) and one non-AD patient with vascular encephalopathy (70 years old).

All procedures involving human samples were performed in accordance with appropriate guidelines and regulations. All experiments involving human tissue were approved by the Bioethical Committee of the University of Barcelona.

Antibodies and reagents

The following antibodies were used as primary antibodies: mouse monoclonal IgG1 against NeuN (clone A60; 1:200; MAB377; MerckMillipore, Darmstadt, Germany), mouse monoclonal IgG1 against GFAP (clone GA5; 1:800; MAB360; MerckMillipore), mouse monoclonal IgG2a against class III beta-tubulin (clone TUJ1; 1:50; 801201; Biolegend, San Diego, CA, USA), mouse monoclonal IgG1 against S100 β-subunit (clone SH-B1; 1:500; S2532; Sigma-Aldrich), mouse monoclonal IgG2a against p62 (1:200; ab56416; Abcam, Cambridge, UK), rabbit monoclonal IgG against GS (1:100; 15B1; Cell Signaling, Leiden, Netherlands), mouse monoclonal IgG1 against ubiquitin (clone Ubi-1; 1:200; ab7254; Abcam), mouse monoclonal IgG1 against HSP70 (clone C92F3A-5; 1:100; MA1-10889; Thermo Fisher Scientific, Rockford, IL, USA), rabbit polyclonal IgG against AQP4 (1:100; AB3594; MerckMillipore), rabbit polyclonal IgG against MMP2 (1:200; AB19167; MerckMillipore) and rabbit polyclonal IgG against LC3 (LC3B; 1:200; NB100-2220; Novus Biologicals, Abingdon, UK).

The following antibodies were used as secondary antibodies: goat anti-rabbit IgM µ chain conjugated to fluorescein isothiocyanate (FITC) (1:250; ab98458; Abcam), Alexa Fluor (AF) 488 goat anti-mouse IgM µ chain specific (1:250; 115-545-075; Jackson ImmunoResearch Laboratories, Newmarket, UK), AF594 goat anti-mouse IgG1 (1:250; A-21125; Life Technologies); AF488 goat anti-mouse IgG2a (1:250; A-21131; Life Technologies), AF594 goat anti-mouse IgG2a (1:250; A-21135; Life Technologies), AF488 goat anti-mouse IgG1 (1:250; A-21121; Life Technologies), AF555 donkey anti-rabbit IgG directed against both their heavy and their light chains (1:250; A-31572; Life Technologies) and AF488 donkey anti-rabbit IgG directed against both their heavy and their light chains (1:250; A-21206; Life Technologies).

Immunohistochemistry

For the immunohistochemistry, the frozen hippocampal sections (6 µm thick), stored at −80°C, were air dried for 10 min and then fixed with acetone for 10 min at 4ºC. After 2 h of drying, sections were rehydrated with phosphate-buffered saline (PBS) and then blocked and permeabilized with 1% bovine serum albumin in PBS (Sigma-Aldrich) (Blocking buffer, BB) with 0.1% Triton X-100 (Sigma-Aldrich) for 20 min. They were then washed with PBS and the primary incubation was overnight at 4°C. Next, the slides were washed and incubated for 1 h at room temperature with the secondary antibody. Nuclear staining was performed with Hoechst (2 µg/mL, H-33258, Fluka, Madrid, Spain) and the slides were washed and coverslipped with Fluoromount (Electron Microscopy Sciences, Hatfield, PA, USA). Staining controls were performed by incubating the secondary antibody after the incubation with BB instead of the primary antibody. In double stainings, controls for cross reactivity of the antibodies were also performed.

Image acquisition and processing

Images were captured with a fluorescence laser and optical microscope (BX41, Olympus, Germany) and stored in TIFF format. All the images were acquired using the same microscope, laser and software settings. Exposure time was adapted to each staining, but the respective control images were acquired with the same exposure time. Image analysis and treatment were performed using the ImageJ program (National Institute of Health, USA). Images that were modified for contrast and brightness to enhance their visualization were processed in the same way as the images corresponding to their respective controls. In some images from double staining, the histogram profile of the intensity of the different colors along one drawn line was obtained by the ImageJ program.

In order to study the distribution of some markers on CA, image stacks were taken with a confocal laser scanning microscopes (LSM 880, Zeiss, Germany) and 3D animations were obtained by means of the Image J program (National Institute of Health, USA).

REFERENCES

1. Cavanagh, J. B. Corpora-amylacea and the family of polyglucosan diseases. *Brain Res. Rev.* **29**, 265–295 (1999).
2. Cissé, S., Perry, G., Lacoste-Royal, G., Cabana, T. & Gauvreau, D. Immunochemical identification of ubiquitin and heat-shock proteins in corpora amylacea from normal aged and Alzheimer's disease brains. *Acta Neuropathol.* **85**, 233-240 (1993).
3. Keller, J.N. Age-related neuropathology, cognitive decline, and Alzheimer's disease. *Ageing Res. Rev.* **5**, 1-13 (2006).
4. Mizutani, T., Satoh, J. & Morimatsu, Y. Axonal polyglucosan body in the ventral posterolateral nucleus of the human thalamus in relation to aging. *Acta Neuropathol.* **74**, 9–12 (1987).
5. Mrak, R.E., Griffin, S.T. & Graham, D.I. Aging-associated changes in human brain. *J. Neuropathol. Exp. Neurol.* **56**, 1269-1275 (1997).
6. Nishio, S. *et al*. Corpora amylacea replace the hippocampal pyramidal cell layer in a patient with temporal lobe epilepsy. *Epilepsia* **42**, 960-962 (2001).
7. Radhakrishnan, A. *et al*. Corpora amylacea in mesial temporal lobe epilepsy: clinico-pathological correlations. *Epilepsy Res.* **74**, 81-90 (2007).
8. Song, W. *et al*. Astroglial heme oxygenase-1 and the origin of corpora amylacea in aging and degenerating neural tissues. *Exp. Neurol*. **254**, 78-89 (2014).
9. Singhrao, S.K., Neal, J.W., Piddlesden, S.J. & Newman, G.R. New immunocytochemical evidence for a neuronal/oligodendroglial origin for corpora amylacea. *Neuropathol. Appl. Neurobiol.* **20**, 66-73 (1994).
10. Sakai, M., Austin, J., Witmer, F. & Trueb, L. Studies of corpora amylacea: Isolation and preliminary characterization by chemical and histochemical techniques. *Arch. Neurol*. **21,** 526–544 (1969).
11. Rohn, T.T. Corpora amylacea in neurodegenerative diseases: cause or effect? *Int. J. Neurol. Neurother.* **2**, 31 (2015).
12. Ferraro, A. & Damon, L. A. The histogenesis of amyloid bodies in the central nervous system. *Arch. Pathol.* **12**, 229-244 (1931).
13. Selmaj, K. *et al*. Corpora amylacea from multiple sclerosis brain tissue consists of aggregated neuronal cells. *Acta Biochim. Pol.* **55**, 43-49 (2008).
14. Meng, H., Zhang, X., Blaivas, M. & Wang, M. M. Localization of blood proteins thrombospondin1 and ADAMTS13 to cerebral corpora amylacea. *Neuropathology* **29**, 664-671 (2009).
15. Suzuki, A. *et al.* Phagocytized corpora amylacea as a histological hallmark of astrocytic injury in neuromyelitis optica. *Neuropathology* **32**, 597-594 (2012).
16. Libard, S. *et al*. Human cytomegalovirus tegument protein pp65 is detected in all intra- and extra-axial brain tumours independent of the tumour type or grade. *PLoS One*. **9**, e108861; 10.1371/journal.pone.0108861 (2014).
17. Pisa, D., Alonso, R., Rábano, A. & Carrasco, L. Corpora amylacea of brain tissue from neurodegenerative diseases are stained with specific antifungal antibodies. *Front. Neurosci.* **10**, 86 (2016).
18. Augé, E., Cabezón, I., Pelegrí, C. & Vilaplana, J. New perspectives on corpora amylacea in the human brain. *Sci. Rep.* **7**, 41807 (2017).

19. Manich, G. *et al*. Presence of a neo-epitope and absence of amyloid beta and tau protein in degenerative hippocampal granules of aged mice. *Age* **36**,151-165 (2014).

20. Manich, G. *et al.* Neo-epitopes emerging in the neurodegenerative hippocampal granules of aged mice can be recognized by natural IgM auto-antibodies. *Immun. Ageing* **12**, 23-30 (2015).

21. Day, R. J., Mason, M. J., Thomas, C., Poon, W. W. & Rohn, T. T. Caspase-cleaved tau co-localizes with early tangle markers in the human vascular dementia brain. *PLoS One.* **10**, e0132637; 10.1371/journal.pone.0132637 (2015).

22. Loeffler, K.U., Edward, D.P. & Tso, M.O. Tau-2 immunoreactivity of corpora amylacea in the human retina and optic nerve. *Invest. Ophthalmol. Vis. Sci.* **34**, 2600-2603 (1993).

23. Wilhelmus, M.M. *et al*. Novel role of transglutaminase 1 in corpora amylacea formation? *Neurobiol. Aging* **32**, 845-856 (2011).

24. Notter, T. & Knuesel, I. Reelin immunoreactivity in neuritic varicosities in the human hippocampal formation of non-demented subjects and Alzheimer's disease patients. *Acta Neuropathol. Commun.* **1**, 27 (2013).

25. Pirici, D. & Margaritescu, C. Corpora amylacea in aging brain and age-related brain disorders. *J. Aging Gerontol.* **2**, 33-57 (2014).

26. Buervenich, S., Olson, L. & Galter, D. Nestin-like immunoreactivity of corpora amylacea in aged human brain. *Brain Res. Mol. Brain Res.* **94**, 204-208 (2001).

27. Korzhevskiĭ, D.E. & Giliarov, A.V. Demonstration of nuclear protein neun in the human brain corpora amylacea. *Morfologiia* **131**, 75-76 (2007).

28. Bakić, M & Jovanović, I. Morphological features of corpora amylacea in human parahippocampal cortex during aging. *Acta Medica Int.* **4**, 25-31 (2017).

29. Nam, I.H. *et al*. Association of corpora amylacea formation with astrocytes and cerebrospinal fluid in the aged human brain. *Korean J. Phys. Anthropol*. **25**, 177-184 (2012).

30. Pirici, I. *et al*. Corpora amylacea in the brain form highly branched three-dimensional lattices. *Rom. J. Morphol. Embryol*. **55**, 1071-1077 (2014).

31. Gáti, I. & Leel-Ossy, L. Heat shock protein 60 in corpora amylacea. *Pathol. Oncol. Res.* **7**, 140-144 (2001).

32. Martin, J. E. *et al*. Heat shock protein expression in corpora amylacea in the central nervous system: clues to their origin. *Neuropathol. Appl. Neurobiol*. **17**, 113-119 (1991).

33. Sbarbati, A., Carner, M., Colletti, V. & Osculati, F. Extrusion of corpora amylacea from the marginal glia at the vestibular root entry zone. *J. Neuropathol. Exp. Neurol.* **55**, 196-201 (1996).

34. Cha-Molstad, H. *et al.* p62/SQSTM1/Sequestosome-1 is an N-recognin of the N-end rule pathway which modulates autophagosome biogenesis. *Nat. Commun.* **8**,102 (2017).

35. Isakson, P., Holland, P., Simonsen, A. The role of ALFY in selective autophagy. Cell Death Differ.**20**, 12–20 (2013).

36. Ponpuak, M. *et al.* Secretory autophagy. Curr. Opin. Cell Biol. **35**, 106-116 (2015).

37. Ethell, I.M. & Ethell D.W. Matrix metalloproteinases in brain development and remodeling: synaptic functions and targets. *J. Neurosci. Res.* **85**, 2813–2823 (2007).
38. Sinadinos, C. *et al*. Neuronal glycogen synthesis contributes to physiological aging. *Aging Cell,* **13**, 935–945 (2014).
39. Valles-Ortega, J. *et al*. Neurodegeneration and functional impairments associated with glycogen synthase accumulation in a mouse model of Lafora disease. *EMBO Mol. Med.* **3**, 667–681 (2011).
40. Duran, J., Gruart, A., Garcia-Rocha, M., Delgado-Garcia, J.M., & Guinovart, J.J. Glycogen accumulation underlies neurodegeneration and autophagy impairment in Lafora disease. *Hum. Mol. Genet.* **23**, 3147–3156 (2014).

ACKNOWLEDGEMENTS

This study was funded by grants BFU2013-47382-P, BFU2016-78398-P and BFU2017-84345-P awarded by the Spanish Ministerio de Economía y Competitividad (MINECO), by Agencia Estatal de Investigación (AEI) and by European Regional Development Funds and by the Centros de Investigación Biomédica en Red (CIBER) at the Instituto de Salud Carlos III. We thank the Generalitat de Catalunya for funding our research group (2017/SGR625). E. Augé received the pre-doctoral Ajuts de Personal Investigador en Formació fellowship from the Universitat de Barcelona (APIF-UB). We are sincerely grateful to Lídia Bardia, from the Advanced Digital Microscopy of the Institute for Research in Biomedicine - IRB Barcelona, for her help in the confocal studies, and to Michael Maudsley for correcting the English version of the manuscript.

AUTHOR CONTRIBUTIONS

E.A., J.D., J.G., C.P. and J.V. participated in the design of the study. E.A., C.P. and J.V. performed the experimental procedures, the microscope and data analysis, and the interpretation of results. E.A., J.D., J.G., C.P. and J.V. drafted the manuscript and participated in the critical review. All the authors have read and approved the final manuscript. C.P. and J.V. contributed equally to this study.

ADDITIONAL INFORMATION

Competing financial interests: The authors declare no competing financial interests.

FIGURE 1

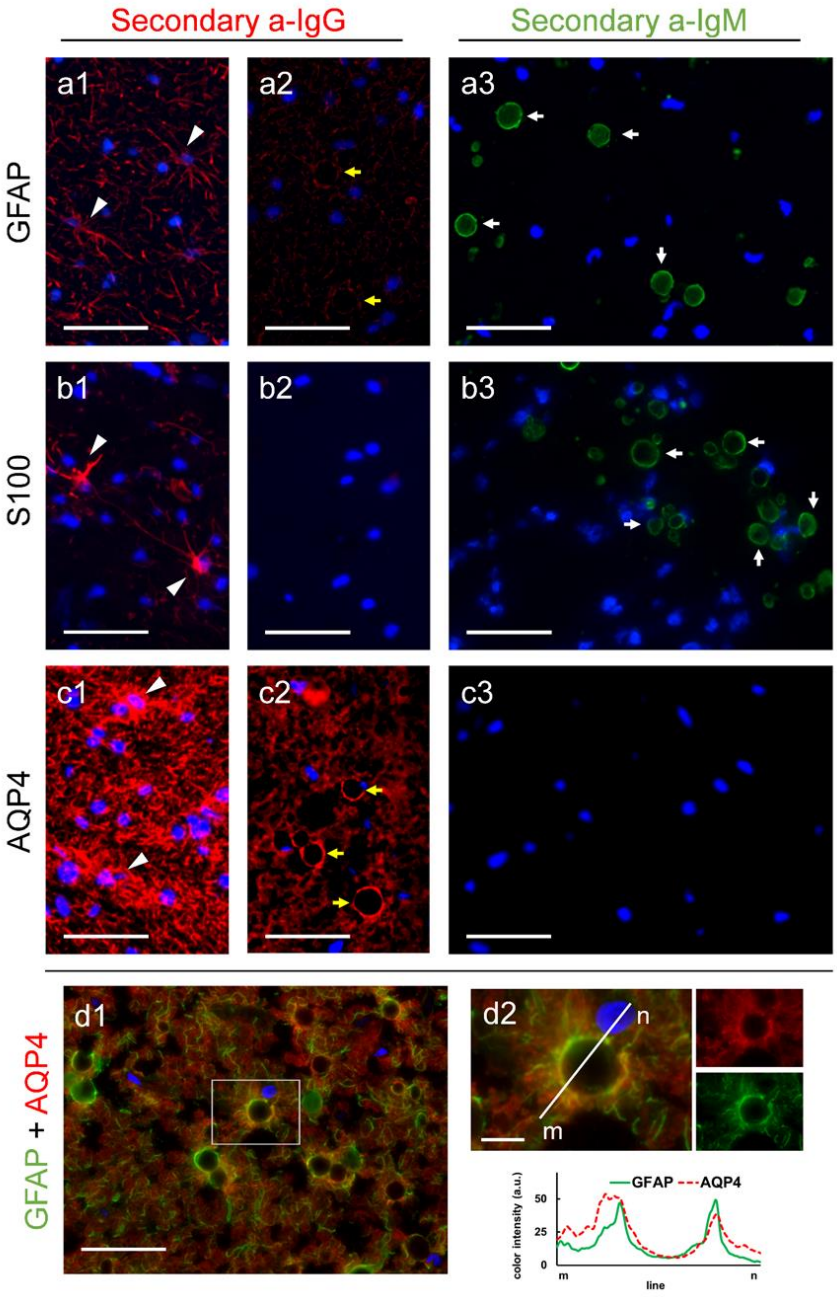

Figure 1. Absence of GFAP, S100 and AQP4 in CA. Representative images of human brain hippocampus sections immunostained with GFAP (a), S100 (b) and AQP4 (c). When using isotype-specific anti-IgG antibodies (a1, a2, b1 and b2) or anti-IgG(H+L) antibodies (c1-c2) conjugated to a red fluorochrome in the second incubation, the positive labeling of astrocytes can be observed (arrowheads in a1, b1 and c1), but CA are not labelled and are visible just as a dark hole when astrocyte processes encircled them (yellow arrows in a2 and c2). By using an isotype-specific anti-IgM antibody conjugated to a green fluorochrome in the second incubation, labeling of CA can be observed as shown in a3 and b3 (white arrows) but not in c3, indicating that GFAP and S100, but not AQP4, are IgM contaminated. Double immunostaining with GFAP and AQP4 show these two markers surrounding the CA (d1). D2 shows an inset of d1, where a CA is magnified. The different color channels are shown in small images next to the corresponding ones, and the histogram profiles

of green and red intensities on the plotted line show the similar distribution of both markers around the CA. Hoechst (blue) was used for nuclear staining. Scale bar in d2: 10 µm, other scale bars: 50 µm.

FIGURE 2

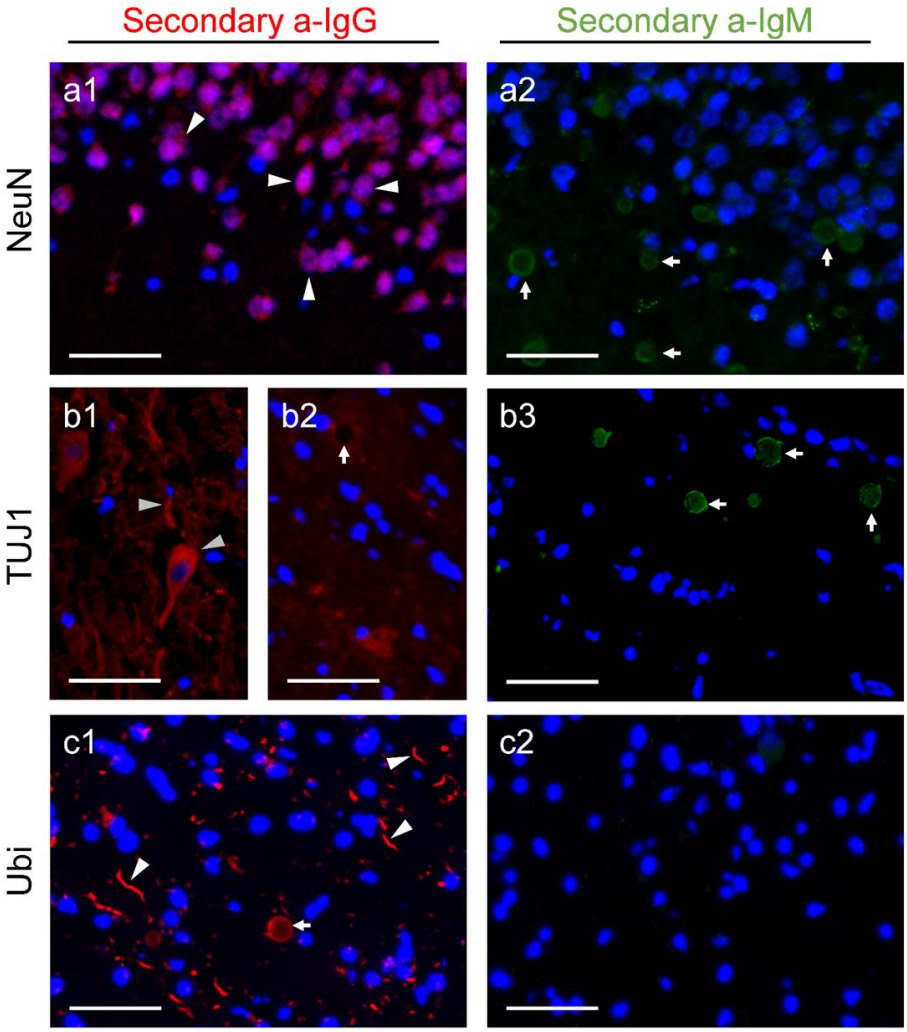

Figure 2. Absence of NeuN and TUJ1 and presence of ubiquitin in CA. Representative images of human brain hippocampus sections immunostained with NeuN (a), TUJ1 (b) and Ubi (c). As expected, when using isotype-specific anti-IgG antibodies conjugated to a red fluorochrome in the second incubation, NeuN stained the neuronal soma (arrowheads in a1), Tuj1 stains both neuronal soma and neurites (arrowheads in b1), and Ubi stained some dystrophic neurites (arrowheads in c1). CA were not labeled with NeuN (a1) and Tuj1 (arrow in b2), but became labeled with Ubi (arrow in C1). When using isotype-specific anti-IgM antibodies conjugated to a green fluorochrome in the second incubation, labeling of CA was observed in a2 and b3 (arrows), but not in c2, indicating the presence of contaminant IgMs in the vials of NeuN and Tuj1, but not in the Ubi vial. Hoechst (blue) was used for nuclear staining. Scale bar: 50 µm.

FIGURE 3

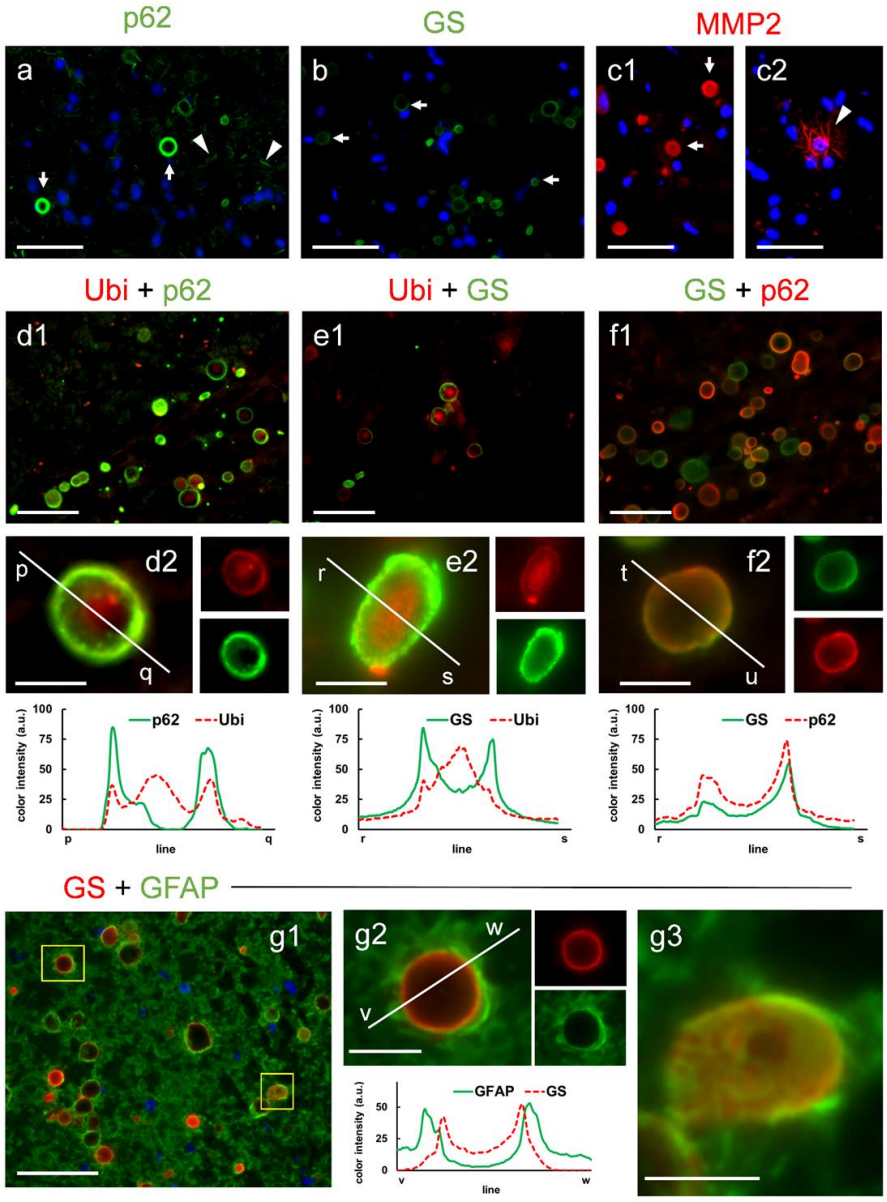

Figure 3. Immunolabeling of CA with the markers p62, GS and MMP2.
Representative images of human brain hippocampus sections immunostained with p62 (a), GS (b) and MMP2 (c1 and c2). The three markers positively stained the CA (arrows). p62 also stained some dystrophic neurites (arrowheads in a), while MMP2 stained some thin filaments (arrowheads in c2). Hoechst (blue) was used for nuclear staining. d1-d2: double immunostaining with Ubi (red) and p62 (green); e1-e2: double immunostaining with Ubi (red) and GS (green); f1-f2: double immunostaining with GS (green) and p62 (red). In some CA, p62 and GS are clearly visible in the peripheral region (d2, e2 and f2), while Ubi is concentrated in the central zone (d2 and e2). The different color channels from d2, e2 and f2 are shown in small images next to the corresponding ones. The histogram profiles of green and red intensities on the plotted lines illustrate the peripheral location of p62 and GS, and show that Ubi is concentrated in the central zone but is also present at the periphery. Double staining with GS and GFAP showed that GFAP staining is surrounding that of GS, which indicated that the astrocytic processes are surrounding CA (Figure 3 g1). This is clearly shown when CA

is magnified (Figure 3 g2). When the histogram profiles are traced, it can be observed that the peaks of intensity of GFAP staining appear externally to those of GS staining. In some cases, CA become sliced in a tangential plane, and then the GS staining appear throughout the surface of the CA, and the astrocytic processes stained with GFAP are surrounding this surface (Fig 3 g3). Scale bars on d2, e2, f2, g2 and g3: 10 µm; other scale bars: 50 µm.

TABLE I

Table I. Retrospective data collection of the positive and negative immunolabeling of CA.

Antibody	Epitope	CA staining	Reference
Directed against Tau protein			
Tau-2	phosphatase-independent epitope of tau	+	Loeffler et al., 1993
Tau 1, Clone PC1C6	non-phosphorylated epitope of the tau	-	Loeffler et al., 1993
PHF-1	phosphorylation at serines 396 and 404	+	Day et al., 2015
TauC3	caspase cleaved tau truncated at Asp 421	+	Day et al., 2015
AT8	tau phosphorylated ser202/thr205	-	Day et al., 2015
HT7	full-lenght tau	-	Day et al., 2015
Tau46	tau C-terminal specific	+	Day et al., 2015
AT8	tau phosphorylated Ser202/thr205	-	Wilhelmus et al., 2011
Tau-2	human tau	+	Wilhelmus et al., 2011
PHF, clone AT100 (#MN1060)	tau phosphorylated Thr212/Ser214 PHF	-	Notter and Knuesel, 2013
Tau pS422 (#44-764G)	tau phosphorylated on serine 422	-	Notter and Knuesel, 2013
Tau-5 (MAB361)	anti-tau 210–241 AA	-	Augé et al., 2017
5E2 (05–348)	anti-tau	-	Augé et al., 2017
Directed against Amyloid-β (Aβ) or amyloid-β protein precursor (APP)			
4G8	Aβ 17-24 aminoacids	-	Pirici and Margaritescu, 2014
anti-Aβ 1-42 (#ab10148)	human Aβ 1-42 aminoacids	-	Wilhelmus et al., 2011
anti-Aβ (#AB5076) P2	Aβ 1-40/42 aminoacids extracytoplasmic APP site	+ +	Notter and Knuesel, 2013 Tate-Ostroff et al., 1988
APP-A4, clone 22C11 (#MAB348)	N-terminal domain of APP	+	Notter and Knuesel, 2013
anti-Aβ1–42, 12F4 (SIG-39142)	Aβ 1-42 aminoacids	-	Augé et al., 2017
anti-Aβ 1–16, 6E10 (SIG-39320)	Aβ 1-16 aminoacids	-	Augé et al., 2017
Directed against nestin			
anti-nestin	nestin	-	Pirici and Margaritescu, 2014
anti-nestin	nestin	+	Buervenich et al., 2001
Directed against NeuN			
anti-NeuN	NeuN protein	+ (some)	Pirici and Margaritescu, 2014
anti-NeuN	NeuN protein	+	Buervenich et al., 2001
anti-NeuN	NeuN protein	+	Korzhevskii and Giliarov, 2007
Directed against synuclein (syn)			
α/β/γ-syn, FL-140 (#SC-10717)	human synuclein	+	Wilhelmus et al., 2011
anti-α-syn (#ab52168)	α-synuclein protein	+	Notter and Knuesel, 2013
anti-α-syn	α-synuclein protein	-/+	Buervenich et al., 2001
Directed against parkin			
anti-parkin (#AB5240)	human parkin	+	Wilhelmus et al., 2011
Directed against reelin			
G10 (#MAB5364)	reelin N-terminus	+	Notter and Knuesel, 2013
clone 142 (#MAB5366)	reelin N-terminus	+	Notter and Knuesel, 2013
R12/14	reelin C-terminus	+	Notter and Knuesel, 2013
Directed against microtubule-associated protein 2 (MAP2)			
anti-MAP2 (#AB5622)	MAP2	+	Notter and Knuesel, 2013
anti-MAP2	MAP2	+	Nam et al., 2012
Directed against neurofilaments			
2F11	Neurofilament protein	+ (some)	Pirici and Margaritescu, 2014
anti-NF70	Neurofilament protein	- (all but one)	Buervenich et al., 2001
Directed against S100			
S100 antisera	S100 proteins (different types)	+ (except S100B)	Hoyaux et al., 2000
anti-S100	glial S100 protein	+	Buervenich et al., 2001
anti-S100	glial S100 protein	+	Pirici and Margaritescu, 2014
anti-S100	glial S100 protein	+	Bakic and Jovanovic, 2017
Directed against glial fibrillary acidic protein (GFAP)			
anti- GFAP	GFAP	- to +	Buervenich et al., 2001
anti-GFAP	GFAP	+	Pirici and Margaritescu, 2014
anti-GFAP (#Z0334)	GFAP	- (outlined)	Notter and Knuesel, 2013
anti-GFAP (#MAB360)	GFAP	- (outlined)	Notter and Knuesel, 2013
anti-GFAP (#ABIN125137)	GFAP	- (outlined)	Pirici et al., 2014
anti-GFAP	GFAP	- (outlined)	Nam et al., 2012
anti-GFAP	GFAP	- (outlined)	Bakic and Jovanovic, 2017
Directed against ubiquitin			
anti-ubiquitin anti-ubiquitin6	ubiquitin ubiquitin	+ +	Day et al., 2015 Pirici and Margaritescu, 2014
anti-ubiquitin (#Z0458)	human ubiquitin	+	Pirici et al., 2014
anti-ubiquitin (#Z0458)	human ubiquitin	+	Wilhelmus et al., 2011
anti-ubiquitin	ubiquitin	+	Cissé et al., 1993

Directed against heat-shock proteins (HSP)			
anti-HSP70	HSP70	+	Buervenich et al., 2001
anti-HSP27	HSP27	- (some outlined)	Erdamar et al., 2000
anti-HSP70-72	HSP70-72	- (some outlined)	Erdamar et al., 2000
anti-HSP90	HSP90	- (some outlined)	Erdamar et al., 2000
anti-HSP28	HSP28	+	Cissé et al., 1993
anti-HSP70	HSP70	+	Cissé et al., 1993
anti-HSP72	HSP72	- (outlined) to +	Martin et al., 1991
anti-HSP60 (#H4149)	HSP60 (383-447 AA)	+	Gáti et al., 2001
Directed against aquaporin 4 (AQP4)			
anti-aquaporin 4	AQP4	+	Pirici and Margaritescu, 2014
anti-aquaporin 4 (#MA1-34259)	AQP4	- (outlined)	Pirici et al., 2014
Directed against advanced glycation end-products (AGE)			
6D12	CML (N-(carboxymethyl)lysine)	+	Kimura et al., 1998
anti-pentosidine	pentosidine	+	Kimura et al., 1998
Directed against proteoglycans			
?	keratan sulfate proteoglycan	+	Liu et al., 1987
?	mannose rich glycoconjugate	+	Liu et al., 1987
Directed against mitochondrial (mit.) epitopes			
anti-Bcl-2	mit. membrane associated protein Bcl-2	+	Botez et al., 2001
Directed against transcriptional factors			
anti-c-Jun/AP1	activator protein 1 transcriptional factor c-Jun	+	Botez et al., 2001
Directed against transglutaminases (TGs)			
anti-TG2 (#06-471)	guinea pig TG2	-	Wilhelmus et al., 2011
anti-TG2 (#Ab-3)	guinea pig TG2	-	Wilhelmus et al., 2011
anti-TG1 (#SC-18129)	human TG1	+	Wilhelmus et al., 2011
TG-catalyzed cross-links, 81D4	anti-H-Glu(H-Lys-OH)-OH	+	Wilhelmus et al., 2011
Directed against cytoskeletal proteins			
anti- β-tubulin III (#T8660)	β-tubulin III	+	Wilhelmus et al., 2011
anti- β-actin (#AB8226)	β-actin	+	Wilhelmus et al., 2011
Directed against thrombospondin			
anti-thrombospondin1, A6.1	thrombospondin1	+	Meng et al., 2009
anti-thrombospondin1, SPM321	thrombospondin1	+	Meng et al., 2009
Directed against ADAMTS3			
anti-ADAMTS13	ADAMTS13	+	Meng et al., 2009
Directed against hypoxia-inducible factor 1-alpha (HIF-1α)			
anti-HIF-1α	HIF-1α	+	Pirici and Margaritescu, 2014
Directed against fungal proteins			
antifungal antibodies	*C.glabrata, C. famata, C. albicans, ...*	+ (neurodeg.)	Pisa et al., 2016
Directed against herpesvirus			
anti-cytomegalovirus (MAB8127)	*tegument protein pp65*	+	Libard et al., 2014
Directed against endothelin B receptor			
anti-ETBR (E9905)	*endothelin B receptor*	+	Vasaikar et al., 2018

TABLE II

Table II. Summary of the results obtained with the antibodies used for Immunohistochemistry

		CA staining secondary antibody				Positive controls secondary antibody		
		α-IgG isotype-specific	α-IgG non-isotype-specific[1]	α-IgM	Presence on CA[2]	α-IgG isotype-specific	α-IgG non-isotype-specific	α-IgM
primary antibody (IgG)	GFAP	-		+	negative	astrocytes		-
	S100	-		+	negative	astrocytes		-
	AQP4		-	-	negative		astrocytes	-
	NeuN	-		+	negative	neuronal soma		-
	Tuj1	-		+	negative	neuronal mt.		-
	HSP70	-		+	doubtful	*not observed*		-
	Ubi	+		-	**positive**	dys. neurites		-
	p62	+		-	**positive**	dys. neurites		-
	GS		+	-	**positive**		polyglucosans	-
	MMP2		+	-	**positive**		thin filaments	-
	LC3B		+	+	doubtful		*not observed*	-

[1]α-IgG non-isotype-specific secondary antibodies were used when the isotype-specific antibodies were unavailable. [2]positive presence can be assumed only when the positive controls stain the expected structures and a) the secondary antibody is isotype-specific, or b) the secondary is non-isotype-specific but the vial of the primary antibody is not IgM contaminated. mt: microtubules; dys: dystrophic

FIGURE S1

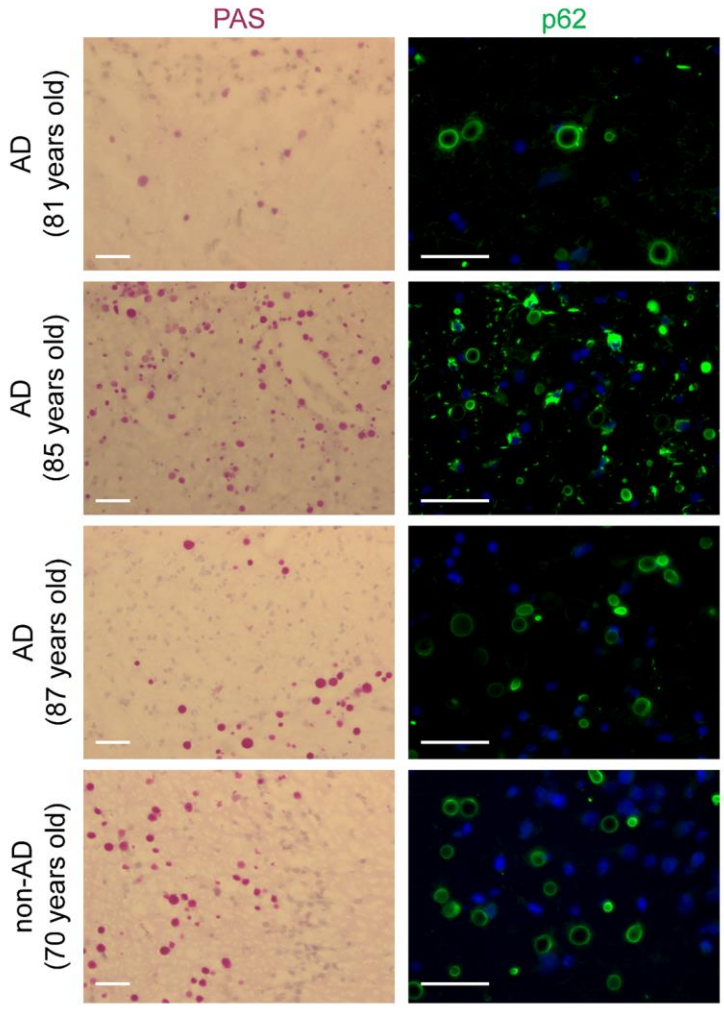

Figure S1. CA do not show staining differences depending on the presence or absence of AD pathology. Representative images of human brain hippocampus sections from three different AD and one non-AD cases stained with periodic acid Schiff (PAS) reaction and counterstained with hematoxylin (a, c, e and g). Representative images of human brain hippocampus sections from the same cases immunostained for p62 (green) and stained with Hoechst (blue) (b, d, f, h). Scale bars: 50 µm. Experimental procedure for PAS staining was performed as described previously in Augé et al., 2017.

ARTICLE 5

ASTROCYTES AND NEURONS PRODUCE DISTINCT TYPES OF POLYGLUCOSAN BODIES IN LAFORA DISEASE

Elisabet Augé, Carme Pelegrí, Gemma Manich, Itsaso Cabezón, Joan J. Guinovart, Jordi Duran i Jordi Vilaplana

GLIA 2018, en premsa

DOI: 10.1002/glia.23463

RESUM

Objectius: Explorar els tipus de PGBs que apareixen en el cervell d'un model murí de la malaltia de Lafora, així com també estudiar la presència de neo-epítops en aquestes estructures.

Material i mètodes: Es van utilitzar ratolins malin *knock-out* (KO), PTG *overexpressed* (OE), MGS^{KO} i els corresponents animals control (C57BL/6). També es van utilitzar ratolins de la soca SAMP8. Tots els experiments es van realitzar amb animals d'entre 60-80 setmanes d'edat i es van utilitzar 4 animals per grup experimental. Es van obtenir seccions criostàtiques o de parafina per realitzar diferents assaigs immunohistoquímics. Per obtenir les seccions criostàtiques, els animals es van anestesiar i es van perfondre amb sèrum fisiològic. Es va procedir a l'extracció del seu encèfal, que es va congelar en isopentà i es va guardar a -80ºC. Es van realitzar seccions coronals que es van fixar amb acetona i congelar a -20ºC. Per obtenir les seccions de parafina, els animals es van anestesiar i es van perfondre amb paraformaldehid al 4% en PBS. Es va procedir a l'extracció del seu encèfal, que es va post fixar *overnight* amb paraformaldehid al 4% en PBS i incloure posteriorment en parafina. Finalment, es van realitzar seccions coronals amb micròtom. Es van realitzar diferents assaigs immunohistoquímics utilitzant anticossos primaris dirigits contra GFAP, NeuN, GS i p62, i també utilitzant IgMs purificades que detecten els neo-epítops. Les mostres es van analitzar per microscòpia de fluorescència. Per dur a terme les quantificacions es va realitzar la tècnica convencional de PAS, i es va mesurar el diàmetre i la densitat en diferents regions cerebrals dels PGBs utilitzant el programa Image J. L'anàlisi estadístic es va realitzar amb el programa SPSS.

Resultats: Els animals $malin^{KO}$ presenten dos tipus de PGBs diferents: un d'ells associats al soma neuronal, de mida més gran i localitzats preferentment a l'escorça cerebral; i un altre tipus de cossos associats a astròcits, de mida més petita, agrupats en clústers i localitzats preferentment a l'hipocamp. Aquests últims també es troben presents en els animals control i en els ratolins SAMP8, però la densitat d'aquests cossos és significativament més gran en els ratolins $malin^{KO}$ que en les altres soques estudiades. A més a més, els marcatges amb les IgMs purificades posen de manifest la presència de neo-epítops en els cossos associats a astròcits, però no en els cossos associats a neurones dels ratolins $malin^{KO}$. En canvi, la proteïna p62, un marcador d'autofàgia, s'acumula en els dos tipus de cossos. D'altra banda, els ratolins MGS^{KO} no presenten cap tipus de PGBs i tampoc cap tipus de marcatge amb les IgMs, fet que posa de manifest que l'estructura de poliglucosà és necessària per a la detecció del neo-

epítop. Els ratolins PTG^{OE} només acumulen PGBs que presenten neo-epítops i no s'observa al seu cervell cap estructura similar als cossos associats a neurones que acumulen els ratolins malin^{KO}.

Conclusions: Els ratolins malin^{KO}, model de la malaltia de Lafora, presenten dos tipus de PGBs a nivell cerebral: uns associats a neurones, principalment corticals i que no presenten neo-epítops; i uns altres associats a astròcits, principalment hipocampals, que presenten neo-epítops i que no són exclusius d'aquests animals però que es troben en major presència en aquesta soca que en d'altres. Els primers poden ser referits com a *neuronal Lafora bodies* i els segons com a *corpora amylacea-like granules*. Així doncs, l'absència de malina indueix a la formació de PGBs en neurones i incrementa la seva formació en astròcits. D'altra banda, la presència de GS és indispensable per a la formació de PGBs i l'augment de la seva activitat incrementa la formació de *corpora amylacea-like granules,* però no dels *neuronal Lafora bodies.* Tots aquests resultats suggereixen que, en contra del estudis publicats fins l'actualitat, els astròcits poden jugar un paper important en la malaltia de Lafora.

Astrocytes and neurons produce distinct types of polyglucosan bodies in Lafora Disease

Journal:	*GLIA*
Manuscript ID	GLIA-00483-2017.R1
Wiley - Manuscript type:	Original Research Article
Date Submitted by the Author:	n/a
Complete List of Authors:	Augé, Elisabet; Universitat de Barcelona, Departament de Bioquímica i Fisiologia Pelegrí, Carme; Universitat de Barcelona, Departament de Bioquímica i Fisiologia Manich, Gemma; Autonomous University of Barcelona (UAB), Cell Biology, Physiology and Immunology Cabezón, Itsaso; Universitat de Barcelona, Departament de Bioquímica i Fisiologia Guinovart, Joan; Institute for Research in Biomedicine (IRB Barcelona), The Barcelona Institute of Science and Technology Duran, Jordi; Institute for Research in Biomedicine (IRB Barcelona), The Barcelona Institute of Science and Technology Vilaplana, Jordi; Universitat de Barcelona, Departament de Bioquímica i Fisiologia
Key Words:	Lafora body, Corpora amylacea, Neo-epitope, Natural antibody, Malin

SCHOLARONE™
Manuscripts

Title:

Astrocytes and neurons produce distinct types of polyglucosan bodies in Lafora Disease

Short title:

Polyglucosan bodies in Lafora Disease

Authors:

Elisabet Augé[1,2], Carme Pelegrí[1,2,3], Gemma Manich[1], Itsaso Cabezón[1,2], Joan J. Guinovart[4,5,6], Jordi Duran[4,5]*, Jordi Vilaplana[1,2,3] *

Affiliations:

[1] Secció de Fisiologia, Departament de Bioquímica i Fisiologia, Universitat de Barcelona, Barcelona, Spain

[2] Institut de Neurociències, Universitat de Barcelona, Barcelona, Spain

[3] Centros de Biomedicina en Red de Enfermedades Neurodegenerativas (CIBERNED), Spain.

[4] Institute for Research in Biomedicine (IRB Barcelona), The Barcelona Institute of Science and Technology, Barcelona, Spain

[5] Centro de Investigación Biomédica en Red de Diabetes y Enfermedades Metabólicas Asociadas (CIBERDEM), Spain

[6] Departament de Bioquímica i Biomedicina Molecular, Universitat de Barcelona, Barcelona, Spain

* **Corresponding authors** (these authors contributed equally to these work):

- Dr. Jordi Duran, Institute for Research in Biomedicine (IRB Barcelona), The Barcelona Institute of Science and Technology, Carrer de Baldiri Reixac 10-12, 08028 Barcelona, Spain. Tel. (+34) 93 4037162 E-mail: jordi.duran@irbbarcelona.org
- Dr. Jordi Vilaplana, Secció de Fisiologia, Departament de Bioquímica i Fisiologia, Facultat de Farmàcia i Ciències de l'Alimentació, Av. Joan XXIII 27-31, 08028 Barcelona, Spain. Tel. (+34) 93 4024505. E-mail: vilaplana@ub.edu

Acknowledgements:

IRB Barcelona is the recipient of a Severo Ochoa Award of Excellence from MINECO (Government of Spain). This study was supported by grants BFU2013-47382-P, SAF-2014-54525-P and BFU2016-78398-P from MINECO, by the Agencia Estatal de Investigación (AEI), by European Regional Development Funds and a grant from the National Institute of Health (NIH-NINDS) P01NS097197. It was also funded by *CIBER de Diabetes y Enfermedades Metabólicas* and *CIBER de Enfermedades Neurodegenerativas* from the *Instituto de Salud Carlos III*. We thank the *Generalitat de Catalunya* for funding our research group (2014/SGR525). I. Cabezón and E. Augé received pre-doctoral "Ajuts de Personal Investigador en Formació" fellowships from the *Universitat de Barcelona* (APIF-UB). None of the supporting agencies had any role in performing the study or writing the manuscript.

Conflict of interest: The authors declare no competing financial interests

Number of words for Abstract (233) Introduction (1245), and Discussion (1260)
Materials and Methods (1365), Results (2046)
Total word count (10134)

Abstract

Lafora disease (LD), the most devastating adolescence-onset epilepsy, is caused by mutations in the *EPM2A* or *EPM2B* genes, which encode the proteins laforin and malin, respectively. Loss of function of one of these proteins, which are involved in the regulation of glycogen synthesis, induces the accumulation of polyglucosan bodies (PGBs)—known as Lafora bodies (LBs) and associated with neurons—in the brain. Ageing and some neurodegenerative conditions lead to the appearance of another type of PGB called corpora amylacea, which are associated with astrocytes and contain neo-epitopes that can be recognized by natural antibodies. Here we studied the PGBs in the cerebral cortex and hippocampus of malin knockout mice, a mouse model of LD. These animals presented not only LBs associated with neurons but also a significant number of PGBs associated with astrocytes. These astrocytic PGBs were also increased in mice from senescence-accelerated mouse-prone 8 (SAMP8) strain and mice with overexpression of Protein Targeting to Glycogen (PTG^{OE}), indicating that they are not exclusive of LD. The astrocytic PGBs, but not neuronal LBs, contained neo-epitopes that are recognized by natural antibodies. The astrocytic PGBs appeared predominantly in the hippocampus but were also present in some cortical brain regions, while neuronal LBs were found mainly in the brain cortex and the pyramidal layer of hippocampal regions CA2 and CA3. Our results indicate that astrocytes, contrary to current belief, are involved in the etiopathogenesis of LD.

Keywords

Lafora body, *Corpora amylacea*, Malin, Neo-epitope, Natural antibody.

Main points

- Absence of malin triggers the formation of polyglucosan bodies in neurons and enhances their development in astrocytes.
- These astrocytic polyglucosan bodies contain neo-epitopes that are recognized by natural antibodies.
- Astrocytes are involved in the etiopathogenesis of Lafora disease.

TOCI

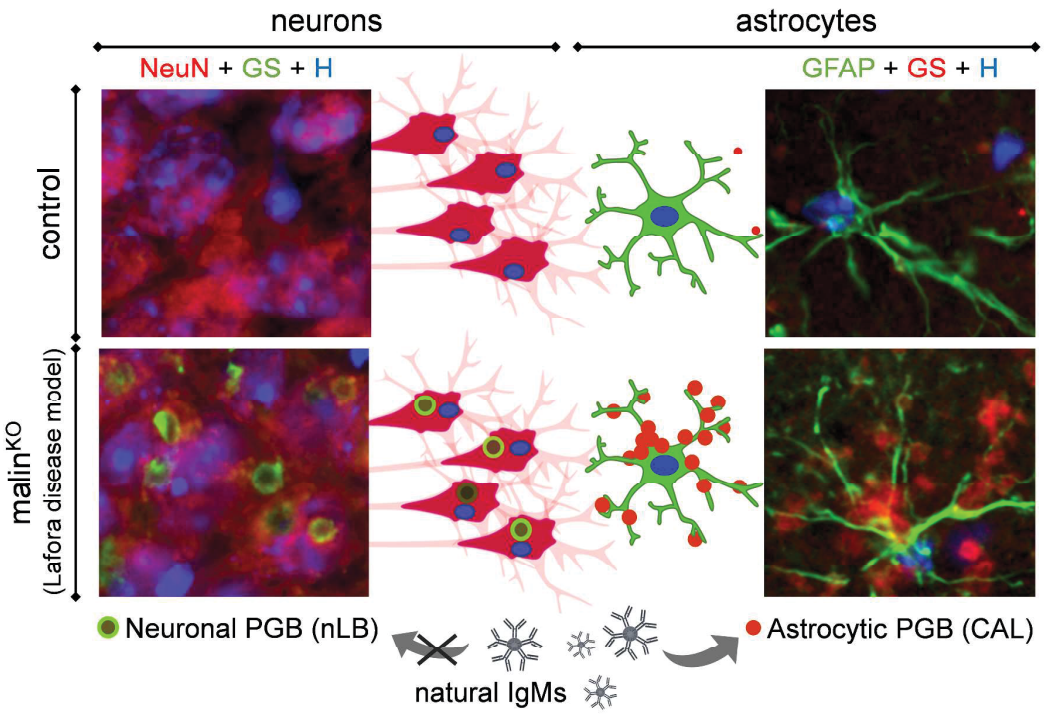

John Wiley & Sons, Inc.

Introduction

The term “polyglucosan bodies” (PGBs) refers to complex molecular aggregates composed of relatively large glucose polymers reaching diameters of tens of micrometres. PGBs have been reported in the central nervous system, but also in other organs and tissues, such as heart, skeletal muscle and liver (Cavanagh, 1999). While these aggregates have been described in humans and other species, they have been most widely studied in mammals. Various forms of PGB are linked to specific diseases. For example, *corpora amylacea* (CA) accumulate in the human brain during normal aging and to a greater extent in several neurodegenerative conditions, including Alzheimer’s, Parkinson’s, Huntington’s and Pick’s diseases (Pirici and Margaritescu, 2014; Rohn, 2015). Although human brain CA are formed mainly by aggregates of polymerized glucose, the presence of waste elements is a recurrent feature of these structures. This observation suggests that that they are involved in the trapping and sequestration of potentially hazardous products (Cavanagh, 1999; Pirici and Margaritescu, 2014; Rohn, 2015). We recently demonstrated that brain CA contain a number of neo-epitopes (Augé et al., 2017). The neo-epitopes are specific epitopes that are not present in healthy brain structures but appear in situations of cellular stress and tissue damage (Binder, 2010). We also found that the neo-epitopes present in CA are recognized by natural IgM antibodies, thus revealing the potential role of the natural immune system in CA removal (Augé et al., 2017). That study of the interaction between CA and the natural immune system was based on previous findings obtained in mice (Manich et al., 2015; Manich et al., 2016). In the same way in which CA accumulate with age in the human brain, aging in the mouse brain leads to the progressive appearance of PGBs, these generally referred to as “PAS granules” because of their positive staining with Periodic acid-Schiff (PAS). Given that the term “PAS granules” used to describe these mouse inclusions leads to misinterpretation because all PGBs are stained by PAS, in the present study we refer to them as CA-like (CAL) granules, because of their similarities to the CA of the human brain. CAL granules are present in a wide range of mouse strains, but they are particularly

abundant in the senescence-accelerated mouse prone 8 (SAMP8) model (Manich et al., 2016). The SAMP8 model is a non-genetically modified strain of mice with a characteristic accelerated aging process that shares characteristics with aged humans, such as a reduced lifespan, lordosis, hair loss, and reduced physical activity (Hamamoto et al., 1984; Takeda et al., 1994). In these animals, CAL granules appear in various regions of the brain as early as three months of age, and their number increases faster than in other strains (Del Valle et al., 2010; Jucker et al., 1994a, 1994b; Kuo et al., 1996). CAL granules arise from a degenerative process that affects astrocytic processes and their surrounding neuropil, and the granules are organized into clusters, each one associated with a specific astrocyte (Manich et al., 2014a). As observed for CA, some neo-epitopes appear during CAL granule formation (Manich et al., 2014b), and they are recognized by natural IgMs (Manich et al., 2015; Manich et al., 2016). We also found that many commercial antibodies are contaminated with natural IgMs, thus leading to false positive staining in immunohistochemical studies of CAL granules in mice (Manich et al., 2014b; Manich et al., 2016) and of CA in the human brain (Augé et al., 2017). These false positive immunostainings contribute to explaining the controversial results of research addressing CA and CAL granules and reveal the need to re-examine many of the immunohistochemical studies carried out to date.

Human diseases like Adult Polyglucosan Body Disease (APBD) and Lafora disease (LD) are also characterized by the accumulation of PGBs in the brain (Cavanagh, 1999; Pirici and Margaritescu, 2014). LD, the most devastating form of adolescence-onset epilepsy, is perhaps the most striking example of the accumulation of PBGs in this organ. These PGBs are referred to as Lafora bodies (LBs). LBs are formed by abnormal poorly branched glycogen that aggregates and amasses into large neuronal inclusions over time (Duran and Guinovart, 2015). LB deposition in the brain leads to the onset and inexorable worsening of neurodegeneration and epilepsy, leading to death by early adulthood (Cavanagh, 1999; Minassian, 2001; Pirici and Margaritescu, 2014). LD is an autosomal recessive myoclonus

epilepsy caused by mutations in one of the following two genes: *EPM2A*, which encodes laforin, a dual-specificity protein phosphatase with a functional carbohydrate-binding domain (Minassian et al., 1998; Serratosa et al., 1999); and *EPM2B*, which encodes malin, an E3 ubiquitin ligase (Chan et al., 2003). Individuals with mutations in *EPM2A* or *EPM2B* are neurologically and histologically indistinguishable. Laforin can function as a glucan phosphatase, removing the phosphate groups attached to glycogen (Tagliabracci et al., 2007). This finding, along with the hyperphosphorylation of glycogen in laforin knockout mice (laforin ^{KO}), led to the hypothesis that elevated levels of phosphate esters cause the abnormal glycogen structure and trigger LB formation (Roach, 2015; Tagliabracci et al., 2008). However, the phosphatase activity of laforin does not appear to be required to prevent the disease (Gayarre et al., 2014), and glycogen hyperphosphorylation does not cause the formation of LBs (Nitschke et al., 2017). Also, there is evidence that laforin and malin form a complex, and these proteins have been described to regulate glycogen accumulation through proteasome-dependent control of glycogen-related proteins, such as Protein Targeting to Glycogen (PTG) (Vilchez et al., 2007; Worby et al., 2008), Muscle Glycogen Synthase (MGS) (Vilchez et al., 2007) and glycogen debranching enzyme (Cheng et al., 2007). In addition, it has been reported that laforin and malin are involved in the clearance of misfolded proteins through the ubiquitin–proteasome system (Garyali et al., 2009; Rao et al., 2010) and in the autophagy degradation pathway (Aguado et al., 2010; Criado et al., 2012; Knecht et al., 2010; Puri et al., 2012). In previous studies, we generated a malin knockout mouse (malin^{KO}) as a model of LD, and combined it with a mouse with a specific deletion of MGS in the brain (MGS^{KO}) (Duran et al., 2013), to generate a double malin^{KO}+MGS^{KO} mouse. We observed that malin^{KO} animals accumulate LBs in the brain and other tissues and show neurodegeneration and functional impairments, including disrupted autophagy (Vallés-Ortega et al., 2011; Duran et al., 2014). The malin^{KO}+MGS^{KO} mouse did not show the accumulation of LBs, neurodegeneration or autophagy impairment seen in the malin^{KO} animals (Duran et al., 2014), thereby suggesting that all these defects are a consequence of glycogen accumulation. Moreover, mice overexpressing PTG

(PTG^{OE}), in which GS activity is increased, present high accumulation of PGBs in the brain (Duran et al., 2014). It is remarkable that although accumulations of CA have been described in several neurodegenerative conditions, including Alzheimer's, Parkinson's, Huntington's and Pick's diseases, the studies of PGBs in LD are centered in neuronal LBs, and the presence of astrocytic CAL granules in mouse models of LD has not yet been studied.

In this study, we explore, on the one hand, the presence of astrocytic CAL granules in the brain of a mouse model of LD, with the aim to determine whether this disease is characterized not only by altered neuronal function but also by the involvement of astrocytes. On the other hand, we address whether the LBs present in LD contain neo-epitopes that are recognized by natural IgMs. To this end, we used malin^{KO} mice and compared them with mice from other strains or models, such as SAMP8, MGS^{KO} and PTG^{OE} animals.

Materials and methods

Mice

Malin^{KO}, PTG^{OE} and MGS^{KO} mice were generated as previously described (Duran et al., 2014). After weaning, at 3 weeks of age, tail clippings were taken for genotyping by qPCR (performed by Transnetyx). Wild-type littermates from the different colonies were used as controls. SAMP8 mice were obtained from the *Servei d'Estabulari de la Facultat de Farmàcia i Ciències de l'Alimentació* (*Universitat de Barcelona*). All procedures were approved by the Barcelona Science Park's Animal Experimentation Committee and the Ethical Committee for Animal Experimentation of the *Universitat de Barcelona* and were carried out in accordance with the European Community Council Directive and National Institutes of Health guidelines for the care and use of laboratory animals. Mice were maintained on a 12/12 h light/dark cycle under standard room temperature (RT) and allowed free access to a commercial chow diet and water throughout the study. All experiments were performed with animals aged between 60 and 80 weeks (n=4 for each experimental group).

Brain processing

Frozen or paraffin-embedded brain sections were used. To obtain frozen sections, animals were anesthetized intraperitoneally with sodium pentobarbital (80 mg/kg) and given an intracardiac gravity-dependent perfusion of 50 mL of saline solution. Brains were dissected and frozen by immersion in isopentane and then chilled in dry ice. Frozen brains were then cut at the coronal plane into 20-µm-thick sections on a cryostat (Leica Microsystems, Germany) at −22°C and placed on slides. Coronal sections from bregma around −2.30 were selected, and the studies were performed considering the hippocampus and the cortex located between the retrosplenial granular region and the primary somatosensory cortex as the regions of interest. Sections were fixed with acetone for 10 min at 4°C and frozen at −20°C. To obtain paraffin-embedded sections (used in PTG^{OE} mice), animals were

perfused transcardially with phosphate-buffered saline (PBS) containing 4% of paraformaldehyde (PF). Brains were removed, postfixed overnight with PBS 4% PF, and embedded in paraffin. Paraffin sections were then cut to a thickness of 5 µm in a microtome.

PAS staining

Frozen sections were stained with PAS following the standard procedure. Briefly, sections were fixed for 10 min in Carnoy's solution (60% ethanol, 30% chloroform and 10% glacial acetic acid). The slides were then pretreated for 10 min with 0.25% periodic acid (19324-50, Electron Microscopy Sciences) in distilled water, followed by a washing step for 3 min with distilled water. They were then immersed in Schiff's reagent (26052-06, Electron Microscopy Sciences) for 10 min. Next, the slides were washed for 5 min in distilled water. Nuclei were counterstained for 1 min with a hematoxylin solution following Mayer (3870, J.T. Baker, Center Valley, USA). The slides were then washed, dehydrated with xylene, and coverslipped with quick-mounting medium (Eukitt, Fluka Analytical, Germany).

Immunofluorescence

Frozen sections were rehydrated with PBS and then blocked and permeabilized with 1% bovine serum albumin (Sigma-Aldrich) (Blocking buffer, BB) and 0.1% Triton X-100 (Sigma-Aldrich) in PBS for 20 min. They were washed with PBS and incubated with the corresponding primary antibodies overnight at 4ºC. Slides were washed and incubated for 1 h at RT with the corresponding secondary antibodies. Nuclear staining was performed with Hoechst (H-33258, Fluka, Madrid, Spain), and slides were washed and coverslipped with Fluoromount (Electron Microscopy Sciences, Hatfield, PA, USA).

PF-paraffin-embedded sections were deparaffinized and required an antigen retrieval step before immunostaining. Thus, slides were immersed in sodium citrate buffer (10 mM, pH=6.0) heated to 100°C for 40 min and then cooled to RT for 30 min. The slides were

washed, and the permeabilization step and immunofluorescence were then performed as described for the frozen sections.

The following were used as primary antibodies: rabbit monoclonal against GS (#15B1, Cell Signaling, Leiden, Netherlands); mouse monoclonal IgG1 against NeuN (#MAB377, MerckMillipore, Darmstadt, Germany); chicken polyclonal against GFAP (#AB5541, MerckMillipore); mouse monoclonal IgG2a against p62 (#ab56416, Abcam, Cambridge, UK); and human IgM purified immunoglobulins (OBT1524; AbD Serotec, Kidlington, UK). The following were used as secondary antibodies: Alexa Fluor (AF) 488 donkey anti-rabbit IgG (H+L); AF555 donkey anti-rabbit IgG (H+L); AF488 goat anti-chicken IgG (H+L); AF594 goat anti-mouse IgG1; AF594 goat anti-mouse IgG2a; and AF488 goat anti-human IgM heavy chain (Life Technologies, Eugene, OR, USA).

Staining controls were performed by incubating brain sections with BB instead of the primary antibody. In double staining, antibody cross-reactivity controls were also performed. In the case of p62 and GS staining, and in order to discard possible false positive staining produced by the presence of contaminant IgMs in the vials, secondary incubations with AF488 goat anti-mouse IgM (Jackson ImmunoResearch Laboratories) or goat anti-rabbit IgM conjugated to fluorescein isothiocyanate (FITC) (Abcam) antibodies were performed.

Image acquisition

Images were taken with a fluorescence laser and optic microscope (BX41, Olympus, Germany) and stored in tiff format. In immunofluorescence studies, and for each staining, all images were acquired using the same microscope, laser and software settings. Image treatment and analysis were performed by means of the ImageJ program (National Institute of Health, USA).

Quantification of the density of the different types of PGBs in mouse brain

To quantify the density of the different types of PGB (i.e. neuronal LBs (nLBs) and CAL granules) in the brains of mice from different strains, a minimum of four animals from each strain were used. Images of coronal sections were obtained with a Hamamatsu NanoZoomer Digital Slide Scanner (40× magnification). From each scanned coronal section, we then exported two tiff images containing the left and right brain hemispheres, each image including the hippocampus and the cortex from the retrosplenial granular region to the primary somatosensory cortex. The tiff images were then processed to calculate the number of nLBs or CAL granules using the ImageJ program (National Institute of Health, USA). For each tiff image, the process performed by this program included the following: a) splitting the color channels in order to obtain the green channel; b) transforming this new image into an 8-bit image; c) establishing the threshold in order to binarize the image; d) binarizing the image; d) applying the watershed; e) selecting, in the original image, the region where granules will be counted, i.e. the Region of Interest (ROI); f) saving the ROI in the ROI manager; g) applying the saved ROI in the corresponding binarized image; and h) to count the particles (i.e. PGBs) contained in the ROI. An example of image treatment and quantification of granules is summarized in Figure S1 (Supplementary material). To perform the quantification in non-continuous regions, we used the “combine” option in the ROI manager. The green channel of the original image was selected because it allowed better differentiation of the PGBs from other structures, such as nuclei and vessels walls. The threshold was visually and accurately set on each image, obtaining the best discrimination of granules. Watershed was applied because it allowed us to split some granules that were fused on binarized images. The size of particles to be counted was limited, in order to discard large structures. After the entire process, for each tiff image, we obtained the number of CAL granules in the hippocampus and in the cortex and that of nLBs in each of these regions in the case of malin^{KO} mice (nLBs are present only in malin^{KO} mice, not in the other strains studied). Finally, to obtain an approximation of the density of CAL or nLBs in a given hippocampal or cortical region, the total number of granules was divided by the total

volume (area of the hippocampal or cortical region x section thickness). Data were tabulated for further descriptive and statistical analysis.

Measurement of PGB size

To determine the size of the different types of PGB (i.e. nLBs and CAL granules) in malin^{KO} animals, representative images from the brain cortex stained with the PAS method were acquired at a 40x magnification with a BX41 Olympus microscope (Germany). Four animals were used, and four images were acquired for each animal. The diameter of the PGBs in the images was then manually measured using the “straight” tool of the ImageJ program (National Institute of Health, USA). Data were tabulated for further descriptive and statistical analysis.

Statistical analysis

Statistical analysis was performed with the ANOVA module of the IBM SPSS Statistics (IBM corp.©). Scheffe test was used for post-hoc comparisons. Significant differences were considered when $p<0.05$.

Results

Malin^{KO} mice accumulate two types of PGB

To characterize and differentiate PGBs in mouse brain, several immunostainings were performed in control, malin^{KO} and SAMP8 brain sections from animals aged 60-80 weeks. To detect PGBs, an antibody directed against GS, the only enzyme able to synthesize glucose polymers in mammals and a marker of PGBs (Vallés-Ortega *et al*. 2011), was used. Simultaneous fluorescence immunostaining on hippocampal sections with anti-GS and anti-GFAP antibodies allowed observation of the PGBs (Figure 1). As expected from previous descriptions (del Valle et al., 2010; Manich et al., 2016), a high number of astrocytic CAL granules were observed in SAMP8 mice (Figure 1a). These bodies were abundant in the hippocampus and tended to form clusters. The granules were in contact with astrocytic processes, as shown by GFAP staining, and, occasionally, the whole astrocyte that formed the cluster of granules was clearly visible. As previously indicated, CAL granules carry some neo-epitopes that are recognized by natural IgM antibodies, and the presence of these IgMs as contaminants in commercial antibodies has led to false positive staining and misinterpretations (Manich et al., 2015). In the present work, in order to discard false positive staining produced by such contaminant IgMs in the vial of anti-GS obtained in rabbit, we stained some sections with anti-GS as a primary antibody and a fluorochrome-labeled anti-rabbit IgM as a secondary antibody. The absence of staining on astrocytic CAL granules indicated that the anti-GS vial did not contain IgMs (Supplementary material, Figure S2), and thus confirmed that the GS staining of CAL granules was specific and not caused by IgMs. Of note, malin^{KO} brain sections double immunostained with anti-GS and anti-GFAP also contained clusters of astrocytic CAL granules, which were distributed in practically all hippocampal layers (Figure 1b), while these clusters were observed only sporadically in the hippocampus of control animals (Figure 1c). In addition, the hippocampus of malin^{KO} mice showed some PGBs that differed from CAL granules. These PGBs were located in the hippocampal pyramidal layer mainly of the CA2-CA3 region and were adjacent to nuclei, presumably neuronal nuclei (Figure 1b). These PGBs

were spherical and appeared to be larger than astrocytic CAL granules, they did not form clusters, and they were unrelated to GFAP processes. SAMP8 and control animals did not present this second type of PGB. The PGBs that differed from astrocytic CAL granules were also detected in the brain cortex of malin^{KO} mice (Figure 1e) but not in the cortex of control or SAMP8 animals (Figures 1d and f). In contrast, sporadic clusters of astrocytic CAL granules were detected in the cortex of the malin^{KO} animals (Figure 1e). Thereafter, simultaneous immunostaining was also performed with anti-GS to label the PGBs and with NeuN antibody, which labels the perikarya of neuronal cells. These immunostainings confirmed that the hippocampal and cortical PGBs in malin^{KO} mice that differ from astrocytic CAL granules are located inside the neuronal soma, near to the neuronal nuclei (Figure 2b and 2e). As these granules are exclusive to the malin^{KO} mice (the model of LD) and are formed in neurons, we will refer to them as neuronal Lafora bodies (nLBs). CAL granules, visible in the SAMP8, malin^{KO} and control animals with the anti-GS staining, did not colocalize with the neuronal NeuN staining.

To compare the size of astrocytic CAL granules with that of nLBs in malin^{KO} mice, the size of the granules from the cortical region was measured on representative images from sections stained with PAS and obtained from four malin^{KO} animals. A total of 259 CAL granules and 167 nLBs were measured. Thereafter, ANOVA was performed considering “size of granules” as the dependent variable, “type of granule” (nLB or CAL granule) as independent variable defined as a fixed factor and “animal” as independent variable defined as random factor. ANOVA indicated that the variable “type of granule” had a significant effect on “size of granules”, while the variable “animal” and the interaction between the independent variables did not. The mean size (±SEM) of CAL granules was 1.59 (±0.03) μm, while that of nLBs was 2.82 (±0.08) μm (Figures 3a and 3b). These observations allow us to conclude that nLBS attain larger sizes than CAL granules.

In the case of malin^{KO} mice, we also determined the density of CAL granules and nLBs in the hippocampus and cortex of four animals. Thereafter, ANOVA was performed considering “density of granules” as the dependent variable and “type of granules” (CAL or nLBs), “brain region” (hippocampus or cortex) and “animal” as independent variables. The variables “type of granules” and “brain region” were defined as fixed factors and “animal” as random factor. The ANOVA indicated that the variables “type of granules” and “brain region” and the interaction between them had a significant effect on “density of granules”. The mean density (±SEM) of the CAL granules in the cortex and hippocampus was 4936.45 (±594.91) granules/mm^3 and 176709.32 (±16058.40) granules/mm^3 respectively, and the mean density (±SEM) of nLBs in the cortex and hippocampus was 33671.06 (±2217.18) granules/mm^3 and 9324.92 (±592.69) granules/mm^3, respectively (Figure 3d). Post hoc comparisons indicated that the density of CAL granules was higher in the hippocampus than in the cortex, the density of nLBs was higher in the cortex than in the hippocampus, the density of CAL granules in the hippocampus was higher than that of nLBs in the hippocampus, and the density of nLBs in the cortex was higher than the density of CAL granules in the cortex. These results indicate that CAL granules predominate in the hippocampus while nLBs predominate in the cortex. Of note is the high density of CAL granules in the hippocampus compared to the other densities measured.

As CAL granules are also present in SAMP8 and control animals, we also determined the density of astrocytic CAL granules in each brain region in these mouse strains. In this case, ANOVA was performed considering “density of granules” as the dependent variable and “strain” (SAMP8, malin^{KO} and control) and “brain region” (hippocampus or cortex) as the independent variables, defined as fixed factors. ANOVA indicated that the variables “strain” and “brain region” had a significant effect on “density of granules” and the interaction between both variables is also significant. In SAMP8 animals, the mean density (±SEM) of the CAL granules in the hippocampus was 27560.24 (±1742.26) granules/mm^3. In malin^{KO} animals, as indicated before, the mean density (±SEM) of CAL granules in the cortex and

hippocampus was 4936.45 (±594.91) granules/mm^3 and 176709.32 (±16058.40) granules/mm^3, respectively. In control animals, the mean density (±SEM) of CAL granules in the hippocampus was 2388.17 (±428.63) granules/mm^3. CAL granules were not observed in the cortex of SAMP8 or control animals. Histograms of mean densities are shown in Figure 3e. The results indicate that the density of CAL granules was higher in the hippocampus than in the cortex in all the mouse strains and that the density of CAL granules was higher in malin^{KO} and SAMP8 animals than in controls, being also higher in malin^{KO} than in SAMP8 mice. Thus, we can assume that the absence of malin in malin^{KO} animals enhances the formation of CAL granules, although this increase can also be observed in other conditions like senescence, as observed in SAMP8 animals.

Taken together, these observations indicate that malin^{KO} animals present two types of PGB: a) CAL granules, which tend to form clusters, are associated with astrocytes, and predominate in the hippocampus, although some clusters can also be observed in the cortex; and b) nLBs, which are larger than CAL granules, are isolated granules, are related to neurons, and are found in the brain cortex and the pyramidal layer of the hippocampus. Of note, nLBs were exclusive to malin^{KO} mice, while astrocytic CAL granules, which were also present in SAMP8 and in control animals, were enhanced in both malin^{KO} and SAMP8 animals. These results are summarized in Table I.

Astrocytic CAL granules, but not nLBs, carry neo-epitopes recognized by natural IgMs

Human CA, as well as CAL granules of SAMP8 and ICR-CD1 mice, contain neo-epitopes that can be recognized by natural IgMs (Augé et al., 2017; Manich et al., 2015). To analyze whether PGBs from malin^{KO} mice also carry these neo-epitopes, double immunostaining was performed with anti-GS and purified human IgMs in the first incubation and the fluorochrome-labeled respective isotype specific antibodies in the second one. As expected, astrocytic CAL granules were immunostained with both antibodies, thereby revealing the presence of neo-epitopes on these structures (Figure 4a). In contrast, nLBs

were not positive for IgMs, thus indicating the absence of neo-epitopes (Figure 4b). All together, these observations reveal that the two types of PGB found in malin^{KO} animals differ in terms of neo-epitope presence.

Polyglucosan structure of CAL granules is required for the presence of the neo-epitopes

The brains of MGS^{KO} mice do not present PGBs and, consequently, MGS activity is a requisite for the formation of these bodies (Sinadinos et al., 2014; Duran et al., 2014). Accordingly, we examined whether the absence of the astrocytic CAL granules in MGS^{KO} animals (76-80 weeks-old) correlated with the absence of the neo-epitopes. Accordingly, we immunostained brain sections from MGS^{KO} animals with both anti-GS antibody and human IgMs. As expected, CAL granules were not detected with the anti-GS antibody in any brain region. Moreover, staining with human IgMs did not reveal the presence of neo-epitopes either (Figure 5). These results suggest that the neo-epitopes are part of the polyglucosan structure of the PGBs or that this polyglucosan structure is required for the addition of components that carry the neo-epitopes.

PTG^{OE} mice present CAL granules but not nLBs

PTG is a protein that orchestrates the signaling of several metabolic enzymes involved in glycogen synthesis. In this regard, the brains of PTG^{OE} mice show enhanced PGB accumulation (Duran et al., 2014). We therefore examined the nature of these PGBs and the presence of neo-epitopes on them. Double immunostaining with both the anti-GS antibody and human IgMs in brain sections of PTG^{OE} mice aged 60-64 weeks showed the presence of CAL granules, forming the characteristic clusters. These granules were immunostained with both anti-GS antibody and human IgMs and were located mainly in the hippocampus (Figure 6). No nLBs were found in this mouse model. Based on these observations, we postulate that the overexpression of PTG is not sufficient to trigger the formation of nLBs in neurons but is sufficient to increase the formation of CAL granules in astrocytes.

p62 is present in both CAL granules and nLBs

p62 is an ubiquitin-binding scaffold protein that interacts with ubiquitinated proteins via its C-terminal ubiquitin-associated (UBA) domain. The direct binding of p62 to LC3 and GABARAP family proteins, that serves as membrane linked protein-binding platforms (Qiu et al., 2017), allows p62 to guide ubiquitinated proteins to autophagosomes and to autophagic processes (Isakson et al., 2013). Moreover, p62 is also related to secretory autophagy, in which the content of the autophagosome is extruded from the cell (Ponpuak et al., 2016). Impaired autophagy has been described in LD mouse models, and it has been reported that p62 is increased in the brains of malin^{KO} mice (Duran et al., 2014). To determine whether the PGBs of malin^{KO} mice contain this protein, we performed double immunostaining with anti-GS and anti-p62 antibodies on brain sections of these animals. Both CAL granules and nLBs were stained with anti-p62 antibody, thereby indicating the presence of these proteins in both types of PGB (Figure 7). The presence of p62 in nLBs, which are located in the neuronal soma, near the nuclei, suggests that nLBs are related to lysosomal degradative autophagy. CAL granules, however, are located in astrocytic processes. As we will further discuss, the presence of p62 in these cells is perhaps related to secretory autophagy. It should be noted that to avoid false staining produced by contaminant IgMs in the vial, in the second incubations we used specific anti-IgG secondary antibodies that do not recognize the IgMs. In a complementary manner, and as performed for the anti-GS, we also examined whether mouse IgMs were present in the vial of anti-p62 antibody obtained in mouse. To this end, we stained some sections with anti-p62 antibody in the first incubation and with a secondary fluorochrome-labeled anti-mouse IgM antibody in the second one. The absence of staining in CAL granules indicated that the anti-p62 vial did not contain IgMs (Supporting Information, Figure S2).

Discussion

LD is characterized by the accumulation of PBGs in the brain, in the form of the so-called LBs. Traditionally, LBs are considered to be neuronal inclusions that occur concomitantly with neurodegeneration and epilepsy and they are related to the inexorable worsening of the condition until death in early adulthood (Lafora & Glueck, 1911). The extensive neuronal loss and severe neuropathological phenotypes observed in patients and animal models of LD suggest that neurons are particularly vulnerable to excess glycogen accumulation (Delgado-Escueta, 2007; Duran et al., 2014; López-González et al., 2017; Vallés-Ortega et al., 2011). Consistent with this, we have demonstrated that glycogen accumulation in neurons induces their death by apoptosis (Duran et al., 2012).

In this study, however, we demonstrate that malin^{KO} mice present high numbers of two types of PGB in the brain, one affecting neurons (nLBs) and the other astrocytes (CAL granules). The CAL granules, referred to in some cases as “PAS granules” in the literature, are also abundant in SAMP8 mice and in aged mice of other strains (Akiyama et al., 1986; Jucker et al., 1994b; Kuo et al., 1996; Manich et al., 2011; Manich et al., 2014a). We observed that the number of CAL granules was also increased in PTG^{OE} mice, indicating that the enhanced activity of MGS promotes their formation. Also, we found that CAL granules were absent in MGS^{KO} animals, thereby indicating that the synthesis of glycogen is indispensable for their formation. In a recent study, Oe et al. (2016) found that levels of glycogen from young C57BL/6 mice were high in the hippocampus. The accumulation of this glycogen was mainly in astrocytes, predominantly in their processes. In addition, these cells showed a patchy distribution of glycogen, each patch corresponding to an individual astrocyte. This patchy distribution diminished in aged mice, when PGBs appeared. The results obtained in the study by Oe et al. are thus consistent with our work, considering that the shifting from patchy glycogen to aberrant polyglucosan that forms the PGBs could be enhanced in malin^{KO}, PTG^{OE} and SAMP8 but not in MGS^{KO} animals. The other type of PGB that we found in malin^{KO} mice, located in the perikarya of the neurons, near to neuronal

nuclei, and referred to here as nLBs, appears to be exclusive to this animal model since it has not been observed in any other strain. All together, these results indicate that the absence of malin triggers the formation of PGBs in neurons and enhances the development of these bodies in astrocytes.

Accordingly, although it is widely assumed that all the PGBs in the brains of LD patients are neuronal, we propose that the two types of PGB described here are present: one type, probably CA, derived from astrocytes and the other type derived from neurons. Therefore, the term LBs should be limited to refer to nLBs. Moreover, based on the observations made in the malin^{KO} mouse model, the amount of the different types of PGB in the brains of LD patients is expected to be dependent on the brain region. The probable significant presence of both types of PGB in the brains of these individuals reinforces the need to make a distinction between LBs and CA, as previously stressed by various authors (Cervós-Navarro, 1991; Leel-Ossy, 2001; Ramsey, 1964; Seitelberger, 1968; Yoshimura, 1977).

As indicated earlier, we previously described the presence of neo-epitopes on both CAL granules from mouse brains and CA from human brains (Augé et al., 2017; Manich et al.,2014b). Although the composition of CA must be re-examined due to the possible false positive staining in immunohistochemical studies (Augé et al., 2017), there is wide consensus that CA contain waste products (Cavanagh, 1999; Pirici and Margaritescu, 2014) and ubiquitin (Cissé et al., 1995; Day et al., 2015; Pirici et al., 2014; Pirici and Margaritescu, 2014; Wilhelmus et al., 2011). It has been proposed that the presence of neo-epitopes on CA is related to the removal of these bodies via the natural immune system after their extrusion (Augé et al., 2017). In this regard, here we show that CAL granules contain p62 protein, which has a ubiquitin-binding domain and is involved in the sequestration of ubiquitinated proteins and organelles (Liu et al., 2016). Also, p62 is related to secretory autophagy, a process in which the content of the autophagosome extrudes

from the cell (Ponpuak et al., 2016). Therefore, the presence of p62 in CAL granules is consistent with the extrusion of CA from human brains.

Furthermore, the presence of a high number of CAL granules in the malin^{KO} mouse model suggests that the absence of malin alters glycogen metabolism not only in neurons but also in astrocytes. In the case of PTG^{OE} mice, CAL granules, but not nLBs, are also present in high numbers. This observation thus indicates distinct routes or key regulators in the genesis of nLBs and CAL granules. However, the activity of MGS is required for the formation of both types of granule, as can be deduced from the observation that CAL granules are absent in MGS^{KO} animals and that both types of PGB are absent in the double mutant malin^{KO}+MGS^{KO} mouse (Duran et al., 2014). CAL granules differ from nLBs in terms of distribution in the brain, size, clustering, and presence of neo-epitopes recognized by IgMs. We previously described the presence of PGBs in astrocytes of the malin^{KO} mouse model (Valles-Ortega et al., 2011). In the present work, we identify astrocytic PGBs as CAL granules and an important pool of PGBs in LD. Since astrocytes serve essential roles in brain function, the impairment of astrocytic activity caused by the accumulation of CAL granules may contribute to the pathophysiology of LD. In this regard, astrocytic uptake of potassium and glutamate is essential for the regulation of neuronal excitability, and the malfunction of astrocytes in LD could explain the epileptic phenotype of the disease (Amédée et al., 1997; Coulter and Eid, 2012). Given that aged mice and the PTG^{OE} mouse model show increased accumulation of CAL granules, it would be of interest to study the epileptic phenotype of these animals.

LBs have been classified as type I or type II on the basis of their size and shape (Van Hoof et al., 1967; Machado-Salas J et al., 2012). Furthermore, it has been hypothesized that these two types are different stages of the same process, in which the accumulation of type I LBs would activate the formation of type II LBs (Machado-Salas et al., 2012). On the basis of the results and images presented in that study, it seems that type I LBs correspond to

CAL granules and type II to nLBs. Therefore, if this correspondence is correct, it is not possible that type I LBs would activate the formation of type II, because of the different cellular origin and different brain region preferences of CAL granules and nLBs. Moreover, given the presence of possible IgM contaminants in the antibodies used and the false staining that IgMs can produce (Manich et al., 2015), we propose that immunohistochemistry studies of PGBs should be reanalyzed.

In conclusion, here we report that the absence of malin enhances the formation of astrocytic CAL granules and triggers the formation of nLBs. These findings should be considered when studying LD, and further work should be done to determine the involvement of each type of PGB in the etiopathogeny of this disease. Greater knowledge of the effects of CAL granules on astrocytes and those of nLBs on neurons, as well as the interaction between the neo-epitopes present in CAL granules and the natural immune system, is expected to contribute to unravelling LD.

References

Aguado, C., Sarkar, S., Korolchuk, V.I., Criado, O., Vernia, S., Boya, P., Sanz, P., de Córdoba S.R., Knecht, E., & Rubinsztein, D.C. (2010). Laforin, the most common protein mutated in Lafora disease, regulates autophagy. Human Molecular Genetics, *19*, 2867–2876. doi: 10.1093/hmg/ddq190.

Akiyama, H., Kameyama, M., Akiguchi, I., Sugiyama, H., Kawamata, T., Fukuyama, H., Kimura, H., Matsushita, M., & Takeda, T. (1986). Periodic acid-Schiff (PAS)-positive: granular structures increase in the brain of senescence accelerated mouse (SAM). Acta Neuropathologica, *72*, 124–129.

Amédée, T., Robert, A., & Coles, J.A. (1997). Potassium homeostasis and glial energy metabolism. Glia, *21*, 46-55.

Augé, E., Cabezón, I., Pelegrí, C., & Vilaplana, J. (2017). New perspectives on corpora amylacea in the human brain. Scientific Reports, *7*, 41807. doi:10.1038/srep41807.

Baumgarth, N., Tung, J.W., & Herzenberg, L.A. (2005). Inherent specificities in natural antibodies: a key to immune defense against pathogen invasion. Springer Seminars in Immunopathology, *26*, 347–362. doi:10.1007/s00281-004-0182-2

Binder, C.J. (2010). Natural IgM antibodies against oxidation-specific epitopes. Journal of Clinical Immunology, *30*, S56-S60. doi: 10.1007/s10875-010-9396-3.

Cavanagh, J.B. (1999). Corpora-amylacea and the family of polyglucosan diseases. Brain Research Reviews, *29*, 265–295.

Cervós-Navarro, J. (1991). *Polyglukosaneinschlüsse im Nervengewebe. In: Pathologie des Nervensystems V: Degenerative und metabolische Erkrankungen*. Berlin, Germany: Springer Verlag.

Chan, E.M., Young, E.J., Ianzano, L., Munteanu, I., Zhao, X., Christopoulos, C.C., Avanzini, G., Elia, M., Ackerley, C.A., Jovic, N.J., Bohlega, S., Andermann, E., Rouleau, G.A., Delgado-Escueta, A.V., Minassian. B.A., & Scherer, S.W. (2003). Mutations in NHLRC1 cause progressive myoclonus epilepsy. Nature Genetics, *35*, 125–127. doi: 10.1038/ng1238.

Cheng, A., Zhang, M., Gentry, M.S., Worby, C.A., Dixon, J.E., & Saltiel, A.R. (2007). A role for AGL ubiquitination in the glycogen storage disorders of Lafora and Cori's disease. Genes & Development, *21*, 2399–2409. doi: 10.1101/gad.1553207.

Cissé, S., Perry, G., Lacoste-Royal, G., Cabana, T., & Gauvreau, D. (1993). Immunochemical identification of ubiquitin and heat-shock proteins in corpora amylacea from normal aged and Alzheimer's disease brains. Acta Neuropathologica, *85*, 233–240.

Coulter, D.A. & Eid, T. (2012). Astrocytic regulation of glutamate homeostasis in epilepsy. Glia, *60*, 1215-1226. doi: 10.1002/glia.22341.

Criado, O., Aguado, C., Gayarre, J., Duran-Trio, L., Garcia-Cabrero, A.M., Vernia, S., San Millán, B., Heredia, M., Romá-Mateo, C., Mouron, S., Juana-López, L., Domínguez, M., Navarro, C., Serratosa, J.M., Sanchez, M., Sanz, P., Bovolenta, P., Knecht, E., & Rodriguez de Cordoba, S. (2012). Lafora bodies and neurological defects in malin-deficient mice correlate with impaired autophagy. Human Molecular Genetics, *21*, 1521–1533. doi: 10.1093/hmg/ddr590.

Day, R. J., Mason, M. J., Thomas, C., Poon, W.W., & Rohn, T. T. (2015). Caspase-cleaved tau co-localizes with early tangle markers in the human vascular dementia brain. PLOS One, *10*, e0132637. doi: 10.1371/journal.pone.0132637.

Del Valle, J., Duran-Vilaregut, J., Manich, G., Casadesús, G., Smith, M.A., Camins, A., Pallàs, M., Pelegrí, C., & Vilaplana, J. (2010). Early amyloid accumulation in the hippocampus of SAMP8 mice. Journal of Alzheimer's disease, *19*, 1303–1315. doi: 10.3233/JAD-2010-1321.

Delgado-Escueta, A.V. (2007). Advances in Lafora progressive myoclonus epilepsy. Current Neurology and Neuroscience Reports, *7*, 428- 433.

Doehner, J., Madhusudan, A., Konietzko, U., Fritschy, J.M., & Knuesel, I. (2010). Co-localization of Reelin and proteolytic AbetaPP fragments in hippocampal plaques in aged wild-type mice. Journal of Alzheimer's Disease, *19*, 1339–1357. doi: 10.3233/JAD-2010-1333.

Duran, J., & Guinovart, J.J. (2015). Brain glycogen in health and disease. Molecular Aspects of Medicine, *46*, 70-77. doi: 10.1016/j.mam.2015.08.007.

Duran, J., Tevy, M.F., Garcia-Rocha, M., Calbó, J., Milán, M., & Guinovart, J.J. (2012). Deleterious effects of neuronal accumulation of glycogen in flies and mice. EMBO Molecular Medicine, *4*, 719-729. doi: 10.1002/emmm.201200241.

Duran J., Saez I., Gruart A., Guinovart JJ., & Delgado-García J.M. (2013). Impairment in long-term memory formation and learning-dependent synaptic plasticity in mice lacking glycogen synthase in the brain. Journal of Cerebral Blood Flow and Metabolism, 33, 550-556. doi: 10.1038/jcbfm.2012.200.

Duran, J., Gruart, A., Garcia-Rocha, M., Delgado-Garcia, J.M., & Guinovart, J.J. (2014). Glycogen accumulation underlies neurodegeneration and autophagy impairment in Lafora disease. Human Molecular Genetics, *23*, 3147–3156. doi: 10.1093/hmg/ddu024.

Garyali, P., Siwach, P., Singh, P.K., Puri, R., Mittal, S., Sengupta, S., Parihar, R., & Ganesh, S. (2009). The malin-laforin complex suppresses the cellular toxicity of misfolded proteins by promoting their degradation through the ubiquitin-proteasome system. Human Molecular Genetics, *18*, 688– 700. doi: 10.1093/hmg/ddn398.

Gayarre, J., Duran-Trio, L., Garcia, O.C., Aguado, C., Juana-Lopez, L., Crespo, I., Knecht, E., Bovolenta, P., & de Cordoba, S.R. (2014). The phosphatase activity of laforin is dispensable to rescue Epm2a−/− mice from Lafora disease. Brain, *137*, 806–818. doi: 10.1093/brain/awt353.

Grönwall, C., Vas, J., & Silverman, G. J. (2012). Protective roles of natural IgM antibodies. Frontiers in Immunology, *3*, 66. doi: 10.3389/fimmu.2012.00066.

Hamamoto, H., Honma, A., Irino, M., Matsushita, T., Toda, K., Matsumura, M., & Takeda, T. (1984). Grading score system: A method for evaluation of the degree of senescence in senescence accelerated mouse (SAM). Mechanisms of Ageing and Development, *26*, 91-102.

Isakson, P., Holland, P., Simonsen, A., (2103). The role of ALFY in selective autophagy. Cell Death and Differentiation, 20, 12–20.

Jucker, M., Walker, L.C., Kuo, H., Tian, M., & Ingram, D.K. (1994a). Age-related fibrillar deposits in brains of C57BL/6 mice. A review of localization, staining characteristics, and strain specificity. Molecular Neurobiology, *9*, 125–133.

Jucker, M., Walker, L.C., Schwarb, P., Hengemihle, J., Kuo, H., Snow, A.D, Bamert, F., & Ingram, D.K. (1994b). Age-related deposition of glia-associated fibrillar material in brains of C57BL/6 mice. Neuroscience, *60*, 875–889.

Knecht, E., Aguado, C., Sarkar, S., Korolchuk, V.I., Criado-Garcia, O., Vernia, S., Boya, P., Sanz, P., Rodríguez de Córdoba, S., & Rubinsztein, D.C. (2010). Impaired autophagy in Lafora disease. Autophagy, *6*, 991–993. doi: 10.4161/auto6.7.13308.

Kuo, H., Ingram, D.K., Walker, L.C., Tian, M., Hengemihle, J.M., & Jucker, M. (1996). Similarities in the age-related hippocampal deposition of periodic acid-schiff-positive granules in the senescence-accelerated mouse P8 and C57BL/6 mouse strains. Neuroscience, *74*, 733–740.

Lafora, G.R., & Glueck, B. (1911). Beitrag zur Histopathologie der myoklonischen epilepsie. Zeitschrift für die Gesamte Neurologie und Psychiatrie, *6*, 1–14.

Leel-Ossy, L. (2001). New data on the ultrastructure of the corpus amylaceum (polyglucosan body). Pathology Oncology Research, *7*, 145-150.

López-González, I., Viana, R., Sanz, P., & Ferrer, I. (2017). Inflammation in Lafora disease: Evolution with disease progression in laforin and malin knock-out mouse models. Molecular Neurobiology, *54*, 3119-3130. doi: 10.1007/s12035-016-9884-4.

Liu, W.J., Ye, L., Huang, W.F., Gui, L.J., Xu, G., Wu, H.L., Yang, C., & Liu, H.F. (2016) p62 links the autophagy pathway and the ubiquitin-proteosome system upon ubiquitinated protein degradation. Cellular & Molecular Biology Letters, *13*, 21-29. doi: 10.1186/s11658-016-0031-z.

Machado-Salas, J., Avila-Costa, M.R., Guevara, P., Guevara, J., Durón, R.M., Bai, D., Tanaka, M., Yamakawa, K., & Delgado-Escueta, A.V. (2012). Ontogeny of Lafora bodies and neurocytoskeleton changes in Laforin-deficient mice. Experimental Neurology, *236*, 131-140. doi: 10.1016/j.expneurol.2012.04.008.

Madhusudan, A., Sidler, C., & Knuesel, I. (2009). Accumulation of reelin-positive plaques is accompanied by a decline in basal forebrain projection neurons during normal aging. The European Journal of Neuroscience. *30*, 1064–1076. doi: 10.1111/j.1460-9568.2009.06884.x.

Manich, G., Augé, E., Cabezón, I., Pallàs, M., Vilaplana, J., & Pelegrí, C. (2015). Neo-epitopes emerging in the neurodegenerative hippocampal granules of aged mice can be recognized by natural IgM auto-antibodies. Immunity & Ageing, *12*, 23. doi: 10.1186/s12979-015-0050-z.

Manich, G., Cabezón, I., Augé, E., Pelegrí, C., & Vilaplana, J. (2016). Periodic acid-Schiff granules in the brain of aged mice: From amyloid aggregates to degenerative structures containing neo-epitopes. Ageing Research Reviews, *27*, 42–55. doi: 10.1016/j.arr.2016.03.001.

Manich, G., Cabezón, I., Camins, A., Pallàs, M., Liberski, P.P., Vilaplana, J., & Pelegrí, C. (2014a). Clustered granules present in the hippocampus of aged mice result from a degenerative process affecting astrocytes and their surrounding neuropil. Age, *36*, 9690. doi: 10.1007/s11357-014-9690-8.

Manich, G., Del Valle, J., Cabezón, I., Camins, A., Pallàs, M., Pelegrí, C., & Vilaplana, J. (2014b). Presence of a neo-epitope and absence of amyloid beta and tau protein in degenerative hippocampal granules of aged mice. Age, *36*, 151–165. doi: 10.1007/s11357-013-9560-9.

Minassian, B.A. (2001). Lafora's disease: towards a clinical, pathologic, and molecular synthesis. Pediatric Neurology, *25*, 21-29.

Minassian, B.A., Lee, J.R., Herbrick, J.A., Huizenga, J., Soder, S., Mungall, A.J., Dunham, I., Gardner, R., Fong, C.Y., Carpenter, S., Jardim, L., Satishchandra, P., Andermann, E., Snead, O.C., Lopes-Cendes, I., Tsui, L.C., Delgado-Escueta, A.V., Rouleau, G.A., & Scherer, S.W. (1998). Mutations in a gene encoding a novel protein tyrosine phosphatase cause progressive myoclonus epilepsy. Nature Genetics, *20*, 171–174.

Nitschke, F., Sullivan, M.A., Wang, P., Zhao, X., Chown, E.E., Perri, A.M., Israelian, L., Juana-Lopez, L., Bovolenta, P., Rodriguez de Cordoba, S., Steup, M.; & Minassian, B.A. (2017). Abnormal glycogen chain length pattern, not hyperphosphorylation, is critical in Lafora disease. EMBO Molecular Medicine, *9*, 906–917. doi: 10.15252/emmm.201707608.

Oe, Y., Baba, O., Ashida, H., Nakamura, K.C., & Hirase, H. (2016). Glycogen distribution in the microwave-fixed mouse brain reveals heterogeneous astrocytic patterns. Glia, *64*, 1532-1545. doi: 10.1002/glia.23020.

Pirici, I., Margaritescu, C., Mogoanta, L., Petrescu, F., Simionescu, C.E., Popescu, E.S., Cecoltan, S., & Pirici, D. (2014). Corpora amylacea in the brain form highly branched three-dimensional lattices. Romanian Journal of Morphology and Embryology, *55*, 1071–1077.

Pirici, D., & Margaritescu, C. (2014). Corpora amylacea in aging brain and age-related brain disorders. Journal of Aging Gerontology, *2*, 33–57. doi: http://dx.doi.org/10.12974/2309-6128.2014.02.01.6.

Puri, R., Suzuki, T., Yamakawa, K., & Ganesh, S. (2012). Dysfunctions in endosomal-lysosomal and autophagy pathways underlie neuropathology in a mouse model for Lafora disease. Human Molecular Genetics, *21*, 175–184. doi: 10.1093/hmg/ddr452.

Qiu, Y., Zheng, Y., Wu, K.P., & Schulman, B.A. (2017). Insights into links between autophagy and the ubiquitin system from the structure of LC3B bound to the LIR motif from the E3 ligase NEDD4. Protein Science, *26*, 1674-1680. doi: 10.1002/pro.3186

Ramsey, H.I. (1965). Ultrastructure of corpora amylacea. Journal of Neuropathology and Experimental Neurology, *24*, 25-39.

Rao, S.N., Maity, R., Sharma, J., Dey, P., Shankar, S.K., Satishchandra, P., & Jana, N.R. (2010). Sequestration of chaperones and proteasome into Lafora bodies and proteasomal dysfunction induced by Lafora disease-associated mutations of malin. Human Molecular Genetics, *19*, 4726–4734. doi: 10.1093/hmg/ddq407.

Roach, P.J. (2015). Glycogen phosphorylation and Lafora disease. Molecular Aspects of Medicine, *46*, 78–84. doi: 10.1016/j.mam.2015.08.003.

Robertson, T.A., Dutton, N.S., Martins, R.N., Roses, A.D., Kakulas, B.A., & Papadimitriou, J.M. (1998). Age-related congophilic inclusions in the brains of apolipoprotein E-deficient mice. Neuroscience, *82*, 171–180.

Rohn, T.T. (2015). Corpora amylacea in neurodegenerative diseases: cause or effect? International Journal of Neurology and Neurotherapy, *2*, 3.

Sbarbati, A., Carner, M., Colletti, V., & Osculati, F. (1996). Extrusion of corpora amylacea from the marginal glia at the vestibular root entry zone. Journal of Neuropathology Experimental Neurology, *55*, 196–201.

Seitelberger, F. (1968). *Myoclonus body disease. In: Pathology of the nervous system*. New York, NY: NMcGraw-Hill.

Serratosa, J.M., Gomez-Garre, P., Gallardo, M.E., Anta, B., de Bernabe, D.B., Lindhout, D., Augustijn, P.B., Tassinari, C.A., Malafosse, R.M., Topcu, M., Grid, D., Dravet, C., Berkovic, S.F., & De Córdoba, S.R. (1999). A novel protein tyrosine phosphatase gene is mutated in progressive myoclonus epilepsy of the Lafora type (*EPM2*). Human Molecular Genetics, *8*, 345–352.

Sharma, J., Rao, S.N., Shankar, S.K., Satishchandra, P., & Jana, N.R. (2011). Lafora disease ubiquitin ligase malin promotes proteasomal degradation of neuronatin and regulates glycogen synthesis. Neurobiology of Disease, *44*, 133–141. doi: 10.1016/j.nbd.2011.06.013.

Sinadinos, C., Valles-Ortega, J., Boulan, L., Solsona, E., Tevy, M.F., Marquez, M., Duran, J., Lopez-Iglesias, C., Calbó, J., Blasco, E., Pumarola, M., Milán, M., & Guinovart, J.J. (2014). Neuronal glycogen synthesis contributes to physiological aging. Aging Cell, *13*, 935–945. doi: 10.1111/acel.12254.

Suzuki, A., Yokoo, H., Kakita, A., Takahashi, H., Harigaya, Y., Ikota, H., & Nakazato, Y. (2012). Phagocytized corpora amylacea as a histological hallmark of astrocytic injury in neuromyelitis optica. Neuropathology, *32*, 597–594. doi: 10.1111/j.1440-1789.2012.01299.x.

Tagliabracci, V.S., Girard, J.M., Segvich, D., Meyer, C., Turnbull, J., Zhao, X.C., Minassian, B.A., DePaoli-Roach, A.A., & Roach, P.J. (2008). Abnormal metabolism of glycogen phosphate as a cause for Lafora disease. Journal of Biological Chemistry, *283*, 33816–33825. doi: 10.1074/jbc.M807428200.

Tagliabracci, V.S., Turnbull, J., Wang, W., Girard, J.M., Zhao, X., Skurat, A.V., Delgado-Escueta, A.V., Minassian, B.A., DePaoli-Roach, A.A., & Roach, P.J. (2007). Laforin is a glycogen phosphatase, deficiency of which leads to elevated phosphorylation of glycogen in vivo. Proceedings of the National Academy of Sciences USA, *104*, 19262–19266. doi: 10.1073/pnas.0707952104

Takeda, T., Hosokawa, M., & Higuchi, K. (1994). *Senescence accelerated mouse (SAM), a novel murine model of aging.* In The SAM model of senescence, Takeda, T., ed. Elsevier, Amsterdam, pp. 15-22.

Valles-Ortega, J., Duran, J., Garcia-Rocha, M., Bosch, C., Saez, I., Pujadas, L., Serafin, A., Cañas, X., Soriano, E., Delgado-García, J.M., Gruart, A., & Guinovart, J.J. (2011). Neurodegeneration and functional impairments associated with glycogen synthase accumulation in a mouse model of Lafora disease. EMBO Molecular Medicine, *3*, 667–681. doi: 10.1002/emmm.201100174.

Van Hoof, F., & Hageman-Bal, M. (1967). Progressive familial myoclonic epilepsy with Lafora bodies. Electron microscopic and histochemical study of a cerebral biopsy. Acta Neuropathologica, *7*, 315–336.

Vilchez, D., Ros, S., Cifuentes, D., Pujadas, L., Valles, J., Garcia-Fojeda, B., Criado-García, O., Fernández-Sánchez, E., Medraño-Fernández, I., Domínguez, J., García-Rocha, M., Soriano, E., Rodríguez de Córdoba, S., & Guinovart, J.J. (2007). Mechanism suppressing glycogen synthesis in neurons and its demise in progressive myoclonus epilepsy. Nature Neuroscience, *10*, 1407–1413. doi: 10.1038/nn1998

Wilhelmus, M. M. M., Verhaar, R., Bol, J.G., Van Dam, A.M., Hoozemans, J.J., Rozemuller, A.J., & Drukarch, B. (2011). Novel role of transglutaminase 1 in corpora amylacea formation? Neurobiology of Aging, *32*, 845–856. doi: 10.1016/j.neurobiolaging.2009.04.019.

Worby, C.A., Gentry, M.S., & Dixon, J.E. (2008). Malin decreases glycogen accumulation by promoting the degradation of protein targeting to glycogen (PTG). The Journal of Biological Chemistry, *283*, 4069–4076. doi: 10.1074/jbc.M708712200

Yoshimura, T. (1977). Beiträge zu den klinisch - und histopathologischen Untersuchungen über die Fälle der Lafora-ähnlichen Einschlusskörperchen. Folia Psychiatrica et Neurologica Japonica, *31*, 89-102.

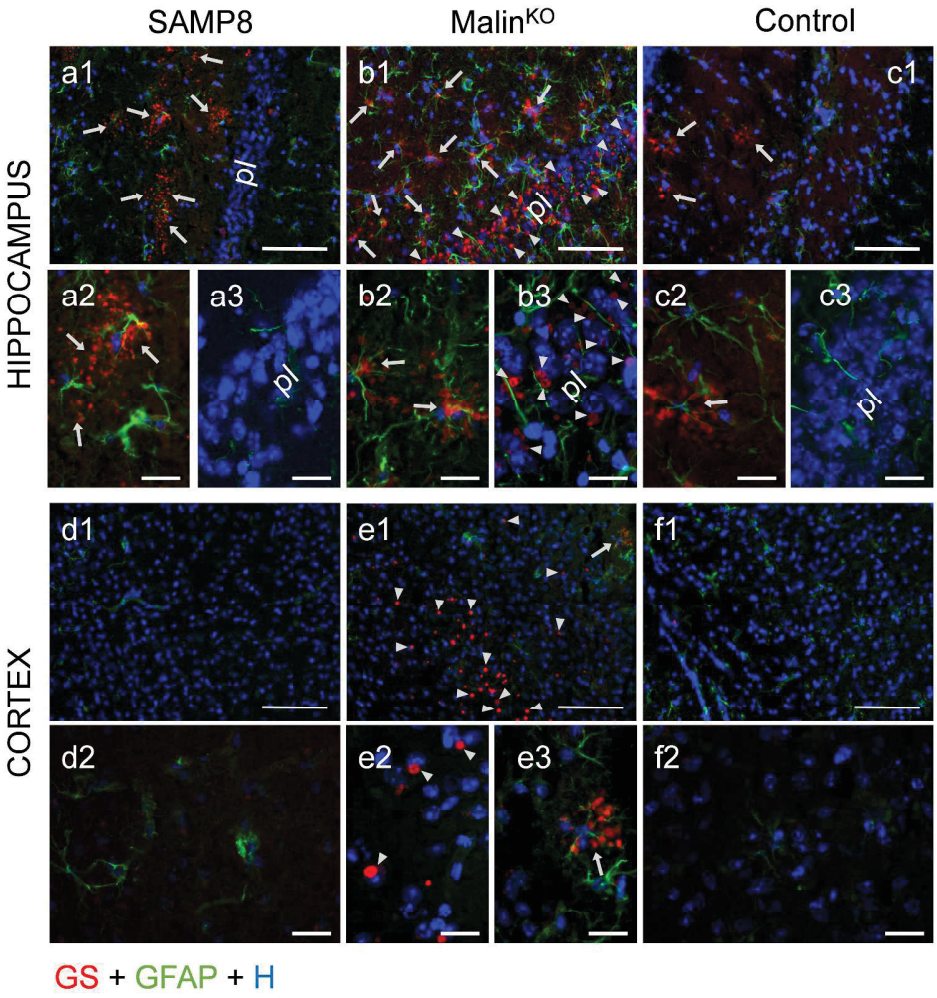

Figure 1. PGBs associated with astrocytes in SAMP8, malinKO and control animals. Representative images of hippocampal and cortical brain sections from SAMP8, malinKO and control mice double immunostained with anti-GS (red) and anti-GFAP (green) antibodies. Hoechst (blue) was used for nuclear staining. Hippocampal brain sections from SAMP8, malinKO mice, and, sporadically, control mice, show clusters of astrocyte-associated CAL granules (arrows in a1, b1 and c1). In some cases, the whole astrocyte involved in the formation of a cluster of CAL granules can be observed (a2, b2 and c2). MalinKO mice also present some non-astrocyte-associated PGBs (arrowheads), located mainly in the pyramidal layer (pl) of the hippocampal CA3 region (b1 and b3). These non-astrocyte-associated PGBs are not detected in SAMP8 or control animals (a3, c3). Cortex brain sections from malinKO mice also contain non-astrocyte-associated PGBs (arrowheads in e1), which are located near to some nuclei (e2), and only a few clusters of CAL granules (e3). The cortex of SAMP8 and control animals do not show PGBs (d1, d2, f1 and f2). Arrows: clusters of astrocyte-associated CAL granules. Arrowheads: non-astrocyte-associated PGBs. Scale bar a1-f1: 100 µm; a2-f2, a3-c3 and e3: 20 µm.

439x462mm (300 x 300 DPI)

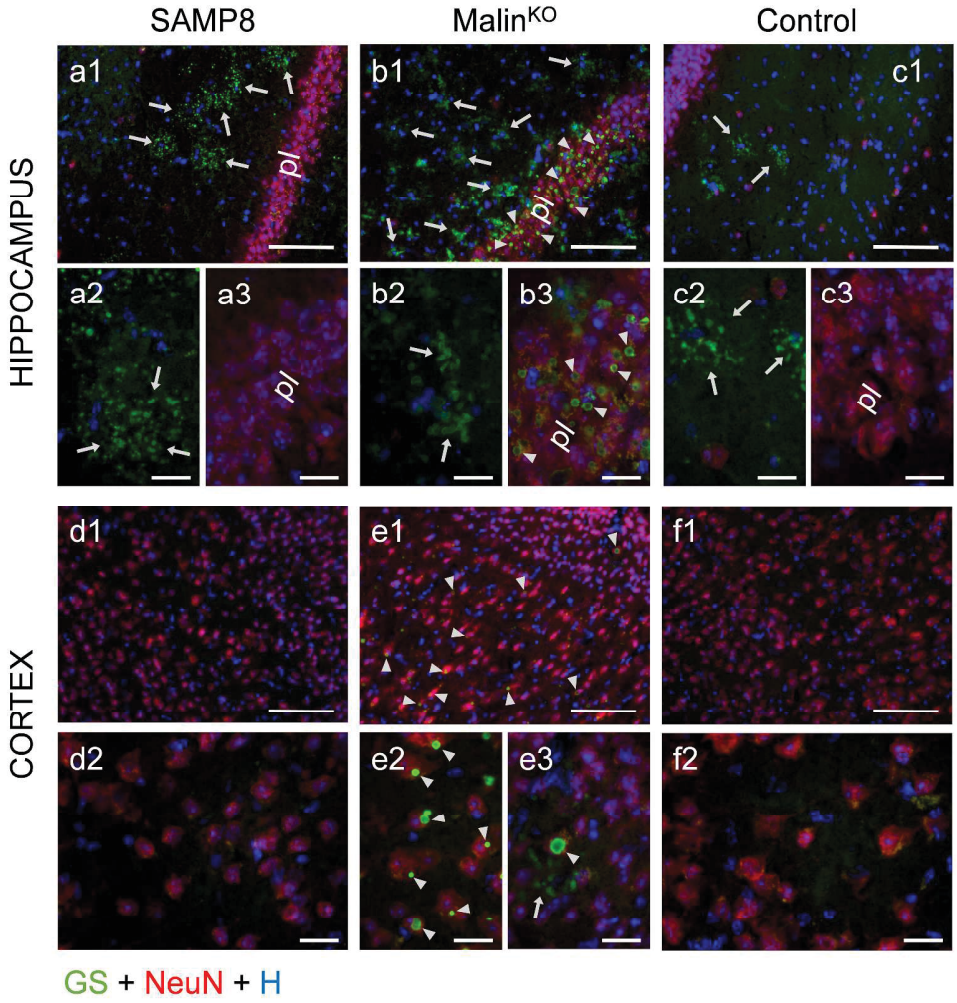

Figure 2. PGBs associated with neurons in malinKO animals. Representative images of hippocampal and cortical brain sections from SAMP8, malinKO and control mice double immunostained with anti-GS (green) and NeuN (red) antibodies. Hoechst (blue) was used for nuclear staining. MalinKO mice show neuronal PGBs (arrowheads in b1 and b3) and clusters of CAL granules (arrows in b1 and b2) in the hippocampus. Neuronal PGBs are mainly in the pyramidal layer. Hippocampal sections of SAMP8 mice show CAL granules (a1 and a2). Clustered CAL granules are also observed in control animals (c1 and c2), but in low numbers. Neither SAMP8 or control mice show neuron-associated PGBs in the hippocampus (a3 and c3). Neuron-associated and some non-neuron-associated PGBs can be observed in the cortex of malinKO animals (e1, e2 and e3). No PGBs were observed in the cortex of SAMP8 or control animals (d1, d2, f1 and f2). As neuronal PGBs are exclusive to the malinKO mouse, a model of Lafora disease, and they are found in neurons, they are referred to as neuronal Lafora bodies (nLBs). Arrows: clusters of CAL granules. Arrowheads: nLBs. pl: pyramidal layer of the hippocampus. Scale bar a1-f1: 100 μm; a2-f2, a3-c3 and e3: 20 μm.

440x465mm (300 x 300 DPI)

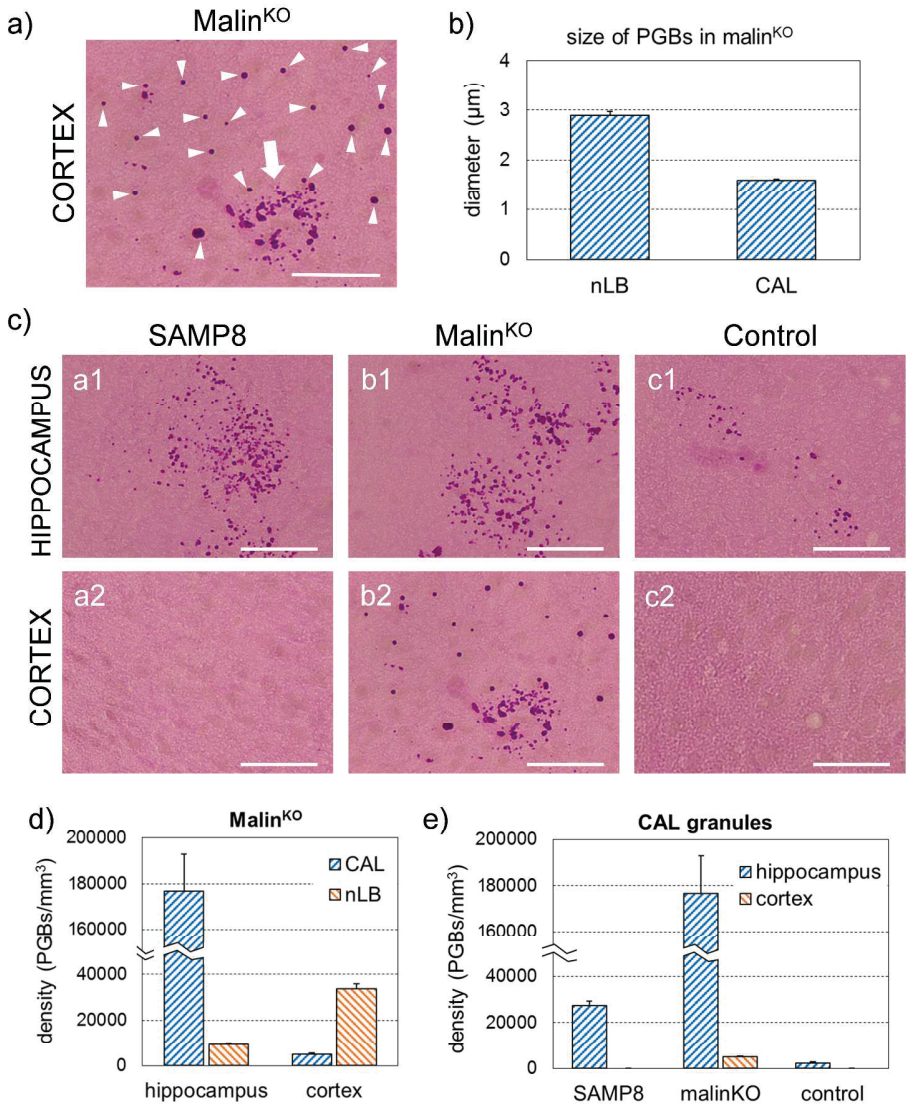

Figure 3. CAL granules, smaller than nLBs, predominate in the hippocampus while nLBs predominate in the cortex. (a) Representative image of the cortex of a malinKO mouse immunostained with PAS, in which nLBs (arrowheads) and a cluster of CAL granules (arrow) can be observed. (b) Histogram showing the mean diameter (and SEM) of nLBs and CAL granules in the cortex of malinKO mice. (c) Representative images of the hippocampus and cortex of SAMP8, malinKO and control mice. Clusters of CAL granules can be observed in the hippocampus of all animals. Some clusters of CAL granules are also observed in the cortex of malinKO mice, which also includes nLBs (see detail in image a). (d) Histogram showing the density of CAL granules and nLBs in the hippocampus and cortex of malinKO animals. (e) Histogram showing the density of CAL granules in the hippocampus and cortex of SAMP8, malinKO and control animals. All histograms express the mean and SEM, and significant differences are detailed in the text. Scale bars: 100 µm.

450x565mm (300 x 300 DPI)

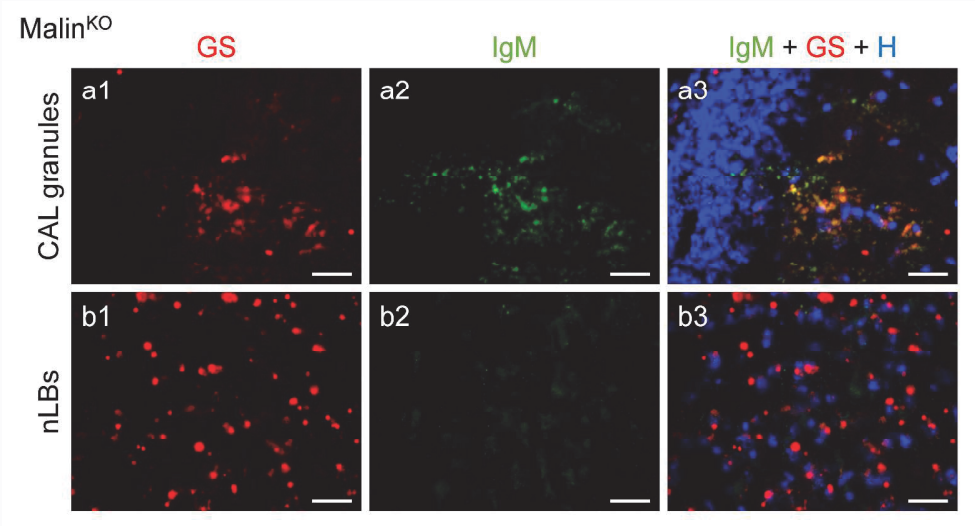

Figure 4. CAL granules, but not nLBs, contain neo-epitopes. Representative images of hippocampal (a1-a3) and cortex (b1-b3) regions of malinKO mice double immunostained with anti-GS antibody (red) and anti-NEs IgMs (green). Hoechst (H, blue) was used for nuclear staining. A cluster of CAL granules from the hippocampus is stained with GS (a1) and also with IgMs (a2). Colocalization (yellow to orange) can be observed in the merged image (a3), indicating that CAL granules contain neo-epitopes. PGBs associated with neurons (nLBs) are stained with anti-GS antibody (b1) but not with the anti-NEs IgMs (b2). The absence of colocalization (b3) indicates that nLBs do not contain neo-epitopes. Scale bar: 20 μm.

494x266mm (300 x 300 DPI)

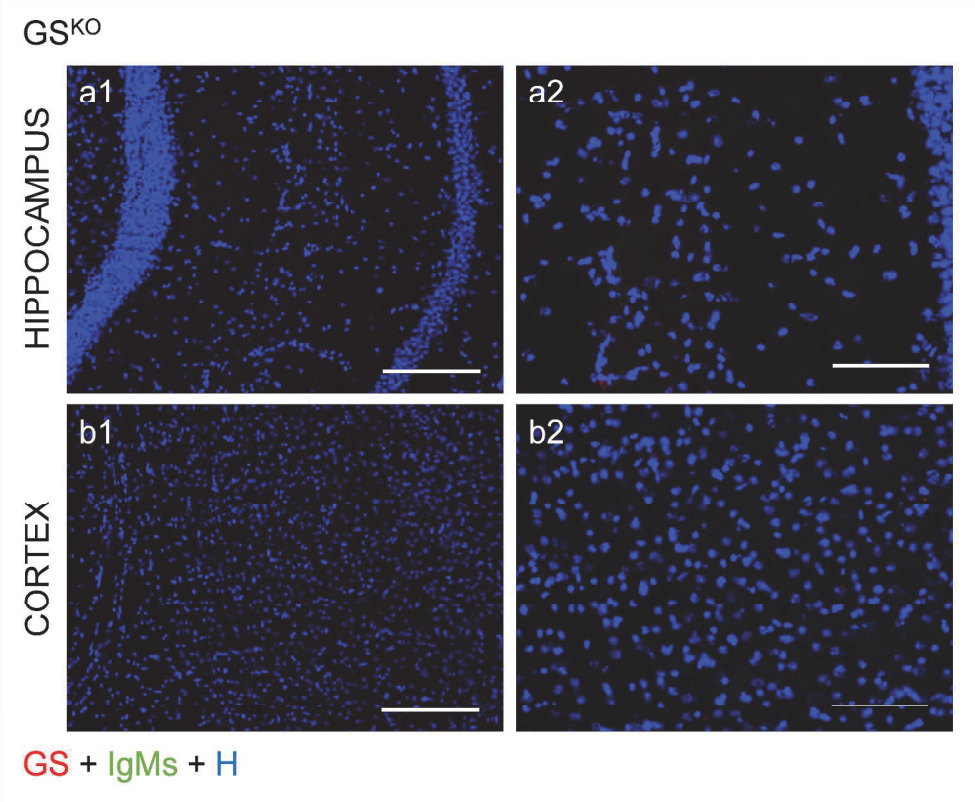

Figure 5. GS is necessary for the detection of clusters of granules containing neo-epitopes. Representative images of hippocampal and cerebral cortex regions of MGSKO mice double immunostained with anti-GS antibody (red) and anti-NEs IgMs (green). Hoechst (H, blue) was used for nuclear staining. The absence of clusters of granules containing neo-epitopes indicate that the glycosidic structure of CAL granules is necessary for the presence of these epitopes. Scale bar a1 and b1: 200 μm; a2 and b2: 100 μm.

418x344mm (300 x 300 DPI)

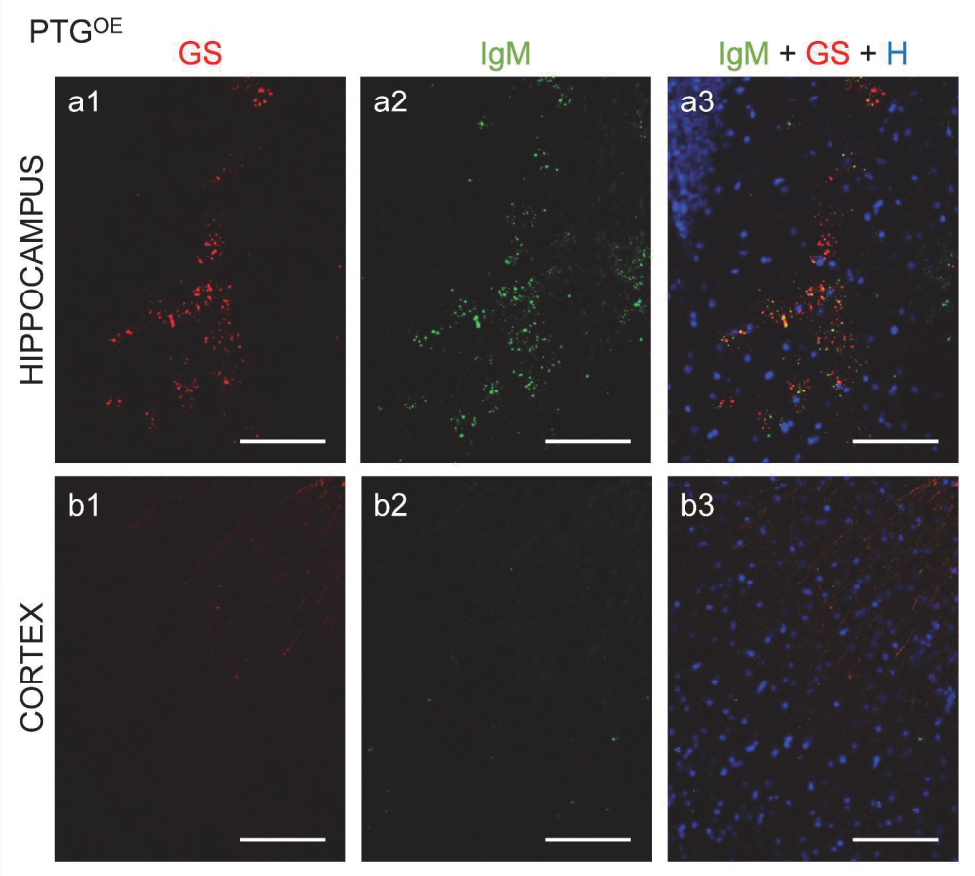

Figure 6. PTGOE animals present CAL granules but not nLBs. Representative images of hippocampal and cerebral cortex regions of PTGOE mice double immunostained with anti-GS antibody (red) and anti-NEs IgMs (green). Hoechst (H, blue) was used for nuclear staining. CAL granules stained with anti-GS antibody (a1) and anti-NEs IgMs (a2) can be observed in the hippocampus, and they are also visible in the merged image (a3). These animals, however, do not present nLBs, as can be seen in cortex images stained with anti-GS antibody (b1) and anti-NEs IgMs (b2) or in the merged image (b3). Scale bar: 100 μm.

438x394mm (300 x 300 DPI)

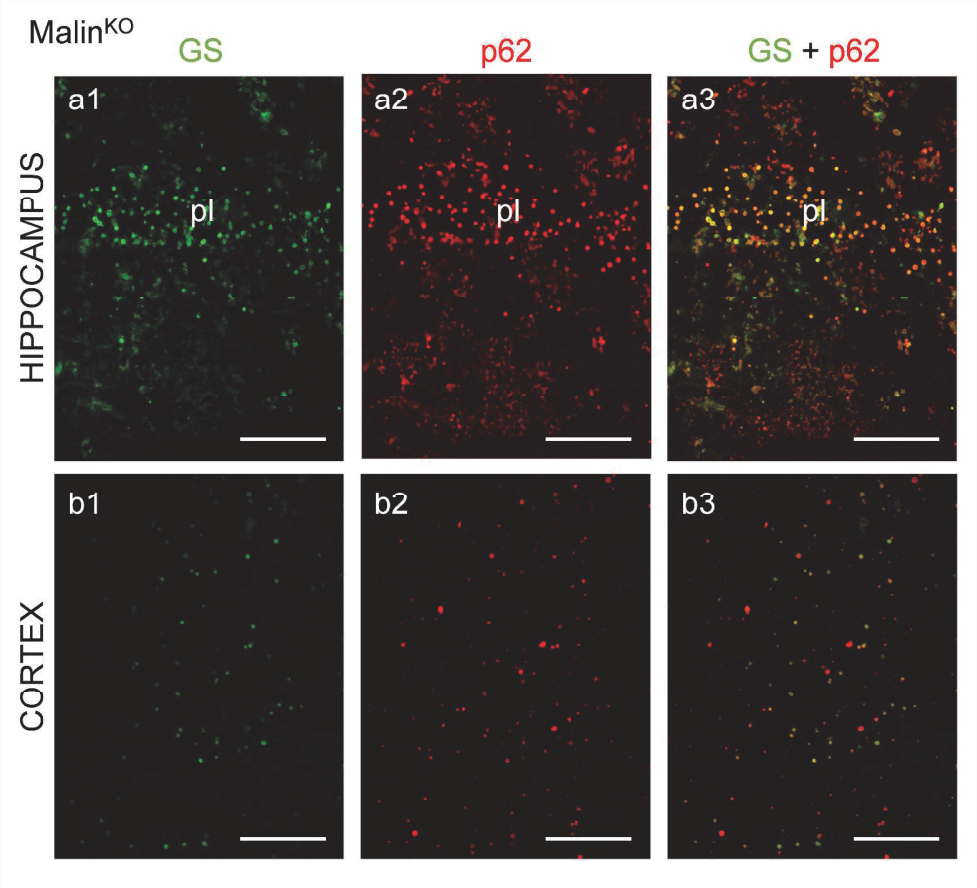

Figure 7. Autophagy marker p62 is present in both CAL granules and nLBs. Representative images of hippocampal and cerebral cortex regions of malinKO mice double immunostained with anti-GS (green) and anti-p62 (red) antibodies. Hoechst (H, blue) was used for nuclear staining. CAL granules and nLBs stained with both anti-GS (a1) and anti-p62 (a2) antibodies can be observed in the hippocampus. nLBs, also stained with anti-GS (b1) and anti-p62 (b2) antibodies, can also be seen in the cortices of the animals. Both types of granules can be also appreciated in the merged images (a3, b3). These results indicate that both types of PGB contain the p62 autophagy marker. pl: pyramidal layer of the hippocampus. Scale bar: 100 μm.

437x398mm (300 x 300 DPI)

Table I. Type and features of PGBs present in each strain or transgenic mouse model

	Type of PGBs	Formed in	Presen-tation	Density[1] in Cx (PGBs/mm^3)	Density[1] in Hc (PGBs/mm^3)	Size[1] (µm)	Neo-epitopes
Malin^{KO}	nLBs	neurons	isolated	33671.06 (±2217.18)	9324.92 (±592.69)	2.83 (±0.22)	absent
	CAL	astrocytes	clustered	4936.45 (±594.91)	176709.32 (±16058.40)	1.59 (±0.18)	present
C57BL/6	CAL	astrocytes	clustered	---	2388.17 (±428.63)	n.a.	present
SAMP8	CAL	astrocytes	clustered	---	27560.24 (±1742.26)	n.a.	present
PTG^{OE}	CAL	astrocytes	clustered	n.a.	n.a.	n.a.	present
MGS^{KO}	---	---	---	---	---	---	---

PGBs: polyglucosan bodies; nLBs: neuronal Lafora bodies; CAL: *corpora amylacea*-like granules; Hp: hippocampus; Cx: cerebral cortex. --- indicates absence of granules. n.a.: data not available. [1] expressed as mean (± standard error of the mean).

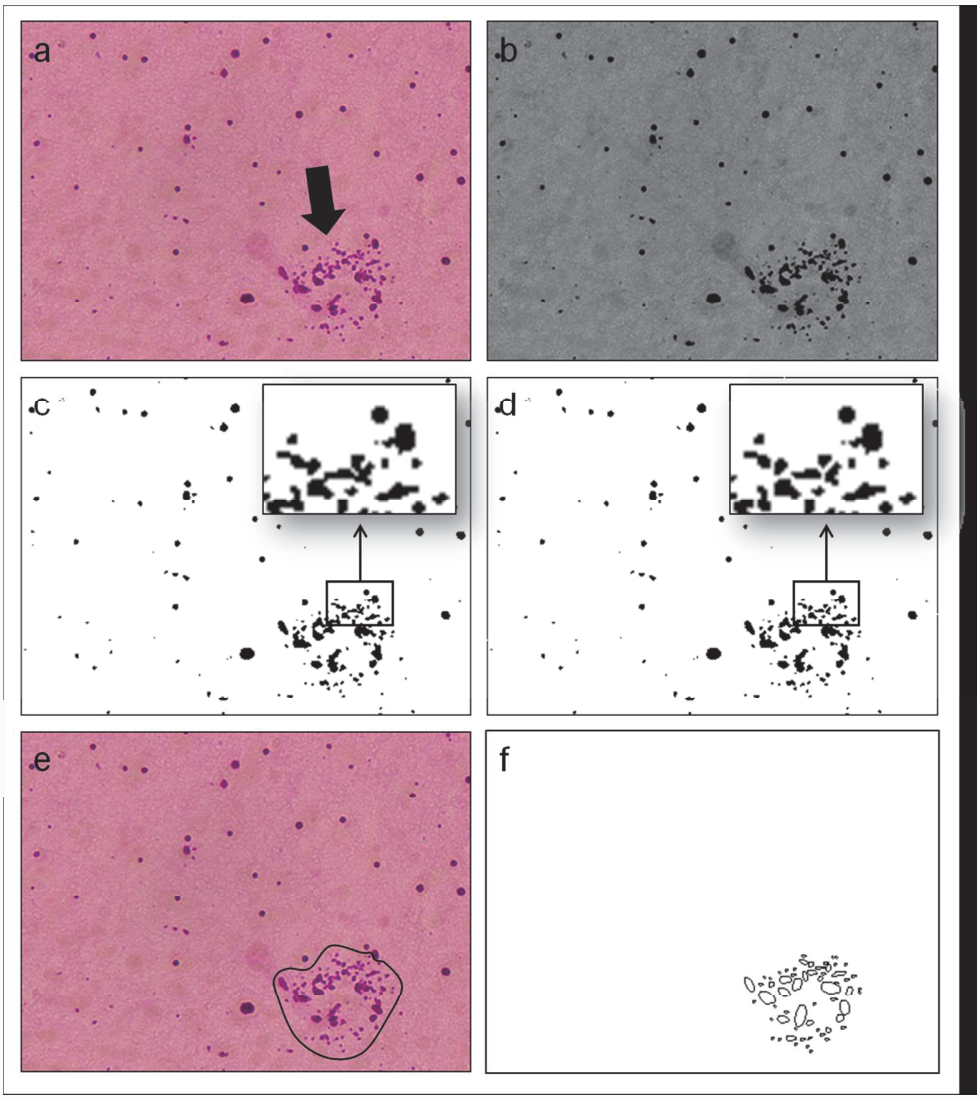

Figure S1 (Supplementary material). Example of image processing to quantify granules using the ImageJ program. a) Original image from a cortical region of a malinKO mouse stained with PAS, in which the granules present in the cluster (arrow) were quantified. b) Image of the green channel transformed to 8 bits, obtained after splitting the color channels. c) Binarized image after establishing the threshold. d) Binarized image after applying the watershed, in which some fused granules become separated (see insets in c and d). e) The region of interest (ROI) is defined in the original image; in this example, the ROI contains only one cluster of granules. f) Image showing the granules that were detected by analyzing the particles on the image d after applying the ROI defined in image e. In this case, 48 granules were detected.

101x113mm (300 x 300 DPI)

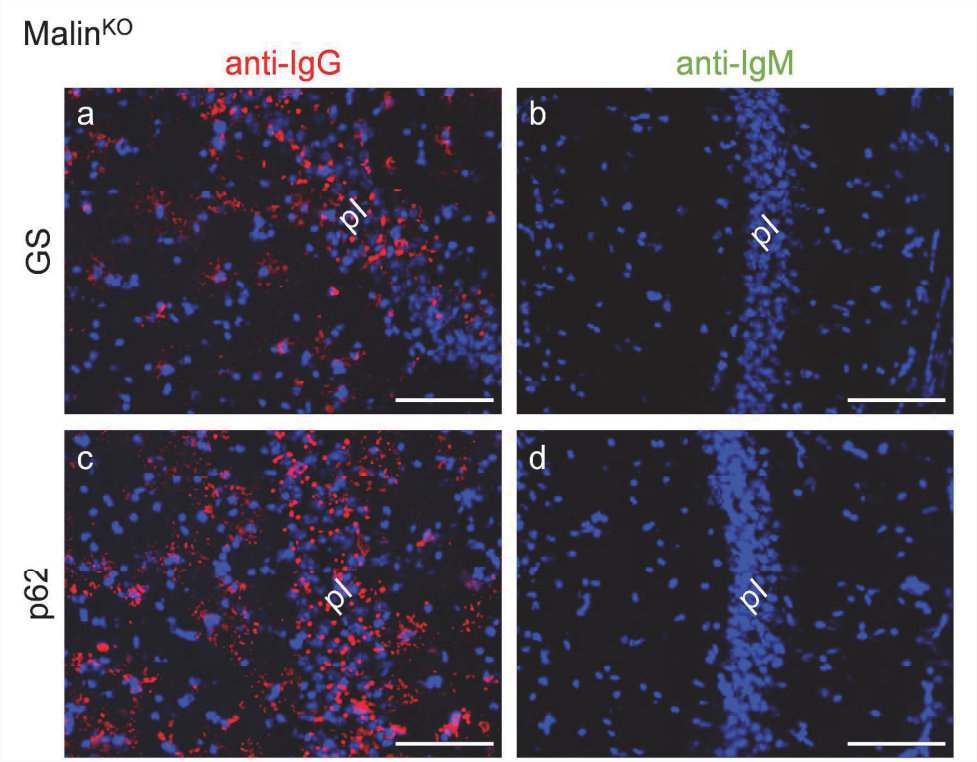

Figure S2 (Supplementary material). The vials of GS and p62 antibodies do not contain contaminant IgMs. Representative images of hippocampal regions of malinKO mice immunostained with a) primary antibody anti-GS and secondary antibody AF555 anti-IgG (red staining), b) anti-GS and FITC anti-IgM (green staining), c) anti-p62 and AF555 anti-IgG (red staining), and d) anti-p62 and AF488 anti-IgM (green staining). Hoechst (blue) was used for nuclear staining. CAL granules are not stained when secondary anti-IgM antibody is used, indicating the absence of IgM contamination, while they are stained when the secondary antibody is anti-IgG. pl: pyramidal layer of the hippocampus. Scale bar: 100 μm.

418x325mm (300 x 300 DPI)

IV. DISCUSSIÓ

L'envelliment cerebral en ratolins condueix a la formació d'uns PGBs anomenats grànuls PAS. Els grànuls PAS van ser descrits per primera vegada per Lamar *et al.* (1976) en ratolins envellits de la soca C57BL/6. Tot i que s'han anat publicant diversos estudis sobre aquests cossos des de la seva primera descripció, no ha estat fins a estudis recents del nostre grup de recerca que s'ha estat descrit la presència d'uns neo-epítops en aquestes estructures (Manich *et al.,* 2014b). Per una banda, la identificació d'aquests neo-epítops ha permès posar de manifest l'existència de falsos marcatges positius que apareixen quan es duen a terme assaigs immunohistoquímics amb la finalitat de caracteritzar aquestes estructures. Aquests neo-epítops poden ser reconeguts per anticossos de l'isotip IgM que sovint es troben presents com a contaminants en alguns anticossos comercials i poden donar lloc a falsos marcatges. De fet, alguns estudis previs ja havien postulat possibles inespecificitats en els marcatges dels grànuls PAS després d'observar marcatge positiu dels agregats quan es duien a terme els controls de pre-adsorció corresponents (Jucker *et al.,* 1992). Per altra banda, l'aparició de neo-epítops en aquestes estructures cerebrals ha permès postular un nou significat fisiopatològic dels grànuls PAS. La generació de neo-epítops és un fet que es dóna en diferents situacions fisiològiques i patològiques, com per exemple com a conseqüència de la peroxidació de lípids, i s'ha vist que esdevenen una diana per als ANs (Binder, 2010).

Amb la finalitat de determinar si els anticossos que reconeixen els neo-epítops dels grànuls PAS són ANs, diferents assaigs immunohistoquímics es van dur a terme en seccions cerebrals de ratolí. Es van utilitzar els sèrums de ratolins de diferents edats i soques com a anticossos primaris per veure si mostraven reactivitat amb els grànuls PAS. En tots ells es van detectar IgMs que reconeixien els neo-epítops d'aquestes estructures. A més a més, els ANs es caracteritzen per estar presents en el plasma dels organismes sense necessitat d'una estimulació externa i la seva presència ha estat determinada en el sèrum de ratolins que no han estat en contacte previ amb patògens externs (Dighiero *et al.,* 1983; Hooijkaas *et al.,* 1984; Wardemann *et al.,* 2003). Per verificar que aquest fet es complia en els anticossos que reconeixen els neo-epítops dels grànuls PAS, es va analitzar la presència d'anticossos dirigits contra els neo-epítops en els sèrums de ratolins mantinguts en condicions SOPF. En tots ells es va determinar la presència d'IgMs que reconeixien els grànuls PAS en observar marcatge positiu de les estructures granulars quan es va dur a terme l'assaig immunohistoquímic. Una altra característica d'aquest tipus d'anticossos és que el seu repertori i el seu patró de reactivitat és estable no només dins d'una mateixa espècie sinó fins i tot també entre diferents espècies (Avrameas, 1991). Així doncs, també es va comprovar si els

anticossos que reconeixen els neo-epítops que apareixen en les estructures granulars es troben presents en altres espècies animals. Es va confirmar que els sèrums de cabra, rata i conill contenien IgMs dirigides contra els neo-epítops dels agregats granulars. Tots aquests resultats permetien confirmar que els anticossos que reconeixien els neo-epítops eren ANs. Per tal de determinar si es tractaven d'AANs, es van realitzar marcatges en les seccions cerebrals dels diferents ratolins utilitzats per a l'estudi amb els seus propis sèrums. Es va poder confirmar que eren AANs, ja que en tots ells es va produir marcatge dels grànuls. En alguns casos no es va poder confirmar aquest fet ja que l'animal no presentava aquestes estructures en el seu hipocamp. Tot i així, encara que alguns animals no presentessin grànuls PAS, els seus sèrums contenien IgMs dirigides contra els neo-epítops. A més a més, es va poder comprovar que, a causa probablement de la barrera hematoencefàlica, aquestes IgMs que es troben en el plasma dels animals no podien accedir al parènquima cerebral en condicions fisiològiques.

Amb aquests resultats es posa de manifest un nou vincle entre les estructures granulars degeneratives que apareixen amb l'envelliment a l'hipocamp de diferents soques de ratolí i el sistema immunitari innat. Els neo-epítops dels grànuls PAS es podrien formar per mecanismes relacionats amb processos d'envelliment, com per exemple mecanismes relacionats amb l'increment d'estrès oxidatiu. Es formarien, doncs, unes estructures antigèniques que esdevenen dianes per als ANs, i podrien desencadenar, per exemple, respostes immunitàries per facilitar l'eliminació de les estructures que els contenen, en cas d'alterar-se la barrera hematoencefàlica o en cas que les IgMs poguessin accedir-hi. Els epítops específics d'oxidació, que representen estructures alterades que es generen com a conseqüència de la peroxidació lipídica, han estat àmpliament documentats en algunes situacions patològiques, com l'aterosclerosi (Hartvigsen *et al.,* 2009). A més a més, les mateixes estructures s'han trobat en les membranes de cèl·lules apoptòtiques (Chang *et al.,* 1999; Chang *et al.,* 2004). Així doncs, els epítops específics d'oxidació constitueixen els *tags* o dianes perfectes per a la identificació de substàncies biològiques de rebuig i per a la diferenciació de cèl·lules no viables de cèl·lules viables i facilitar l'eliminació de les primeres (Chou *et al.,* 2009). Així doncs, les IgMs naturals podrien participar en l'eliminació d'aquests agregats hipocampals en cas de tenir-hi accés.

L'acumulació d'agregats de tipus poliglucosà que apareixen amb l'envelliment en el cervell no és un fet exclusiu dels ratolins. En el cervell humà també s'acumulen durant l'envelliment uns cossos d'aquesta naturalesa glucídica, els CA. Diferents estudis han posat de manifest les similituds i les diferències que presenten ambdues estructures. Els

estudis duts a terme per Jucker *et al*. (1992, 1994a, 1994b) i per Jucker i Ingram (1994) remarquen l'estreta relació que existeix entre els CA i els clústers de grànuls que apareixen en ratolí. Tot i que puntualitzen que hi ha alguns trets que difereixen entre aquestes dues estructures, principalment la seva distribució i la seva mida, afirmen que els grànuls PAS presenten similituds amb els cossos cerebrals humans, i aquest fet pot proporcionar informació pel que fa al significat fisiopatològic i al desenvolupament dels CA. Robertson *et al*. (1998) també van comparar les estructures granulars PAS positives que s'acumulen al cervell de ratolins deficients d'ApoE i els CA humans. Tot i que emfatitzen que són estructures similars, manifesten que existeixen diferències pel que fa al perfil histoquímic i a les característiques que presenten a nivell ultrastructural. Mitsuno *et al*. (1999) també relacionen els agregats de poliglucosà que apareixen a l'hipocamp, i en menor quantitat al cerebel i bulb olfactori, dels ratolins de la soca AKR i els CA humans, afirmant que es tractaria d'estructures similars. A més a més, per marcar els grànuls de ratolí utilitzen un anticòs monoclonal dirigit contra un poliglucosà, el KM279, el qual també s'havia demostrat que tenia reactivitat per als CA. Estudis més recents (Sinadinos *et al*., 2014) també associen els CA humans amb els grànuls PAS de ratolí. Estudien la formació dels agregats en ratolins de la soca C57BL/6 a mesura que els animals envelleixen, així com també estudien la presència de diferents marcadors descrits prèviament en els CA humans. La seva associació amb l'envelliment, la presència de determinats components i la seva base glucídica, els permet postular que els grànuls PAS de ratolí serien els equivalents als CA humans.

Així doncs, el segon plantejament que ens vam fer era conèixer si els CA humans presenten neo-epítops que poden ser reconeguts per anticossos d'origen natural. Amb aquesta finalitat, es van realitzar diferents assaigs immunohistoquímics en seccions coronals d'hipocamp humà de diferents casos. Primer de tot es va verificar la presència d'aquests cossos en tots els casos utilitzats en l'estudi mitjançant la tinció de PAS. Posteriorment, en seccions consecutives, i utilitzant els plasmes humans de diferents donants de sang sans, es va demostrar la presència d'anticossos de l'isotip IgM en el plasma d'aquests donants que reaccionaven amb alguns epítops dels CA i els marcaven. Per descartar la presència d'un receptor per a Fc en aquestes estructures i demostrar que el marcatge de les IgMs fos específic, es van seguir dos procediments. Per una banda, es va incubar només el fragment Fc de les IgMs i es va observar que no hi havia marcatge dels CA. Per altra banda, es va utilitzar, prèviament a la incubació de les IgMs humanes, un reactiu comercial que bloquejava els receptors Fc de tots els isotips d'immunoglobulines. En aquest últim cas, es va seguir observant marcatge. D'aquesta manera es va descartar la presència d'un receptor Fc en aquestes estructures

i es va confirmar que la unió de les IgMs amb els CA era a través de les regions variables de l'*antigen binding fragment* (Fab), que és la regió que conté el lloc de reconeixement per a l'antigen. Tal com s'ha comentat amb anterioritat, els ANs es caracteritzen per estar presents en diferents espècies animals, així com també per estar presents en el plasma dels organismes sense la necessitat de contacte previ amb antígens externs. Tal com s'havia abordat en el cas dels grànuls de ratolí, per confirmar que les IgMs que reconeixien els CA eren ANs, es van realitzar diferents marcatges utilitzant sèrums de cabra, rata, conill i ratolí. També es va fer el marcatge amb el sèrums de ratolins mantinguts en condicions SOPF. En tots els casos es va confirmar la presència d'anticossos de l'isotip IgM que marcaven les estructures humanes. També es va analitzar la presència d'aquestes IgMs en els sèrums obtinguts de sang de cordó umbilical. El repertori d'AANs s'ha estudiat en el sèrum de cordó umbilical humà (Merbl *et al*. 2007). A diferència de les IgGs, les IgMs no poden creuar la placenta, i per tant, aquelles que es troben presents en el sèrum de cordó umbilical s'originen amb independència d'una estimulació externa. Tal com vàrem poder observar, el marcatge dels CA es produïa també utilitzant les IgMs purificades dels sèrums de diferents cordons umbilicals, verificant la presència d'IgMs que podien reconèixer els neo-epítops dels CA, i confirmant que es tractaven d'ANs.

Per tant, amb aquests resultats es posa de manifest un nou vincle entre els CA cerebrals humans i el sistema immunitari innat. Així doncs, com passa amb els grànuls PAS de ratolí, els CA cerebrals contenen epítops que poden ser reconeguts per anticossos que es troben presents en el plasma de diferents organismes sense la necessitat que hi hagi un estímul extern. Aquests epítops no es troben en altres estructures del cervell i, com s'ha descrit per als grànuls PAS (Manich *et al*. 2014a), és probable que els epítops dels CA humans es formin durant el procés de formació del cos i és per això que poden ser considerats com a neo-epítops. Probablement, com s'ha comentat amb anterioritat per als grànuls PAS, durant la seva formació existeixen mecanismes involucrats que podrien estar relacionats amb l'envelliment. Els ANs tenen la capacitat de reconèixer estructures pròpies que sovint representen neo-estructures alterades o induïdes per estrès que es generen durant diversos processos biològics. Aquesta capacitat de reconèixer determinats antígens propis permet que els ANs reconeguin material de rebuig o cèl·lules apoptòtiques i en promoguin la seva eliminació. Tot i que es desconeix encara avui dia l'origen i la funció dels CA, s'ha hipotetitzat que podrien estar implicats en la captació de substàncies de rebuig o de productes perjudicials (Cavanagh, 1999). Tenint en compte aquest fet, l'aparició dels neo-epítops ens els CA podria ser conseqüència de la presència d'algun component alterat, com per exemple productes resultants de la

peroxidació lipídica, com el malondialdehid (Chou *et al.,* 2009; Grönwall *et al.,* 2012). Tot i així, els CA no són una acumulació aleatòria de diferents components, sinó que són unes estructures compactes amb un alt contingut glucídic que tenen una localització concreta: perivascular i periventricular majoritàriament. L'estudi de Sbarbati *et al*. (1996), en base a les seves observacions, suggereix que els CA, després de formar-se als astròcits, són extruïts al teixit connectiu pial a través de la membrana limitant glial. Així doncs, els CA serien uns elements que formarien part d'un sistema glio-pial encarregat de l'eliminació de substàncies del sistema nerviós. Per tant, l'existència d'ANs dirigits contra neo-epítops dels CA és congruent amb aquest fet ja que, tal com s'ha explicat prèviament, una de les principals funcions dels ANs és identificar cèl·lules apoptòtiques o substàncies de rebuig i promoure'n la seva eliminació mitjançant processos fagocítics sense desencadenar una resposta inflamatòria en el teixit (Chou *et al.,* 2009; Grönwall *et al.,* 2012; Wang *et al.,* 2016). Així doncs, la presència de neo-epítops en els CA que poden ser reconeguts per ANs suggereix que els CA podrien ser fagocitats un cop expulsats del SNC, en concordança amb el mecanisme potencial de neteja atribuït als CA (Sbarbati *et al.,* 1996). De fet, s'ha demostrat que la presència de CA al cervell no es correlaciona amb processos inflamatoris locals i a més, en casos de neuromielitis òptica, els CA situats en les regions afectades són reconeguts per macròfags infiltrants (Suzuki *et al.,* 2012).

Com s'ha descrit per als grànuls PAS (Manich *et al.,* 2014b), les IgMs naturals que reconeixen els neo-epítops d'aquestes estructures són la font de falsos marcatges positius quan es troben com a contaminants en alguns anticossos comercials. De fet, l'estudi de Manich *et al*. (2014b) determina que la majoria d'anticossos comercials contenen aquestes IgMs, i tenint en compte aquest fet, descarta la presència d'alguns components dels grànuls que havien estat descrits amb anterioritat, com són la proteïna tau i el pèptid Aβ. S'han descrit nombrosos components per als CA del cervell humà; un gran ventall de proteïnes i d'altres marcadors que han permès postular diferents orígens i funcions per a aquestes estructures. Tot i així, per a alguns d'ells hi ha hagut certa controvèrsia. De fet, Erdamar *et al*. (2000), quan van estudiar la presència de HSP70-72 en els CA, i a diferència d'estudis anteriors duts a terme per Martin *et al*. (1991), no van observar cap tipus de marcatge en els cossos quan van dur a terme estudis immunohistoquímics. En aquest estudi, Erdamar *et al*. (2000) conclouen que aquesta variabilitat de marcatge pot ser deguda a la patologia de cada cas estudiat, als anticossos utilitzats, a les pròpies HSP o a algun altre factor no establert. Així doncs, aquest altre factor que anomena Erdamar *et al.* (2000) podrien ser les IgMs naturals. Per verificar que les IgMs naturals es poden trobar en anticossos comercials i donar lloc

a falsos marcatges positius dels CA, es va utilitzar l'anticòs JJ319. Aquest anticòs ja havia estat utilitzat amb anterioritat per confirmar la presència d'IgMs contaminants que marcaven els gränuls PAS (Manich *et al.,* 2014b). Com en aquest últim cas, l'anticòs marcava els CA cerebrals humans, tot i no tenir reactivitat per cap epítop present en el cervell humà. Es va confirmar que el marcatge no era específic i era causat per la presència d'IgMs naturals en aquest anticòs, susceptibles a ser reconegudes per anticossos secundaris que reconeixen tant la cadena pesada com la cadena lleugera de les IgGs. De la mateixa manera, aquest fet es podria produir en altres anticossos comercials no purificats, o purificats amb un mètode que no hagués eliminat correctament les IgMs, algunes d'elles ANs.

Respecte la composició dels CA, diferents estudis han posat de manifest la presència de la proteïna tau (Day *et al.,* 2015; Loeffler *et al.,* 1993; Wilhelmus *et al.,* 2011) i el pèptid Aβ (Notter i Knuesel, 2013) en aquests agregats humans mitjançant estudis immunohistoquímics. Tot i així, altres autors, fins i tot en alguns casos els mateixos autors d'aquests estudis, han obtingut resultats oposats (Notter i Knuesel, 2013; Pirici i Margaritescu, 2014; Wilhelmus *et al.,* 2011). En aquesta tesi es va re-avaluar la presència d'aquests dos components als CA, tenint en compte la possible presència d'IgMs naturals en alguns anticossos comercials, així com també el possible creuament d'alguns anticossos secundaris amb aquestes IgMs. Així doncs, es va evitar utilitzar anticossos secundaris que reconeguessin tant les cadenes pesades com les cadenes lleugeres de les IgG i es van fer controls de pre-adsorció de tots els marcatges. Es va observar que el marcatge dels CA humans estava produït per les IgMs naturals que es trobaven presents en alguns dels anticossos comercials i que aquest no desapareixia quan es feia el control de pre-adsorció corresponent. El marcatge específic de la proteïna tau o els pèptids Aβ, en canvi, es detectava en els cabdells o plaques dels casos de malaltia d'Alzheimer, i el marcatge desapareixia quan es feia el corresponent control de pre-adsorció. Aquests resultats indiquen que els CA no presenten cap d'aquests dos components, tal com s'havia observat en alguns estudis anteriors. A més a més, es posa de manifest el motiu pel qual s'obtenien resultats contradictoris en els estudis immunohistoquímics i es planteja si altres marcadors descrits anteriorment en els CA també podrien ser el resultat de falsos marcatges positius.

La composició bioquímica dels CA va ser analitzada per Sakai *et al*. (1969), i van determinar que, un cop purificats per centrifugació i després de ser tractats amb pepsina se n'obté una fracció aquosa que conté un 87.9% d'hexosa, un 4.7 % de proteïna i un 2.5% de fosfats. Diferents estudis immunohistoquímics s'han dut a terme per caracteritzar quines són les proteïnes que es troben contingudes en aquests cossos. La

interpretació de la funció i l'origen dels CA ha anat variant durant el temps, i nombroses teories sobre aquests cossos s'han formulat, en part, degut a la descripció de nous components identificats per estudis immunohistoquímics. Han estat descrits components vinculats amb un possible origen neuronal, com l'α-sinucleïna (Buervenich *et al.,* 2001; Notter i Knuesel, 2013; Wilhelmus *et al.,* 2011), la reelina (Notter i Knuesel, 2013), la MAP2 (Nam *et al.,* 2012; Notter i Knuesel, 2013) i la β-tubulina classe III (Wilhelmus *et al.,* 2011). També s'ha demostrat que presenten reactivitat per NeuN (Buervenich *et al.,* 2001; Korzhevskii i Giliarov, 2007; Pirici i Margaritescu, 2014) i per nestina (Buervenich *et al.,* 2001), tot i que aquesta última no ha pogut ser detectada pels estudis duts a terme per Pirici i Margaritescu (2014). També han estat descrits alguns components vinculats amb un possible origen glial. Reaccions positives en els CA amb anticossos dirigits contra la proteïna bàsica de mielina, la proteïna proteolipídica, el galactosilcerebroside i la glicoproteïna de mielina de l'oligodendròcit (Singhrao *et al.,* 1994) indiquen que metabòlits oligodendroglials podrien contribuir a la seva composició. També han estat determinades proteïnes vinculades a l'astroglia, com proteïnes específiques de la família S100 (Buervenich *et al.,* 2001; Hoyaux *et al.,* 2000; Pirici i Margaritescu, 2014), AQP4 (Pirici i Margaritescu, 2014) o GFAP. Pel que fa a aquesta última, mentre que alguns autors descriuen un marcatge positiu dels CA (Buervenich *et al.,* 2001; Pirici i Margaritescu, 2014), altres conclouen que la immunoreactivitat per a GFAP es limita al marge d'aquests dipòsits (Nam *et al.,* 2012; Notter i Knuesel, 2013; Pirici *et al.,* 2014). A més a més, també s'ha observat que els CA són immunoreactius a HSP (Cissé *et al.,* 1993; Gáti i Leel-Ossy, 2001; Martin *et al.,* 1991), tot i que Erdamar *et al*. (2000), com s'ha comentat anteriorment, no va poder reproduir el marcatge d'algunes d'elles, i a la ubiqüitina (Cissé *et al.,* 1993; Day *et al.,* 2015; Pirici i Margaritescu, 2014; Pirici *et al.,* 2014; Wilhelmus *et al.,* 2011).

Amb la finalitat de determinar si, com passa amb la proteïna tau i el pèptid Aβ, altres components dels CA descrits amb anterioritat resultaven ser el resultat de falsos marcatges positius, es van dur a terme diferents assaigs immunohistoquímics en seccions coronals criostàtiques d'hipocamp humà de diferents casos. Es va re-avaluar la presència de GFAP, AQP4, S100B, NeuN, β-tubulina classe III i ubiqüitina en els CA. Tenint en compte la presència de possibles IgMs contaminants en els vials dels anticossos comercials, es va descartar la presència de tots aquests components, excepte la presència d'ubiqüitina. Aquests resultats reforcen la necessitat de revisar els altres components que han estat descrits amb anterioritat mitjançant tècniques immunohistoquímiques, ja sigui aquells que només han estat descrits un cop o aquells que han estat descrits en diversos estudis donant lloc a resultats contradictoris. Elucidar

quins components realment formen part dels CA permetrà clarificar quina és la funció d'aquests cossos.

La presència en els CA d'ubiqüitina, una proteïna implicada en la senyalització de substrats per a ser degradats, i els neo-epítops reconeguts per IgMs naturals, reforça la idea que els CA podrien ser estructures involucrades en la captació de substàncies de rebuig o productes perjudicials (Cavanagh, 1999), que posteriorment serien extruïdes del sistema nerviós i eliminades per processos de fagocitosi (Sbarbati *et al.,* 1996). En relació a aquesta possible funció, es va estudiar la presència de p62 i MMP2 als CA, així com també la presència de GS, l'únic enzim capaç de sintetitzar polímers de glucosa i que s'ha descrit que resulta essencial per a la formació de PGBs (Sinadinos *et al.,* 2014). Els resultats obtinguts confirmen la presència d'aquests components. La proteïna MMP2 és una metal·loproteïnasa implicada en el remodelatge extracel·lular (Ethell i Ethell*,* 2007), i la seva presència podria estar relacionada en facilitar el procés d'extrusió dels CA des dels astròcits marginals al líquid cefaloraquidi. A més a més, l'estudi de la relació que presenten la ubiqüitina, la p62 i la GS permet observar que la p62 i la GS tenen un marcatge perifèric, mentre que la ubiqüitina es troba tant a la perifèria com a l'interior del cos. Així doncs, aquests resultats suggereixen que els CA no són només l'agregació de polímers de glucosa insolubles que contenen proteïnes, sinó estructures amb dues regions diferenciades. La part perifèrica esdevindria la part activa o en creixement, on la GS aniria formant nous polímers de glucosa, i la p62 podria interaccionar amb les substàncies ubiqüitinades; mentre que la part central seria la regió estable on els polímers de glucosa retindrien les substàncies ubiqüitinades.

Una hipòtesi alternativa seria que els polímers de glucosa fossin per ells mateixos les substàncies de rebuig. De fet, els PGBs presenten alteracions de ramificació, de nivells de fosfat i de solubilitat respecte el glicogen fisiològic (Cavanagh, 1999; Minassian, 2001). A més a més, en un model de la malaltia de Lafora, una malaltia neurodegenerativa que es caracteritza per presentar PGBs a nivell cerebral, la deficiència de GS contribueix a prevenir la progressió de la malaltia (Duran *et al.,* 2014), suggerint que l'acumulació dels polímers de glucosa són les substàncies de rebuig en aquest cas.

L'anàlisi ultrastructural dels CA realitzat en estudis previs revela que aquests estan formats per una estructura complexa de fibres linears orientades a l'atzar (8-12 nm). Normalment són cossos arrodonits, que no contenen una membrana pròpia i sovint estan envoltats per fibres glials (Ramsey, 1965). Diferents autors indiquen que es troben localitzats en processos astrocítics (Leel-Ossy, 2001; Palmucci *et al*., 1982; Ramsey,

1965; Sbarbati *et al*., 1996), mentre que d'altres els han descrit com a inclusions intra-axonals (Mizutani *et al.*, 1987; Takahashi *et al*., 1975; Woodford i Tso, 1980). Tot i així, mai han estat localitzats al soma neuronal.

Els resultats dels nostres estudis ultrastructurals confirmen que els CA són inclusions intracitoplasmàtiques constituïdes per una massa compacta formada per estructures linears. Aquesta massa és envoltada sovint per filaments intermedis i alguns elements membranosos i mitocòndries, observacions consistents amb descripcions anteriors dels CA (Leel-Ossy 2001; Ramsey 1965; Woodford i Tso 1980). A nivell de microscòpia de fluorescència s'observa que els filaments intermedis que envolten els CA corresponen a filaments GFAP, tal com suggereixen diferents autors (Leel-Ossy 2001; Notter i Knuesel, 2013; Palmucci *et al*., 1982; Ramsey, 1965). Tot i així, altres autors no descarten la seva presència en axons (Anzil *et al*., 1974; Mizutani *et al*., 1987; Takahashi *et al*., 1975; Woodford i Tso, 1980). Els nostres resultats també mostren CA en estadis primerencs. Aquests CA es caracteritzen per presentar una massa central menys compacta la qual conté restes cel·lulars, estructures membranoses i mitocòndries, localitzades tant a l'interior de l'estructura com al voltant. Aquestes observacions són consistents amb els autors que suggereixen que els CA són unes estructures encarregades de captar productes de rebuig generats per processos relacionats amb el procés d'envelliment (Cavanagh, 1999; Leel-Ossy, 2001; Schipper, 2004).

L'estudi de microscòpia electrònica dels CA permet identificar similituds a nivell d'ultrastructura entre aquestes inclusions i els grànuls PAS de ratolí. Tant els CA com els grànuls PAS estan envoltats per una membrana plasmàtica i presenten una regió central compacta, formada per estructures fibril·lars, que acostuma a estar envoltada per mitocòndries i estructures membranoses (Doehner *et al.,* 2010; Kuo *et al.,* 1996; Manich *et al.,* 2014a; Mitsuno *et al.,* 1999; Robertson *et al.,* 1998). A més a més, la regió central dels grànuls PAS també està envoltada per fibres GFAP (Manich *et al.,* 2014a). L'estudi de l'ultraestructura dels grànuls PAS immadurs (Manich *et al.,* 2014a) demostra que aquests presenten una regió central menys compacta, tal com s'observa en els CA en estadis primerencs. Tot i que la mida, distribució i algunes propietats histoquímiques són diferents entre els dos tipus d'inclusions, les similituds que presenten a nivell ultraestructural reforcen la idea que els CA i els grànuls PAS són estructures equivalents.

Pel que fa a l'estudi de la distribució dels neo-epítops en els CA es demostra, mitjançant assaigs d'immunofluorescència en seccions semi fines, que aquests es troben distribuïts per tot el cos. Aquests resultats són consistents amb l'estudi de la localització dels neo-

epítops en els grànuls PAS de ratolí (Manich *et al.,* 2014a), en el qual s'observa a nivell ultrastructural que els neo-epítops es troben localitzats en les estructures fibril·lars que conformen el grànuls. Tot i que el marcatge de seccions ultrafines utilitzant anticossos secundaris conjugats amb partícules d'or ofereix millors resultats per a una localització més precisa a nivell ultrastructural, en el cas de mostres cerebrals humanes la manipulació i preservació del teixit fa que aquest procés sigui dificultós degut principalment al *post-mortem delay* que provoca el deteriorament del teixit.

D'altra banda, la malaltia de Lafora és una malaltia neurodegenerativa que es caracteritza per l'acumulació d'uns PGBs que reben el nom de LBs. Aquests cossos s'acumulen en diferents teixits, però el major òrgan afectat és el cervell. Tot i que els LBs i els CA tenen una estructura i composició similar (Sakai *et al.,* 1969; Sakai *et al.,* 1970), existeixen un parell de característiques que els diferencien: els LBs es troben exclusivament associats a neurones, principalment al soma neuronal, i tenen una estructura més compacta a la part central (Cavanagh, 1999).

Degut a la naturalesa de poliglucosà que presenten tant els CA com els LBs, resulta interessant estudiar si aquests últims contenen neo-epítops que puguin ser reconeguts per ANs. Tot i que alguns autors han considerat que aquestes estructures són diferents estadis d'un mateix procés (Sinadinos *et al.,* 2014), altres autors emfatitzen que es tracta d'estructures completament diferents (Cervós-Navarro, 1991; Leel-Ossy, 2001; Ramsey, 1965).

En les últimes dècades s'han desenvolupat diferents models murins per estudiar els mecanismes patogènics de la malaltia de Lafora. Un d'aquests models és el ratolí deficient de malina. Els ratolins malin^{KO} reprodueixen la malaltia perquè presenten LBs en diferents teixits, incloent el cervell, i un contingut de glicogen cerebral que duplica el dels animals control i correspon a una fracció insoluble i poc ramificada del polisacàrid. A més a més, presenten neurodegeneració, increment de l'excitabilitat sinàptica i propensió a patir convulsions mioclòniques (Vallès-Ortega *et al.,* 2011).

Amb la finalitat d'estudiar amb més profunditat els PGBs que apareixen en el model malin^{KO}, així com l'expressió de neo-epítops en aquestes estructures, es van realitzar diferents assaigs immunohistoquímics en seccions cerebrals d'aquests animals. A més a més, l'estudi es va complementar amb altres ratolins Tg: PTG^{OE} i MGS^{KO}. Els resultats d'aquest estudi permeten concloure que en els cervells dels animals malin^{KO} s'acumulen dos tipus de PGBs: uns cossos que es presenten majoritàriament a l'escorça cerebral, els quals estan associats al soma neuronal i tenen una mida més gran; i uns altres cossos que es troben principalment a l'hipocamp, associats a astròcits, agregats en

forma de clúster i de mida més petita. Aquests últims cossos també es troben en els ratolins control, ratolins de la soca SAMP8 i ratolins PTG^{OE}. Aquests resultats indiquen que els cossos associats a neurones són LBs (*neuronal Lafora bodies,* nLBs), mentre que els associats a astròcits són de tipus grànuls PAS (Akiyama *et al.,* 1986; Jucker *et al.,* 1994b; Kuo *et al.,* 1996; Manich *et al.,* 2011; Manich *et al.,* 2014a). A causa de les similituds que s'han anat comentant al llarg d'aquesta tesi entre els CA humans i els grànuls PAS de ratolí, hem anomenat aquests últims com a CA *like granules* (CAL). Aquests CAL, a més, es troben incrementats significativament en els animals malin^{KO} respecte els seus corresponents controls. Per tant, l'absència de malina indueix la formació de nLBs i incrementa la formació de CAL.

Els resultats obtinguts concorden amb els estudis prèviament publicats en quant a la localització neuronal dels LBs en humans (Busard *et al.,* 1987b; Jenis *et al.,* 1970; Ramon y Cajal *et al.,* 1974; Vanderhaeghen, 1971). Estudis anteriors indiquen que el tipus de cèl·lules on s'acumulen els PGBs és un tret que permet diferenciar els uns dels altres i podria explicar el fenotip que s'observa en una situació o altra (Cavanagh, 1999; Minassian, 2001). Així doncs, el sever fenotip neuropatològic que s'observa a la malaltia de Lafora suggereix que les neurones són particularment vulnerables a l'excés de les acumulacions de glicogen (Delgado-Escueta, 2007; Duran *et al.,* 2014; López-González *et al.,* 2017; Vallès-Ortega *et al.,* 2011). Tot i així, en el model murí malin^{KO} de la malaltia de Lafora no només s'observen nLBs sinó que també incrementen significativament els grànuls CAL, fet que posa de manifest una possible contribució d'aquests cossos en la patogènesi de la malaltia. L'augment de CAL a l'hipocamp és una nova troballa, que obligarà a reenfocar l'estudi d'aquesta malaltia.

Un altre resultat important, i a destacar, és que els PGBs de tipus CAL dels animals malin^{KO} presenten neo-epítops, mentre que els nLBs no. Aquesta observació concorda amb els resultats anteriors i confirma que el model murí de malaltia de Lafora presenta dos tipus de PGBs diferents. Tot i així, com indiquen estudis previs (Duran *et al.,* 2014; Sinadinos *et al.,* 2014) l'absència de GS evita la formació de qualsevol tipus de PGBs, posant de manifest un mecanisme de formació comú per aquests dos tipus de PGBs. En el present estudi, a més a més, s'observa que la detecció dels neo-epítops dels CAL està directament relacionada amb la formació de les estructures de poliglucosà.

D'altra banda, els animals PTG^{OE} presenten un nombre elevat de CAL, però no de nLBs, fet que indica que l'increment de l'activitat de la GS, produïda per l'expressió constitutiva de PTG, promou la formació d'un tipus de PGBs, però no de l'altre, suggerint diferents

rutes o elements reguladors en la gènesi dels nLBs i els grànuls CAL, malgrat que per a la formació dels dos tipus de cossos la GS sigui necessària.

Els grànuls CAL difereixen dels nLBs en termes de localització cerebral, mida, patró d'acumulació i presència de neo-epítops reconeguts per IgMs naturals. La presència de PGBs en astròcits en el model de malin^{KO} ja havia estat descrita (Sinadinos *et al.,* 2014; Vallès-Ortega *et al.,* 2011). Els resultats obtinguts en el nostre estudi, però, identifiquen aquests PGBs com a grànuls CAL i com un *pool* important dels PGBs que apareixen en el model de la malaltia de Lafora. Els astròcits participen en funcions essencials del cervell i un acúmul de grànuls CAL en aquestes cèl·lules podria contribuir a la fisiopatologia de la malaltia. En aquest sentit, la captació astrocítica de potassi i glutamat és essencial per a l'excitabilitat de les neurones, i un mal funcionament dels astròcits en la malaltia de Lafora, podria explicar el fenotip epilèptic d'aquesta (Amédée *et al.,* 1997; Coulter i Eid, 2012).

Tal com havia estat descrit en estudis previs (Del Valle *et al.,* 2010), els animals de la soca SAMP8, que es caracteritza per presentar un procés d'envelliment accelerat, presenten un elevat nombre de CAL. La relació entre l'envelliment i els CAL ha estat àmpliament demostrada. Tenint en compte les característiques multifactorials de l'envelliment, els factors relacionats amb l'aparició dels CAL podrien ser nombrosos i diversos. Tot i així, un dels factors que podria jugar un paper important és l'estrès oxidatiu. S'ha observat en diferents dissenys experimentals que l'aparició i progressió dels CAL es troba alterada quan els nivells d'estrès oxidatiu són modificats. En ratolins deficients d'ApoE, l'administració d'una dieta *high-fat* suplementada amb antioxidants redueix de manera significativa el nombre de clústers de grànuls en comparació amb els animals alimentats tant amb la mateixa dieta sense el suplement d'antioxidants o amb una dieta normal (Veurink *et al.,* 2003). En un altre estudi, es va observar una correlació positiva entre els nivells plasmàtics de lipoproteïnes d'alta densitat (HDL) i el nombre de clústers de grànuls en animals alimentats amb una dieta aterogènica (Krass *et al.,* 2003). També s'ha observat que hi ha una reducció significativa dels clústers de grànuls en animals SAMP8 alimentats amb un antioxidant com el resveratrol (Porquet *et al.,* 2013).

Un altre factor important és el rerefons genètic de l'animal perquè diferents soques de ratolí han mostrat una tendència diferent en la presentació de grànuls (apartat 1.3.2). Això suggereix que el rerefons genètic podria estar relacionat amb la presència de diferents al·lels o mutacions genètiques que afectarien el metabolisme o els nivells d'estrès oxidatiu. De la mateixa manera, els ratolins Tg presenten diferències en quant a l'increment de grànuls, com ho fan els ratolins deficients d'ApoE, els quals presenten

un increment en el nombre de grànuls respecte als animals control (Robertson *et al.,* 1998). Així doncs, l'absència de malina o l'increment de l'expressió de PTG són modificacions que podrien donar lloc a l'increment de CAL a través de modular el metabolisme energètic i els nivells d'estrès oxidatiu.

Alguns autors han considerat que hi ha dos tipus de LBs, classificats amb els termes tipus I i tipus II en base a la seva mida i forma (Van Hoof i Hageman-Bal, 1967; Machado-Salas *et al.,* 2012). A més a més, s'havia hipotetitzat que aquests dos tipus de LBs són diferents estadis d'un mateix procés, on l'acumulació del tipus I activaria la formació del tipus II (Machado-Salas *et al.,* 2012). Tot i així, els resultats obtinguts en el nostre estudi no confirmen aquesta hipòtesi, sinó que mostren que els anomenats tipus I per aquests autors correspondrien als grànuls CAL i els tipus II als nLBs. Per tant, seria poc probable que els tipus I produissin els tipus II, degut al diferent origen cel·lular i a les diferents regions cerebrals on tendeixen a acumular-se uns i altres. A més a més, a causa de la possible presència d'IgMs naturals com a contaminants en alguns anticossos comercials i els falsos marcatges positius que aquestes poden produir en els grànuls CAL, els resultats obtinguts fins a l'actualitat sobre la composició dels PGBs haurien de re-analitzar-se.

Tenint en compte els resultats obtinguts en aquesta tesi i les dades actuals disponibles, els PGBs es podrien classificar en dues grans categories (Figura 9). D'una banda, en situacions fisiològiques, la GS d'astròcits s'activa (1), i es formen les partícules de glicogen i els PGBs (2). Els productes de rebuig (WE) o proteïnes alterades s'acumulen en aquests PGBs (3) i són extruïts del SNC a través de mecanismes d'autofàgia secretòria cap a l'espai de Virchow-Robin (4) o directament al líquid cefalorraquidi. Entraran posteriorment al sistema limfàtic, on poden ser reconeguts per IgMs naturals. En situacions on hi ha un increment de WE, com l'envelliment i certes malalties neurodegeneratives, com la malaltia d'Alzheimer, aquests PGBs es veuen incrementats. D'altra banda, en el cas de la malaltia de Lafora, l'absència del complex malina-laforina en els astròcits (A) fa augmentar l'activitat de la GS i la formació de WE, augmentant, doncs, la formació de PGBs astrocítics. L'acúmul excessiu de PGBs astrocítics podria acabar afectant la funcionalitat d'aquest tipus cel·lular i participar en el fenotip epilèptic de la malaltia. L'absència del complex malina-laforina en neurones (B) també activa la maquinària de síntesi de PGBs neuronals, però aquest tipus de PGBs serien dirigits cap al sistema de glicofàgia, en les zones properes al nucli (5), enlloc de ser extruïts. La seva acumulació bloquejaria, almenys en part, el sistema d'autofàgia neuronal i seria la responsable de la neurodegeneració que s'observa en aquesta malaltia.

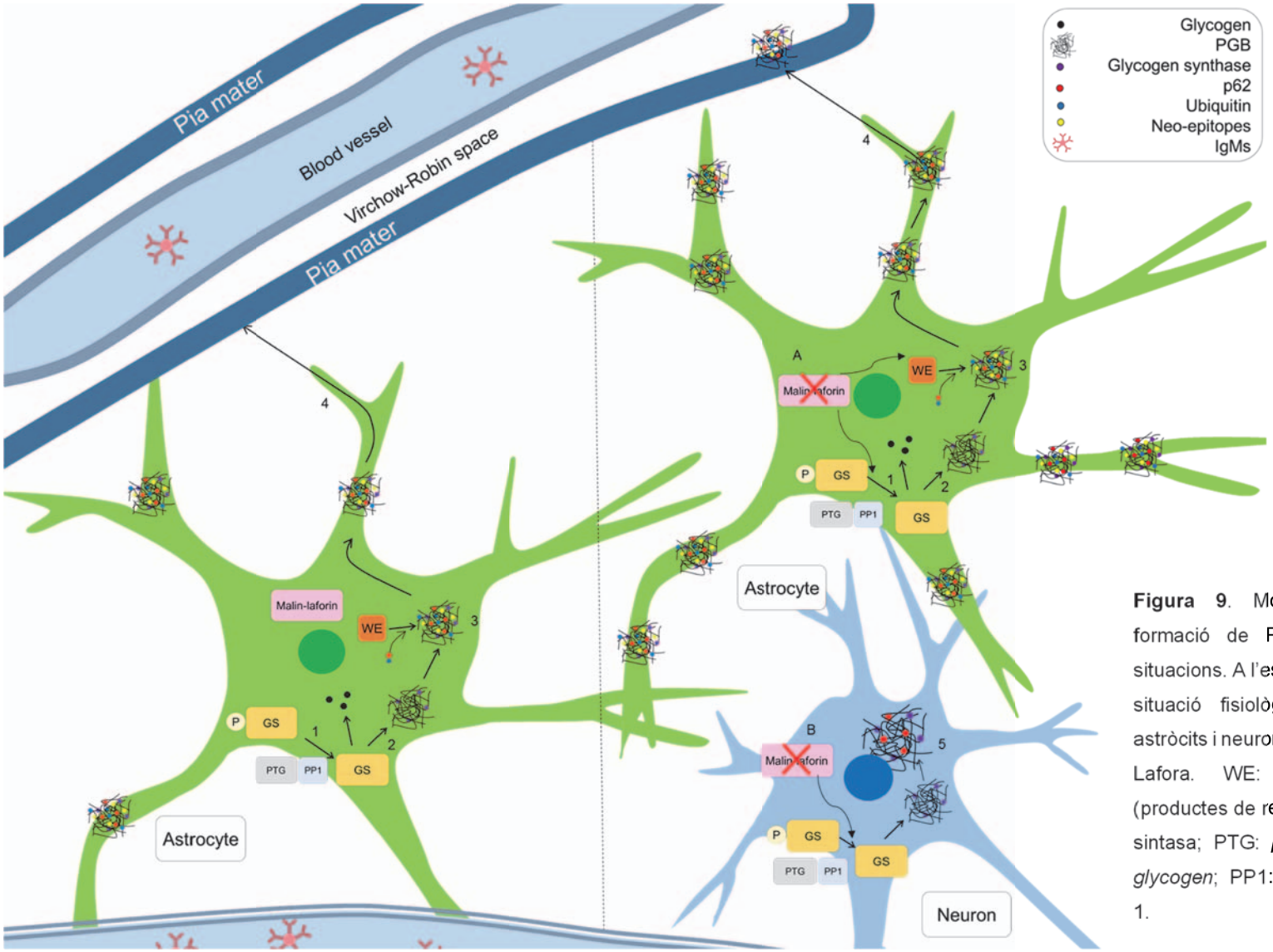

Figura 9. Model proposat de formació de PGBs en diferents situacions. A l'esquerra, astròcits en situació fisiològica. A la dreta, astròcits i neurones en la malaltia de Lafora. WE: *waste elements* (productes de rebuig); GS: glicogen sintasa; PTG: *protein targeting to glycogen*; PP1: proteïna fosfatasa 1.

V. *CONCLUSIONS*

1. The neo-epitopes found in the PAS granules of the hippocampus of aged mice can be recognized by natural IgM antibodies.

2. These natural IgMs are present in mouse plasma, independently of the existence of granules in the brain.

3. The presence of both the neo-epitopes in PAS granules and the natural IgMs against them in plasma open a new approach in the study of pathological brain processes.

4. *Corpora amylacea* from human brain are intracytoplasmic inclusions located in astrocytes.

5. The formation of c*orpora amylacea* takes place inside the cell, where some products become aggregated.

6. *Corpora amylacea* contain neo-epitopes that can be recognized by plasmatic IgMs.

7. The neo-epitopes on *corpora amylacea* are located throughout the whole body.

8. The IgMs that recognize the neo-epitopes of *corpora amylacea* are natural antibodies.

9. Some commercial antibodies contain contaminant natural IgM antibodies that recognize the neo-epitopes of *corpora amylacea.*

10. Contaminant natural IgM antibodies can produce false positive staining on *corpora amylacea.*

11. These structures do not contain tau protein, β-amyloid peptides, neuronal nuclei antigen, class III β-tubulin, aquaporin 4, S100B protein or glial fibrillary acidic protein, against that described previously.

12. *Corpora amylacea* contain glycogen synthase, an indispensable enzyme to form glucose polymers.

13. *Corpora amylacea* contain ubiquitin and p62, which are related to the elimination of waste elements.

14. *Corpora amylacea* contain matrix metalloproteinase 2, which is related to the reorganization of extracellular matrix.

15. *Corpora amylacea* can be physiological structures related to the extrusion of waste substances out of the brain.

16. Because of the similarities between *corpora amylacea* from human brain and PAS granules from mouse brain, these last bodies can be referred to as *corpora amylacea*-like granules.

17. Malin deficient mice, a mouse model of Lafora disease, contain two types of polyglucosan bodies in the brain: neuronal Lafora bodies and *corpora amylacea*-like granules.

18. Neuronal Lafora bodies are specific of Lafora disease and do not contain neo-epitopes.

19. *Corpora amylacea*-like granules, formed in astrocytes, are not specific of Lafora disease and contain neo-epitopes.

20. Although not specific of Lafora disease, the formation of *corpora amylacea*-like granules is highly increased in malin deficient mice.

21. Contrary to current belief, astrocytes can be involved in the etiopathogenesis of Lafora disease.

22. Glycogen synthase is indispensable for the formation of *corpora amylacea*-like granules.

23. The absence of *corpora amylacea*-like granules induced by the absence of glycogen synthase makes the aggregation of neo-epitopes impossible.

24. Protein targeting to glycogen overexpression, which enhances glycogen synthase activity, triggers the formation of *corpora amylacea*-like granules but not that of neuronal Lafora bodies.

25. Although glycogen synthase is necessary for the formation of both types of bodies, the routes of genesis may be different.

VI. BIBLIOGRAFIA

A

Acharya JN, Satishchandra P, Shankar SK. Familial progressive myoclonus epilepsy: Clinical and electrophysiologic observations. Epilepsia. 1995; 36:429-34.

Aguado C, Sarkar S, Korolchuk VI, Criado O, Vernia S, Boya P, Sanz P, Rodríguez de Córdoba S, Knecht E, Rubinsztein DC. Laforin, the most common protein mutated in Lafora disease, regulates autophagy. Hum Mol Genet. 2010; 19:2867–76.

Akiyama H, Kameyama M, Akiguchi I, Sugiyama H, Kawamata T, Fukuyama H, Kimura H, Matsushita M, Takeda T. Periodic acid-Schiff (PAS)-positive: granular structures increase in the brain of senescence accelerated mouse (SAM). Acta Neuropathol. 1986; 72:124-129.

Amédée T, Robert A, Coles JA. Potassium homeostasis and glial energy metabolism. Glia. 1997;21:46-55.

Andrade DM, Ackerley CA, Minett TS, Teive HA, Bohlega S, Scherer SW, Minassian BA. Skin biopsy in Lafora disease: genotype-phenotype correlations and diagnostic pitfalls. Neurology. 2003;61:1611-4.

Anzil AP, Herrlinger H, Blinzinger K, Kronski, D. Intraneuritic corpora amylacea. Virchows Arch A Pathol Anat Histol. 1974; 364:297–301.

Avendano J, Rodrigues MM, Hackett JJ, Gaskins R. Corpora amylacea of the optic nerve and retina: A form of neuronal degeneration. Invest Ophthalmol Vis Sci. 1980; 19:550–5.

Averback P. Parasynaptic corpora amylacea in the striatum. Arch Pathol. 1981; 105:334–5.

Avrameas S, Ternynck T, Tsonis IA, Lymberi P. Naturally occurring B-cell autoreactivity: a critical overview. J Autoimmun. 2007;29:213-8.

Avrameas S, Ternynck T. Natural autoantibodies: the other side of the immune system. Res Immunol. 1995;146:235-48.

Avrameas S. Natural autoantibodies: from 'horror autotoxicus' to 'gnothi seauton'. Immunol Today. 1991;12:154-9.

B

Balea IA, Illes P, Schobert R. Affinity of corpora amylacea for oligonucleotides sequence dependency and proteinaceous binding motif. Neuropathology. 2006;26:277-82.

Berard-Badier M, Pellissier JF, Gambarelli D, de Barsy T, Roger J, Toga M. The retina in Lafora disease: light and electron microscopy. Albrecht Von Graefes Arch Klin Exp Ophthalmol. 1980; 212:285-94.

Berkovic SF, Cochius J, Andermann E, Andermann F. Progressive myoclonus epilepsies: Clinical and genetic aspects. Epilepsia. 1993; 34:S19-30.

Binder CJ, Shaw PX, Chang MK, Boullier A, Hartvigsen K, Hörkkö S, Miller YI, Woelkers DA, Corr M, Witztum JL. The role of natural antibodies in atherogenesis. J Lipid Res. 2005; 46:1353–63.

Binder CJ. Natural IgM antibodies against oxidation-specific epitopes. J Clin Immunol. 2010; 30:S56-60.

Botez G, Rami A. Immunoreactivity for Bcl-2 and C-Jun/AP1 in hippocampal corpora amylacea after ischaemia in humans. Neuropathol Appl Neurobiol. 2001; 27:474-80.

Buervenich S, Olson L , Galter D. Nestin-like immunoreactivity of corpora amylacea in aged human brain. Brain Res Mol Brain Res. 2001; 94:204–8.

Busard HL, Gobreels-Festen AA, Renih WU, Gabreels FJ, Stadhouders AM. Axilla skin biopsy; a reliable test for the diagnosis of Lafora's disease. Ann Neurol. 1987a; 21:599-601.

Busard HL, Renier WO, Gabreëls FJ, Jaspar HH, Slooff JL, Janssen AJ, Van Haelst UJ. Lafora disease: a quantitative morphological and biochemical study of the cerebral cortex. Clin Neuropathol. 1987b; 6:1-6.

Busard HL, Span JP, Renkawek K, Renier WO, Gabreëls FJ, Slooff JL, Van't Hof MA. Polyglucosan bodies in brain tissue: a systematic study. Clin Neuropathol. 1994; 13:60-3.

Buzzard EF, Greenfield JG. Pathology of the nervous system. London. Constable; 1921.

C

Carpenter S, Karpati G. Sweat gland duct cells in Lafora disease: Diagnosis by skin biopsy. Neurology. 1981; 31:1564-8.

Casali P, Notkins A. $CD5^+$ B lymphocytes, polyreactive antibodies and the human B-cell repertoire. Immunol Today. 1989; 10:364–368.

Casali P, Schettino EW. Structure and function of natural antibodies. Curr Top Microbiol Immunol. 1996; 210:167–79.

Cavanagh JB. Corpora-amylacea and the family of polyglucosan diseases. Brain Res Brain Res Rev. 1999; 29:265–95.

Cervós-Navarro J. Polyglukosaneinschlüsse im Nervengewebe. In: Pathologie des Nervensystems. V. Ed Cervós-Navarro J. Springer Verl, Berlin. Heidelberg; 1991. p. 99-115.

Chan EM, Ackerley CA, Lohi H, Ianzano L, Cortez MA, Shannon P, Scherer SW, Minassian BA. Laforin preferentially binds the neurotoxic starch-like polyglucosans, which form in its absence in progressive myoclonus epilepsy. Hum Mol Genet. 2004; 13:1117-29.

Chan EM, Young EJ, Ianzano L, Munteanu I, Zhao X, Christopoulos CC, Avanzini G, Elia M, Ackerley CA, Jovic NJ, Bohlega S, Andermann E, Rouleau GA, Delgado-Escueta AV, Minassian BA, Scherer SW. Mutations in NHLRC1 cause progressive myoclonus epilepsy. Nat Genet. 2003; 35:125–17.

Chang MK, Bergmark C, Laurila A, Hörkkö S, Han KH, Friedman P, Dennis EA, Witztum JL. Monoclonal antibodies against oxidized low-density lipoprotein bind to apoptotic cells and inhibit their phagocytosis by elicited macrophages: evidence that oxidation specific epitopes mediate macrophage recognition. Proc Natl Acad Sci U S A. 1999; 96:6353–8.

Chang MK, Binder CJ, Miller YI, Subbanagounder G, Silverman GJ, Berliner JA, Witztum JL. Apoptotic cells with oxidation-specific epitopes are immunogenic and proinflammatory. J Exp Med. 2004; 200:1359–70.

Chen C, Stenzel-Poore MP, Rittenberg MB. Natural auto- and polyreactive antibodies differing from antigen-induced antibodies in the H chain CDR3. J Immunol. 1991; 147: 2359-67.

Cheng A, Zhang M, Gentry MS, Worby CA, Dixon JE, Saltiel AR. A role for AGL ubiquitination in the glycogen storage disorders of Lafora and Cori's disease. Genes Dev. 2007; 21:2399-409.

Chou MY, Fogelstrand L, Hartvigsen K, Hansen LF, Woelkers D, Shaw PX, Choi J, Perkmann T, Bäckhed F, Miller YI, Hörkkö S, Corr M, Witztum JL, Binder CJ. Oxidation-specific epitopes are dominant targets of innate natural antibodies in mice and humans. J Clin Invest. 2009; 119:1335–49.

Chung MH, Horoupian DS. Corpora amylacea: a marker for mesial temporal sclerosis. J Neuropathol Exp Neurol. 1996; 55:403–8.

Cisse S, Lacoste-Royal G, Laperriere J, Cabana T, Gavreau D. Ubiquitin is a component of polypeptides purified from corpora amylacea of aged human brain. Neurochem Res. 1991; 16:429–33.

Cissé S, Perry G, Lacoste-Royal G, Cabana T, Gauvreau D. Immunochemical identification of ubiquitin and heat-shock proteins in corpora amylacea from normal aged and Alzheimer's disease brains. Acta Neuropathol. 1993; 85:233–40.

Coulter DA, Eid T. Astrocytic regulation of glutamate homeostasis in epilepsy. Glia. 2012; 60:1215-26.

Criado O, Aguado C, Gayarre J, Duran-Trio L, Garcia-Cabrero AM, Vernia S, San Millán B, Heredia M, Romá-Mateo C, Mouron S, Juana-López L, Domínguez M, Navarro C, Serratosa JM, Sanchez M, Sanz P, Bovolenta P, Knecht E, Rodriguez de Cordoba S. Lafora bodies and neurological defects in malin-deficient mica correlate with impaired autophagy. Hum Mol Genet. 2012; 21:1521-33.

D

Day RJ, Mason MJ, Thomas C, Poon WW, Rohn TT. Caspase-cleaved tau co-localizes with early tangle markers in the human vascular dementia brain. PLoS One. 2015;10:e0132637.

Del Valle J, Duran-Vilaregut J, Manich G, Casadesús G, Smith MA, Camins A, Pallàs M, Pelegrí C, Vilaplana J. Early amyloid accumulation in the hippocampus of SAMP8 mice. J Alzheimers Dis. 2010; 19:1303–15.

Delgado-Escueta AV. Advances in lafora progressive myoclonus epilepsy. Curr Neurol Neurosci Rep. 2007; 7:428–33.

DePaoli-Roach AA, Tagliabracci VS, Segvich DM, Meyer CM, Irimia JM, Roach PJ. Genetic depletion of the malin E3 ubiquitin ligase in mice leads to lafora bodies and the accumulation of insoluble laforin. J Biol Chem. 2010; 285:25372-81.

Dighiero G, Lymberi P, Holmberg D, Lundquist I, Coutinho A, Avrameas S. High frequency of natural autoantibodies in normal newborn mice. J Immunol. 1985;134:765-71.

Dighiero G, Lymberi P, Mazie JC, Rouyre S, Butler-Browne GS, Whalen RG, Avrameas S. Murine hybridomas secreting natural monoclonal antibodies reacting with self antigens. J Immunol. 1983; 131:2267-72.

Doehner J, Genoud C, Imhof C, Krstic D, Knuesel I. Extrusion of misfolded and aggregated proteins--a protective strategy of aging neurons? Eur J Neurosci. 2012; 35:1938-50.

Doehner J, Madhusudan A, Konietzko U, Fritschy JM, Knuesel I. Co-localization of Reelin and proteolytic AbetaPP fragments in hippocampal plaques in aged wild-type mice. J Alzheimers Dis. 2010; 19:1339-57.

Dolman CL, McCormick Q, Drance SM. Aging of the optic nerve. Arch Ophthalmol. 1980; 98:2053–8.

Duan B, Morel L. Role of B-1a cells in autoimmunity. Autoimmun Rev. 2006; 5:403-8.

Duran J, Gruart A, García-Rocha M, Delgado-García JM, Guinovart JJ. Glycogen accumulation underlies neurodegeneration and autophagy impairment in Lafora disease. Hum Mol Genet. 2014; 23:3147-56.

Duran J, Tevy MF, Garcia-Rocha M, Calbó J, Milán M, Guinovart JJ. Deleterious effects of neuronal accumulation of glycogen in flies and mice. EMBO Mol Med. 2012; 4:719-29.

E

Erdamar S, Zhu ZQ, Hamilton WJ, Armstrong DL, Grossman RG. Corpora amylacea and heat shock protein 27 in Ammon's horn sclerosis. J Neuropathol Exp Neurol. 2000; 59:698-706.

Ethell IM, Ethell DW. Matrix metalloproteinases in brain development and remodeling: synaptic functions and targets. J Neurosci Res. 2007; 85:2813-23.

F

Faria-Neto JR, Chyu KY, Li X, Dimayuga PC, Ferreira C, Yano J, Cercek B, Shah PK. Passive immunization with monoclonal IgM antibodies against phosphorylcholine reduces accelerated vein graft atherosclerosis in apolipoprotein E-null mice. Atherosclerosis. 2006; 189:83-90.

Flajnik MF, Rumfelt LL. Early and natural antibodies in non-mammalian vertebrates. Curr Top Microbiol Immunol. 2000; 252:233-40.

Fujii M, Goto N, Okada A, Kida A, Kikuchi K. Distribution of amyloid bodies in the aged human vestibulocochlear nerve. Acta Oto-Laryngol. 1996; 116:566–71.

G

Ganesh S, Delgado-Escueta AV, Sakamoto T, Avila MR, Machado-Salas J, Hoshii Y, Akagi T, Gomi H, Suzuki T, Amano K, Agarwala KL, Hasegawa Y, Bai DS, Ishihara T, Hashikawa T, Itohara S, Cornford EM, Niki H, Yamakawa K. Targeted disruption of the Epm2a gene causes formation of Lafora inclusion bodies, neurodegeneration, ataxia, myoclonus epilepsy and impaired behavioral response in mice. Hum Molec Genet. 2002; 11:1251-62.

Gardai S, Bratton D. Recognition ligands on apoptotic cells: a perspective. J Leukoc Biol. 2006; 79:896–903.

Garyali P, Siwach P, Singh PK, Puri R, Mittal S, Sengupta S, Parihar R, Ganesh S. The malin-laforin complex suppresses the cellular toxicity of misfolded proteins by promoting their degradation through the ubiquitin-proteasome system. Hum Mol Genet. 2009; 18:688-700.

Gáti I, Leel-Ossy L. Heat shock protein 60 in corpora amylacea. Pathol Oncol Res. 2001; 7:140-4.

Gómez-Abad C, Gómez-Garre P, Gutiérrez-Delicado E, Saygi S, Michelucci R, Tassinari CA, Rodríguez de Córdoba S, Serratosa JM. Lafora disease due to EPM2B mutations: a clinical and genetic study. Neurology. 2005; 64:982-6.

Gonzalez R, Charlemagne J, Mahana W, Avrameas S. Specificity of natural serum antibodies present in phylogenetically distinct fish species. Immunology. 1988; 63:31-6.

Greene V, Papasozomenos SC. Tau-protein immunoreactivity in Lafora body disease and in corpora amylacea. J Neuropathol Exp Neurol. 1987; 46:345.

Grönwall C, Vas J, Silverman GJ. Protective roles of natural IgM antibodies. Front Immunol. 2012; 3:66.

H

Hara T, Nakamura K, Matsui M, Yamamoto A, Nakahara Y, Suzuki-Migishima R, Yokoyama M, Mishima K, Saito I, Okano H, Mizushima N. Suppression of basal autophagy in neural cells causes neurodegenerative disease in mice. Nature. 2006; 441:885–9.

Hartvigsen K, Chou MY, Hansen LF, Shaw PX, Tsimikas S, Binder CJ, Witztum JL. The role of innate immunity in atherogenesis. J Lipid Res. 2009; 50:S388-93.

Hedberg-Oldfors C, Oldfors A. Polyglucosan storage myopathies. Mol Aspects Med. 2015; 46:85-100.

Hooijkaas H, Benner R, Pleasants JR, Wostmann BS. Isotypes and specificities of immunoglobulins produced by germ-free mice fed chemically defined ultrafiltered "antigen-free" diet. Eur J Immunol. 1984; 14:1127-30.

Hörkkö S, Bird DA, Miller E, Itabe H, Leitinger N, Subbanagounder G, Berliner JA, Friedman P, Dennis EA, Curtiss LK, Palinski W, Witztum JL. Monoclonal autoantibodies specific for oxidized phospholipids or oxidized phospholipid-protein adducts inhibit macrophage uptake of oxidized low-density lipoproteins. J Clin Invest. 1999; 103: 117-28.

Hoyaux D, Decaestecker C, Heizmann CW, Vogl T, Schäfer BW, Salmon I, Kiss R, Pochet R. S100 proteins in corpora amylacea from normal human brain. Brain Res. 2000; 867:280-8.

I

Irino M, Akiguchi I, Takeda T. Ultrastructural study of PAS-positive granular structures in brains of SAMP8. Takeda T. International Congress Series. The Sam Model Of Senescence; 1994. p. 371-374

Iwaki T, Hamada Y, Tateishi J. Advanced glycosylation end-products and heat shock proteins accumulate in the basophilic degeneration of the myocardium and the corpora amylacea of the glia. Pathol Int. 1996; 46:757-63.

J

Jenis EH, Schochet SS, Earle KM. Myoclonus epilepsy with Lafora bodies: case report with electron microscopic observation. Mil Med. 1970; 135:116-9.

Jucker M, Ingram DK. Age-related fibrillar material in mouse brain. Assessing its potential as a biomarker of aging and as a model of human neurodegenerative disease. Ann N Y Acad Sci. 1994; 719:238-47.

Jucker M, Walker L, Kuo H, Tian M, Ingram DK. Age-related fibrillar deposits in brains of C57BL/6 mice. A review of localization, staining characteristics, and strain specificity. Mol Neurobiol. 1994a; 9:125-33.

Jucker M, Walker L, Martin L, Kitt C, Kleinman H, Ingram DK, Price D. Age-associated inclusions in normal and transgenic mouse brain. Science. 1992; 255:1443-5.

Jucker M, Walker L, Schwarb P, Hengemihle J, Kuo H, Snow D, Bamert F, Ingram DK. Age-related deposition of glia-associated fibrillar material in brains of C57BL/6 mice. Neuroscience. 1994b; 60:875–89.

K

Keller JN. Age-related neuropathology, cognitive decline, and Alzheimer's disease. Ageing Res Rev. 2006; 5:1-13.

Kern DS, Maclean KN, Jiang H, Synder EY, Sladek JR Jr, Bjugstad KB. Neural stem cells reduce hippocampal tau and reelin accumulation in aged Ts65Dn Down syndrome mice. Cell Transplant. 2011; 20:371-9.

Kim SJ, Gershov D, Ma X, Brot N, Elkon KB. I-PLA(2) activation during apoptosis promotes the exposure of membrane lysophosphatidylcholine leading to binding

by natural immunoglobulin M antibodies and complement activation. J Exp Med. 2002; 196:655-65.

Knecht E, Aguado C, Sarkar S, Korolchuk VI, Criado-García O, Vernia S, Boya P, Sanz P, Rodríguez de Córdoba S, Rubinsztein DC. Impaired autophagy in Lafora disease. Autophagy. 2010; 6:991-3.

Knuesel I, Nyffeler M, Mormède C, Muhia M, Meyer U, Pietropaolo S, Yee BK, Pryce CR, LaFerla FM, Marighetto A, Feldon J. Age-related accumulation of Reelin in amyloid-like deposits. Neurobiol Aging. 2009; 30:697–716.

Kobayashi K, Iyoda K, Ohtsuka Y, Ohtahara S, Yamada M. Longitudinal clinicoelectrophysiologic study of a case of Lafora disease proven by skin biopsy. Epilepsia. 1990; 31:194-201.

Kocherhans S, Madhusudan A, Doehner J, Breu KS, Nitsch RM, Fritschy JM, Knuesel I. Reduced Reelin expression accelerates amyloid-beta plaque formation and tau pathology in transgenic Alzheimer's disease mice. J Neurosci. 2010; 30:9228-40.

Komatsu M, Waguri S, Chiba T, Murata S, Iwata J, Tanida I, Ueno T, Koike M, Uchiyama Y, Kominami E, Tanaka K. Loss of autophagy in the central nervous system causes neurodegeneration in mice. Nature. 2006; 441:880–4.

Korzhevskiĭ DE, Giliarov AV. Demonstration of nuclear protein neun in the human brain corpora amylacea. Morfologiia. 2007; 131:75-6.

Krass KL, Colinayo V, Ghazalpour A, Vinters HV, Lusis AJ, Drakec TA. Genetic loci contributing to age-related hippocampal lesions in mice. Neurobiol Dis. 2003; 13:102–8.

Kubota T, Holbach LM, Naumann GO. Corpora amylacea in glaucomatous and non-glaucomatous optic nerve and retina. Graefes Arch Clin Exp Ophthalmol. 1993; 231:7–11.

Kubota T, Naumann GO. Reduction in number of corpora amylacea with advancing histological changes of glaucoma. Graefes Arch Clin. Exp Ophthalmol. 1993; 231:249–53.

Kuo H, Ingram DK, Walker LC, Tian M, Hengemihle JM, Jucker M. Similarities in the age-related hippocampal deposition of periodic acid-schiff-positive granules in

the senescence-accelerated mouse P8 and C57BL/6 mouse strains. Neuroscience. 1996; 74:733–40.

L

Lacroix-Desmazes S, Kaveri SV, Mouthon L, Ayouba A, Malanchère E, Coutinho A, Kazatchkine MD. Self-reactive antibodies (natural autoantibodies) in healthy individuals. J Immunol Methods. 1998; 216:117-37.

Lafora GR, Glueck B. Beitrag zur Histopathologie der myoklonis chen. Epilepsie. Zeitschrift fur die gesamte Neurologie und Psychiatrie; 1911; 6:1–14.

Lafora GR. Uber das Vorkommen amyloider Korperchen im Innern der Ganglienzellen: zugleich en Beitrag zum Studium der amyloiden Substanz im Nervensystem. Virchows Arch Pathol Anat Physiol Klin Med. 1911; 205:295–303.

Lamar CH, Hinsman EJ, Henrikson CK. Alterations in the hippocampus of aged mice. Acta Neuropathol. 1976; 36:387–391.

Leel-Ossy L. New data on the ultrastructure of the corpus amylaceum (polyglucosan body). Pathol Oncol Res. 2001; 7:145-50.

Lehesjoki AE, Koskiniemi M, Sistonen P, Miao J, Hästbacka J, Norio R, de la Chapelle A. Localization of a gene for progressive myoclonus epilepsy to chromosome 21q22. Proc Natl Acad Sci U S A. 1991; 88:3696-9.

Leibundgut G, Witztum JL, Tsimikas S. Oxidation-specific epitopes and immunological responses: Translational biotheranostic implications for atherosclerosis. Curr Opin Pharmacol. 2013; 13:168-79.

Lewis PD, Evans DJ, Shambayati B. Immunocytochemical anti-lectin-binding studies on Lafora bodies. Clin Neuropathol. 1990; 9:7–9.

Litvack ML, Palaniyar N. Review: Soluble innate immune pattern-recognition proteins for clearing dying cells and cellular components: implications on exacerbating or resolving inflammation. Innate Immun. 2010; 16:191-200.

Liu HM, Anderson K, Caterson B. Demonstration of a keratin sulfate proteoglycan and a mannose-rich glycoconjugate in corpora amylacea of the brain by immunocytochemical and lectin-binding methods. J Neuroimmunol. 1987; 14:49–60.

Liu Y, Wang Y, Wu C, Liu Y, Zheng P. Deletions and missense mutations of EPM2A exacerbate unfolded protein response and apoptosis of neuronal cells induced by endoplasm reticulum stress. Hum Mol Genet. 2009; 18:2622-31.

Lodeiro M, Puerta E, Ismail MA, Rodriguez-Rodriguez P, Rönnbäck A, Codita A, Parrado-Fernandez C, Maioli S, Gil-Bea F, Merino-Serrais P, Cedazo-Minguez A. Aggregation of the inflammatory S100A8 precedes Aβ plaque formation in transgenic APP mice: positive feedback for S100A8 and Aβ productions. J Gerontol A Biol Sci Med Sci. 2017; 72:319-328.

Loeffler KU, Edward DP, Tso MO. Tau-2 immunoreactivity of corpora amylacea in the human retina and optic nerve. Invest Ophthalmol Vis Sci. 1993; 34:2600–3.

López-González I, Viana R, Sanz P, Ferrer I. Inflammation in Lafora disease: Evolution with disease progression in laforin and malin knock-out mouse models. Mol Neurobiol. 2017; 54:3119-30.

Lutz HU, Binder CJ, Kaveri S. Naturally occurring auto-antibodies in homeostasis and disease. Trends Immunol. 2009; 30:43-51.

M

Machado-Salas J, Avila-Costa MR, Guevara P, Guevara J, Durón RM, Bai D, Tanaka M, Yamakawa K, Delgado-Escueta AV. Ontogeny of Lafora bodies and neurocytoskeleton changes in Laforin-deficient mice. Exp Neurol. 2012; 236:131-40.

Madhusudan A, Sidler C, Knuesel I. Accumulation of reelin-positive plaques is accompanied by a decline in basal forebrain projection neurons during normal aging. Eur J Neurosci. 2009; 30:1064-76.

Mandybur TI, Ormsby I, Zemlan FP. Cerebral aging: a quantitative study of gliosis in old nude mice. Acta Neuropathol. 1989;77:507-13.

Manich G, Cabezón I, Camins A, Pallàs M, Liberski PP, Vilaplana J, Pelegrí C. Clustered granules present in the hippocampus of aged mice result from a degenerative process affecting astrocytes and their surrounding neuropil. Age. 2014a; 36:9690.

Manich G, del Valle J, Cabezón I, Camins A, Pallàs M, Pelegrí C, Vilaplana J. Presence of a neo-epitope and absence of amyloid beta and tau protein in degenerative hippocampal granules of aged mice. Age. 2014b; 36:151-65.

Manich G, Mercader C, del Valle J, Duran-Vilaregut J, Camins A, Pallàs M, Vilaplana J, Pelegrí C. Characterization of amyloid-β granules in the hippocampus of SAMP8 mice. J Alzheimers Dis. 2011; 25:535-46.

Mannoor K, Xu Y, Chen C. Natural autoantibodies and associated B cells in immunity and autoimmunity. Autoimmunity. 2013;46:138–47.

Maqbool A, Tahir M. Corpora amylacea in human cadaveric brain age related differences. Biomedica. 2008; 24:92-5.

Mariuzza RA. Multiple paths to multispecificity. Immunity. 2006; 24:359–61.

Martin JE, Mather K, Swash M, Garafalo O, Leigh PN, Anderton BH. Heat shock protein expression in corpora amylacea in the central nervous system: clue to their origin. Neuropathol Appl Neurobiol. 1991; 17:113–9.

McMahon J, Huang X, Yang J, Komatsu M, Yue Z, Qian J, Zhu X, Huang Y. Impaired autophagy in neurons after disinhibition of mammalian target of rapamycin and its contribution to epileptogenesis. J Neurosci. 2012; 32:15704–14.

Meng H, Zhang X, Blaivas M, Wang MM. Localization of blood proteins thrombospondin1 and ADAMTS13 to cerebral corpora amylacea. Neuropathology. 2009; 29:664-71.

Merbl Y, Zucker-Toledano M, Quintana FJ, Cohen IR. Newborn humans manifest autoantibodies to defined self molecules detected by antigen microarray informatics. J Clin Invest. 2007; 117:712-8.

Miller YI, Choi SH, Wiesner P, Fang L, Harkewicz R, Hartvigsen K, Boullier A, Gonen A, Diehl CJ, Que X, Montano E, Shaw PX, Tsimikas S, Binder CJ, Witztum JL. Oxidation-specific epitopes are danger-associated molecular patterns recognized by pattern recognition receptors of innate immunity. Circ Res. 2011; 108:235-48.

Minassian BA, Lee JR, Herbrick JA, Huizenga J, Soder S, Mungall AJ, Dunham I, Gardner R, Fong CY, Carpenter S, Jardim L, Satishchandra P, Andermann E,

Snead OC 3rd, Lopes-Cendes I, Tsui LC, Delgado-Escueta AV, Rouleau GA, Scherer SW. Mutations in a gene encoding a novel protein tyrosine phosphatase cause progressive myoclonus epilepsy. Nat Genet. 1998; 20:171-4.

Minassian BA. Lafora's disease: towards a clinical, pathologic, and molecular synthesis. Pediatr Neurol. 2001; 25:21-9.

Mitsuno S, Takahashi M, Gondo T, Hoshii Y, Hanai N, Ishihara T, Yamada M. Immunohistochemical, conventional and immunoelectron microscopical characteristics of periodic acid-Schiff-positive granules in the mouse brain. Acta Neuropathol. 1999; 98:31-8.

Mittal KR, Olszewski WA. Widening of inter-Purkinje cell distances in association with corpora amylacea. J Gerontol. 1985; 40:700-2.

Mizutani T, Satoh J, Morimatsu Y. Axonal polyglucosan body in the ventral posterolateral nucleus of the human thalamus in relation to aging. Acta Neuropathol. 1987; 74:9–12.

Montecino-Rodriguez E, Dorshkind K. New perspectives in B-1 B cell development and function. Trends Immunol. 2006; 27:428-33.

Mrak RE, Griffin ST, Graham DI. Aging-associated changes in human brain. J Neuropathol Exp Neurol. 1997; 56:1269-75.

N

Nakamura S, Akiguchi I, Seriu N, Ohnishi K, Takemura M, Ueno M, Tomimoto H, Kawamata T, Kimura J, Hosokawa M. Monoamine oxidase-B-positive granular structures in the hippocampus of aged senescence-accelerated mouse (SAMP8). Acta Neuropathol. 1995; 90:626-32.

Nam IH, Kim DW, Song H, Kim S, Lee KS, Lee YH. Association of corpora amylacea formation with astrocytes and cerebrospinal fluid in the aged human brain. Korean J Phys Anthropol. 2012; 25:177-84.

Nanduri AS, Kaushal N, Clusmann H, Binder DK. The maestro don Gonzalo Rodríguez-Lafora. Epilepsia. 2008; 49:943-7.

Nishio S, Morioka T, Kawamura T, Fukui K, Nonaka H, Matsushima M. Corpora amylacea replace the hippocampal pyramidal cell layer in a patient with temporal lobe epilepsy. Epilepsia. 2001; 42:960-2.

Notkins AL. Polyreactivity of antibody molecules. Trends Immunol. 2004; 25:174-9.

Notter T, Knuesel I. Reelin immunoreactivity in neuritic varicosities in the human hippocampal formation of non-demented subjects and Alzheimer's disease patients. Acta Neuropathol Commun. 2013; 1:27.

O

Oddo S, Caccamo A, Shepherd JD, Murphy MP, Golde TE, Kayed R, Metherate R, Mattson MP, Akbari Y, LaFerla FM. Triple-transgenic model of Alzheimer's disease with plaques and tangles: intracellular Abeta and synaptic dysfunction. Neuron. 2003; 39:409-21.

P

Palinski W, Rosenfeld ME, Ylä-Herttuala S, Gurtner GC, Socher SS, Butler SW, Parthasarathy S, Carew TE, Steinberg D, Witztum JL. Low density lipoprotein undergoes oxidative modification in vivo. Proc Natl Acad Sci USA. 1989; 86:1372-6.

Palmucci L, Anzil AP, Luh S. Intra-astrocytic glycogen granules and corpora amylacea stain positively for polyglucosans: a cytochemical contribution on the fine structural polymorphism of particulate polysaccharides. Acta Neuropathol. 1982; 57:99-102.

Pederson BA, Turnbull J, Epp JR, Weaver SA, Zhao X, Pencea N, Roach PJ, Frankland PW, Ackerley CA, Minassian BA. Inhibiting glycogen synthesis prevents Lafora disease in a mouse model. Ann Neurol. 2013; 74:297-300.

Pirici D, Margaritescu C. Corpora amylacea in aging brain and age-related brain disorders. J Aging Gerontol. 2014; 2:33-57.

Pirici I, Mărgăritescu C, Mogoantă L, Petrescu F, Simionescu CE, Popescu ES, Cecoltan S, Pirici D. Corpora amylacea in the brain form highly branched three-dimensional lattices. Rom J Morphol Embryol. 2014; 55:1071-7.

Pisa D, Alonso R, Rábano A, Carrasco L. Corpora amylacea of brain tissue from neurodegenerative diseases are stained with specific antifungal antibodies. Front Neurosci. 2016; 10:86.

Porquet D, Casadesús G, Bayod S, Vicente A, Canudas AM, Vilaplana J, Pelegrí C, Sanfeliu C, Camins A, Pallàs M, del Valle J. Dietary resveratrol prevents Alzheimer's markers and increases life span in SAMP8. Age. 2013; 35:1851-65.

Puri R, Suzuki T, Yamakawa K, Ganesh S. Dysfunctions in endosomal-lysosomal and autophagy pathways underlie neuropathology in a mouse model for Lafora disease. Hum Mol Genet. 2012; 21:175-84.

R

Rachubinski AL, Maclean KN, Evans JR, Bjugstad KB. Modulating cognitive deficits and tau accumulation in a mouse model of aging Down syndrome through neonatal implantation of neural progenitor cells. Exp Gerontol. 2012; 47:723-33.

Radhakrishnan A, Radhakrishnan K, Radhakrishnan VV, Mary PR, Kesavadas C, Alexander A, Sarma PS. Corpora amylacea in mesial temporal lobe epilepsy: clinico-pathological correlations. Epilepsy Res. 2007; 74:81-90.

Ramachandran N, Girard JM, Turnbull J, Minassian BA. The autosomal recessively inherited progressive myoclonus epilepsies and their genes. Epilepsia. 2009; 50: 29-36.

Ramon y Cajal S, Blanes A, Martinez A, Saenz E, Gutierrez M. Lafora's Disease. An ultrastructural and histochemical study. Acta Neuropathol. 1974; 30:189–96.

Ramsey HI. Ultrastructure of corpora amylacea. J Neuropathol Exp Neurol. 1965; 24: 25-39.

Rao SN, Maity R, Sharma J, Dey P, Shankar SK, Satishchandra P, Jana NR Sequestration of chaperones and proteasome into Lafora bodies and proteasomal dysfunction induced by Lafora disease-associated mutations of malin. Hum Mol Genet. 2010; 19:4726-34.

Robertson TA, Dutton NS, Martins RN, Roses AD, Kakulas BA, Papadimitriou JM. Age-related congophilic inclusions in the brains of apolipoprotein E-deficient mice. Neuroscience. 1998; 82:171-80.

Robertson TA, Dutton NS, Martins RN, Taddei K, Papadimitriou JM. Comparison of astrocytic and myocytic metabolic dysregulation in apolipoprotein E deficient and human apolipoprotein E transgenic mice. Neuroscience. 2000; 98:353-9.

Robitaille Y, Carpenter S, Karpati G, DiMauro SD. A distinct form of adult polyglucosan body disease with massive involvement of central and peripheral neuronal processes and astrocytes: a report of four cases and a review of the occurrence of polyglucosan bodies in other conditions such as Lafora's disease and normal ageing. Brain. 1980; 103:315-36.

S

Sakai M, Austin J, Witmer F, Trueb L. Studies in myoclonus epilepsy (Lafora body form). II. Polyglucosans in the systemic deposits of myoclonus epilepsy and in corpora amylacea. Neurology. 1970; 20:160-76.

Sakai M, Austin J, Witmer F, Trueb L. Studies of corpora amylacea. I. Isolation and preliminary characterization by chemical and histochemical techniques. Arch Neurol. 1969; 21:526-44.

Sbarbati A, Carner M, Colletti V, Osculati F. Extrusion of corpora amylacea from the marginal glia at the vestibular root entry zone. J Neuropathol Exp Neurol. 1996; 55:196-201.

Schipper HM, Cissé S. Mitochondrial constituents of corpora amylacea and autofluorescent astrocytic inclusions in senescent human brain. Glia. 1995; 14:55-64.

Schipper HM. Brain iron deposition and the free radical-mitochondrial theory of ageing. Ageing Res Rev. 2004; 3:265-301.

Schwartz-Albiez R, Laban S. Eichmüller S, Kirschfink M.. Cytotoxic natural antibodies against human tumours: an option for anti-cancer immunotherapy? Autoimmun Rev. 2008; 7:491–5.

Schwartz-Albiez R. Naturally occurring antibodies directed against carbohydrate tumor antigens. Adv Exp Med Biol. 2012; 750:27–43.

Schwarz GA, Yanoff M. Lafora’s disease. Distinct clinico-pathologic form of unverricht’s syndrome. Arch Neurol. 1965; 12:172-88.

Selmaj K, Pawłowska Z, Walczak A, Koziołkiewicz W, Raine CS, Cierniewski CS. Corpora amylacea from multiple sclerosis brain tissue consists of aggregated neuronal cells. Acta Biochim Pol. 2008; 55:43-9.

Sengupta S, Badhwar I, Upadhyay M, Singh S, Ganesh S. Malin and laforin are essential components of a protein complex that protects cells from thermal stress. J Cell Sci. 2011; 124:2277-86.

Serratosa JM, Gómez-Garre P, Gallardo ME, Anta B, de Bernabé DB, Lindhout D, Augustijn PB, Tassinari CA, Malafosse RM, Topcu M, Grid D, Dravet C, Berkovic SF, de Córdoba SR. A novel protein tyrosine phosphatase gene is mutated in progressive myoclonus epilepsy of the Lafora type (EPM2). Hum Mol Genet. 1999; 8:345-52.

Sethi DK, Agarwal A, Manivel V, Rao KV, Salunke DM. Differential epitope positioning within the germline antibody paratope enhances promiscuity in the primary immune response. Immunity. 2006; 24:429e38

Sharma J, Rao SN, Shankar SK, Satishchandra P, Jana NR. Lafora disease ubiquitin ligase malin promotes proteasomal degradation of neuronatin and regulates glycogen synthesis. Neurobiol Dis. 2011; 44:133-41.

Sinadinos C, Valles-Ortega J, Boulan L, Solsona E, Tevy MF, Marquez M, Duran J, Lopez-Iglesias C, Calbó J, Blasco E, Pumarola M, Milán M, Guinovart JJ. Neuronal glycogen synthesis contributes to physiological aging. Aging Cell. 2014; 13:935-45.

Singh S, Ganesh S. Lafora progressive myoclonus epilepsy: a meta-analysis of reported mutations in the first decade following the discovery of the EPM2A and NHLRC1 genes. Hum Mutat. 2009; 30:715-23.

Singh S, Sethi I, Francheschetti S, Riggio C, Avanzini G, Yamakawa K, Delgado-Escueta AV, Ganesh S. Novel NHLRC1 mutations and genotype-phenotype correlations in patients with Lafora's progressive myoclonic epilepsy. J Med Genet. 2006; 43:e48.

Singh S, Suzuki T, Uchiyama A, Kumada S, Moriyama N, Hirose S, Takahashi Y, Sugie H, Mizoguchi K, Inoue Y, Kimura K, Sawaishi Y, Yamakawa K, Ganesh S. Mutations in the NHLRC1 gene are the common cause for Lafora disease in the Japanese population. J Hum Genet. 2005; 50:347-52.

Singhrao SK, Morgan BP, Neal JW, Newman GR. A functional role for corpora amylacea based on evidence from complement studies. Neurodegeneration. 1995; 4:335-45.

Singhrao SK, Neal JW, Newman GR. Corpora amylacea could be an indicator of neurodegeneration. Neuropathol Appl Neurobiol. 1993; 19:269-76.

Singhrao SK, Neal JW, Piddlesden SJ, Newman GR. New immunocytochemical evidence for a neuronal/oligodendroglial origin for corpora amylacea. Neuropathol Appl Neurobiol. 1994; 20:66-73.

Song W, Zukor H, Liberman A, Kaduri S, Arvanitakis Z, Bennett DA, Schipper HM. Astroglial heme oxygenase-1 and the origin of corpora amylacea in aging and degenerating neural tissues. Exp Neurol. 2014; 254:78-89.

Soontornniyomkij V, Risbrough VB, Young JW, Soontornniyomkij B, Jeste DV, Achim CL. Increased hippocampal accumulation of autophagosomes predicts short-term recognition memory impairment in aged mice. Age. 2012; 34:305-16.

Stam FC, Roukema PA. Histochemical and biochemical aspects of corpora amylacea. Acta Neuropathol. 1973; 25:95-102.

Steyaert A, Cissé S, Merhi Y, Kalbakji A, Reid N, Gauvreau D, Lacoste-Royal G. Purification and polypeptide composition of corpora amylacea from aged human brain. J Neurosci Methods. 1990; 31:59-64.

Suzuki A, Yokoo H, Kakita A, Takahashi H, Harigaya Y, Ikota H, Nakazato Y. Phagocytized corpora amylacea as a histological hallmark of astrocytic injury in neuromyelitis optica. Neuropathology. 2012; 32:587-94.

T

Tagliabracci VS, Heiss C, Karthik C, Contreras CJ, Glushka J, Ishihara M, Azadi P, Hurley TD, DePaoli-Roach AA, Roach PJ. Phosphate incorporation during glycogen synthesis and Lafora disease. Cell Metab. 2011; 13:274-82.

Tagliabracci VS, Turnbull J, Wang W, Girard JM, Zhao X, Skurat AV, Delgado-Escueta AV, Minassian BA, Depaoli-Roach AA, Roach PJ. Laforin is a glycogen phosphatase, deficiency of which leads to elevated phosphorylation of glycogen in vivo. Proc Natl Acad Sci USA. 2007; 104:19262-6.

Takahashi K, Agari M, Nakamura H. Intra-axonal corpora amylacea in ventral and lateral horns of the spinal cord. Acta Neuropathol. 1975; 11:151–8.

Takemura M, Nakamura S, Akiguchi I, Ueno M, Oka N, Ishikawa S, Shimada A, Kimura J, Takeda T. Beta/A4 proteinlike immunoreactive granular structures in the brain of senescence-accelerated mouse. Am J Pathol. 1993; 142:1887-97.

Ternynck T, Avrameas S. Murine natural monoclonal autoantibodies: a study of their polyspecificities and their affinities. Immunol Rev. 1986; 94:99-112.

Tsuiji H, Inoue I, Takeuchi M, Furuya A, Yamakage Y, Watanabe S, Koike M, Hattori M, Yamanaka K. TDP-43 accelerates age-dependent degeneration of interneurons. Sci Rep. 2017; 7:14972.

Turnbull J, DePaoli-Roach AA, Zhao X, Cortez MA, Pencea N, Tiberia E, Piliguian M, Roach PJ, Wang P, Ackerley CA, Minassian BA. PTG depletion removes Lafora bodies and rescues the fatal epilepsy of Lafora disease. PLoS Genet. 2011; 7:e1002037.

Turnbull J, Epp JR, Goldsmith D, Zhao X, Pencea N, Wang P, Frankland PW, Ackerley CA, Minassian BA. PTG protein depletion rescues malin-deficient Lafora disease in mouse. Ann Neurol. 2014; 75:442-6.

Turnbull J, Wang P, Girard JM, Ruggieri A, Wang TJ, Draginov AG, Kameka AP, Pencea N, Zhao X, Ackerley CA, Minassian BA. Glycogen hyperphosphorylation underlies lafora body formation. Ann Neurol. 2010; 68:925-33.

V

Valles-Ortega J, Duran J, Garcia-Rocha M, Bosch C, Saez I, Pujadas L, Serafin A, Cañas X, Soriano E, Delgado-García JM, Gruart A, Guinovart JJ. Neurodegeneration and functional impairments associated with glycogen synthase accumulation in a mouse model of Lafora disease. EMBO Mol Med. 2011; 3:667-81.

Van Heycop ten Ham MW, de Jager H. Progressive myoclonus epilepsy with Lafora bodies. Epilepsia. 1963; 4:95–119.

Van Hoof F, Hageman-Bal M. Progressive familial myoclonic epilepsy with Lafora bodies. Electron microscopic and histochemical study of a cerebral biopsy. Acta Neuropathol. 1967; 7:315-36.

Vanderhaeghen JJ. Correlation between ultrastructure and histochemistry of lafora bodies. Acta Neuropathol. 1971; 17:24-36.

Vernia S, Rubio T, Heredia M, Rodríguez de Córdoba S, Sanz P. Increased endoplasmic reticulum stress and decreased proteasomal function in lafora disease models lacking the phosphatase laforin. PLoS One. 2009; 4:e5907.

Veurink G, Liu D, Taddei K, Perry G, Smith MA, Robertson TA, Hone E, Groth DM, Atwood CS, Martins RN. Reduction of inclusion body pathology in ApoE-deficient mice fed a combination of antioxidants. Free Radic Biol Med. 2003; 34:1070-7.

Vilchez D, Ros S, Cifuentes D, Pujadas L, Vallès J, García-Fojeda B, Criado-García O, Fernández-Sánchez E, Medraño-Fernández I, Domínguez J, García-Rocha M, Soriano E, Rodríguez de Córdoba S, Guinovart JJ. Mechanism suppressing glycogen synthesis in neurons and its demise in progressive myoclonus epilepsy. Nat Neurosci. 2007; 10:1407-13.

Virchow R. Ueber eine Gehirn und Ruckenmark des Menschen aufgefundene Substanz mit der chemischen Reaction der Cellulose. Arch Path Anat u Physiol u Klin Med. 1854; 6:135–8.

Vollmers HP, Brändlein S. Natural antibodies and cancer. J Autoimmun. 2007; 29:295-302.

W

Wang H, Coligan JE, Morse HC. Emerging functions of natural IgM and its Fc receptor FCMR in immune homeostasis. Front Immunol. 2016; 7:99.

Wardemann H, Yurasov S, Schaefer A, Young JW, Meffre E, Nussenzweig MC. Predominant autoantibody production by early human B cell precursors. Science. 2003; 301:1374-7.

Weismann D, Binder CJ. The innate immune response to products of phospholipid peroxidation. Biochim Biophys Acta. 2012; 1818:2465-75.

Wilhelmus MM, Verhaar R, Bol JG, van Dam AM, Hoozemans JJ, Rozemuller AJ, Drukarch B. Novel role of transglutaminase 1 in corpora amylacea formation? Neurobiol Aging. 2011; 32:845-56.

Wirak DO, Bayney R, Ramabhadran TV, Fracasso RP, Hart JT, Hauer PE, Hsiau P, Pekar SK, Scangos GA, Trapp BD, Unterbeck AJ. Deposits of amyloid beta protein in the central nervous system of transgenic mice .Science. 1991; 253:323-5.

Woodford B, Tso MO. An ultrastructural study of the corpora amylacea of the optic nerve head and retina. Am J Ophthalmol. 1980; 90:492-502.

Wootla B, Watzlawik JO, Warrington AE, Wittenberg NJ, Denic A, Xu X, Jordan LR, Papke LM, Zoecklein LJ, Pierce ML, Oh SH, Kantarci OH, Rodriguez M. Naturally occurring monoclonal antibodies and their therapeutic potential for neurologic diseases. JAMA Neurol. 2015; 72:1346-53.

Worby CA, Gentry MS, Dixon JE. Malin decreases glycogen accumulation by promoting the degradation of protein targeting to glycogen (PTG). J Biol Chem. 2008; 283:4069-76.

Y

Ye X, Meeker HC, Kozlowski P, Carp RI. The occurrence of vacuolation, and periodic acid-Schiff (PAS)-positive granules and plaques in the brains of C57BL/6J, AKR, senescence-prone (SAMP8) and senescence-resistant (SAMR1) mice infected with various scrapie strains. Brain Res. 2004; 995:158-66.

Yokoi S, Nakayama H, Negishi T. Biochemical studies on tissues from a patient with Lafora disease. Clin Chim Acta. 1975; 62:415-23.

VII. ANNEX

Ageing Research Reviews 27 (2016) 42–55

Contents lists available at ScienceDirect

Ageing Research Reviews

journal homepage: www.elsevier.com/locate/arr

Review

Periodic acid-Schiff granules in the brain of aged mice: From amyloid aggregates to degenerative structures containing neo-epitopes

Gemma Manich[a], Itsaso Cabezón[a], Elisabet Augé[a], Carme Pelegrí[a,b,*,1], Jordi Vilaplana[a,b,1]

[a] Departament de Fisiologia, Facultat de Farmàcia, Universitat de Barcelona, Av. Joan XXIII s/n, 08028 Barcelona, Spain
[b] CIBERNED Centros de Biomedicina en Red de Enfermedades Neurodegenerativas, Spain

ARTICLE INFO

Article history:
Received 24 July 2015
Received in revised form 22 January 2016
Accepted 2 March 2016
Available online 9 March 2016

Keywords:
Ageing
Hippocampus
Periodic acid-Schiff
Neo-epitope
Natural antibody
Amyloid

ABSTRACT

Brain ageing in mice leads to the progressive appearance and expansion of degenerative granular structures frequently referred as "PAS granules" because of their positive staining with periodic acid-Schiff (PAS). PAS granules are present mainly in the hippocampus, although they have also been described in other brain areas such as piriform and entorhinal cortices, and have been observed in other mammals than mice, like rats and monkeys. PAS granules have been identified as a wide range of brain deposits related to numerous neurodegenerative diseases, such as amyloid deposits, neurofibrillary tangles, Lafora bodies, corpora amylacea and polyglucosan bodies, and these identifications have generated controversy and particular theories about them. We have recently reported the presence of a neo-epitope in mice hippocampal PAS granules and the existence of natural IgM auto-antibodies directed against the neo-epitope in the plasma of the animals. The significance of the neo-epitope and the autoantibodies is discussed in this review. Moreover, we observed that the IgM anti-neo-epitope is frequently present as a contaminant in numerous commercial antibodies and is responsible of a considerable amount of false positive immunostainings, which may produce misinterpretations in the identification of the granules. Now that this point has been clarified, this article reviews and reconsiders the nature and physiopathological significance of these degenerative granules. Moreover, we suggest that neo-epitopes may turn into a useful brain-ageing biomarker and that autoimmunity could become a new focus in the study of age-related degenerative processes.

© 2016 Elsevier B.V. All rights reserved.

Contents

* Corresponding author at: Departament de Fisiologia, Facultat de Farmàcia, Av. Joan XXIII s/n, 08028 Barcelona, Spain. Fax: +34 93 4035901.
E-mail address: carmepelegri@ub.edu (C. Pelegrí).
[1] These authors contributed equally to this study.

http://dx.doi.org/10.1016/j.arr.2016.03.001
1568-1637/© 2016 Elsevier B.V. All rights reserved.

1. Introduction

Ageing has been broadly defined as a time-dependent functional decline affecting most living organisms and is mainly characterised by a progressive loss of physiological integrity that leads to impaired function and increased vulnerability to death (López-Otín et al., 2013). In the human brain, ageing involves alterations to learning and memory, as well as motor performance (Yeoman et al., 2012). Moreover, ageing is the main risk factor for several neurodegenerative diseases. Because the molecular mechanisms of human brain ageing are not fully understood, animal models of ageing and age-related diseases are useful for acquiring greater insight into these pathways.

Brain ageing in mice leads to morphological and functional changes that can be considered a result of abnormal or pathological processes. One of these is the appearance of pathological granular structures in the hippocampus and their progressive expansion with age. These round-to-ovoid structures are organised into clusters and one of their main features is that they stain positively with periodic acid-Schiff (PAS). For this reason, they have been frequently named as PAS granules, as it will be done in this review. They are found in a wide range of mouse strains, but a noticeable amount of PAS granules has been observed in the senescence-accelerated mouse prone 8 (SAMP8) strain, which exhibits an accelerated ageing process (Akiyama et al., 1986; Del Valle et al., 2010; Kuo et al., 1996). Although PAS granules have mainly been studied in mice, they have also been described in the brains of aged individuals of other animal species, such as other rodents and non-human primates (Knuesel et al., 2009; Kuo et al., 1996).

PAS granules were first described by Lamar et al. (1976) in old C57BL/6 mice and they were later reported in SAMP8 mice (Akiyama et al., 1986). These structures, alternatively named Wirak bodies, became relevant when they were accidentally identified as beta-amyloid (Aβ) aggregates developed in $A\beta PP_{(1-42)}$ transgenic mice (Wirak et al., 1991). The results reported in that article were shown to be actually caused by false-positive immunohistochemical stainings, due to a non-specific binding of the anti-Aβ antibodies to the PAS granules (Jucker et al., 1992). Since then, there has been a large disparity when describing PAS granules composition, cell origin and physiopathological role. However, there is a consensus on relating these structures with the ageing phenomenon (Akiyama et al., 1986; Doehner et al., 2012; Jucker et al., 1994b; Kuo et al., 1996).

The recent identification of the reason behind the false-positive staining results (Manich et al., 2014b) has helped clarify current evidence relating to PAS granules and paved the way for a new approach to studying neurodegenerative diseases. This review aims to address these questions.

2. Main features of PAS granules

2.1. Morphology and brain location of PAS granules

PAS granules are round-to-ovoid structures found in the brain parenchyma of several animal species. In mice, these structures are mainly located in the hippocampus, where they first appear in the *stratum radiatum* of the CA1 region, from where they gradually extend to other hippocampal layers and regions. Granules measure up to 3 μm in diameter and tend to form clusters measuring about 80 μm in diameter, each containing approximately 40–50 granules (Akiyama et al., 1986; Jucker et al., 1994b; Kuo et al., 1996; Ye et al., 2004) and occasionally reaching 100 granules per cluster (Jucker et al., 1992; Robertson et al., 2000). Fig. 1 shows a representative granule cluster in mouse hippocampus.

Clustered PAS granules have mainly been studied in the mouse hippocampus, although they have also been found in other brain regions. Studies on the topographical distribution of clustered granules in aged mouse brains indicated the presence of these structures in the hippocampus, piriform and entorhinal cortices, olfactory bulb, cerebellum and trapezoid body (Akiyama et al., 1986; Jucker et al., 1994b; Knuesel et al., 2009; Kern et al., 2011; Mitsuno et al., 1999; Robertson et al., 1998), as it has been illustrated in Fig. 2. Clustered granules are present in a high amount in the *stratum radiatum* and *lacunosum moleculare* layers of the hippocampus, and are distributed throughout the CA1, CA2, CA3 and dentate gyrus regions (Nakamura et al., 1995). In the cerebellum, the PAS granule clusters are mainly located in the granular and Purkinje cell layers (Jucker et al., 1994b; Mitsuno et al., 1999). Slight morphological differences have been encountered in the clusters of the cerebellum, since these have a smaller number of granules per cluster and a more diffused pattern compared to those of the hippocampus. However, both the morphology and the reactivity pattern indicate that the PAS granules of the cerebellum and the hippocampus are the result of the same process. Moreover, clustered granules have occasionally been reported in the diencephalon, striatum and amygdala of the oldest mice (Jucker et al., 1994b; Knuesel et al., 2009). Overall, it could be highlighted that PAS granules develop mainly in the allocortices but not in the neocortices (Akiyama et al., 1986; Soontornniyomkij et al., 2012).

In general, the distribution and progression of granule clusters in the brain regions follow a similar pattern in all mice that develop these structures. The main differences relating to the onset, evolution and speed of expansion of granule clusters in mice are linked to age and strain. These determining factors will be explained in more detail in the following sections.

2.2. Animal species and mouse strain specificities in granule cluster presence

PAS granule clusters were first discovered in mice and have been mainly studied in them. However, this phenomenon is not restricted to this specie as these structures have also been observed in other rodents. For example, PAS granules have been found in the hippocampus of old individuals of the genre *Peromyscus* (Jucker et al., 1994b; Kuo et al., 1996) and in Wistar rats (Knuesel et al., 2009). Likewise, hippocampal granule clusters have also been detected in young and old monkeys of the specie *Callithrix jacchus* (Knuesel et al., 2009). In all these cases the morphology of the granule clusters and their distribution was similar to that described in mice, and an increase of granule clusters was observed with age-

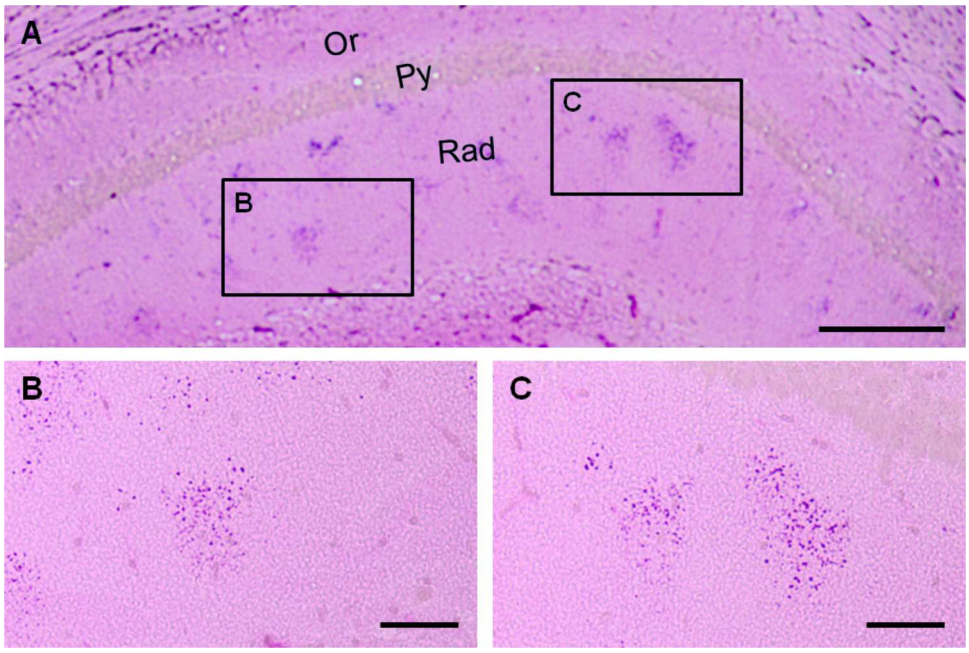

Fig. 1. Clusters of granules in the CA1 region of the hippocampus of a 12-month-old SAMP8 mouse stained with PAS. As it can be observed in (B) and (C) magnifications, clusters constituted by 40–50 granules are intensively stained. Or: Oriens layer, Py: pyramidal layer, Rad: *stratum radiatum*. Scale bars: (A) 200 μm, (B) and (C) 50 μm.

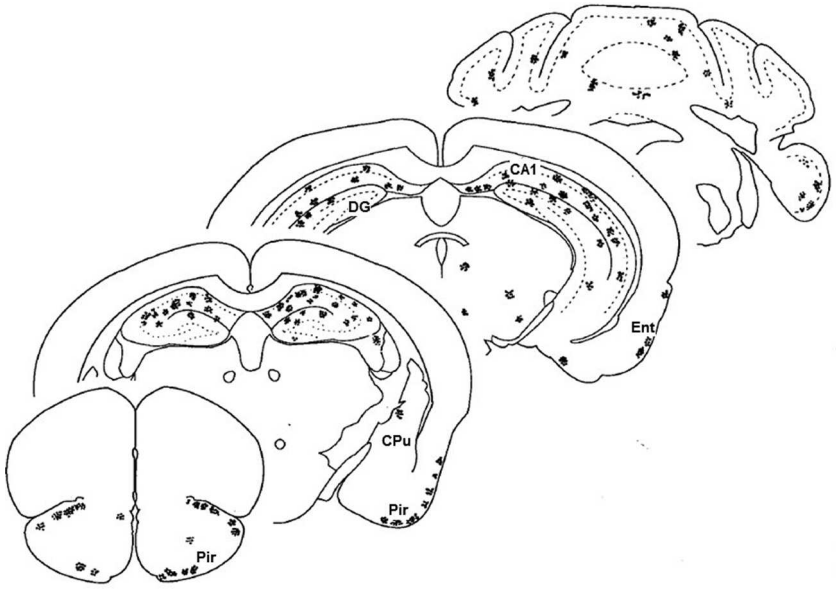

Fig. 2. Schematic distribution of clusters in 18-month-old C57BL/6 mice. Clusters in the caudate-putamen, fimbria-fornix and telencephalon have been observed only occasionally in a few aged animals. Pir, piriform cortex; CPu, caudate-putamen; DO, dentate gyrus; Ent, entorhinal cortex; CA1, CA1 field of the hippocampus.
Source: from Jucker et al. (1994b).

ing. The evidence available suggests that PAS granule clusters are present in other species, but deeper studies would be needed to ascertain these results. Moreover, it should be taken into account a possible variability in different strains of the same specie, as it can be inferred from the studies performed in mice that are summarized below.

Numerous studies have reported the presence of clustered granules in many mouse strains (Table 1). These structures have been extensively studied in the brains of aged C57BL/6 mice (Jucker et al., 1992; Lamar et al., 1976), SAMP8 and senescence-accelerated mouse resistant-1 (SAMR1) mice (Del Valle et al., 2010; Porquet et al., 2013), and AKR mice (Mitsuno et al., 1999). In BALB/c, DBA/2, C3H and CBA strains, PAS granules are only occasionally found in small amounts in some old animals (Jucker et al., 1994a, 1994b; Krass et al., 2003 and unpublished observations by the authors). These structures also appear in transgenic mice with a genetic background of a strain that develops clustered granules. Some of these transgenic mice present variations in the speed of appearance and the quantity of hippocampal clustered granules compared to the parental strain (Robertson et al., 1998, 2000). The strain differences made it possible to study the inheritance of this trait and thus prove the importance of the genetic background of the strain in the onset of clustered granules (see Section 4.2).

Table 1
Appearance and increase of hippocampal granule clusters with age in mouse strains.

Mouse strain (genetic background)	Age (months)	Sex (F/M)	Granule clusters	References
129Sv (ec)	10	F	+	Jucker et al. (1994b)
A/J	7–9	M	◊	Jucker et al., (1994b)
AKR	7–18	M/F	+ . . . +++[a]	Mitsuno et al. (1999)
	10	M/F	+/++	
	15	M	+	
	16	M/F	++/+++	
Athymic nude mice	2	F	◊	Mandybur et al. (1989)
	18–29	F	+++	
BALB/c				
BALB/c cOlaHsd	3	M	◊	Unpublished observations[b]
	12	M	+	Unpublished observations[b]
BALB/cByJ	2	M/F	◊	Jucker et al. (1992, 1994b)
BALB/cJ	7–9	M/F	◊	
BALB/cAnNCrlBR	7–9	M/F	◊	
BALB/cByJ	21	M/F	◊	
C3H/He	7–9	M/F	+	Jucker et al. (1992)
C3H/HeJ	7–9	M/F	◊	Jucker et al. (1994b)
C3H/HeNCrlBR	7–9	M/F	◊	
C57BL/6	1, 2, 4 w	M/F	◊	Robertson et al. (1998)
	2, 3, 4	M/F	◊	Lamar et al. (1976), Robertson et al. (1998), Madhusudan et al. (2009) and Doehner et al. (2010)
	4–30	M	+ . . . +++[a]	Kuo et al. (1996)
C57BL/6Jico	4–5	M	+	Knuesel et al. (2009)
	6	M/F	+	Robertson et al. (1998, 2000) and Soontornniyomkij et al. (2012)
C57BL/6J	7–9	M/F	+++/++	Jucker et al. (1992, 1994b) and Madhusudan et al. (2009)
C57BL/6NCrlBR	7–9	M/F	++/+	Jucker et al. (1992, 1994b)
	8	M/F	++	Lamar et al. (1976) and Robertson et al. (1998, 2000)
C57BL/6Zur	10–12	M/F	++	Jucker et al. (1994b) and Robertson et al. (1998)
C57BL/6J	12	M/F	+++	Madhusudan et al. (2009)
C57BL/6Jico	11–14	M	+++	Knuesel et al. (2009)
	16	M/F	+++	Lamar et al. (1976) and Krass et al. (2003)
	14, 15, 18	M/F	+++	Robertson et al. (1998) and Doehner et al. (2010)
	26	M	+++	Soontornniyomkij et al. (2012)
C57BL/6Jico	20–23	M	+++	Knuesel et al. (2009)
	24–31		+++	Jucker et al. (1992, 1994b)
CBA				Jucker et al. (1994b)
CBA/J	7	M	◊	
CBANCrlNia2	17	M	◊	
Crl:CFW(SW)BR	17	M	◊	Jucker et al. (1994a)
DBA				
DBA/2J	10–12	M	◊	Jucker et al. (1994b)
DBA/2J	16	F	+	Krass et al. (2003)
DBA/NCrlNia2	17	M	◊	Jucker et al. (1994b)
DDD	<10	M/F	◊	Akiyama et al. (1986)
	>10	M/F	+	
	>20		++	
ICR-CD1	3	M	◊	Del Valle et al. (2010, 2011)
	6	M	◊	Del Valle et al. (2010, 2011) and Manich et al. (2011)
	9, 12	M	+	Del Valle et al. (2011)
	9, 12, 15	M	+ . . . ++[a]	Del Valle et al. (2010)
SAMP8	2	M	◊	Nakamura et al.,(1995)
	2–16	M/F	◊ . . . +++[a]	Akiyama et al. (1986) and Kuo et al. (1996)
	3, 6	M	+/++	Del Valle et al. (2010, 2011) and Manich et al. (2011)
SAMP8/Ta/Nia	9	M	+++	Jucker et al. (1994b)
	9	M	+++	Del Valle et al. (2010, 2011), Manich et al. (2011, 2014a, 2014b) and Porquet et al. (2013)
	9–11	M	+++	Nakamura et al. (1995) and Manich et al. (2014b)
	12	M	+++	Del Valle et al. (2010, 2011) and Manich et al. (2011)
	14, 15	M	+++	Del Valle et al. (2010) and Manich et al. (2014a, 2014b)
SAMR1	2	M	◊	Nakamura et al. (1995)
	3, 6	M	◊	Akiyama et al. (1986) and Del Valle et al. (2010)
SAMR1/Ta/Nia	9	M	◊	Jucker et al. (1994b)
	9	M	◊	Del Valle et al. (2010) and Porquet et al. (2013)
	11–12	M	+	Akiyama et al. (1986) and Nakamura et al. (1995)
	12, 15	M	+/++	Del Valle et al. (2010)
	20	M/F	++	Akiyama et al. (1986)
Transgenic mice strains				
3xTgAD (129Sv × C57BL/6				
++/+	6, 12	M	−/++	Oddo et al. (2003)
−/− and ++/+	15	M	+/++	Knuesel et al. (2009)
AβPP konckout (129 Sv × C57BL/6)				Doehner et al. (2010)
−/−	15		+	

Table 1 (*Continued*)

Mouse strain (genetic background)	Age (months)	Sex (F/M)	Granule clusters	References
$A\beta PP_{swe}$-PSENdE1 (C57BL/6)				Manich et al. (2014b)
+/− and −/−	9–17	M	+ . . . ++[a]	
$A\beta PP_{swe}$/arc (C57BL/6)				Doehner et al. (2010)
+/+	15		++	
AE101, AE301 (C57BL/6 × DBA/2)				Wirak et al. (1991)
−/−	12		◊	
+/+	12		++	
AD11 (C57BL/6 × SJLF2)				Corsetti et al. (2008)
−/−	15		+	
+/+			+++	
ApoE-knockout (C57BL/6)				
−/−	1, 2 w	M/F	◊	Robertson et al. (1998)
	4 w/2	M/F	+	
	4, 6, 8, 12	M/F	++ . . . +++[a]	Robertson et al. (1998, 2000)
	10, 14, 18	M/F	++ . . . +++[a]	Robertson et al. (1998)
	15	F	+++	Veurink et al. (2003)
Human ApoE-2, human ApoE-3 or human ApoE-4 (ApoE-knockout C57BL/6)				Robertson et al. (2000)
−/+ (hemizygous)	4, 6, 8, 12	M/F	+ . . . ++[a]	
Reeler or reelin heterozygous knockout (C57BL/6 x C3H)				Kocherhans et al. (2010)
+/−	3, 9		+/++	
+/+	3, 9		◊/+	
Reeler orleans (BALB/c)				
−/−	15	F	◊	Doehner et al. (2010)
SynGap (C57BL/6)				Knuesel et al. (2009)
+/− and +/+	6,	F	+	
+/− and +/+	12,	M/F	++/+++[c]	
+/− and +/+	24	F	++	
Ts65Dn (C57BL/6)				
Disomic	12	M	+	Kern et al. (2011) and Rachubinski et al. (2012)
Trisomic	12	M	+++	

In the first column, the strain or the genetic background of the transgenic mouse strain is identified, also when animals were generated by cross-breeding. In the latter, genotypes used in the study are also specified (−/− wild-type; +/− heterozygous or hemizygous; +/+ or ++/+ homozygous). Sex is indicated as male (M) or female (F). Ages are indicated in months, or in weeks (w) when indicated. Hippocampal granule cluster number has been approximately summarized following this score: ◊ no clusters or a sparse cluster; + few clusters; ++ generalised presence of clusters; +++ profuse number of clusters.

[a] Increase in the number of granule clusters between indicated ages.

[b] Unpublished observations made by the authors.

[c] Observed differences due to the genotype.

2.3. Age and sex influences in the onset of granule cluster

Age is undoubtedly a key factor in the onset and growth of granule clusters. Although the increase of these clusters in the hippocampus, entorhinal cortex and piriform cortex correlates with age (Madhusudan et al., 2009), the age at which granule clusters appear and grow varies substantially between mice strains. In SAMP8 mice, the PAS granules appear as early as three months of age, which is earlier than in other strains, and the number of clusters and granules increases and spreads faster than in other strains (Del Valle et al., 2010; Jucker et al., 1994a, 1994b; Kuo et al., 1996). In a study that compared the number of hippocampal granule clusters between ICR-CD1, SAMR1 and SAMP8 mice from 3 to 15 months of age, the latter showed a greater increase in granule clusters at all ages analysed. At 3 months of age, the number of clusters in SAMP8 mice was higher, although not significantly, than the other strains. However, the differences were statistically significant at 6, 9, 12 and 15 months of age. Nevertheless, the number of granule clusters increased slightly with age in both ICR-CD1 and SAMR1 strains, especially between 12 and 15 months of age. As shown in Fig. 3 the granule clusters occupied almost the entire hippocampus in a 12-month-old SAMP8 mouse (Del Valle et al., 2010). Differences in the increase in granule clusters with age have been also observed in transgenic mice, with respect to controls, including reeler mice (Kocherhans et al., 2010), 3xTg-AD (Knuesel et al., 2009; Oddo et al., 2003), Ts65Dn (Kern et al., 2011; Rachubinski et al., 2012) and malin knockout mice (Valles-Ortega et al., 2011). However, transgenic ApoE-deficient mice have been reported to develop the earliest PAS granule structures, as early as four to six weeks of age (Robertson et al., 1998, 2000).

Generally, a higher variability is observed in the number of hippocampal granule clusters with advancing age. In the oldest mice, the accumulative trend of granule clusters stalls and may even see a slight decrease (Jucker et al., 1994b). Moreover, there is greater granule cluster dispersion in these older animals, perhaps as a result of the increase in granule diameter or the blending of small granules into larger ones (Jucker et al., 1994b; Robertson et al., 2000), as previously observed at ultrastructural level (Doehner et al., 2012).

While age clearly influences the onset of granule clusters, different results have been reported between male and female mice. Female C57BL/6 mice usually present more granule clusters than males (Jucker et al., 1992, 1994b; Knuesel et al., 2009; Lamar et al., 1976). Therefore, age-related changes in steroidal hormones and the neuroendocrine axis have been hypothesised to influence hippocampal granule cluster formation. However, early studies in SAMP8 mice contradict these differences between sexes (Akiyama et al., 1986), so it is unclear whether there are real variations between male and female mice.

2.4. PAS granules ultrastructure

Analysing the granule ultrastructure makes it possible to differentiate a central core of electron-dense crystalline-like fibrillary deposits, generally surrounded by a halo or electron-lucent region (Fig. 4). This halo is externally delimited by a slightly discontinuous plasma membrane, which suggests an intracellular location. The central core is round to ovoid in shape and contains membrane-like

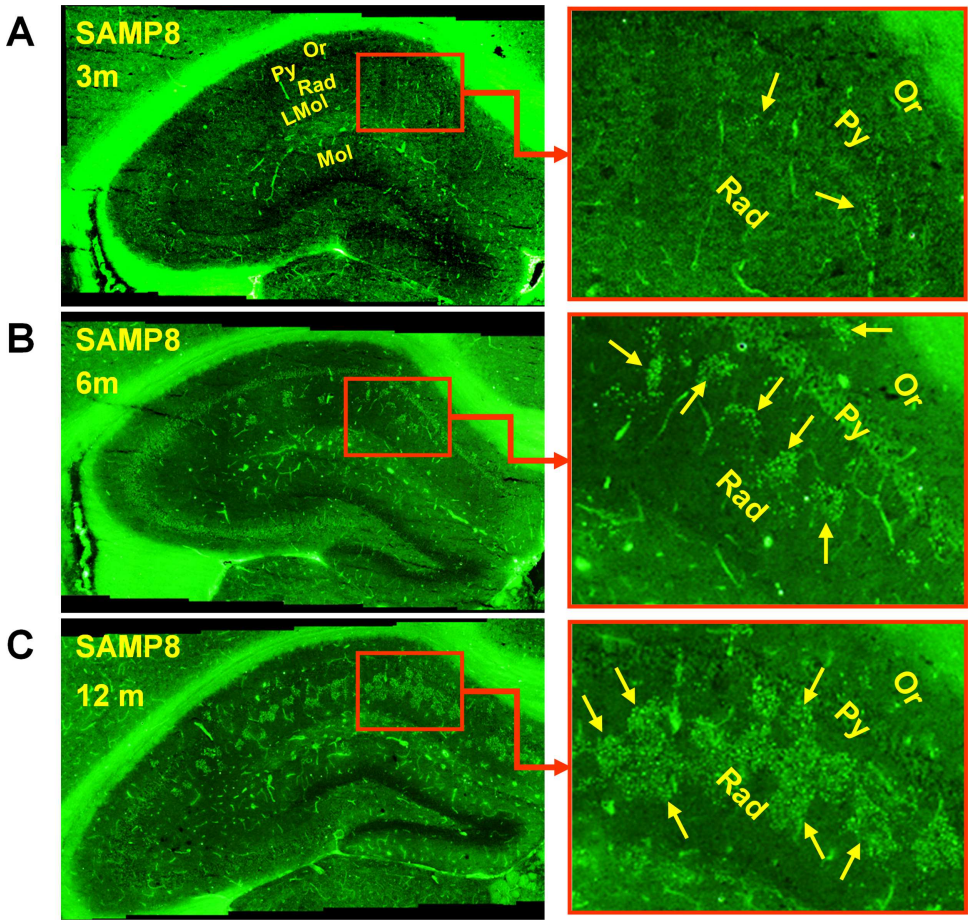

Fig. 3. Coronal hippocampal sections presenting PAS granule clusters of SAMP8 mice aged 3, 6 and 12 months (A, B and C, respectively). Granules were immunostained with 4G8 antibody directed against Aβ peptides but containing anti-neo-epitope IgM antibodies. Granule clusters start to appear in the CA1 hippocampal region and they spread throughout the hippocampus with increasing age. Or: *oriens* layer, Py: pyramidal layer, Rad: *stratum radiatum*, LMol: *lacunosum moleculare* layer, Mol: molecular layer of the dentate gyrus.

Source: adapted from Del Valle et al. (2010).

structures that are 5–8 nm thick, are haphazardly aggregated and do not resemble any cell organelles (Kuo et al., 1996; Manich et al., 2014a; Robertson et al., 2000). In fact, cytoplasmic organelles such as the endoplasmic reticulum, polyribosomes, intermediate filaments, multivesicular bodies and mitochondria have occasionally been described in the halo region, usually in a state of degeneration (Doehner et al., 2010; Kuo et al., 1996; Manich et al., 2014a; Mitsuno et al., 1999; Robertson et al., 1998). These organelles are accompanied by many blebs or large cisterns, some of which originate from the invagination of the surrounding plasma membrane, and which are located in the translucent area and show close contact with the core of the granule (Manich et al., 2014a). The membrane surrounding the granule has special contacts that are characteristic of astrocyte-astrocyte junctions (Kuo et al., 1996; Manich et al., 2014a). In general, the structures in the area immediately surrounding the mature granules do not present perceivable morphological alterations. However, some symptoms of deterioration such as degenerating dendrites have occasionally been detected (Manich et al., 2014a). Although the granule ultrastructure has been mainly studied in the hippocampus, similar ultrastructural features have been described in the cerebellum, like the intracellular halo and surrounding membrane or the hydropic changes in the cytoplasm of the affected cells (Mitsuno et al., 1999).

2.5. PAS granules composition

The first steps to identifying the PAS granule composition were performed using a wide range of histochemical staining procedures in order to find out the general nature of the granule compounds (Table 2).

As the name of these granules suggests, the granule clusters characteristically stain intensely positive with PAS (Lamar et al., 1976). This staining method is used to detect glycogen and macromolecules that contain glycans, proteoglycans and glycolipids (Spicer and Schulte, 1992), although proteins containing serine and threonine may show slightly PAS-positive staining (Spicer, 1961). Furthermore, other general staining procedures related to glycoconjugates have been reported to positively stain the granules, e.g., iodine (Mitsuno et al., 1999), or modifications of the PAS staining, e.g., Gomori's methenamine silver stain (Akiyama et al., 1986; Jucker et al., 1994a, 1994b). Previous brain slice digestion with α-amylase or diastase only slightly reduced PAS granule staining, which rules out the possibility of high amounts of glycogen in these structures (Akiyama et al., 1986; Lamar et al., 1976; Mitsuno et al., 1999). In any case, although glycogen is not the main component, these staining results suggest that the PAS granules contain high levels of polysaccharides.

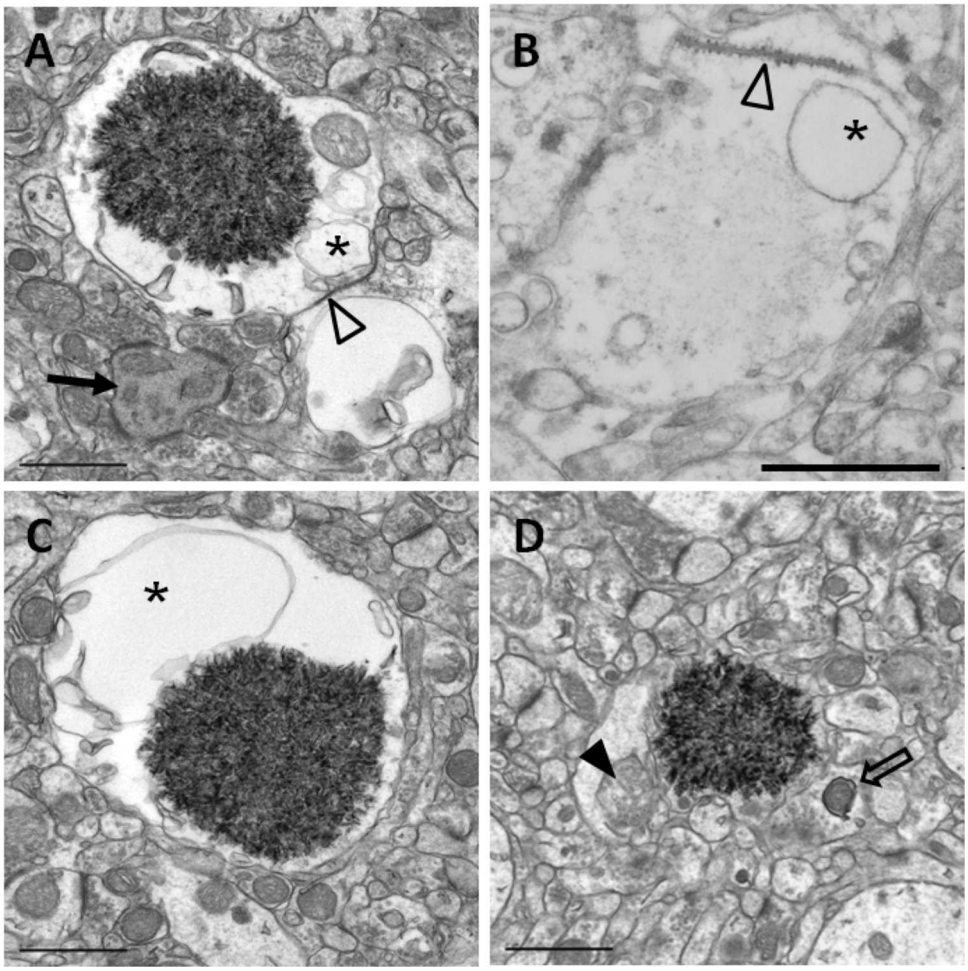

Fig. 4. Electron microscopy images of hippocampal mature granules from a 14-month-old SAMP8 mouse. Mature granules measured up to 3 μm. When tissue was embedded in Spurr and treated with OsO_4, granules showed an electron-dense core formed by a dense mesh of fibrillar membranous-like structures, generally encircled by a translucent halo (A, C and D). When tissue was embedded in Lowicryl, the core appeared smoothly stained (B). Blebs or big cisterns (*), as well as degenerating mitochondria (full arrowhead) were located in the translucent area. A characteristic junction with a membrane of an adjacent cell could be observed (empty arrowhead). In the surroundings of the mature granule, a degenerating dendrite (full arrow) and a mitophagy process (empty arrow) could be visualized. Scale bar: 1 μm.
Source: adapted from Manich et al. (2014a).

However, some controversy has arisen from the results of other general staining methods. This was the case for thioflavin S stain, which has produced positive staining results in some cases (Doehner et al., 2010; Jucker et al., 1992; Kocherhans et al., 2010) and negative results in others (Jucker et al., 1994a; Mandybur et al., 1989; Manich et al., 2014b; Takemura et al., 1993), and the Congo red stain, another amyloid marker, which has also produced contradictory results (Jucker et al., 1994a; Robertson et al., 1998). Indeed, the ultrastructural observation of the PAS granules does not reveal the presence of amyloid in these structures, or at least not as a major constituent (Jucker et al., 1992; Manich et al., 2014a).

Tests performed using enzyme histochemistry reported monoamine oxidase (MAO)-B positive enzymatic activity in the hippocampal PAS granules of aged SAMP8 mice (Nakamura et al., 1995). MAO-B is typically located in the external mitochondrial membrane of glial cells and in serotonergic and histaminergic neurons (Shih et al., 1999), and this enzyme has been also reported to be involved in Parkinson's disease and ageing (Jenner, 2012).

The granule composition has also been extensively addressed in immunohistochemistry studies, which are detailed below.

2.6. Presence of a neo-epitope in PAS granules

In a recent work, we described the presence of a neo-epitope of carbohydrate nature in the PAS granules that is not present in other brain areas (Manich et al., 2014b). Ultrastructural studies indicated that the neo-epitopes are located in the core of the granules, specifically in the membranous fragments. However, some of them could also be observed in the plasma membrane of the astrocytic process and in the membranes of the structures nearest to the neuropil. The neo-epitope is similarly observed in these same areas in immature granules and in the core spread matrix (Manich et al., 2014a). These observations led to the conclusion that the neo-epitope is actually generated during the granule formation process. The neo-epitopes found in the PAS granules are a target of natural IgM auto-antibodies present in the serum of all mice strains tested and in other animal species (Manich et al., 2015; see Section 4.3). It is important to note that the profuse presence of these IgMs directed against the neo-epitope as a contaminant in commercial and non-commercial antibodies is responsible for numerous false-positive staining results when immunohistochemical procedures are used, as detailed below (Manich et al., 2014b).

Table 2
Histochemical stainings performed in hippocampal brain sections to identify the granule composition.

Histochemical staining	Result	References
α-Amylase	d	Akiyama et al. (1986)
β-Amylase	–	Akiyama et al. (1986)
Alcian's blue	–	Akiyama et al. (1986)
Bielchowsky silver	–	Lamar et al. (1976)
Bodian silver impregnation/Bodian protargol	w	Akiyama et al. (1986) and Mandybur et al. (1989)
Blumer-PAS-dimedione	+	Akiyama et al. (1986)
Chrome-alum haematoxylin	–	Robertson et al. (1998)
Congo red	–	Akiyama et al. (1986), Jucker et al. (1992, 1994a), Mandybur et al. (1989), Mitsuno et al. (1999) and Takemura et al. (1993)
Congo red (Askanas modification)	+	Robertson et al. (1998, 2000)
Cresyl violet/Nissl staining	–	Jucker et al. (1992), Kern et al. (2011), Knuesel et al. (2009) and Mandybur et al. (1989)
Gomori Aldehyde Fuchsin	–	Robertson et al. (1998)
Gomori's methenamine silver (Grocott's modification)	+	Jucker et al. (1992, 1994a, 1994b)
Haematoxylin & Eosin	–	Akiyama et al. (1986), Jucker et al. (1992), Lamar et al. (1976), Mandybur et al. (1989), Mitsuno et al. (1999), Robertson et al. (1998, 2000), Takemura et al. (1993) and Ye et al. (2004)
Iodine	+	Mitsuno et al. (1999)
	w	Akiyama et al. (1986)
Klüver–Barrera	–	Akiyama et al. (1986) and Mandybur et al. (1989)
Luxol fast blue	–	Jucker et al. (1992)
Millon Schiff	–	Akiyama et al. (1986)
Neutral red	–	Takemura et al. (1993)
Ninhydrin–Schiff	–	Akiyama et al. (1986)
Oil red O	–	Akiyama et al. (1986)
Okamoto α-naphtol	–	Akiyama et al. (1986)
PAS (Periodic Acid Schiff)	+	Akiyama et al. (1986), Jucker et al. (1992), Kern et al. (2011), Kuo et al. (1996), Lamar et al. (1976), Mandybur et al. (1989), Mitsuno et al. (1999), Nakamura et al. (1995), Robertson et al. (1998, 2000), Takemura et al. (1993), Veurink et al. (2003) and Ye et al. (2004)
PAS with diastase digestion	d	Lamar et al. (1976) and Mitsuno et al. (1999)
Perl's Prussian blue	–	Robertson et al. (1998)
Schiff	–	Akiyama et al. (1986)
Silver staining	+	Doehner et al. (2012)
Sudan Black B	–	Akiyama et al. (1986)
Thioflavin	+	Doehner et al. (2010) and Jucker et al. (1992, 1994a, 1994b)
S	–	Manich et al. (2014b), Mandybur et al. (1989) and Takemura et al. (1993)
Thionin	–	Jucker et al. (1992)
Toluidine blue	–	Akiyama et al. (1986) and Robertson et al. (1998)

Results of the granule cluster staining have been indicated as: positive (+), negative (–), weak positive staining (w), and decrease of the staining after enzymatic treatment of tissue sections (d).

2.7. Immunohistochemical studies of PAS granules

Because a wide range of antibodies produced in mouse and rabbit ascites and serum contained these IgMs, even some antibodies that were supplied as purified antibodies, they stained the hippocampal PAS granules thus providing false-positive stainings. These findings cast doubt on most of the information available on PAS granule composition from immunohistochemical studies.

Several immunostaining processes detected glycoproteins and proteoglycans (Akiyama et al., 1986; Kuo et al., 1996; Takemura et al., 1993), as well as polyglucosan components, which led to consider the PAS granules as equivalent to Lafora bodies (Valles-Ortega et al., 2011). The presence of several extracellular matrix proteins has also been described, including heparin sulphate proteoglycan and laminin (Jucker et al., 1992, 1994b; Kuo et al., 1996), syndecan-2 (Manich et al., 2011) and reelin (Knuesel et al., 2009; Doehner et al., 2012). Furthermore, the antibody KM279 generated against corpora amylacea intensely stained the granules in aged AKR mice (Mitsuno et al., 1999). Also, some proteins involved in neurodegenerative diseases were targeted, i.e. Aβ peptides (Del Valle et al., 2010; Doehner et al., 2012; Knuesel et al., 2009; Oddo et al., 2003; Robertson et al., 1998; Wirak et al., 1991), ubiquitin (Robertson et al., 1998; Soontornniyomkij et al., 2012), α-synuclein (Krass et al., 2003) and tau protein (Kern et al., 2011; Manich et al., 2011; Rachubinski et al., 2012). The PAS granules positive immunostainings have not only been restricted to the hippocampus, as positive stainings for reelin, ubiquitin, synapsin II, p62 or MAP2 have been observed in the PAS granules of the olfactory bulb and the cerebellar cortex (Doehner et al., 2010; Soontornniyomkij et al., 2012) and anti-reelin antibodies stained clustered granules of the piriform and entorhinal cortices (Knuesel et al., 2009; Madhusudan et al., 2009). These results suggested some concordances of PAS granules with several brain lesions observed in neuropathological diseases.

However, taking into account the possible contaminant IgMs, the presence of all these components in PAS granules reported by means of immunohistochemistry requires confirmation. The correspondence of the PAS granules with Lafora bodies and corpora amylacea based on immunohistochemical procedures might be inconsistent with ultrastructural and histochemical studies. Conversely, the correspondence with senile plaques or neurofibrillary tangles, based on staining with antibodies directed against Aβ peptides and tau protein, has been rejected; the presence of Aβ peptides and tau protein has been revised and discarded (Jucker et al., 1992; Manich et al., 2014b), and the positive staining results explicitly attributed to the presence of IgMs directed against the neo-epitope (Manich et al., 2014b). Although the studies about the antibody specificity have been only performed in the hippocampal granules, their high correspondence with the PAS granules present in other brain areas allow to assume that false-positive stainings could affect the clustered granules of these areas.

2.8. PAS granules formation

The granule formation process is still unclear, since the information available is minimal and confusing. However, ultrastructural studies have shed light on the fine granule structure and helped identify immature granules, which has generated relevant information about the formation of granules.

Although the dense membrane-like mesh that constitutes the core of the granule can be considered to be an accumulation of molecular waste, successive ultrastructural changes from the exterior to the interior of the granules have led some authors to suggest that the pathological process initiates outside the granules and that degenerative structures migrate inward (Kuo et al., 1996). However, Doehner et al. (2012) proposed that granules originate as a protective strategy of aged neurons that extrude damaged or misfolded proteins, which are subsequently engulfed by glia. This hypothesis is based on the presence of AβPP-derived proteolytic fragments on the granules (Doehner et al., 2010), which has since been demonstrated to be false. Nevertheless, the study of the granule formation in the early phases led us to hypothesise that the granules are the result of a degenerative process involving principally astrocytic processes (Fig. 5). The generation of granules includes the appearance of abnormal membranous structures that form intracellular bubbles or blebs of variable sizes and irregular shapes and the instability of the plasmatic membrane. These structures and some organelles degenerate and produce some membranous fragments, and an assembly process of the resulting fragments generates the dense-core nucleus of the mature granule (Manich et al., 2014a). It is important to note that the plasma membrane of the immature granules, and some membranes of the adjacent structures, is often fragmented or unstable, and the boundaries between cells are therefore lost. This membrane disruption has also been observed in mature granules, but is particularly evident in granules being formed, and could lead to part of the neuropil adjacent to the granule being incorporated into it (Manich et al., 2014a).

2.9. Cell origin of PAS granules

The cell origin of the PAS granules has been a controversial topic and conflicting opinions have been expressed about their neuronal or astrocytic origin.

A remarkably tight relationship between the granules and astrocytes has frequently been reported. PAS granules have been observed within protoplasmic astrocytic cell bodies and astrocytic processes that had expanded and whose cytoplasmic organelles were greatly diluted (Robertson et al., 1998). Furthermore, approximately 60–80% of the PAS granules have been associated with glial fibrillary acidic protein (GFAP)-positive astrocyte processes (Akiyama et al., 1986; Jucker et al., 1994b; Madhusudan et al., 2009; Nakamura et al., 1995), and whole granule clusters have even been directly associated with GFAP-positive astrocytes (Jucker et al., 1994b; Manich et al., 2011, 2014a; Nakamura et al., 1995). Ultrastructural studies have identified mature granules in degenerated astrocytic processes containing glycogen accumulations, GFAP-immunostained fibrils and specific astrocyte-astrocyte junctions with adjacent membranes (Kuo et al., 1996; Manich et al., 2014a). Interestingly, immature granules have always been found to originate in astrocytes, and the formation of granules in the different processes of a specific astrocyte has been reported to cause the clustering pattern of the PAS granules, each cluster being the set of granules formed in one astrocyte, as illustrated in Fig. 6 (Manich et al., 2014a). Granules have also been regularly associated with blood capillaries and detected in the astrocyte end-feet surrounding them (Doehner et al., 2010; Manich et al., 2014a; Robertson et al., 1998; Ye et al., 2004). Remarkably, MAO-B histochemical staining reinforces the suggestion that astrocytes participate in the formation of PAS granules, since this enzyme is observed in both hippocampal astrocytes and granule clusters (Nakamura et al., 1995).

Neuronal origin has been suggested based on the fact that synaptic vesicles and terminals are in contact with the plasma membrane of the PAS granules (Mitsuno et al., 1999), and on the ultrastructural observation of granules presumably located in abnormal synaptic terminals (Irino et al., 1994) or granules interconnected through dendrites (Doehner et al., 2012; Wirak et al., 1991). However, as mentioned above, locating the PAS granules can be difficult due to the loss of boundaries between the astrocytes and the adjacent cells during their formation. In addition, neuronal origin has been postulated based on the neuronal components described in these structures, such as Aβ peptides (Del Valle et al., 2010; Knuesel et al., 2009; Robertson et al., 1998), neuronal nuclei protein and tau protein (Kern et al., 2011; Manich et al., 2011; Rachubinski et al., 2012) and reelin protein or ApoE2 receptor (Knuesel et al., 2009). Moreover, some authors have suggested that the PAS granules are dystrophic neurites due to the positive staining with anti-tau antibodies (Corsetti et al., 2008). Some of these components, such as Aβ and tau, have been demonstrated to be absent from PAS granules, while other staining results are uncertain and require verification.

In any case, a general review of the findings reported up to now supports the astrocytic origin of the PAS granules. The remaining cell types, including oligodendrocytes and microglia, do not appear to have a close spatial relationship with granules, although they may interact with these structures (Manich et al., 2014a). High densities of activated and phagocytic microglia have been observed next to the PAS granule clusters (Knuesel et al., 2009; Madhusudan et al., 2009). Actually, a recent report on mice fed with cuprizone showed a diminishment on the number of hippocampal granule clusters (Cana et al., 2015), which could be possibly explained by the increase of the microglial phagocytic activity induced by cuprizone (Gudi et al., 2014).

3. Brain pathology associated with PAS granules

3.1. Memory loss

Possibly age-related disturbances may be found in the immediate surrounding areas of PAS granules, as confirmed by the extent of the affected area and the ultrastructural observation of these structures. Because the hippocampus plays an essential role in memory, several tests to measure memory dysfunction have been used to relate it to the presence of PAS granules in this brain area. In aged C57BL/6 mice, a statistically significant relationship between granule clusters and memory loss was found in the Morris water maze test (Jucker et al., 1994b) and the radial arm maze task (Knuesel et al., 2009). Recent episodic memory was also evaluated in this strain by Soontornniyomkij et al. (2012) using the object recognition test. A signification correlation was observed with granule clusters stained with LC3 and p62, although this may have corresponded to IgM anti-neo-epitope false-positive staining.

3.2. Motor performance

Although granule clusters that are found in the hippocampus have been the main subject of researchers' interest, these structures have also been observed in other brain areas (Section 2.1). The cerebellum also exhibits a considerable presence of granule clusters, and age-related motor impairment could therefore be related to these structures. Nevertheless, a first attempt to study the relationship between motor performance and cerebellar granule clusters

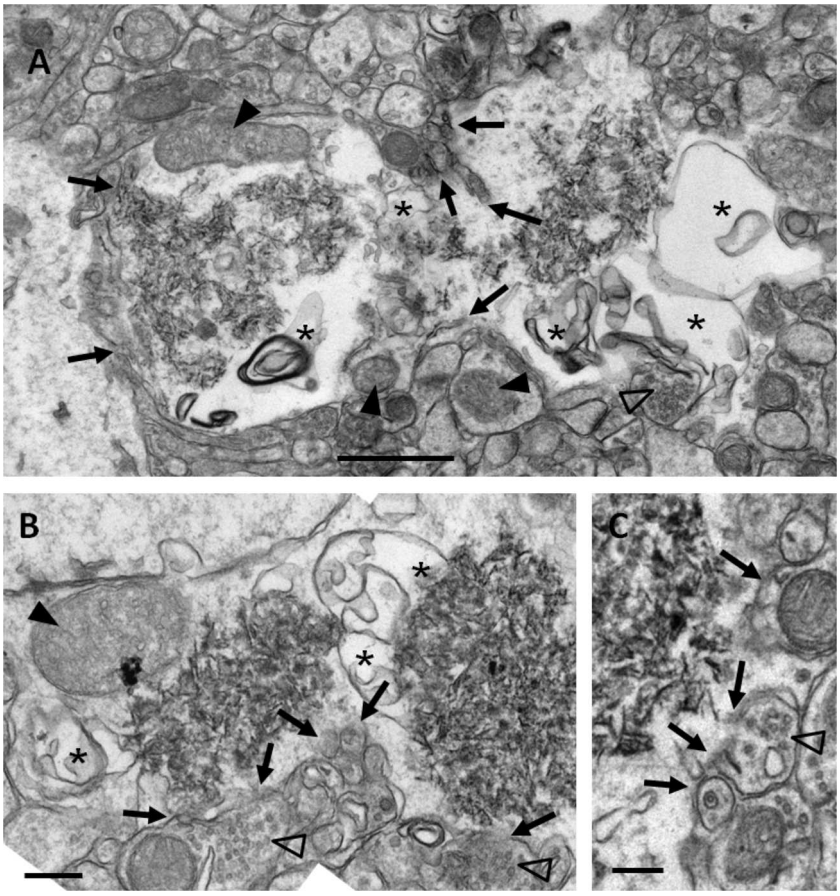

Fig. 5. Electron microscopy images of hippocampal immature granules from a 14-month-old SAMP8 mouse. (A) Immature granules showed some sparse membranous-like structures instead of the electron-dense core. (B) and (C) Granules in a more advanced stage of development. Big blebs or bubbles (*) and degenerating mitochondria (full arrowheads) appeared in the peripheral zone. The plasma membrane and membranes of adjacent structures showed instability and fragmentation (full arrows), causing a loose of the boundaries of these structures. This process of rupture can affect dendritic spines (empty arrowheads), as clearly shown in (C). (D) Inset from (A) in which the instability and the fragmentation of the membranes could be better observed. Scale bar: (A and B): 1 μm; (C)–(E) 200 nm.
Source: adapted from Manich et al. (2014a).

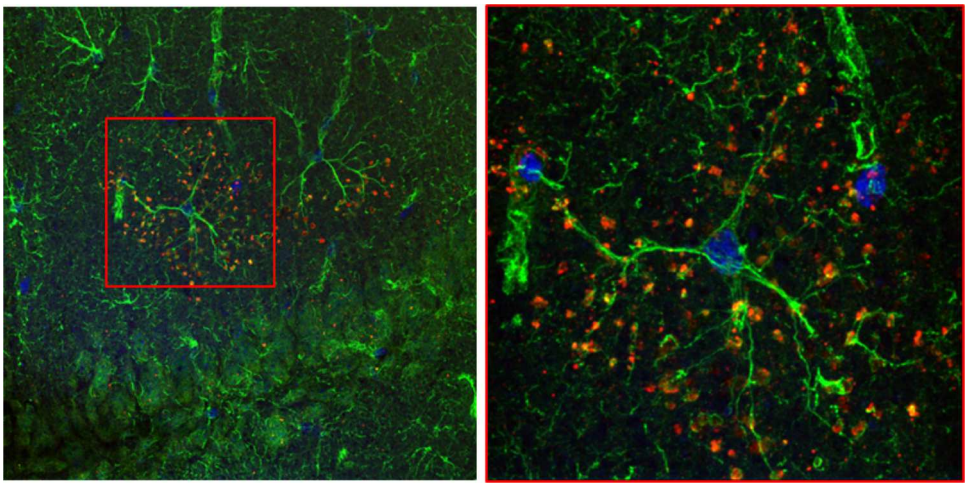

Fig. 6. Confocal microscopy image of a double immunohistochemical staining of the CA1 hippocampus area from a 9-month-old SAMP8 mouse. PAS granules were detected with a mouse IgM antibody against the neo-epitope (red), and reactive astrocytes were detected with an anti-GFAP antibody (green). Nuclei were stained by Hoechst (blue). In this image the close association of some granule clusters and astrocytes is shown. (For interpretation of the references to colour in this figure legend, the reader is referred to the web version of this article.)
Source: adapted from Manich et al. (2014a).

in SAMP8, SAMR1 and C57BL/6 did not reveal any significant correlation (Ingram et al., 1994).

4. Factors related to granule etiopathogeny

4.1. Oxidative stress

One of the principal theories of ageing relates oxidative stress to the decline of physiological functions (Harman, 2006). Because granule clusters are related to ageing, it seems feasible to search for a relationship between oxidative stress and the onset and development of these structures. Indeed, the effect of oxidative stress and anti-oxidant compounds on these hippocampal structures has been assessed in several studies that have mainly focused on feeding mice on high-fat diets for long periods of time.

In an initial study performed using ApoE-deficient mice, the administration of a high-fat diet supplemented with antioxidants for a three-month period showed a significant reduction in the number of granule clusters compared to mice fed either the same high-fat diet without antioxidants or a normal diet (Veurink et al., 2003). In another study on the incidence of hippocampal PAS granules in mice, a positive correlation was observed between plasma HDL levels and the number of granule clusters in mice fed an atherogenic diet (Krass et al., 2003). Moreover, a recent article reported a significantly low incidence of granule clusters in SAMP8 mice fed with resveratrol, a well-known antioxidant compound (Porquet et al., 2013). SAMP8 mice, one of the mouse strains with the highest numbers and earliest appearance of granule clusters, are considered a model of oxidative stress, since high levels of free radicals have been observed in their brains (Perluigi et al., 2014). Furthermore, the MAO-B enzyme, a mitochondrial enzyme that may be related to the formation of reactive oxygen species, has been detected in high amounts in the PAS granules, and its expression is higher in the hippocampal astrocytes of aged animals (Nakamura et al., 1995). Moreover, a recent study on animals fed with a diet supplemented with cuprizone, a copper chelator, produced a diminishment of hippocampal PAS granule clusters (Cana et al., 2015). According to the authors, this effect might be explained by the alteration of the redox-active homeostasis.

On the whole, these findings reinforce the important role played by oxidative stress in the appearance of these structures and point to a definite but as yet unclear relationship between oxidative stress, ageing and the degenerative process that takes place in the mouse hippocampus and leads to granule formation.

4.2. Genetic background

According to previous studies, hippocampal granule clusters show a strain-specific expression with ageing, as mentioned in Section 2.2. In order to take advantage of this feature, intercrosses between susceptible and resistant mouse strains have been used to identify the chromosomal regions involved in granule cluster development. Early studies on intercrosses between C57BL/6 and DBA/2, CH3 or BALB/c revealed a dominant heritability of this trait in the first generation progeny (Jucker et al., 1994a, 1994b). A subsequent study consisting of quantitative trait loci analysis using the first and second progenies of a C57BL/6 and DBA/J strain intercross provided evidence of possible major gene loci involved in the appearance of hippocampal granule clusters (Krass et al., 2003). Specifically, a major gene locus with a dominant effect was identified 26 cM from marker D7Mit91, and two other gene loci, D10Mit15 and D10Mit10, were found to influence this phenotypic trait. Krass et al. (2003) speculated about the possible genes located in these sequences based on the granule components detected by immunohistochemistry, and it was therefore difficult to identify an appropriate candidate. It has been reported that D7Mit91 is involved in fat maintenance under dietary restrictions and is related to the insulin growth factor-1 receptor, and that D10Mit15 is associated with life span and other aspects (www.informatics.jax.org). This data reveals a complex genetic basis related to the onset and development of the PAS granules. Thus, different mutations or gene alleles affecting the metabolism or oxidative stress levels could determine and influence the different degrees of granule formation. For example, as indicated above, ApoE-deficient mice have higher numbers of granules than control animals (Robertson et al., 1998) and malin knockout mice (Valles-Ortega et al., 2011). Therefore, the presence of PAS granules is probably related to a variety of genes and not one specific gene, and the genetic background of each mouse strain could affect the number of granules they present. In any case, oxidative stress may underlie and influence granule formation.

4.3. Natural IgM antibodies directed against the neo-epitope

IgM antibodies directed against the neo-epitope have been found in the sera of mice, as well as rat, goat and rabbit sera. Respect to mice, these antibodies have been detected in one to nine-month-old ICR-CD1, SAMP8 and BALB/c animals, as well as in three-months-old ICR-CD1 and BALB/c animals maintained in specific and opportunistic pathogen-free conditions. Thus, these IgM antibodies must be considered as natural antibodies that are present in the organism without previous exposure to external antigens (Manich et al., 2015). Actually, the presence of these natural IgM antibodies is the reason behind the false-positive staining of the PAS granules when using antibodies obtained from mouse or rabbit ascites or serum. Moreover, the IgM antibodies of each animal can recognize the neo-epitopes present in the granules of their own brain, which would indicate that the anti-neo-epitope IgMs are in fact natural auto-antibodies.

The presence of both these neo-epitopes in the PAS granules and the natural anti-neo-epitope IgMs could be due to the fact that the neo-epitopes are formed by widespread mechanisms related to pathological ageing processes such as those associated with the increase of oxidative stress caused by the production of reactive oxygen or nitrogen species. Oxidative stress may cause advanced glycation end products or oxidised phospholipids, which are a target of natural auto-antibodies and may trigger immune responses aimed at eliminating them and removing the structures that contain them (Binder et al., 2003; Goldin et al., 2006; Singh et al., 2001).

Whether anti-neo-epitope IgMs exert a functional role in the appearance or development of granule clusters is unclear. Because these IgMs are natural antibodies, they could be involved in the removal of senescent structures, since one of their functions is the clearance of tissue debris following degradation (Avrameas and Selmi, 2013). However, the negative immunostaining of the hippocampal PAS granules with only secondary antibodies directed against IgMs indicate that under physiological conditions the IgMs present in mouse plasma do not reach the granules, probably due to the existence of the blood–brain barrier (Manich et al., 2015).

4.4. Other treatments and experimental manipulations

Since it has been alleged that PAS granules have a variety of different identities, various treatments with different experimental aims have been performed and have occasionally achieved an increase or a decrease in the quantity of granule clusters in mouse brains. These experimental treatments include bone marrow replacement in ApoE-deficient mice, which resulted in a reduction in the number of hippocampal granule clusters compared to untreated mice (Robertson et al., 2000), and chronically induced

neuroinflammation, which provoked an increase in the size and number of granules with respect to the control group (Doehner et al., 2012; Knuesel et al., 2009). Moreover, the implantation of neural stem cells in disomic and trisomic Ts65Dn mice showed a significant decrease in the number of granule clusters in the CA1 hippocampal area in both genotypes (Kern et al., 2011). However, further investigation is required in order to interpret and achieve a better understanding of these observations.

5. Discussion and conclusions

Since the PAS granules were first described by Lamar et al. (1976), these structures have been extensively identified as different brain deposits related to numerous neurodegenerative diseases.

A wide range of studies have linked the mouse granule clusters to the corpora amylacea in the human brain (Mitsuno et al., 1999; Sinadinos et al., 2014). These studies have been based on the PAS-positive staining of these deposits, their association with ageing and their formation in both astrocytes and neurons (Cavanagh, 1999). Nevertheless, some other important features of the PAS granules are not consistent with these deposits, e.g. their characteristic brain distribution in the hippocampus, the granule ultrastructure and the conflicting results in other histochemical stainings (Cavanagh, 1999; Robertson et al., 1998). Another glycosidic brain depositions with which the PAS granules have been related are Lafora bodies. However, these deposits develop in neurons, their formation pattern does not present fragmentation or blebbing of the cytoplasm (Ganesh et al., 2002) and their identification has been based on immunohistochemical procedures using anti-advanced glycation end-product (AGE) and anti-ubiquitin antibodies (Valles-Ortega et al., 2011). The PAS granules have been also identified as amyloid aggregates (Del Valle et al., 2010; Doehner et al., 2010; Robertson et al., 2000; Wirak et al., 1991), although this interpretation should be ruled out due to the controversial results and false-positive staining results (Jucker et al., 1992; Kern et al., 2011; Krass et al., 2003; Manich et al., 2014b). Similarly, PAS granules have been interpreted as a sign of tauopathies (Kern et al., 2011; Krass et al., 2003; Manich et al., 2011) and even autophagosomes formed when the proteostasis has been altered (Soontornniyomkij et al., 2012). Again, these statements were based on immunohistochemical studies where antibodies might contain anti-neo-epitope IgM. Finally, a group of studies have hypothesised that the PAS granules are reelin deposits extruded by aged neurons and phagocytised by astrocytes due to a failure in the proteasome/autophagosome system, a parallel process to reelin neuron loss (Doehner et al., 2010, 2012; Knuesel et al., 2009; Kocherhans et al., 2010; Madhusudan et al., 2009). The false-positive staining results could explain the detection of reelin as a granule component.

Each of these identifications has generated a particular theory about their significance and a different set of experiments and proposals. These interpretations, which have appeared and disappeared over time, have generated disagreements and controversy. The principal cause of these controversies is, probably, the high number of false immunostaining results produced by the presence of neo-epitopes on these structures and the existence of natural IgMs directed against them. Now that this point has been clarified, and according to the items exposed previously, the nature and significance of PAS granules should be reconsidered.

An important step to this aim is to use an appropriate nomenclature to the identification of these structures. Due to their unmistakable PAS-positive staining and their still unknown nature, the clustered granules have been named previously and consistently as PAS granules. So far, the reports referring to them have used diverse names, being therefore more difficult to achieve a deeper understanding. Using the name “PAS granules” could be appropriate for future reports.

Throughout this review, degenerative PAS granules have been shown to be primarily described and studied in the mouse hippocampus, although they also exist in other brain structures and in other mammals. The reason for the high specificity and the early development of the hippocampal PAS granules is unknown. Some hypothesis related to a higher sensitivity of the hippocampal cells or other brain areas to oxidative stress have already been suggested (Cana et al., 2015; Manich et al., 2014a) and the appearance of PAS granules has also been related to an increase of oxidative stress and ageing. On the other hand, cross-regional brain differences, and even subregional differences, have been encountered in specific neuronal populations that suffer selective vulnerability to oxidative stress, and exhibit earlier functional decline and cell death during normal ageing, or in age-associated neurodegenerative diseases (Wang and Michaelis, 2010). Concretely, neurons in the hippocampal CA1 region and cerebellar granule cell layer are particularly vulnerable to oxidative stress (Wilde et al., 1997; Wang et al., 2007, 2009). Neurons in the hippocampal CA1 region are shown to be particularly sensitive to oxidative stress, whereas those in CA3 are comparatively resistant (Wang et al., 2007), potentially suggesting compromised astrocyte protection (Cana et al., 2015). Furthermore, hippocampal astrocytes could show selective vulnerability to oxidative stress, as suggested by the results in astrocytes of the CA1 region in comparison to other hippocampal brain areas reported in transitory focal ischemia (Ouyang et al., 2007) . All in all, interactions between glial cells and neurons are essential to the appearance of selective neuron vulnerability among cell populations (Wang and Michaelis, 2010), and this could explain the brain regional development of the PAS granules.

The granules mainly form in astrocyte processes and tend to appear in clusters, where each cluster corresponds to the set of granules of a determined astrocyte. During formation of the granules, the degeneration of cytoplasmic organelles, especially mitochondria, takes place, irregular vacuolar structures emerge and the cytoplasmic membrane occasionally fragments and alters. The cytoplasmic membranes surrounding the neuropil structures may also suffer alterations, and in some cases the cellular boundaries are lost. Once constituted, the granules contain a dense central part formed by the accumulation of membranous fragments and a peripheral zone with a very low density of organelles.

The relationship between hippocampal PAS granules and ageing has been repeatedly and consistently shown. A comprehensive observation of granule formation leads to the identification of global ageing-related features that may be connected to the functional impairment of the ageing brain. In fact, several hallmarks of ageing described by López-Otín et al. (2013) may be present in the granule formation process, including cellular senescence, mitochondrial dysfunction and deregulated nutrient sensing, and some others may be involved in the process, e.g., altered intercellular communication and loss of proteostasis. Therefore, considering the multifactorial characteristics of ageing, it is not surprising that the factors related to the appearance of PAS granules could be numerous and diverse. One seemingly important factor is the level of oxidative stress, since in different experimental designs in which oxidative stress levels are modified (alterations in energy metabolism, use of antioxidants, studies using high-fat diets, etc.), the onset and progression of the PAS granules is altered. Mitochondrial degeneration and the increased enzyme activity of MAO-B in the granules may also be associated with increased oxidative stress. Another factor that seems important is the genetic background of the animal, since different strains of mice have shown different trends in the presentation of these granules. This genetic background might be related to the presence of different alleles or

gene mutations affecting the metabolism or the levels of oxidative stress.

Nevertheless, the appearance of neo-epitopes in hippocampal PAS granules may also be related to ageing and increased oxidative stress. In ageing processes, there is an increase in the generation of AGEs (Goldin et al., 2006), which are formed by the modification of proteins or lipids that become non-enzymatically glycated and oxidised (Schmidt et al., 1994; Singh et al., 2001). Early glycation and oxidation processes result in the formation of Schiff bases and Amadori products, which eventually lead to the generation of AGEs (Schmidt et al., 1994). Although it is unclear whether or not the glycosidic neo-epitopes found in the granules are AGEs, it is important to note that glycosidic neo-epitopes can be targets of immune surveillance and natural IgM antibodies (Brändlein et al., 2003; Vollmers and Brändlein, 2006). Therefore, it is not surprising that the new carbohydrate epitope that appears in the hippocampus PAS granules of mice would be recognised by natural IgM antibodies present in ubiquitous form in the ascites or serum of mice or other species.

From our point of view, the neo-epitopes present in the PAS granules could become a useful brain-ageing biomarker in degenerative brain processes. Moreover, these neo-epitopes and the natural IgMs directed against them suggest that autoimmunity could become a new focus in the study of age-related degenerative processes. Natural antibodies could become a useful new tool for the treatment of age-related neurodegenerative diseases.

Acknowledgements

This study was funded by grant BFU2010-22149 from the Spanish Ministerio de Ciencia e Innovación and grant BFU2013-47382-P from the Spanish Ministerio de Economía y Competitividad, and by the Centros de Investigación Biomédica en Red (CIBER) at the Instituto de Salud Carlos III. We thank the Generalitat de Catalunya for funding the research group (2009/SGR00853, 2014/SGR525) and for awarding a predoctoral fellowship to G. Manich (FI-DGR 2011). I. Cabezón and E. Augé received the predoctoral fellowship Ajuts de Personal Investigador en Formació fellowship from the Universitat de Barcelona (APIF-UB). Authors are grateful to Christopher Evans for revising the English language.

References

Akiyama, H., Kameyama, M., Akiguchi, I., Sugiyama, H., Kawamata, T., Fukuyama, H., Kimura, H., Matsushita, M., Takeda, T., 1986. Periodic acid-Schiff (PAS)-positive: granular structures increase in the brain of senescence accelerated mouse (SAM). Acta Neuropathol. 72, 124–129.

Avrameas, S., Selmi, C., 2013. Natural autoantibodies in the physiology and pathophysiology of the immune system. J. Autoimmun. 41, 46–49.

Binder, C.J., Hörkkö, S., Dewan, A., Chang, M.K., Kieu, E.P., Goodyear, C.S., Shaw, P.X., Palinski, W., Witztum, J.L., Silverman, G.J., 2003. Pneumococcal vaccination decreases atherosclerotic lesion formation: molecular mimicry between *Streptococcus pneumoniae* and oxidized LDL. Nat. Med. 9, 736–743.

Brändlein, S., Pohle, T., Ruoff, N., Wozniak, E., Müller-Hermelink, H.K., Vollmers, H.P., 2003. Natural IgM antibodies and immunosurveillance mechanisms against epithelial cancer cells in humans. Cancer Res. 63, 7995–8005.

Cana, A., Herder, V., Hansmann, F., Beineke, A., Baumgärtner, W., Spitzbarth, I., 2015. Characterization of periodic acid-Schiff-positive granular deposits in the hippocampus of SJL/J mice. Toxicol. Pathol. 43, 737–742.

Cavanagh, J.B., 1999. Corpora-amylacea and the family of polyglucosan diseases. Brain Res. Rev. 29, 265–295.

Corsetti, V., Amadoro, G., Gentile, A., Capsoni, S., Ciotti, M.T., Cencioni, M.T., Atlante, A., Canu, N., Rohn, T.T., Cattaneo, A., Calissano, P., 2008. Identification of a caspase-derived N-terminal tau fragment in cellular and animal Alzheimer's disease models. Mol. Cell Neurosci. 38, 381–392.

Del Valle, J., Duran-Vilaregut, J., Manich, G., Casadesús, G., Smith, M.A., Camins, A., Pallàs, M., Pelegrí, C., Vilaplana, J., 2010. Early amyloid accumulation in the hippocampus of SAMP8 mice. J. Alzheimers Dis. 19, 1303–1315.

Del Valle, J., Duran-Vilaregut, J., Manich, G., Pallàs, M., Camins, A., Vilaplana, J., Pelegrí, C., 2011. Cerebral amyloid angiopathy: blood-brain barrier disruption and amyloid accumulation in SAMP8 mice. Neurodegener. Dis. 8, 421–429.

Doehner, J., Madhusudan, A., Konietzko, U., Fritschy, J.-M., Knuesel, I., 2010. Co-localization of Reelin and proteolytic AbetaPP fragments in hippocampal plaques in aged wild-type mice. J. Alzheimers Dis. 19, 1339–1357.

Doehner, J., Genoud, C., Imhof, C., Krstic, D., Knuesel, I., 2012. Extrusion of misfolded and aggregated proteins—a protective strategy of aging neurons? Eur. J. Neurosci. 35, 1938–1950.

Ganesh, S., Delgado-Escueta, A.V., Sakamoto, T., Avila, M.R., Machado-Salas, J., Hoshii, Y., Akagi, T., Gomi, H., Suzuki, T., Amano, K., Agarwala, K.L., Hasegawa, Y., Bai, D.-S., Ishihara, T., Hashikawa, T., Itohara, S., Cornford, E.M., Niki, H., Yamakawa, K., 2002. Targeted disruption of the Epm2a gene causes formation of Lafora inclusion bodies neurodegeneration, ataxia, myoclonus epilepsy and impaired behavioral response in mice. Hum. Mol. Genet. 11, 1251–1262.

Goldin, A., Beckman, J.A., Schmidt, A.M., Creager, M.A., 2006. Advanced glycation end products: sparking the development of diabetic vascular injury. Circulation 114, 597–605.

Gudi, V., Gingele, S., Skripuletz, T., Stangel, M., 2014. Glial response during cuprizone-induced de- and remyelination in the CNS: lessons learned. Front. Cell. Neurosci. 8, 73.

Harman, D., 2006. Free radical theory of aging: an update: increasing the functional life span. Ann. N. Y. Acad. Sci. 1067, 10–21.

Ingram, D.K., Kuo, H., Hengemihle, A., Shimada, A., Tian, M., Jucker, M., 1994. Motor and memory performance of SAMP8, R1 and C57BL/6 mice: assessing the relationship to PAS positive granules in the brain. In: Takeda, T. (Ed.), International Congress Series, The SAM Model of Senescence. Excerpta Medica, Amsterdam, pp. 73–82.

Irino, M., Akiguchi, I., Takeda, T., 1994. Ultrastructural study of PAS-positive granular structures (PGS) in brains of SAMP8. In: Takeda, T. (Ed.), The SAM Model of Senescence. Excerpta Medica, pp. 371–374.

Jenner, P., 2012. Mitochondria, monoamine oxidase B and Parkinson's disease. Basal Ganglia 2, S3–S7.

Jucker, M., Walker, L.C., Martin, L.J., Kitt, C.A., Kleinman, H.K., Ingram, D.K., Price, D.L., 1992. Age-associated inclusions in normal and transgenic mouse brain. Science 255, 1445.

Jucker, M., Walker, L.C., Kuo, H., Tian, M., 1994a. Age-related fibrillar deposits in brains of C57BL/6 mice: a review of localization staining characteristics incidence of fibrillar deposits with aging. Mol. Neurobiol. 9, 125–133.

Jucker, M., Walker, L.C., Schwarb, P., Hengemihle, J., Kuo, H., Snow, a.D, Bamert, F., Ingram, D.K., 1994b. Age-related deposition of glia-associated fibrillar material in brains of C57BL/6 mice. Neuroscience 60, 875–889.

Kern, D.S., Maclean, K.N., Jiang, H., Synder, E.Y., Sladek, J.R., Bjugstad, K.B., 2011. Neural stem cells reduce hippocampal tau and reelin accumulation in aged Ts65Dn down syndrome mice. Cell Transplant. 20, 371–379.

Knuesel, I., Nyffeler, M., Mormède, C., Muhia, M., Meyer, U., Pietropaolo, S., Yee, B.K., Pryce, C.R., LaFerla, F.M., Marighetto, A., Feldon, J., 2009. Age-related accumulation of reelin in amyloid-like deposits. Neurobiol. Aging 30, 697–716.

Kocherhans, S., Madhusudan, A., Doehner, J., Breu, K.S., Nitsch, R.M., Fritschy, J.-M., Knuesel, I., 2010. Reduced reelin expression accelerates amyloid-beta plaque formation and tau pathology in transgenic Alzheimer's disease mice. J. Neurosci. 30, 9228–9240.

Krass, K.L., Colinayo, V., Ghazalpour, A., Vinters, V.H., Lusis, A.J., Drake, T.A., 2003. Genetic loci contributing to age-related hippocampal lesions in mice. Neurobiol. Dis. 13, 102–108.

Kuo, H., Ingram, D.K., Walker, L.C., Tian, M., Hengemihle, J.M., Jucker, M., 1996. Similarities in the age-related hippocampal deposition of periodic acid-schiff-positive granules in the senescence-accelerated mouse P8 and C57BL/6 mouse strains. Neuroscience 74, 733–741.

Lamar, C.H., Hinsman, E.J., Henrikson, C.K., 1976. Alterations in the hippocampus of aged mice. Acta Neuropathol. 36, 387–391.

López-Otín, C., Blasco, M., a Partridge, L., Serrano, M., Kroemer, G., 2013. The hallmarks of aging. Cell 153, 1194–1217.

Madhusudan, A., Sidler, C., Knuesel, I., 2009. Accumulation of reelin-positive plaques is accompanied by a decline in basal forebrain projection neurons during normal aging. Eur. J. Neurosci. 30, 1064–1076.

Mandybur, T.I., Ormsby, I., Zemlan, F.P., 1989. Cerebral aging: a quantitative study of gliosis in old nude mice. Acta Neuropathol. 77, 507–513.

Manich, G., Mercader, C., del Valle, J., Duran-Vilaregut, J., Camins, A., Pallàs, M., Vilaplana, J., Pelegrí, C., 2011. Characterization of amyloid-β granules in the hippocampus of SAMP8 mice. J. Alzheimers Dis. 25, 535–546.

Manich, G., Cabezón, I., Camins, A., Pallàs, M., Liberski, P.P., Vilaplana, J., Pelegrí, C., 2014a. Clustered granules present in the hippocampus of aged mice result from a degenerative process affecting astrocytes and their surrounding neuropil. Age 36, 9690.

Manich, G., Del Valle, J., Cabezón, I., Camins, A., Pallas, M., Pelegrí, C., Vilaplana, J., 2014b. Presence of a neo-epitope and absence of amyloid beta and tau protein in degenerative hippocampal granules of aged mice. Age 36, 151–165.

Manich, G., Augé, E., Cabezón, I., Pallàs, M., Vilaplana, J., Pelegrí, C., 2015. Neo-epitopes emerging in the neurodegenerative hippocampal granules of aged mice can be recognized by natural IgM auto-antibodies. Immun. Ageing, http://dx.doi.org/10.1186/s12979-015-0050-z (in press).

Mitsuno, S., Takahashi, M., Gondo, T., Hoshii, Y., Hanai, N., Ishihara, T., Yamada, M., 1999. Immunohistochemical: conventional and immunoelectron microscopical characteristics of periodic acid-Schiff-positive granules in the mouse brain. Acta Neuropathol. 98, 31–38.

Nakamura, S., Akiguchi, I., Seriu, N., Ohnishi, K., Takemura, M., Ueno, M., Tomimoto, H., Kawamata, T., Kimura, J., Hosokawa, M., 1995. Monoamine

oxidase-B-positive granular structures in the hippocampus of aged senescence-accelerated mouse (SAMP8). Acta Neuropathol. 90, 626–632.
Oddo, S., Caccamo, A., Shepherd, J.D., Murphy, M.P., Golde, T.E., Kayed, R., Metherate, R., Mattson, M.P., Akbari, Y., Laferla, F.M., 2003. Triple-transgenic model of Alzheimer's disease with plaques and tangles: intracellular abeta and synaptic dysfunction. Neuron 39, 409–421.
Ouyang, Y.B., Volobouéva, L.A., Xu, L.J., Giffard, R.G., 2007. Selective dysfunction of hippocampal CA1 astrocytes contributes to delayed neuronal damage after transient forebrain ischemia. J. Neurosci. 27, 4253–4260.
Perluigi, M., Swomley, A.M., Butterfield, D.A., 2014. Redox proteomics and the dynamic molecular landscape of the aging brain. Ageing Res. Rev. 13, 75–89.
Porquet, D., Casadesús, G., Bayod, S., Vicente, A., Canudas, A.M., Vilaplana, J., Pelegrí, C., Sanfeliu, C., Camins, A., Pallàs, M., Del Valle, J., 2013. Dietary resveratrol prevents Alzheimer's markers and increases life span in SAMP8. Age 35, 1851–1856.
Rachubinski, A.L., Maclean, K.N., Evans, J.R., Bjugstad, K.B., 2012. Modulating cognitive deficits and tau accumulation in a mouse model of aging down syndrome through neonatal implantation of neural progenitor cells. Exp. Gerontol. 47, 723–733.
Robertson, T.A., Dutton, N.S., Martins, R.N., Roses, A.D., Kakulas, B.A., Papadimitriou, J.M., 1998. Age-related congophilic inclusions in the brains of apolipoprotein E-deficient mice. Neuroscience 82, 171–180.
Robertson, T.A., Dutton, N.S., Martins, R.N., Taddei, K., Papadimitriou, J.M., 2000. Comparison of astrocytic and myocytic metabolic dysregulation in apolipoprotein E deficient and human apolipoprotein E transgenic mice. Neuroscience 98, 353–359.
Schmidt, A.M., Hori, O., Brett, J., Yan, S.D., Wautier, J.L., Stern, D., 1994. Cellular receptors for advanced glycation end products implications for induction of oxidant stress and cellular dysfunction in the pathogenesis of vascular lesions. Arterioscler. Thromb. 14, 1521–1528.
Shih, J.C., Chen, K., Ridd, M.J., 1999. Monoamine oxidase: from genes to behavior. Annu. Rev. Neurosci. 22, 197–217.
Sinadinos, C., Valles-Ortega, J., Boulan, L., Solsona, E., Tevy, M.F., Marquez, M., Duran, J., Lopez-Iglesias, C., Calbó, J., Blasco, E., Pumarola, M., Milán, M., Guinovart, J.J., 2014. Neuronal glycogen synthesis contributes to physiological aging. Aging Cell 13, 935–945.
Singh, R., Barden a Mori, T., Beilin, L., 2001. Advanced glycation end-products: a review. Diabetologia 44, 129–146.
Soontornniyomkij, V., Risbrough, V.B., Young, J.W., Soontornniyomkij, B., Jeste, D.V., Achim, C.L., 2012. Increased hippocampal accumulation of autophagosomes predicts short-term recognition memory impairment in aged mice. Age 34, 305–316.
Spicer, S.S., 1961. The use of various cationic reagents in histochemical differentiation of mucopolysaccharides. Am. J. Clin. Pathol. 36, 393–407.
Spicer, S.S., Schulte, B.A., 1992. Diversity of cell glycoconjugates shown histochemically: a perspective. J. Histochem. Cytochem. 40, 1–38.
Takemura, M., Nakamura, S., Akiguchi, I., Ueno, M., Oka, N., Ishikawa, S., Shimada, A., Kimura, J., Takeda, T., 1993. Beta/A4 proteinlike immunoreactive granular structures in the brain of senescence-accelerated mouse. Am. J. Pathol. 142, 1887–1897.
Valles-Ortega, J., Duran, J., García-Rocha, M., Bosch, C., Sáez, I., Pujadas, L., Serafín, A., Cañas, X., Soriano, E., Delgado-García, J.M., Gruart, A., Guinovart, J.J., 2011. Neurodegeneration and functional impairments associated with glycogen synthase accumulation in a mouse model of Lafora disease. EMBO Mol. Med. 3, 667–681.
Veurink, G., Liu, D.A.N., Taddei, K., Perry, G., Smith, M.A., Robertson, T.A., Hone, E., Groth, D.M., Atwood, C.S., Martins, R.N., 2003. Reduction of inclusion body pathology in ApoE-deficient mice fed a combination of antioxidants. Free Radic. Biol. Med. 34, 1070–1077.
Vollmers, H.P., Brändlein, S., 2006. Natural IgM antibodies: the orphaned molecules in immune surveillance. Adv. Drug Deliv. Rev. 58, 755–765.
Wang, X., Pal, R., Chen, X.W., Kumar, K.N., Kim, O.J., Michaelis, E.K., 2007. Genome-wide transcriptome profiling of region-specific vulnerability to oxidative stress in the hippocampus. Genomics 90, 201–212.
Wang, X., Zaidi, A., Pal, R., Garrett, A.S., Braceras, R., Chen, X.W., Michaelis, M.L., Michaelis, E.K., 2009. Genomic and biochemical approaches in the discovery of mechanisms for selective neuronal vulnerability to oxidative stress. BMC Neurosci. 10, 12.
Wang, X., Michaelis, E.K., 2010. Selective neuronal vulnerability to oxidative stress in the brain. Front Aging Neurosci. 2, 12.
Wilde, G.J., Pringle, A.K., Wright, P., Iannotti, F., 1997. Differential vulnerability of the CA1 and CA3 subfields of the hippocampus to superoxide and hydroxyl radicals in vitro. J. Neurochem. 69, 883–886.
Wirak, D.O., Bayney, R., Ramabhadran, T.V., Fracasso, R.P., Hart, J.T., Hauer, P.E., Hsiau, P., Pekar, S.K., Scangos, G.A., Trapp, B.D., 1991. Deposits of amyloid beta protein in the central nervous system of transgenic mice. Science 253, 323–325.
Ye, X., Meeker, H.C., Kozlowski, P., Carp, R.I., 2004. The occurrence of vacuolation, and periodic acid-Schiff (PAS)-positive granules and plaques in the brains of C57BL/6 AKR, senescence-prone (SAMP8) and senescence-resistant (SAMR1) mice infected with various scrapie strains. Brain Res. 995, 158–166.
Yeoman, M., Scutt, G., Faragher, R., 2012. Insights into CNS ageing from animal models of senescence. Nat. Rev. Neurosci. 13, 435–445.